UNDERSTANDING THE MECHANISMS, THERMODYNAMICS AND KINETICS OF COCRYSTALLIZATION TO CONTROL PHASE TRANSFORMATIONS

by

Adivaraha Jayasankar

A dissertation submitted in partial fulfillment
of the requirements for the degree of
Doctor of Philosophy
(Pharmaceutical Sciences)
in The University of Michigan
2008

Doctoral Committee:

Associate Professor Naír Rodríguez-Hornedo, Chair
Professor Gordon L. Amidon
Professor Steven P. Schwendeman
Associate Professor Adam J. Matzger
Research Professor Gregory E. Amidon

To Bhagavan Sri Satya Sai Baba, my parents, and my wife Soumya

ACKNOWLEDGEMENTS

While this dissertation presents the scientific work carried out in the last five years as a graduate student, it does not reflect the love, support, encouragement and guidance of many who have supported my journey through graduate school and deserve more than an acknowledgement.

I would like to specially acknowledge my advisor Dr. Naír Rodríguez-Hornedo for whom I have utmost respect and appreciation. This dissertation was possible mainly because of the opportunity presented to me by Dr. Rodríguez in summer 2003 for joining her group as a part-time research assistant. Her dedication, enthusiasm, and passion for research motivated me to pursue a Ph.D. under her guidance. The training, support, and encouragement she has given me during my years in graduate school will be remembered forever. She has not only molded me into a scientist, but also has influenced me at a personal level to evolve into a better person. Her philosophy and teaching style are unique, and will continue to impact me even after I graduate. The years that I have spent being her student will always be cherished.

The journey through graduate school would have been difficult without the company of my former and current lab mates: Dr. Kurt Seefeldt, Dr. Barbara Rodríguez-Spong, Sarah J. Bethune, Phil Zocharski, David Good, Chinmay Maheshwari, Neal

Huang, Dr. L. Sreenivas Reddy, and Lilly Roy. Being in your company has made graduate school an enjoyable experience. Thank you so much for your support and help during my years in graduate school. I also acknowledge my committee members for providing valuable feedback on my research.

Special thanks to the College of Pharmacy at the University of Michigan for financial support in the form of Upjohn, Schering Plough, and Warner Lambert fellowships. Funding from the Purdue-Michigan consortium and research gift from Boehringer Ingelheim are also acknowledged.

Where I am today is because of my parents, and this dissertation is a reflection of the love and support that my parents have given me throughout my life. They have gone to great extents to make sacrifices for me and to ensure that all of my needs are met. I specially thank my father, Mr. S.A. Sarma, who has made great strides to ensure that my brother and I received the best possible education. He has inspired us to work hard in order to achieve our goals. I will be ever grateful to my parents for all the things they have done for us. I would also like to acknowledge my wife, Soumya, who has motivated me to keep moving through difficult times. Her love and patience has been a tremendous source of strength for me during my years in graduate school. I also thank my in-laws for all the help they have rendered to us during our time in graduate school. What they have done for us will always be remembered. I also thank members of Sri Satya Sai Organization who have helped me feel at home through their support, kindness, and love, especially during my first few years of stay in the US.

Above all, I would like to acknowledge my Guru and Divine Master, Bhagavan Sri Satya Sai Baba, for His divine grace and guidance in accomplishing this work.

Bhagavan is my main source of inner strength and peace. His love and words of encouragement have been a source of inspiration and transformation. I thank Him profusely for everything that He has given me, and pray that He continue to guide me in all my future endeavors.

Finally, a note to the reader; parts or sections of the chapters presented in this dissertation have been submitted for publication or published in the following articles:

1. Jayasankar, A.; Reddy, L. S.; Bethune, S. J.; Rodríguez-Hornedo, N. The Role of Cocrystal and Solution Chemistry on The Formation and Stability of Cocrystals with Different Stoichiometry. *Cryst. Growth Des*. **2008**, submitted.
2. Jayasankar, A.; Good, D. J.; Rodríguez-Hornedo, N. Mechanisms by Which Moisture Generates Cocrystals. *Mol. Pharm*. **2007**, 4, 360-372.
3. Jayasankar, A.; Somwangthanaroj, A.; Shao, Z. J.; Rodríguez-Hornedo, N. Cocrystal Formation During Cogrinding and Storage is Mediated by Amorphous Phase. *Pharm. Res*. **2006**, 23, 2381-2392.
4. Rodríguez-Hornedo, N.; Nehm, S. J.; Jayasankar, A. Cocrystals: Design, Properties and Formation Mechanisms. In *Encyclopedia of Pharmaceutical Technology,* 3rd ed.; Swarbrick, J., Eds.; Informa Health Care: New York, **2006**, pp.615-635.

TABLE OF CONTENTS

LIST OF FIGURES

LIST OF TABLES

LIST OF APPENDICES

ABSTRACT

The solid-state form of a drug influences its physico-chemical and biopharmaceutical properties. Consequently, phase transformations induced during processing/storage affects drug performance. Understanding the transformation mechanisms is valuable for anticipating and controlling phase transformations. In this dissertation, the mechanisms of conversion of crystalline drugs to cocrystals and factors affecting cocrystal stability are reported. Specifically, the objectives are to: (i) identify the factors governing the formation of different stoichiometry cocrystals, (ii) examine coformer, excipients and cosolvents effects on cocrystal hydrate thermodynamic stability, (iii) investigate the propensity and mechanisms of cocrystallization in solid mixtures due to moisture sorption, and (iv) identify the mechanisms by which mechanical activation induces cocrystal formation in mixtures. Model compounds selected in this study include carbamazepine, theophylline and coformers that form cocrystals.

Coformer solution concentration governs the formation and stability of different stoichiometry cocrystals. Studies with 1:1 and 2:1 carbamazepine-4-aminobenzoic acid cocrystals indicate that the cocrystal richer in coformer is more stable at higher coformer concentration. Phase diagrams showing cocrystal solubility and stability domains are generated using mathematical models based on cocrystal and solution chemistry.

Coformer concentration also governs the formation and stability of cocrystal hydrates in aqueous solutions. Studies with theophylline-citric acid and carbamazepine-4-aminobenzoic acid cocrystal hydrates indicate that coformers that modulate the water activity (a_w) of aqueous solutions can induce cocrystal hydrate to anhydrous cocrystal conversion. Addition of excipients or cosolvents to aqueous solutions similarly affects cocrystal hydrate stability by decreasing a_w.

Cocrystallization can also occur in solid mixtures of cocrystal reactants. Cocrystals of carbamazepine-nicotinamide, carbamazepine-saccharin, and caffeine or theophylline with various carboxylic acid coformers are formed due to moisture sorption and deliquescence in reactant mixtures. Transformation mechanism involves moisture uptake, reactant dissolution, cocrystal nucleation and growth. The rate and extent of cocrystal formation depends on RH, moisture uptake, deliquescent material, mixture composition, and reactant dissolution rates.

In the solid-state, cogrinding carbamazepine with saccharin or nicotinamide forms cocrystals. Cocrystal formation is shown to be amorphous phase mediated, and depends on cogrinding temperature, presence of moisture, and reactant hydrated form. Higher cogrinding temperature and water present in crystal lattice or vapor phase enhance cocrystallization.

.

CHAPTER I

INTRODUCTION

Background

An important decision to be made in the early stages of drug development is regarding the selection of an appropriate solid form for an active pharmaceutical ingredient (API). Polymorphs, salts, hydrates and solvates, and amorphous phases of APIs may be selected for development. The API solid form affects its physico-chemical properties such as solubility, dissolution rates, and hygroscopicity, physical and chemical stability, and mechanical properties. For instance, the chemical stability of carbamazepine and cinnamic acid is dependent on the solid-state form.[1, 2] Polymorphs of chloramphenicol palmitate and carbamazepine exhibit different bioavailabilities due to different solubility and dissolution rates of the solid forms.[3-5] Salts of poorly soluble drugs are sometimes used to enhance drug solubility and bioavailability.[6] Amorphous phases of APIs also enable to achieve high drug concentrations.[7] However, they are more prone to physical and chemical instability than the crystalline phases due to high reactivity.[8-10] Hydrates and solvates of API similarly impact the biopharmaceutical properties. API hydrates have lower aqueous solubilities, while solvates have higher aqueous solubilities when compared to anhydrous crystalline phases.[11-14] Consequently,

hydration or dehydration of APIs can impact the biopharmaceutical properties and manufacturability.[15] Differences in the properties of different API solid forms are a consequence of differences in molecular interactions, structure and composition that result in different energetics.[16] A classification of API solid forms based on structure and composition is shown in figure 1.1.

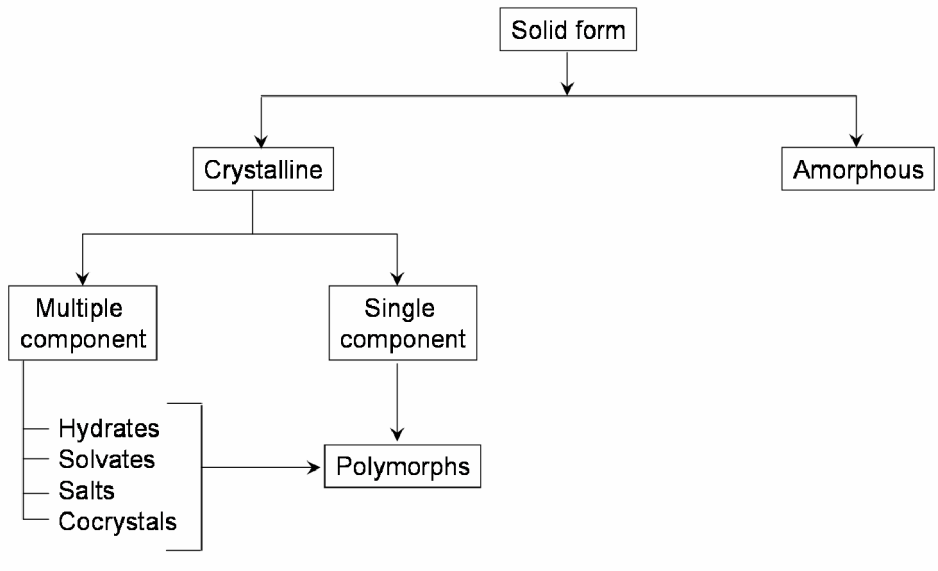

Figure 1.1: Classification of API solid form based on structure and composition.

Cocrystals have recently gained attention as attractive alternate solid forms for drug development. A pharmaceutical cocrystal is a single crystalline homogenous phase consisting of a drug and excipient or another drug.[16-23] The different components in the cocrystal are neutral in nature when compared to salts that have ionized components.[17, 20, 23-25] The components in a cocrystal exist in a definite stoichiometric ratio, and assemble via non-covalent interactions such as hydrogen bonds, ionic bonds, π-π or van der Waals

interactions. Cocrystals thus possess different composition and structure when compared to the crystals of parent components. Table 1.1 compares the crystallographic parameters of some carbamazepine (CBZ) cocrystals with anhydrous form III CBZ. Table 1.2 shows examples of some crystalline drugs for which pharmaceutical cocrystals have been discovered.

Crystal engineering and design of cocrystals

Cocrystal design is based on crystal engineering principles. The term 'crystal engineering' refers to engineering or construction of crystalline solids with desirable properties, and is based on a fundamental understanding of inter-molecular interactions that govern the assembly of molecules into a network superstructure.[26, 27] The molecules in the network are held together by synthons that are basic structural units formed from non-covalent interactions such as van der Waals interactions, $\pi - \pi$ interactions, and hydrogen bonds between the functional groups in the molecules.[28-31] Figure 1.2 shows some examples of commonly occurring synthons in the crystal structures of single and multiple-component materials.

Table 1.1: Crystallographic properties of CBZ(III)[32] and CBZ cocrystals[19]

	CBZ (III)	CBZ-NCT	CBZ-SAC	CBZ-trimesic acid
Stoichiometry	-	1:1	1:1	1:1
Molecular weight	236.27	358.39	419.46	446.40
Crystal system	Monoclinic	Monoclinic	Triclinic	Monoclinic
Space group	$P2_1/n$	$P2_1/n$	P-1	C2/c
a (Å)	7.54	5.09	7.51	32.53
b (Å)	11.16	17.59	10.45	5.27
c (Å)	13.91	19.65	12.68	24.16
α (degree)	90	90	83.64	90
β (degree)	92.86	90.92	85.70	98.19
γ (degree)	90	90	75.41	90
Volume ($Å^3$)	1168.30	1761.6	957.0	4099.3
Density (g/cm^{-3})	1.34	1.35	1.46	1.45

Table 1.2: Examples of pharmaceutical cocrystals

API	Cocrystal Former	Ratio (API:Ligand)	CSD REFCODE
Carbamazepine	Nicotinamide[19]	1:1	UNEZES
	Saccharin[19]	1:1	UNEZAO
	Benzoquinone[19]	1:1	UNEYOB
	Trimesic acid[19]	1:1	UNIBAU
	Terephthalaldehyde[19]	1:1	UNEYUH
	Formamide[19]	1:1	UNIBOI
	Adamantane-1,3,5,7-tetracarboxylic acid[19]	1:1	UNIBIC
	4-aminobenzoic acid[33]	2:1 anhydrous	XAQRAJ
		2:1:1 hydrate	XAQREN
	Malonic acid[34, 35]	2:1	
	Succinic acid[34]	2:1	
	2,6-pyridinedicarboxylic acid[33]		XAQRIR
	Aspirin[36]		TAZRAO
Caffeine	Oxalic acid[21]	2:1	GANXUP
	Adipic acid[37]	1:1	CESKAN
	Malonic acid[21]	2:1	GANYAW
	Maleic acid[21]	1:1	GANYEA
		2:1	
	Glutaric acid[21]	1:1 (Forms I, II)	EXUQUJ
	Citric acid[38]	1:1	KIGKER
	Methyl gallate[39]	1:1	DIJVOH
	4-hydroxybenzoic acid[40]	1:2	
		2:1	
	d-tartaric acid[41]	1:1	NEXWUJ
	1-hydroxy-2-napthoic acid[42]	1:1	KIGKIV
	3-hydroxy-2-napthoic acid[42]	1:1	KIGKOB
	Barbital[43]	2:1	CAFBAR20
	Sulfaproxyline[44]	1:1	VIGVOW
Itraconazole	Fumaric acid[45]	2:1	
	Succinic acid[45]	2:1	IKEQEU
	Malic acid[45]	2:1	
	Tartaric acid[45]	2:1	
Piracetam	Gentisic acid[46]	1:1	DAVPAS
	p-hydroxybenzoic acid[46]	1:1	DAVPEW

Table 1.2 (continued)

API	Cocrystal Former	Ratio (API:Ligand)	CSD REFCODE
Theophylline	5-fluorouracil monohydrate[47]	2:1	ZAYLOA
	Phenobarbital[48]	2:1	THOPBA
	Oxalic acid[22]	2:1	XEJWUF
	Maleic acid[22]	1:1	XEJXEQ
	Glutaric acid[22]	1:1	XEJXIU
	Malonic acid[22]	1:1	XEJXAM
	Citric acid[38]	1:1 anhydrous	
		1:1:1 hydrate	KIGKAN
	Saccharin[35]	1:1	
	Salicyclic acid[25, 49]	1:1	KIGLES
	dl-Tartaric acid[41]	2:1	NEYCIE
	Sorbic acid[25]	1:1	KIGLAO
	5-chlorosalicylic acid[25]	1:1	CSATEO
	4-hydroxybenzoic acid[25]	1:1	KIGLOC
	Sulfathiazole[50]	1:1	SULTHE
	1-hydroxy-2-naphthoic acid[25]	1:1	KIGLIW
	2,4-dihydroxybenzoic acid[25]	1:1	DEYREF
	Acetaminophen[25]	1:1	KIGLUI
Sulfadimidine	Acetylsalicylic acid[51]	1:1	VUGMIT
	4-aminosalicylic acid[51]	1:1	VUGMOZ
	2-aminobenzoic acid[51]	1:1	SORWEB
	4-aminobenzoic acid[51]	1:1	SORWIF
Piroxicam	Fumaric acid[18]	4:1	DIKDIL
	Benzoic acid[18]	1:1	DIKDOR
	Succinic acid[18]	2:1	DIKCIK
	1-hydroxy-2-naphthoic acid[18]	1:1	DIKCOQ
	4-hydroxybenzoic acid[18]	1:1 (form I)	DIKDEH
		1:1 (form II)	NIFKIX
	Malonic acid[18]	1:1	

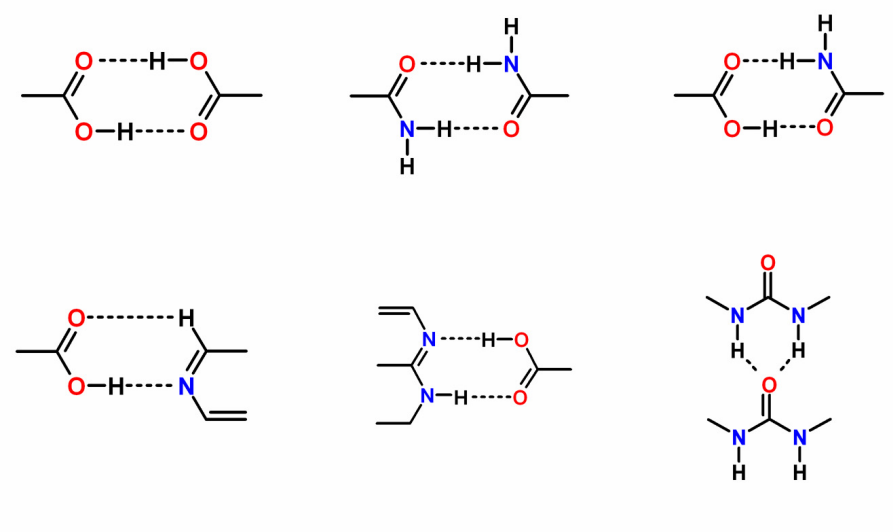

Figure 1.2: Examples of commonly occurring synthons in single and multiple component crystals

Due to their directionality, strength and frequency of occurrence, hydrogen bonds are extensively employed in cocrystal design.[18, 19, 21, 22, 52-55] By studying the packing motifs and hydrogen bond patterns in the crystal structures of large number of organic compounds, Etter and Donohue have proposed the following three hydrogen bonds rules:[52, 56, 57]

(i) all acidic hydrogens in a molecule will be used for hydrogen bond formation

(ii) all good hydrogen bond acceptors will be used when there are available hydrogen bond donors, and

(iii) the best hydrogen bond donor and best acceptor will preferentially form hydrogen bonds to one another.

Using these rules, hydrogen bond and synthon formation between the functionalities of different molecules can be predicted and rank ordered,[58-60] and strategies for cocrystal

design can be derived. This approach was used to design cocrystals of the anti-epileptic drug carbamazepine (CBZ) in 2003.[19]

The molecular structure of CBZ (figure 1.3) shows an azepine ring with a primary amide functional group that has two hydrogen bond donors and two acceptors. The crystal structures of form III CBZ exhibits the carboxamide homodimer (figure 1.4A) due to hydrogen bonding between the amide groups of two CBZ molecules.[27, 61, 62] The anti-NH in the amide group remains free due to steric hindrance from the azepine ring. However, in the crystal structure of carbamazepine dihydrate (CBZ(D)), the anti-NH forms N—H···O hydrogen bonds with water molecules (figure 1.4B). One of the strategies in the design of CBZ cocrystals, therefore, is to utilize the anti-NH of CBZ to form hydrogen bonds with other coformer molecules, such as NCT and SAC, while retaining the CBZ carboxamide dimer[19] as shown in figures 1.4C and 1.4D.

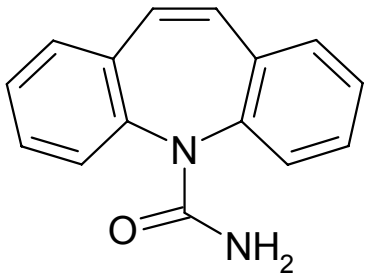

Figure 1.3: Molecular structure of carbamazepine

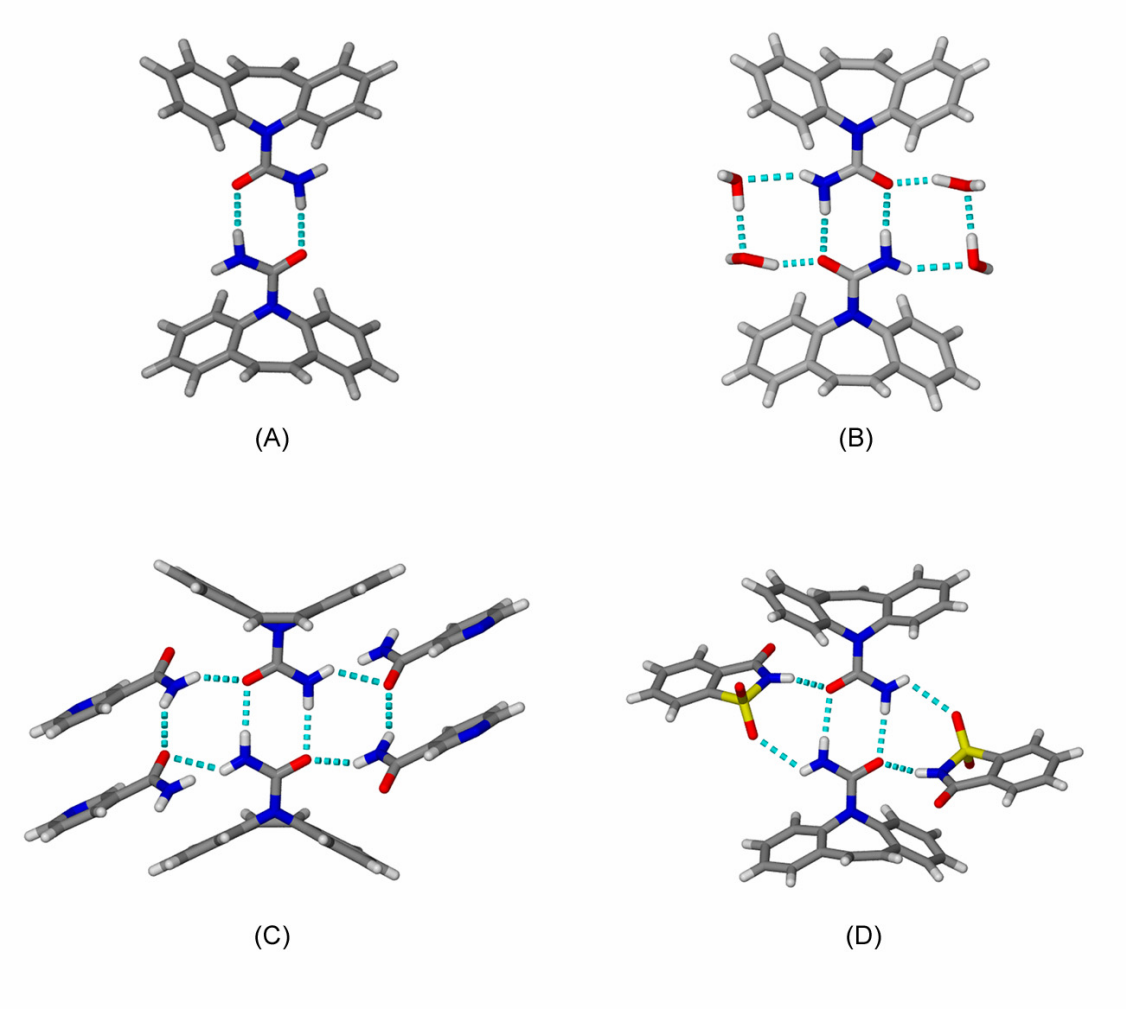

Figure 1.4: Hydrogen bonding patterns in (A) CBZ(III),[32] (B) CBZ(D),[63] (C) CBZ-NCT cocrystal,[19] and (D) CBZ-SAC cocrystal[19]

An alternative strategy for designing CBZ cocrystals is to replace the amide-amide interactions in the carboxamide homodimer with stronger acid-amide interactions resulting in a heterodimer.[19] CBZ cocrystals with trimesic acid, 5-nitroisophhalic acid, and CBZ-malonic acid have been designed in this manner[19, 35] (figure 1.5). Using these strategies, as many as 40 cocrystals of carbamazepine have been discovered to date.[19, 33, 34, 64] Cocrystals thus enhance the diversity of CBZ solid forms.

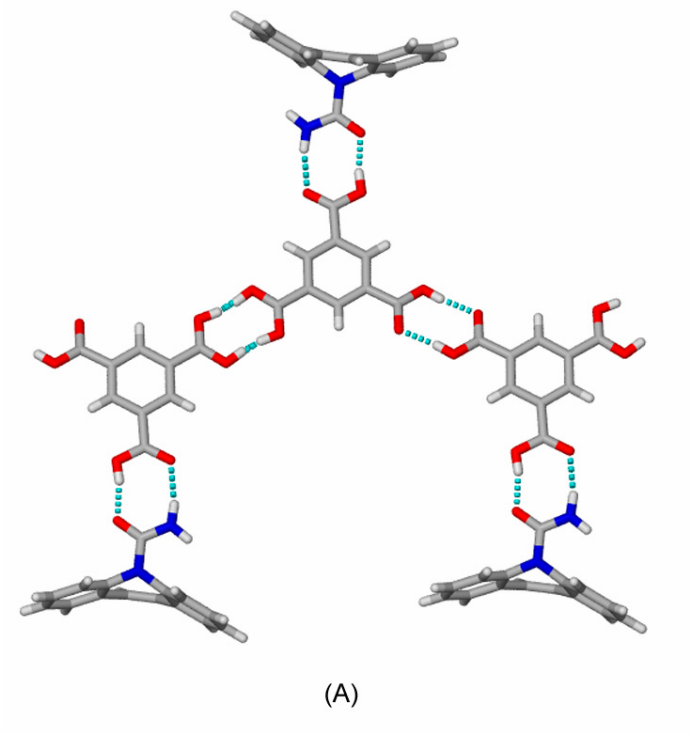

Figure 1.5: Hydrogen bonding patterns in (A) CBZ-trimesic acid,[19] (B) CBZ-5-nitroisophthalic acid,[19] and (C) CBZ-malonic acid[35]

Strategies to design caffeine and theophylline cocrystals were similarly developed based on hydrogen bond rules and synthon formation. Caffeine and theophylline are characterized by basic nitrogen and carbonyl groups in the imidazole and pyrimidine ring that serve as hydrogen bond acceptors. Theophylline, in addition, has a hydrogen bond donor. The molecular structure of these two compounds is shown in figure 1.6.

Cocrystals of caffeine were designed using coformers such as dicarboxylic acids that donate hydrogen bonds.[21, 42] The cocrystals are formed as a result of heteromeric O−H···N and C−H···O interactions that replace the homomeric interactions in the crystal structure of caffeine.[21, 42] Figure 1.7 shows the hydrogen bonding patterns in some caffeine-dicarboxylic acid cocrystals. Cocrystals of theophylline with dicarboxylic acids were similarly designed using dicarboxylic acids that serve as both hydrogen bond donors and acceptors[22] (figure 1.8). In this case, N−H···N interactions between theophylline molecules in anhydrous theophylline are replaced by stronger O−H···N interactions between the carboxylic acid and basic nitrogen of theophylline. The –NH donor in theophylline interacts with the carbonyl of adjacent theophylline via N−H···O interactions to form theophylline dimer.[22]

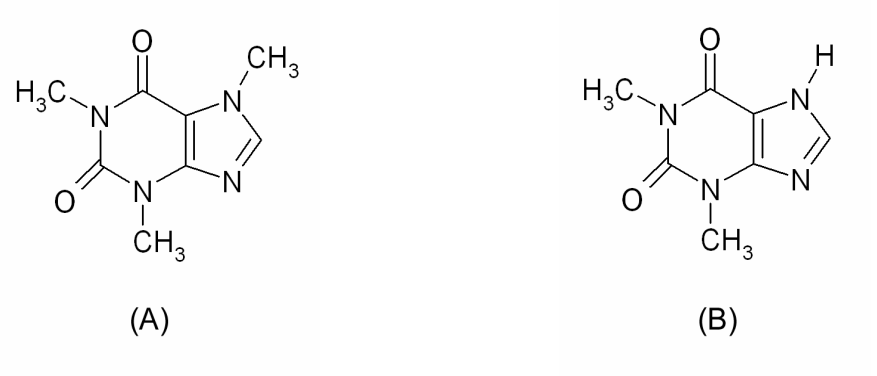

Figure 1.6: Molecular structure of (A) Caffeine, and (B) Theophylline

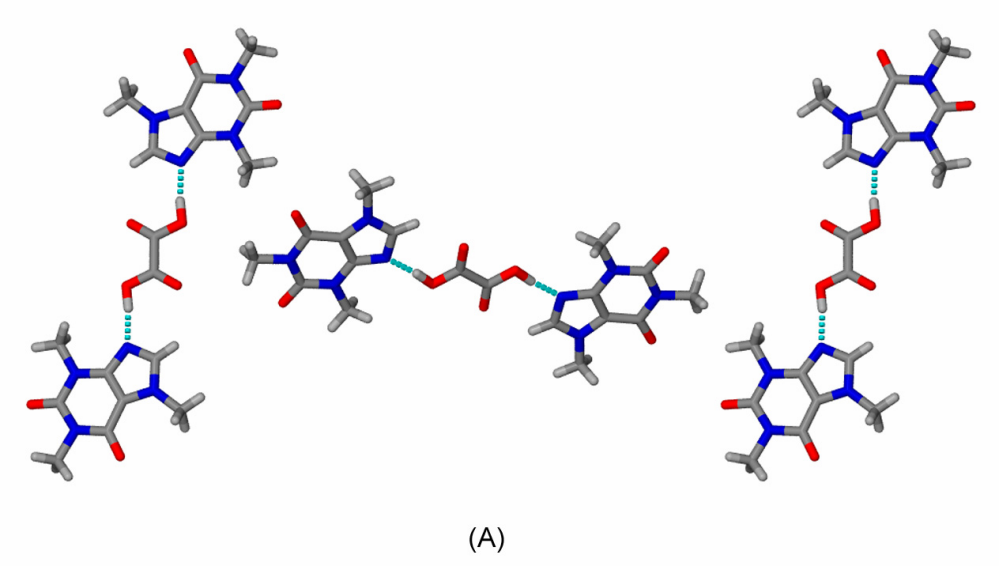

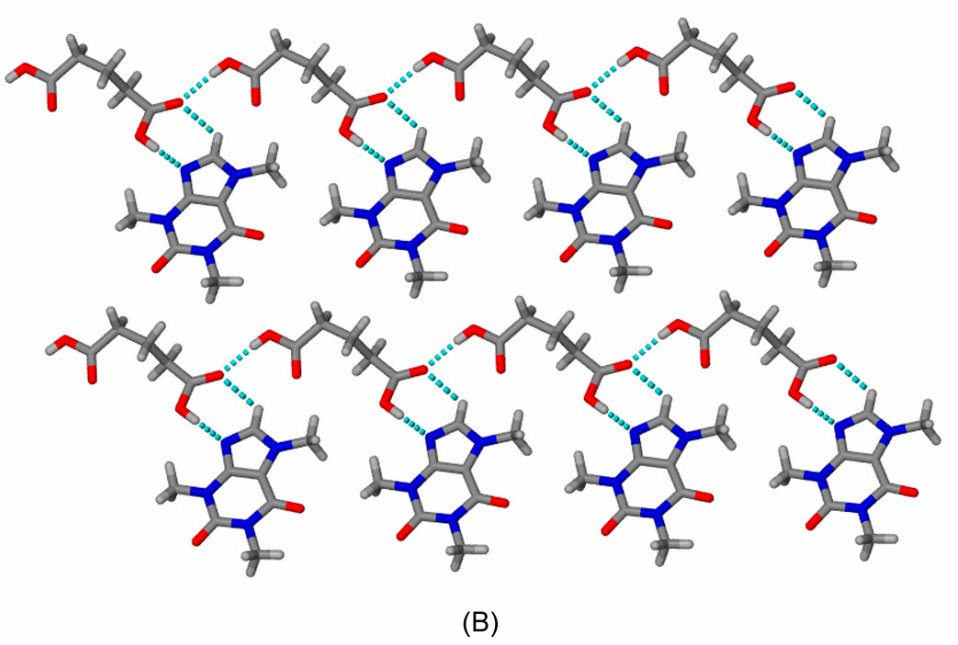

Figure 1.7: Molecular assemblies in caffeine cocrystals: (A) caffeine-oxalic acid,[21] and (B) caffeine-glutaric acid (form I)[21]

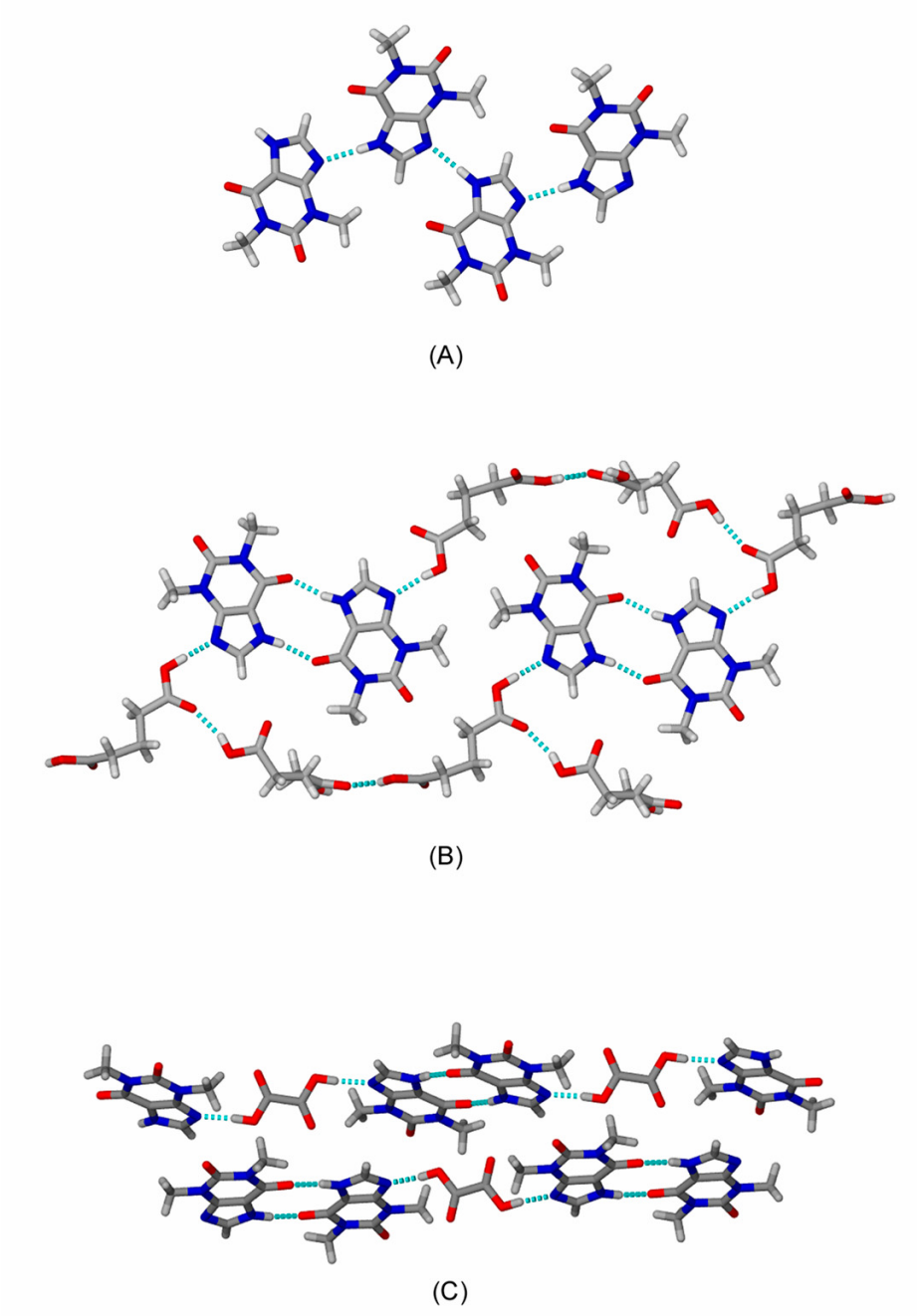

Figure 1.8: Molecular assemblies in (A) anhydrous theophylline,[65] (B) theophylline-glutaric acid cocrystal,[22] and (C) theophylline-oxalic acid cocrystal[22]

Cocrystal properties

Examples in the preceding section show that cocrystallization alters the molecular interactions and composition of pharmaceutical materials. As such one can expect changes in physico-chemical properties such as chemical stability, hygroscopicity, dissolution rates and solubility due to cocrysallization of pharmaceutical materials. This has been demonstrated for a few API cocrystals.

Chemical stability

Cocrystallization can improve the chemical stability of an API. For instance, carbamazepine is reported to undergo chemical degradation to cyclobutyl dimer after forming a hydrate.[2, 66] The degradation reaction requires that the distance between the azepine rings of adjacent CBZ molecules be less than or equal to 4.1Å.[66] Cocrystallization of CBZ with coformers such as saccharin (SAC) or nicotinamide (NCT) alters the molecular interactions and packing arrangement of CBZ molecules. Hence, these cocrystals exhibit greater stability against hydration and degradation.

Melting point

The melting point of cocrystals, in general, differs from those of the individual components due to changes in molecular interactions, composition and structure. Table 1.3 compares the melting points of some drugs, coformers, and the corresponding pharmaceutical cocrystals. Cocrystals with lower melting points can be advantageous during pharmaceutical processing; for example when a melted state of a thermally labile API is desired during some processes such as hot melt extrusion, a cocrystal with a

melting point lower than that of the pure crystalline API will allow for melting at lower temperatures to avoid chemical degradation.

Table 1.3: Melting points of single components and their cocrystals[19, 35, 67-72]

Drug/coformer	M.P. (°C)
Carbamazepine (CBZ)	192
Caffeine (CAFF)	236
Theophylline (THP)	269
Sulfamerazine (SFZ)	237
Nicotinamide (NCT)	126-128
Saccharin (SAC)	229
Glutaric acid (GLA)	98
Salicylic acid (SAA)	158-162

Cocrystal	M.P. (°C)
CBZ-NCT	160
CBZ-SAC	177
CBZ-GLA	125
CAFF-SAC	124
CAFF-GLA	96
THP-SAC	207
THP-GLA	118
SFZ-SAA	201

Hygroscopicity and hydrate formation

Pharmaceutical cocrystals can alter API hygroscopicity and prevent hydrate or solvate in APIs. Hydrate or solvate formation of APIs relies on interactions between the drug and the solvent in the crystal. Replacing these interactions with those between the API and cocrystal former can inhibit API hydrate or solvate formation. This has been shown for CBZ cocrystals with SAC and NCT. Anhydrous carbamazepine transforms to CBZ(D) on exposure to high relative humidities. However, CBZ-NCT and CBZ-SAC cocrystals under similar conditions exhibit greater stability against CBZ(D) formation[66] (figure 1.9). Similar behavior is reported for cocrystals of caffeine and theophylline with dicarboxylic acids.[21, 22]

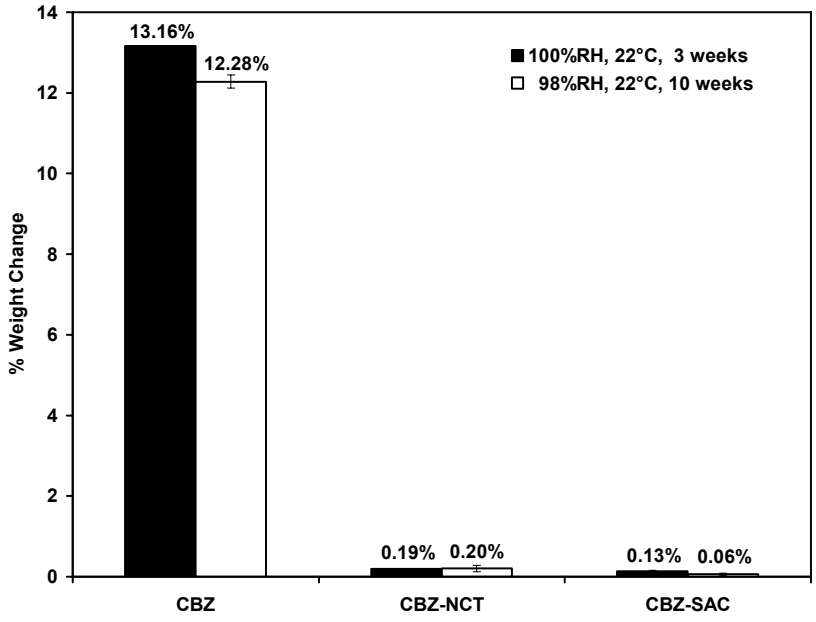

Figure 1.9: Hygroscopicity of carbamazepine (CBZ), nicotinamide (NCT), saccharin (SAC), CBZ-NCT cocrystal, and CBZ-SAC cocrystal[20]

Dissolution rates and solubility

Cocrystals alter the solubility and dissolution rate of crystalline drugs. Itraconazole (ITZ), an antifungal agent, is an API with very low aqueous solubility. 2:1 cocrystals of itraconazole were prepared using 4 dicarboxylic acids (l-tartaric acid, maleic acid, succinic acid, and fumaric acid).[45] Dissolution rates of the cocrystals were compared with that of the pure crystalline and amorphous drug in 0.1N HCl at 25°C.[45] The cocrystals showed 4 – 20 fold faster dissolution relative to the crystalline drug. In the case of ITZ−l-tartaric acid and ITZ−l-malic acid cocrystals, the dissolution profiles were comparable with the amorphous form of the drug.

Cocrystals of fluoxetine hydrochloride, an anti-depressant, were synthesized with benzoic acid, succinic acid and fumaric acid.[73] Powder dissolution studies indicated

rapid dissolution of the cocrystals in water at 20°C.[73] Intrinsic dissolution rate studies were therefore performed to compare the dissolution rates of cocrystals and the crystalline salt. The dissolution rate of 2:1 fumaric acid cocrystal was similar to the pure crystalline fluoxetine hydrochloride, but the dissolution rate for the benzoic acid 1:1 cocrystal was half that of the API. Fluoxetine hydrochloride-succinic acid 2:1 cocrystal had approximately three times higher dissolution rate, but the dissolution was so fast that an accurate value was difficult to measure. Thus cocrystal synthesis with different ligands offers the opportunity to tailor the dissolution rates of drugs.

Solubility studies with carbamazepine-nicotinamide (CBZ-NCT) cocrystal have shown that cocrystal solubility decreases with increasing ligand concentration (figure 1.10).[74] These studies further show that cocrystal solubility dependence on ligand concentration can be predicted using mathematical models based on cocrystal dissociation and complexation equilibria as shown below for a 1:1 cocrystal forming 1:1 solution complex.[74]

$$AB_{solid} \overset{K_{sp}}{\rightleftharpoons} A_{soln} + B_{soln} \quad (1)$$

$$A_{soln} + B_{soln} \overset{K_{11}}{\rightleftharpoons} AB_{soln} \quad (2)$$

Equilibrium constants for these reactions are the solubility product

$$K_{sp} = [A][B] \quad (3)$$

and the binding constant for the 1:1 complex formed in solution

$$K_{11} = \frac{[AB]}{[A][B]} = \frac{[AB]}{K_{sp}} \quad (4)$$

Mass balance on [A] and [B] yields the following relationship:

$$[A]_T = \frac{K_{sp}}{[B]} + K_{11}K_{sp} \quad (5)$$

For a 1:1 cocrystal, cocrystal solubility is given by: $S_{cocrystal} = [A]_T = [B]_T$

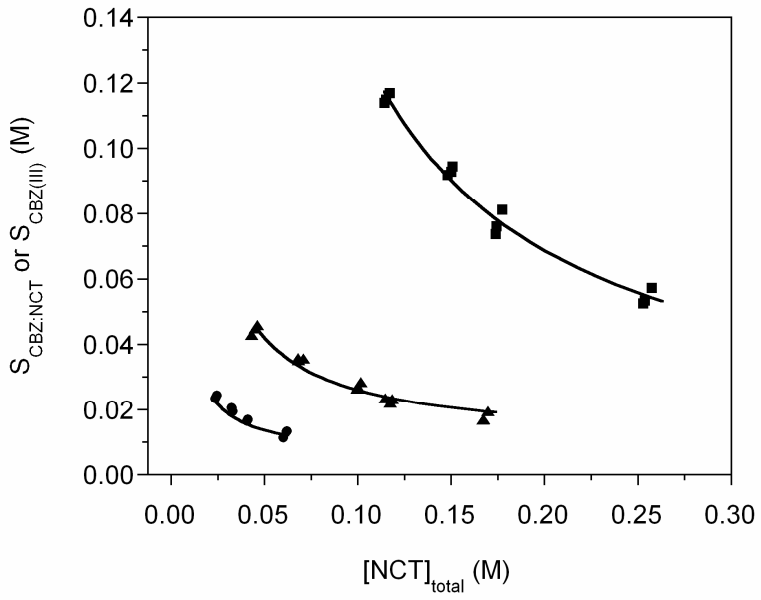

Figure 1.10: Solubility of 1:1 CBZ:NCT cocrystal at 25 °C as a function of total NCT concentration in ethanol, 2-propanol, and ethyl acetate.[74] The solid lines represent the predicted solubility according to equation (5). Filled symbols are experimental cocrystal solubility values in (■) ethanol, (▲) 2-propanol, and (●) ethyl acetate.

For cocrystals with ionizable drug and/or coformer, cocrystal solubility is also dependent on solution pH. This dependence can be predicted using mathematical models based on ionization and cocrystal dissociation equilibria. For a binary cocrystal RHA, where R is the drug and HA is the acidic ligand, the solubility ($S_{cocrystal}$) dependence on pH is given as:[20]

$$S_{cocrystal} = \sqrt{K_{sp}\left(1 + \frac{K_a}{[H^+]}\right)} \quad (6)$$

K_{sp} is the solubility product of the cocrystal, and K_a is the ligand dissociation constant. Figure 1.11 shows the predicted solubility dependence on pH for a cocrystal with weak acidic ligand and neutral drug.[20] Models predicting pH dependent solubility have also been developed for cocrystals with ionizable drug and coformer.[75]

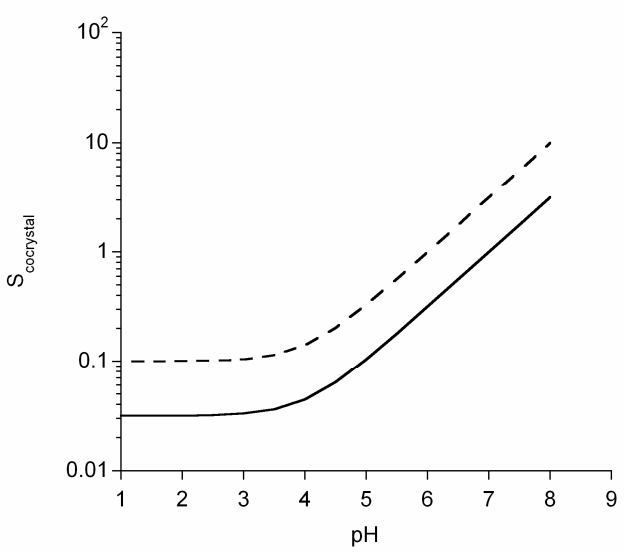

Figure 1.11: pH-solubility dependence for cocrystal with neutral drug and acidic ligand plotted using equation (6) with K_{sp} values of $0.001M^2$ (—) and $0.01M^2$ (- - -), and ligand $pK_a = 4$.[20]

Mechanical property

Due to differences in molecular interactions and crystal structure, cocrystals also exhibit different mechanical properties. For instance, 1:1 cocrystal of caffeine with methyl gallate shows improved tabletability over caffeine and methyl gallate at high compaction pressures (> 240 MPa).[39] In contrast, tablets of caffeine showed lamination

at compaction pressures greater than 180 MPa, and a sharp reduction in tensile strength due to elastic deformation at pressures greater than 240 MPa. Methyl gallate tablets exhibited poor tensile strength and high elastic recovery at low compaction pressures. Improved tabletability of the cocrystal is attributed to the presence of slip planes that are absent in caffeine.[39] Cocrystals of CBZ with SAC and NCT are similarly reported to have improved tableting characteristics when compared to CBZ(D) or CBZ(III). While high pressure (5000 psi) applied for 30 minutes were required to make tablets of CBZ(III) or CBZ(D) to avoid capping, tablets of cocrystals could be made at lower compaction pressures over shorter times.[66]

The preceding examples illustrate the potential offered by cocrystals for altering physico-chemical properties. Considerable effort and time have therefore been expended on cocrystal design and screening.

Cocrystal screening

Screening for cocrystals is performed using solution or solid-state based methods. Cocrystal screening by solution based approaches is usually performed by slow evaporation of organic solvents containing the drug and coformer in stoichiometric molar ratios.[19, 33, 64] While this approach has generally been successful for discovering cocrystals, it is nevertheless empirical, and suffers from the risk of crystallizing single components. A more effective approach for screening cocrystals is the reaction crystallization method where supersaturation with respect to cocrystal is selectively achieved by dissolving the least soluble component, usually the drug, in solutions of the highly soluble component, usually the coformer.[76] Thus, the drug and coformer may be

in non-stoichiometric molar ratios in this method. The effectiveness of this approach for cocrystal screening was demonstrated in a recent study with CBZ cocrystals. Twenty-seven cocrystals of CBZ with several carboxylic acids were discovered using aqueous or organic solvents.[34]

Recent studies have also employed thermal methods for cocrystal screening where the drug and coformer are heated in DSC or hot stage.[35, 77] Cocrystal formation in this case is preceded by the formation of eutectic melt. Cocrysals of carbamazepine, caffeine, sulfamerazine, theophylline and flurbiprofen with several coformers were identified using this approach.[35, 77]

In the solid-state, cocrystal screening is performed by cogrinding the reactants.[51, 52, 78-80] Small quantities of organic solvents or water added to the reactants during grinding have been shown to improve the success of discovering cocrystals.[38, 41, 81, 82] Cocrystals that could not be identified by slow evaporation of organic solvents or by dry grinding were identified by cogrinding reactants with small quantities of solvent, with the outcome being dependent on the nature of solvent.[82-84]

Research objectives

Much of the current emphasis in the field of pharmaceutical cocrystals has been on cocrystal design and screening. Only a few studies have investigated cocrystal properties. Several reports indicate the potential for cocrystals as alternate solid-state forms for drug development, however less is known about the factors affecting cocrystal formation and stability. Lack of such understanding can lead to unanticipated phase changes during processing or storage, and result in poor pharmaceutical product

performance. This has been shown for AMG-517, a class II Amgen compound. Transformation of the drug to cocrystal during development resulted in solubility limited absorption.[85] The objective of the current study, therefore, is to understand the mechanisms of cocrystallization, and to identify the factors that affect cocrystal formation and stability using carbamazepine and theophylline cocrystals as model systems. The specific goals are to:

(i) Identify the factors governing the formation and stability of cocrystals with different stoichiometry,

(ii) Determine the mechanisms by which moisture induces cocrystal formation in reactant mixtures

(iii) Examine the effect of hygroscopic additives, such as sucrose and fructose, and reactant properties on the formation and stability of cocrystals

(iv) Identify the factors governing the formation and thermodynamic stability of anhydrous and hydrated cocrystals

(v) Determine cocrystal formation mechanisms during cogrinding and storage.

Subsequent chapters in this thesis will address the above goals. The remaining portion of the current chapter will present model APIs and cocrystals used in this research. Chapter 2 examines the factors affecting the formation and stability of cocrystals with different stoichiometry. Key parameters to identify cocrystal stability domains are presented. Mathematical models based on heterogenous and homogenous equilibria to (i) predict cocrystal and drug solubilities, and (ii) generate phase solubility

and triangular phase diagrams are presented. The utility of models for estimating cocrystal solubility in pure solvents, and for predicting cocrystal solubilities with minimum number of experiments is demonstrated. Chapter 3 presents the mechanism of cocrystal formation due to moisture sorption and deliquescence in reactant mixtures. The effects of hygroscopic additives and the factors affecting cocrystal formation and stability are addressed. Chapter 4 discusses the role of coformer, excipient and cosolvent aqueous concentrations on the formation and thermodynamic stability of anhydrous and hydrated cocrystals. Phase diagrams showing the solubility and stability dependence of anhydrous and hydrated cocrystals on coformer concentration are presented. Chapter 5 focuses on the mechanism of cocrystal formation during cogrinding. The effects of grinding time, temperature, and solid-state form of reactants on cocrystal formation during cogrinding are presented. Results showing transformations during storage, and the effect of storage conditions on cocrystal formation rates are presented.

Model Compounds and cocrystals

Carbamazepine and theophylline were chosen as the models drugs in this study. Carbamazepine is a BCS class II compounds and has low solubility and high permeability. In contrast, theophylline is a class I compound with high solubility and permeability. Cocrystals of both drugs have been identified with several pharmaceutically relevant coformers using the crystal engineering principles and strategies outlined in a preceding section.

Carbamazepine

Carbamazepine, an anti-convulsant drug, exists in four polymorphic forms.[61, 62] The crystal structures of all four polymorphic forms of carbamazepine exhibit similar molecular conformations and hydrogen bonding patterns resulting in a carboxamide homodimer.[27] The primary difference between the different forms is in the packing arrangements that results in different crystallographic properties as illustrated in table 1.4. Of the four polymorphic forms, monoclinic form III is the thermodynamically stable form at room temperature.[67]

In addition to the four polymorphic forms, carbamazepine also forms a dihydrate and solvates.[19, 86, 87] The crystal structure of carbamazepine dihydrate exhibits the carboxamide dimer motifs similar to those observed in the carbamazepine polymorphs. However, the anti-NH of carbamazepine amide forms hydrogen bonds with water molecules that results in the formation of water channels along the b-axis in carbamazepine dihydrate. Due to these differences in the hydrogen bond patterns and packing arrangements, carbamazepine dihydrate exhibits different crystallographic and physico-chemical properties. Thermal analysis of CBZ(D) shows an endotherm at 50-80°C and a 13% weight loss corresponding to the loss of water from the crystal. CBZ(D) is the thermodynamically stable form at high relative humidities (RH > 70%), and has the lowest solubility in water when compared to the anhydrous forms. Consequently, the anhydrous forms transform to CBZ(D) upon dissolution in water.

Table 1.4: Crystallographic properties of CBZ polymorphs

	CBZ (I)[62]	CBZ (II)[88]	CBZ(III)[32]	CBZ(IV)[61]	CBZ(D)[63]
Crystal system	Triclinic	Trigonal	Monoclinic	Monoclinic	Monoclinic
Space group	P-1	R-3	$P2_1/n$	C2/c	$P2_1/c$
a (Å)	5.17	35.45	7.54	26.61	10.07
b (Å)	20.57	35.45	11.16	6.93	28.72
c (Å)	22.25	5.25	13.91	13.96	4.83
α (degree)	84.12	90	90	90	90
β (degree)	88.01	90	92.86	109.70	103.45
γ (degree)	85.19	120	90	90	90
Volume (cm^3)	2344.8	5718.3	1168.3	2421.9	1358.3
Density (g/cm^{-3})	1.34	1.24	1.34	1.29	1.33

Carbamazepine cocrystals

Approximately 40 cocrystals of carbamazepine (CBZ) have been reported to date,[19, 33, 34, 64] and table 1.2 lists some examples of CBZ cocrystals. Cocrystals of carbamazepine with nicotinamide (NCT), saccharin (SAC) and 4-aminobenzoic acid (4ABA) were selected as model systems in the current study since the crystallographic and physico-chemical properties of these cocrystals are reported.[19, 33]

Both CBZ-NCT and CBZ-SAC cocrystals exhibit polymorphism. Form I CBZ-NCT and CBZ-SAC were first identified in 2003 by slow evaporation of organic solvents containing the reactants in stoichiometric molar ratio.[19] The crystal structures of both

cocrystals and hydrogen bonding patterns have been presented in an earlier section (figure 1.4). Polymorphic form II CBZ-NCT cocrystal was identified by melt-quenching form I cocrystal and reheating the resulting amorphous phase,[89] as well as by polymer mediated nucleation and growth from solutions.[90] Form I is thermodynamically stable phase at room temperature, and is monotropically related to form II cocrystal. Form II exhibits an exothermic transformation to form I at 83-90°C.[89] Upon dissolution in water, form I CBZ-NCT transforms to CBZ(D) due to higher aqueous solubility of the cocrystal.

Form II CBZ-SAC cocrystal polymorph was identified by polymer mediated nucleation.[90] Unlike the form I CBZ-SAC cocrystal, form II CBZ-SAC cocrystal does not retain the CBZ amide homodimer. Instead, the CBZ amide forms heterosynthon by hydrogen bonding with the SAC amide[90] as shown in figure 1.12. Based on thermal analysis and stability study of form II CBZ-SAC cocrystal in suspensions, form I is reported to be the thermodynamically stable phase at room temperature.[90] However, form I CBZ-SAC transforms to CBZ(D) upon dissolution in water due to higher aqueous solubility of the cocrystal.[66]

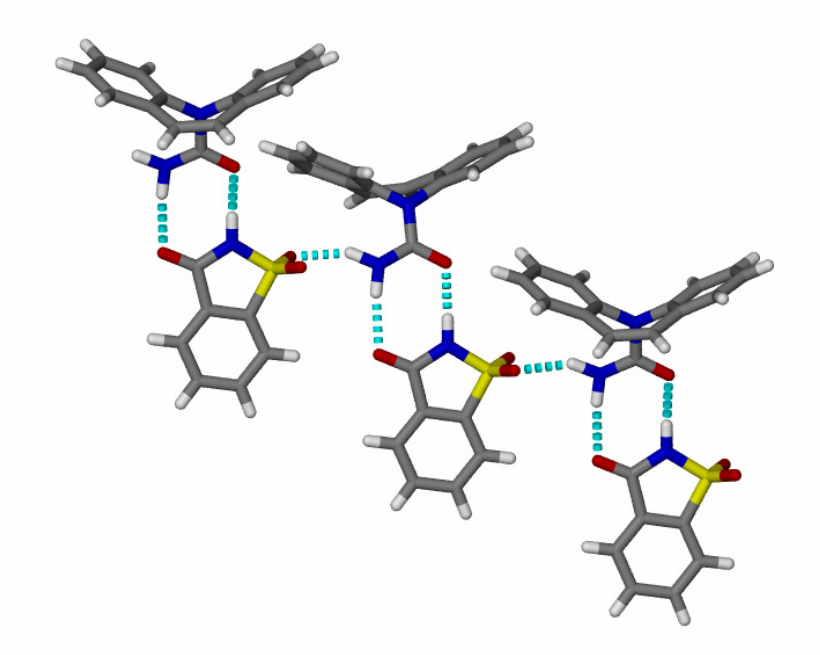

Figure 1.12: Hydrogen bonding in form II CBZ-SAC cocrystal[90]

Carbamazepine-4-aminobenzoic acid (CBZ-4ABA) cocrystal is reported to exist in the anhydrous and hydrated form.[33] The crystal structures of the two cocrystals are shown in figure 1.13. The 2:1 anhydrous structure shows the expected acid–amide heterosynthon as well as an unexpected amide-amide homosynthon. Two acid-amide heterosynthons are connected through N–H_{anti}···O hydrogen bonds to from a tetrameric unit. These tetramers are hydrogen bonded to CBZ homodimers on each side *via* amino N–H···O hydrogen bond (figure 1.13A).[33] In the 2:1 hydrated structure, water molecule interrupts the expected acid–amide heterosynthon. A second CBZ molecule interacts with the water interrupted dimer via O–H···O and N–H···O hydrogen bonds to form a tetramer. These tetramers are in turn connected by amino N–H···O hydrogen bond to form a eight molecule discrete unit (figure 1.13B).[33]

Both the anhydrous and hydrated cocrystals were discovered by slow evaporation of organic solvents containing CBZ and 4ABA in 1:1 mol ratio.[33] However, the relative thermodynamic stabilities of the two cocrystalline phases are not known. Identifying the factors governing the formation and thermodynamic stability of the two cocrystalline phases will enable anticipation of phase transformation, and is therefore a subject matter of interest in the current study.

CBZ-NCT, CBZ-SAC and CBZ-4ABA cocrystals were also selected in the current study as the coformers (NCT, SAC and 4ABA) in these cocrystals exhibit different properties such as solubility, hygroscopicity and melting points. Nicotinamide exists in four polymorphic forms and has a melting point of 126-128°C.[69] It has high aqueous solubility, and is known to self-associate in aqueous solutions.[91] Further, NCT has been shown to enhance the solubility of several drugs significantly by forming complexes in solution.[92, 93] During storage at high relative humidity, NCT sorbs more than 50% water and deliquesces.[66] In contrast, 4-aminobenzoic acid and saccharin are non-hygroscopic and have low aqueous solubility.[94, 95] Both ligands are ionizable. SAC is a weak acid with a pK_a of 1.8,[96] while 4ABA is amphoteric with pK_as of 2.45 and 4.85.[97] The melting point of 4ABA and SAC are higher when compared to NCT. 4ABA melts at 187-189°C,[94] while SAC melts at 229.5°C.[72]

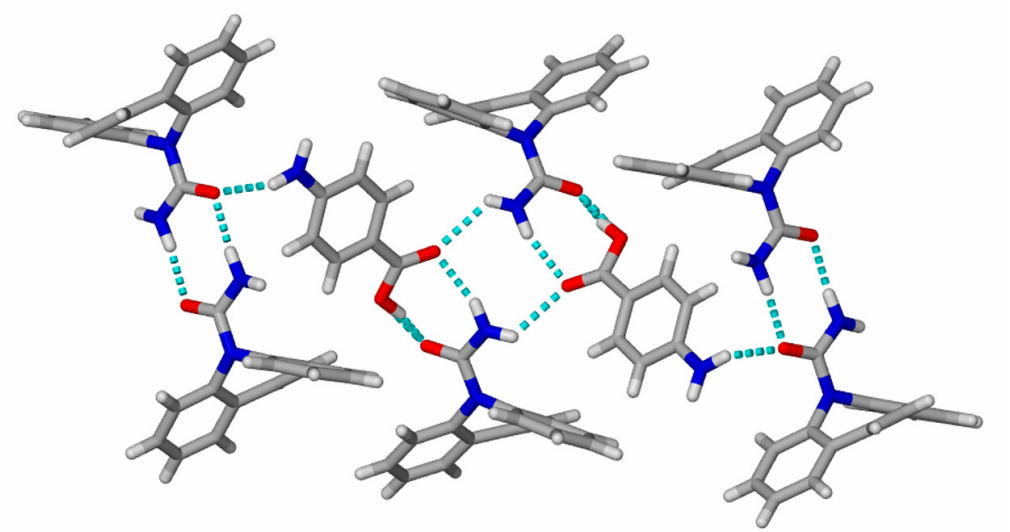

(A)

.

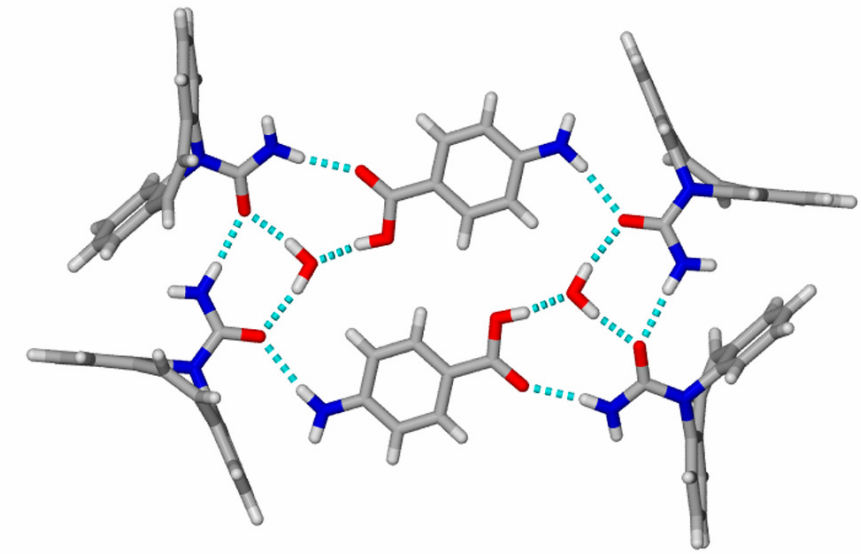

(B)

Figure 1.13: Molecular assemblies in CBZ-4ABA cocrystals[33] (A) 2:1 anhydrous cocrystal, and (B) 2:1:1 cocrystal hydrate

Theophylline

Theophylline (THP), a bronchodialator, exists in 3 polymorphic forms (forms I, I*, I'),[15, 98] and as a hydrate.[99] The molecular structure of theophylline is shown in figure 1.6. Of the three polymorphs, form I is the stable phase at room temperature, while forms I' and I* are meta-stable. Form I* was identified by heating theophylline hydrate,[15] and form I' was identified by heating form I at 260-280°C for 1 hour.[98] Form I' is enantiotropically related to form I, while form I* is monotropically related. All three anhydrous forms transform to theophylline hydrate in water since theophylline hydrate is the least soluble phase in water.[15, 98]

Theophylline has two hydrogen bond acceptors and one hydrogen bond donor (figure 1.6). Hence, it can form cocrystals with coformers capable of donating and accepting hydrogen bonds. Table 1.2 shows examples of theophyline cocrystals with several coformers. While most theophylline cocrystals are anhydrous, the cocrystal with citric acid (CTA) is reported to exist in the anhydrous and hydrated form.[38] The cocrystals were identified by cogrinding reactants.[38] Anhydrous cocrystal was formed by cogrinding anhydrous THP and CTA. Cocrystal hydrate was formed by cogrinding the hydrated reactants or by cogrinding the anhydrous reactants with small quantities of water. Both THP-CTA cocrystals were also identified by slow evaporation of organic solvent containing the reactants in stoichiometric ratios.[38]

Water activity is well known to affect the formation and stability of pharmaceutical hydrates.[100, 101] The water activity can be varied by altering the solution composition.[102] Citric acid is highly water soluble, and increasing citric acid aqueous concentration is known to decrease the water activity.[103] Since cocrystal stability has

been shown to depend on coformer concentration, THP-CTA cocrystals were selected as model systems to examine the effect of coformer concentration on the formation and stability of anhydrous and hydrated cocrystals in aqueous media.

References

1. Byrn, S. R.; Pfeiffer, R. R.; Stowell, J. G., *Solid-State Chemistry of Drugs*. Second; SSCI, Inc.: West Lafayette, 1999.

2. Matsuda, Y.; Akazawa, R.; Teraoka, R.; Otsuka, M. Pharmaceutical Evaluation of Carbamazepine Modifications - Comparative Study for Photostability of Carbamazepine Polymorphs by Using Fourier Transformed Reflection-Absorption Infrared Spectroscopy and Colorimteric Measurement. *J. Pharm. Pharmacol.* 1994, 46, 162-167.

3. Aguiar, A. J.; Krc, J.; Kinkel, A. W.; Samyn, J. C. Effect of Polymorphism on the Absorption of Chloramphenicol from Chloramphenicol Pamitate. *J. Pharm. Sci.* 1967, 56, 847-853.

4. Carino, S. R.; Sperry, D. C.; Hawley, M. Relative Bioavailability Estimation of Carbamazepine Crystal Forms Using an Artificial Stomach-Duodenum Model. *J. Pharm. Sci.* 2006, 95, 116-125.

5. Kobayashi, Y.; Ito, S.; Itai, S.; Yamamoto, K. Physicochemical Properties and Bioavailability of Carbamazepine Polymorphs and Dihydrate. *Int. J. Pharm.* 2000, 193, 137-146.

6. Serajuddin, A. T. M. Salt Formation to Improve Drug Solubility. *Adv. Drug. Del. Rev.* 2007, 59, 603-616.

7. Hancock, B. C.; Pikal, M. What Is the True Solubility Advantage for Amorphous Pharmaceuticals? *Pharm. Res.* 2000, 17, 397-403.

8. Yoshioka, S.; Aso, Y. Correlations between Molecular Mobility and Chemical Stability During Storage of Amorphous Pharmaceuticals. *J. Pharm. Sci.* 2007, 96, 960-981.

9. Andronis, V.; Yoshioka, M.; Zografi, G. Effects of Sorbed Water on the Crystallization of Indomethacin from the Amorphous State. *J. Pharm. Sci.* 1997, 86, 346-351.

10. Andronis, V.; Zografi, G. Crystal Nucleation and Growth of Indomethacin Polymorphs from the Amorphous State. *J. Non-Cryst. Solids.* 2000, 271, 236-248.

11. Zhu, H.; Khankari, R. K.; Padden, B. E.; Munson, E. J.; Gleason, W. B.; Grant, D. J. W. Physicochemical Characterization of Nedocromil Bivalent Metal Salt Hydrates. 1. Nedocromil Magnesium. *J. Pharm. Sci.* 1997, 85, 1026-1034.

12. Zhu, H.; Padden, B. E.; Munson, E. J.; Grant, D. J. W. Physicochemical Characterization of Nedocromil Bivalent Metal Salt Hydrates. 2. Nedocromil Zinc.

J. Pharm. Sci. 1997, 86, 418-429.

13. Zhu, H.; Yuen, C.; Grant, D. J. W. Influence of Water Activity in Organic Solvent + Water Mixtures on the Nature of the Crystallizing Drug Phase . 1. Theophylline. *Int. J. Pharm.* 1996, 135, 151-160.

14. Ghosh, S.; Grant, D. J. W. Determination of the Solubilities of Crystalline Solids in Solvent Media That Induce Phase Changes - Solubilities of 1,2-Dialkyl-3-Hydroxy-4-Pyridones and Their Formic Acid Solvates in Formic Acid and Water. *Int. J. Pharm.* 1995, 114, 185-196.

15. Phadnis, N. V.; Suryanarayanan, R. Polymorphism in Anhydrous Theophylline - Implications on the Dissolution Rate of Theophylline Tablets. *J. Pharm. Sci.* 1997, 86, 1256-1263.

16. Cui, Y. A Material Science Perspective of Pharmaceutical Solids. *Int. J. Pharm.* 2007, 339, 3-18.

17. Aakeroy, C. B.; Salmon, D. J. Building Co-Crystals with Molecular Sense and Supramolecular Sensibility. *CrystEngComm.* 2005, 7, 439-448.

18. Childs, S. L.; Hardcastle, K. I. Cocrystals of Piroxicam with Carboxylic Acids. *Cryst. Growth Des.* 2007, 7, 1291-1304.

19. Fleischman, S. G.; Kuduva, S. S.; McMahon, J. A.; Moulton, B.; Walsh, R. D. B.; Rodríguez-Hornedo, N.; Zaworotko, M. J. Crystal Engineering of the Composition of Pharmaceutical Phases: Multiple-Component Crystalline Solids Involving Carbamazepine. *Cryst. Growth Des.* 2003, 3, 909-919.

20. Rodríguez-Hornedo, N.; Nehm, S. J.; Jayasankar, A. Cocrystals: Design, Properties and Formation Mechanisms. In *Encyclopedia of Pharmaceutical Technology*, 3rd ed.; Swarbrick, J., Eds.; Informa Health Care: 2006; pp 615-635.

21. Trask, A. V.; Motherwell, W. D. S.; Jones, W. Pharmaceutical Cocrystallization: Engineering a Remedy for Caffeine Hydration. *Cryst. Growth Des.* 2005, 5, 1013-1021.

22. Trask, A. V.; Motherwell, W. D. S.; Jones, W. Physical Stability Enhancement of Theophylline Via Cocrystallization. *Int. J. Pharm.* 2006, 320, 114-123.

23. Vishweshwar, P.; McMahon, J. A.; Bis, J. A.; Zaworotko, M. J. Pharmaceutical Co-Crystals. *J. Pharm. Sci.* 2006, 95, 499-516.

24. Aakeroy, C. B.; Fasulo, M. E.; Desper, J. Cocrystal or Salt: Does It Really Matter? *Mol. Pharm.* 2007, 4, 317-322.

25. Childs, S. L.; Stahly, P. G.; Park, A. The Salt-Cocrystal Continuum: The Influence of Crystal Structure on Ionization State. *Mol. Pharm.* 2007, 4, 323-388.

26. Desiraju, G. R. Crystal Engineering: From Molecules to Materials. *J. Mol. Struct.* 2003, 656, 5-15.

27. Rodríguez-Spong, B.; Price, C. P.; Jayasankar, A.; Matzger, A. J.; Rodríguez-Hornedo, N. General Principles of Pharmaceutical Solid Polymorphism: A Supramolecular Perspective. *Adv. Drug. Del. Rev.* 2004, 56, 241-274.

28. Desiraju, G. R. Hydrogen Bridges in Crystal Engineering: Interactions without Borders. *Acc. Chem. Res.* 2002, 35, 565-573.

29. Desiraju, G. R. Supramolecular Synthons in Crystal Engineering - a New Organic Synthesis. *Angew. Chem. Int. Ed.* 1995, 34, 2311-2327.

30. Nangia, A.; Desiraju, G. R. Supramolecular Structures - Reason and Imagination. *Acta Crystallogr.* 1998, A54, 934-944.

31. Nangia, A.; Desiraju, G. R. Supramolecular Synthons and Pattern Recognition. *Top. Curr. Chem.* 1998, 198, 58-95.

32. Himes, V. L.; Mighell, A. D.; DeCamp, W. H. Structure of Carbamazepine: 5h-Dibenz[B,F]Azepine-5-Carboxamide. *Acta Crystallogr.* 1981, B37, 2242-2245.

33. McMahon, J. A.; Bis, J. A.; Vishweshwar, P.; Shattock, T. R.; McLaughlin, O. L.; Zaworotko, M. J. Crystal Engineering of the Composition of Pharmaceutical Phases. 3. Primary Amide Supramolecular Heterosynthons and Their Role in the Design of Pharmaceutical Cocrystals. *Z. Kristallogr.* 2005, 220, 340-350.

34. Childs, S. L.; Rodríguez-Hornedo, N.; Reddy, L. S.; Jayasankar, A.; Maheshwari, C.; McCausland, L.; Shipplett, R.; Stahly, B. C. Screening Strategies Based on Solubility and Solution Composition Generate Pharmaceutically Acceptable Cocrystals of Carbamazepine. *CrystEngComm.* 2008, 10, 856-864.

35. Lu, E.; Rodríguez-Hornedo, N.; Suryanarayanan, R. A Rapid Thermal Method for Cocrystal Screening. *CrystEngComm.* 2008, 10, 665-668.

36. Vishweshwar, P.; McMahon, J. A.; Oliveira, M.; Peterson, M. L.; Zaworotko, M. J. The Predictably Elusive Form II of Aspirin. *J. Am. Chem. Soc.* 2005, 127, 16802-16803.

37. Bučar, D.-K.; Henry, R. F.; Lou, X.; Borchardt, T. B.; Zhang, G. G. Z. A Hidden Cocrystal of Caffeine and Adipic Acid. *Chem. Comm.* 2007, 525-527.

38. Karki, S.; Friščić, T.; Jones, W.; Motherwell, W. D. S. Screening for Pharmaceutical

Cocrystal Hydrates Via Neat and Liquid-Assisted Grinding. *Mol. Pharm.* 2007, 4, 347-354.

39. Sun, C. C.; Hou, H. Improving Mechanical Properties of Caffeine and Methyl Gallate Crystals by Cocrystallization. *Cryst. Growth Des.* 2008, 8, 1575-1579.

40. Zhang, G.; Bučar, D.-K.; Henry, R.; Lou, X.; Duerst, R.; Borchardt, T.; MacGillivray, L. Co-Crystals of Caffeine with Hydroxy- and Dihydroxy-Benzoic Acids Composed of up to Three Supramolecular Heterosynthons. *AAPS J.* 2007.

41. Friščić, T.; Fabian, L.; Burley, J. C.; Jones, W.; Motherwell, W. D. S. Exploring Cocrystal - Cocrystal Reactivity Via Liquid-Assisted Grinding: The Assembling of Racemic and Dismantling of Enantiomeric Cocrystals. *Chem. Comm.* 2006, 48, 5009-5011.

42. Bučar, D.-K.; Henry, R. F.; Lou, X.; Duerst, R. W.; Borchardt, T. B.; MacGillivray, L. R.; Zhang, G. G. Z. Co-Crystals of Caffeine and Hydroxy-2-Napthoic Acids: Unusual Formation of the Carboxylic Acid Dimer in the Presence of a Heterosynthon. *Mol. Pharm.* 2007, 4, 339-346.

43. Craven, B. M.; Gartland, G. L. The 2:1 Crystal Complex of 5,5-Diethylbarbituric Acid (Barbital) and Caffeine. *Acta Crystallogr.* 1974, B30, 1191-1195.

44. Ghosh, M.; Basak, A. K.; Mazumdar, S. K. Structure and Molecular Confirmation of the 1:1 Molecular Complex of Sulfaproxyline-Caffeine. *Acta Crystallogr.* 1991, C47, 577-580.

45. Remenar, J. F.; Morissette, S. L.; Peterson, M. L.; Moulton, B.; MacPhee, J. M.; Guzman, H. R.; Almarsson, O. Crystal Engineering of Novel Cocrystals of a Triazole Drug with 1,4-Dicarboxylic Acids. *J. Am. Chem. Soc.* 2003, 125, 8456-8457.

46. Vishweshwar, P.; McMahon, J. A.; Peterson, M. L.; Hickey, M. B.; Shattock, T. R.; Zaworotko, M. J. Crystal Engineering of Pharmaceutical Co-Crystals from Polymorphic Active Pharmaceutical Ingredients. *Chem. Comm.* 2005, 36, 4601-4603.

47. Zaitu, S.; Miwa, Y.; Taga, T. A 2:1 Molecular Complex of Theophylline and 5-Fluorouracil as the Monohydrate. *Acta Crystallogr.* 1995, C51, 1857-1859.

48. Nakao, S.; Fujii, S.; Sakai, T.; Tomita, K.-I. The Crystal and Molecular Structure of the 2:1 Molecular Complex of Theophylline with Phenobarbital. *Acta Crystallogr.* 1977, B33, 1373-1378.

49. Madarasz, J.; Bombicz, P.; Jarmi, K.; Ban, M.; Pokol, G.; Gal, S. Thermal Ftir and XRD Study on Some 1:1 Molecular Compounds of Theophylline. *J. Therm. Anal.*

Calorim. 2002, 69, 281-290.

50. Shefter, E.; Sackman, P. Structural Studies on Molecular Complexes V: Crystal Structures of Sulfathiazole - Sulfanilamide and Sulfathiazole - Theophylline Complexes. *J. Pharm. Sci.* 2006, 60, 282-286.

51. Caira, M. R.; Nassimbeni, L. R.; Wildervanck, A. F. Selective Formation of Hydrogen Bonded Cocrystals between Sulfonamide and Aromatic Carboxylic Acids in the Solid State. *J. Chem. Soc. Perkin Trans.* 1995, 2, 2213-2216.

52. Etter, M. C. Hydrogen Bonds as Design Elements in Organic Chemistry. *J. Phys. Chem.* 1991, 95, 4601 - 4610.

53. Etter, M. C.; Frankenbach, G. M. Hydrogen-Bond Directed Cocrystallization as a Tool for Designing Acentric Organic Solids. *Chem. Mater.* 1989, 1, 10-12.

54. Etter, M. C.; Frankenbach, G. M.; Adsmond, D. A. Using Hydrogen Bonds to Design Acentric Organic Materials for Nonlinear Optical Users. *Mol. Cryst. Liq. Cryst.* 1990, 187, 25-39.

55. Etter, M. C.; Reutzel, S. M. Hydrogen-Bond Directed Cocrystallization and Molecular Recognition Properties of Acyclic Imides. *J. Am. Chem. Soc.* 1991, 113, 2586-2598.

56. Donohue, J. The Hydrogen Bond in Organic Crystals. *J. Phys. Chem.* 1952, 56, 502-510.

57. Etter, M. C. Encoding and Decoding Hydrogen Bond Patterns of Organic Compounds. *Acc. Chem. Res.* 1990, 23, 120-126.

58. Etter, M. C. Aggregate Structures of Carboxylic Acids and Amides. *Israel J. Chem.* 1985, 25, 312-319.

59. Leiserowitz, L. Molecular Packing Modes. Carboxylic Acids. *Acta Crystallogr.* 1976, B32, 775-801.

60. Leiserowitz, L.; Schmidt, G. M. J. Molecular Packing Modes .3. Primary Amides. *J. Chem. Soc. A.* 1969, 16, 2372.

61. Lang, M.; Kampf, J. W.; Matzger, A. J. Form IV of Carbamazepine. *J. Pharm. Sci.* 2002, 91, 1186-1190.

62. Grzesiak, A.; Lang, M.; Kim, K.; Matzger, A. J. Comparison of the Four Anhydrous Polymorphs of Carbamazepine and the Crystal Structure of Form I. *J. Pharm. Sci.* 2003, 92, 2260-2271.

63. Harris, R. K.; Ghi, P. Y.; Puschmann, H.; Apperley, D. C.; Griesser, U. J.; Hammond, R. B.; Ma, C.; Roberts, K. J.; Pearce, G. J.; Yates, J. R.; Pickard, C. J. Structural Studies of the Polymorphs of Carbamazepine, Its Dihydrate, and Two Solvates. *Org. Process Res.Dev.* 2005, 9, 902 - 910.

64. Babu, N. J.; Reddy, L. S.; Nangia, A. Amide-N-Oxide Heterosynthon and Amide Dimer Homosynthon in Cocrystals of Carboxamide Drugs and Pyridine N-Oxides. *Mol. Pharm.* 2007, 4, 417-434.

65. Ebisuzaki, Y.; Boyle, P. D.; Smith, J. A. Methylxanthines .1. Anhydrous Theophylline. *Acta Crystallogr.* 1997, 53, 777-779.

66. Rodríguez-Spong, B. Enhancing the Pharmaceutical Behavior of Poorly Soluble Drugs through the Formation of Cocrystals and Mesophases. Ph.D. Thesis. University of Michigan, 2005.

67. Behme, R. J.; Brooke, D. Heat of Fusion Measurement of a Low Melting Polymorph of Carbamazepine That Undergoes Multiple-Phase Changes During Differential Scanning Calorimetry Analysis. *J. Pharm. Sci.* 1991, 80, 986-990.

68. Dong, J.-X.; Li, Q.; Tan, Z.-C.; Zhang, Z.-H.; Liu, Y. The Standard Molar Enthalpy of Formation, Molar Heat Capacities, and Thermal Stability of Anhydrous Caffeine. *J. Chem. Thermodyn.* 2007, 39, 108-114.

69. Hino, T.; Ford, J. L.; Powell, M. W. Assessment of Nicotinamide Polymorphs by Differential Scanning Calorimetry. *Thermochim. Acta.* 2001, 374, 85-92.

70. Rodríguez-Spong, B.; Zocharski, P.; Billups, J.; McMahon, J.; Zaworotko, M. J.; Rodríguez-Hornedo, N. Enhancing the Pharmaceutical Behavior of Carbamazepine through the Formation of Cocrystals. *AAPS J.* 2003, 5, Abstract M1298.

71. Zhang, G. G. Z.; Gu, C.; Zell, M. T.; Burkhardt, R. T.; Munson, E. J.; Grant, D. J. W. Crystallization and Transitions of Sulfamerazine Polymorphs. *J. Pharm. Sci.* 2002, 91, 1089-1100.

72. Basavoju, S.; Bostrom, D.; Velaga, S. P. Indomethacin-Saccharin Cocrystal: Design, Synthesis and Preliminary Pharmaceutical Characterization. *Pharm. Res.* 2008, 25, 530-541.

73. Childs, S. L.; Chyall, L. J.; Dunlap, J. T.; Smolenskaya, V. N.; Stahly, B. C.; Stahly, P. G. Crystal Engineering Approach to Forming Cocrystals of Amine Hydrochlorides with Organic Acids. Molecular Complexes of Fluoxetine Hydrochloride with Benzoic, Succinic, and Fumaric Acids. *J. Am. Chem. Soc.* 2004, 126, 13335-13342.

74. Nehm, S. J.; Rodríguez-Spong, B.; Rodríguez-Hornedo, N. Phase Solubility

Diagrams of Cocrystals Are Explained by Solubility Product and Solution Complexation. *Cryst. Growth Des.* 2006, 6, 592-600.

75. Reddy, L. S.; Bethune, S. J.; Kampf, J. W.; Rodríguez-Hornedo, N. Cocrystals and Salts of Gabapentin: Ph Dependent Cocrystal Stability and Solubility. *Cryst. Growth Des.* 2008, accepted.

76. Rodríguez-Hornedo, N.; Nehm, S. J.; Seefeldt, K. F.; Pagán-Torres, Y.; Falkiewicz, C. J. Reaction Crystallization of Pharmaceutical Molecular Complexes. *Mol. Pharm.* 2006, 3, 362-367.

77. Berry, D. J.; Seaton, C. C.; Clegg, W.; Harrington, R. W.; Coles, S. J.; Horton, P. N.; Hursthouse, M. B.; Storey, R.; Jones, W.; Friščić, T.; Blagden, N. Applying Hot-Stage Microscopy to Co-Crystal Screening: A Study of Nicotinamide with Seven Active Pharmaceutical Ingredients. *Cryst. Growth Des.* 2008, 8, 1697-1712.

78. Etter, M. C.; Reutzel, S. M.; Choo, C. G. Self-Organization of Adenine and Thymine in the Solid State. *J. Am. Chem. Soc.* 1993, 115, 4411-4412.

79. Pedireddi, V. R.; Jones, W.; Chorlton, A. P.; Docherty, R. Creation of Crystalline Supramolecular Arrays: A Comparison of Co-Crystal Formation from Solution and by Solid State Grinding. *Chem. Comm.* 1996, 8, 987-988.

80. Trask, A.; Jones, W. Crystal Engineering of Organic Cocrystals by the Solid-State Grinding Approach. *Top. Curr. Chem.* 2005, 254, 41-70.

81. Friščić, T.; Trask, A. V.; Jones, W.; Motherwell, W. D. S. Screening for Inclusion Compounds and Systematic Construction of Three Component Solids by Liquid Assisted Grinding. *Angew. Chem. Int. Ed.* 2006, 45, 7546-7550.

82. Trask, A. V.; Motherwell, W. D. S.; Jones, W. Solvent-Drop Grinding: Green Polymorph Control of Cocrystallisation. *Chem. Comm.* 2004, 7, 890-891.

83. Shan, N.; Toda, F.; Jones, W. Mechanochemistry and Co-Crystal Formation: Effect of Solvent on Reaction Kinetics. *Chem. Comm.* 2002, 2372-2373.

84. Trask, A. V.; vandeStreek, J.; Motherwell, W. D. S.; Jones, W. Achieving Polymorphic and Stoichiometric Diversity in Cocrystal Formation: Importance of Solid-State Grinding, Powder X-Ray Structure Determination, and Seeding. *Cryst. Growth Des.* 2005, 5, 2233-2241.

85. Bak, A.; Gore, A.; Yanez, E.; Stanton, M.; Tufekcic, S.; Syed, R.; Akrami, A.; Rose, M.; Surapaneni, S.; Bostick, T.; King, A.; Neervannan, S.; Ostovic, D.; Koparkar, A. The Co-Crystal Approach to Improve the Exposure of a Water Insoluble Compounds: AMG 517 Sorbic Acid Co-Crystal Characterization and Pharmacokinetics. *J. Pharm. Sci.* 2008, 97, 3942-3956.

86. Fernandes, P.; Bardin, J.; Johnston, A.; Florence, A. J.; Leech, C. K.; David, W. I. F.; Shankland, K. Carbamazepine Trifluoroacetic Acid Solvate. *Acta Crystallogr.* 2007, E63, O4269-U2927.

87. Johnston, A.; Florence, A. J.; Fernandes, P.; Shankland, A.; Kennedy, A. R. 10,11-Dihydrocarbamazepine-Form-Amide Solvate (1/1) *Acta Crystallogr. B.* 2007, E63, O3888-U3750.

88. Lowes, M. M. J.; Caira, M. R.; Lotter, A. P.; Vanderwatt, J. G. Physicochemical Properties and X-Ray Structural Studies of the Trigonal Polymorph of Carbamazepine. *J. Pharm. Sci.* 1987, 76, 744-752.

89. Seefeldt, K. J.; Miller, J.; Alvarez-Núñez, F.; Rodríguez-Hornedo, N. Crystallization Pathways and Kinetics of Carbamazepine-Nicotinamide Cocrystals from the Amorphous State by in Situ Thermomicroscopy, Spectroscopy and Calorimetry Studies *J. Pharm. Sci.* 2007, 96, 1147-1158.

90. Porter III, W. W.; Elie, S. C.; Matzger, A. J. Polymorphism in Carbamazepine Cocrystals. *Cryst. Growth Des.* 2008, 8, 14-16.

91. Coffman, R. E.; Kildsig, D. O. Hydrotropic Solubilization - Mechanistic Studies. *Pharm. Res.* 1996, 13, 1460-1463.

92. Hussain, M. A.; DiLuccio, R. C.; Maurin, M. B. Complexation of Moricizine with Nicotinamide and Evaluation of the Complexation Constants by Various Methods. *J. Pharm. Sci.* 1993, 82, 77-79.

93. Rasool, A. A.; Hussain, A. A.; Dittert, L. W. Solubility Enhancement of Some Water-Insoluble Drugs in the Presence of Nicotinamide and Related Compounds. *J. Pharm. Sci.* 1991, 80, 387-393.

94. Gracin, S.; Rasmuson, Å. C. Polymorphism and Crystallization of P- Aminobenzoic Acid *Cryst. Growth Des.* 2004, 4, 1013-1023.

95. O'Neil, M. J., *The Merck Index*. 13th Merck & Co., Inc: New Jersey, 2001; p.

96. Zubair, M. U.; Hassan, M. M. A. Saccharin. In *Analytical Profiles of Drug Substances*, ed.; Florey, K., Eds.; Academic Press: Orlando, Florida, 1984; pp 487-519.

97. Robinson, R. A.; Biggs, A. I. The Ionization Constants of P-Aminobenzoic Acid in Aqueous Solutions at 25c. *Aust. J. Chem.* 1956, 10, 128-134.

98. Suzuki, E.; Shimomura, K.; Sekiguchi, K. Thermochemical Study of Theophylline and Its Hydrate. *Chem. Pharm. Bull.* 1989, 37, 493-497.

99. Sun, C.; Zhou, D.; Grant, D. J. W.; Jr, V. G. Y. Theophylline Monohydrate. *Acta Crystallogr.* 2002, E58, 368-370.

100. Li, Y.; Chow, P. S.; Tan, R. B. H.; Black, S. N. Effect of Water Activity on the Transformation between Hydrate and Anhydrate of Carbamazepine. *Org. Process Res. Dev.* 2008, 12, 264-270.

101. Ticehurst, M. D.; Storey, R. A.; Watt, C. Application of Slurry Bridging Experiments at Controlled Water Activities to Predict the Solid-State Conversion between Anhydrous and Hydrated Forms Using Theophylline as a Model Drug. *Int. J. Pharm.* 2002, 247, 1-10.

102. Ross, K. D. Estimation of Water Activity in Intermediate Moisture Foods. *Food Tech.* 1975, 29, 26-34.

103. Peng, C.; Chow, A. H. L.; Chan, C. K. Hygroscopic Study of Glucose, Citric Acid, and Sorbitol Using an Electrodynamic Balance: Comparison with Unifac Predictions. *Aerosol Sci. Tech.* 2001, 35, 753-758.

CHAPTER II

THE ROLE OF COCRYSTAL AND SOLUTION CHEMISTRY ON THE FORMATION AND STABILITY OF COCRYSTALS WITH DIFFERENT STOICHIOMETRY

Introduction

Achieving the desired bioavailability is the ultimate goal and a major challenge in drug development. One of the significant ways to achieve this is by generating different crystalline or amorphous forms of an API with a range of physicochemical and pharmaceutical properties.[1-8] Screening for API cocrystals, salts, polymorphs, solvates, hydrates, and amorphous phases with desirable properties is therefore an active and routine procedure in drug discovery and development.[9-14] Cocrystal design based on crystal engineering principles and strategies enables modulation of API properties such as solubility, dissolution rates, physical and chemical stability, and mechanical properties.[15-21]

The number of API cocrystals continues to increase and for some drugs as many as 40 to 50 cocrystals are reported.[15, 19-27] Fifty cocrystals of piroxicam and about 40 for carbamazepine have been discovered.[10, 22, 25-27] API cocrystals of different stoichiometries with the same components have also been reported and are usually discovered by different crystallization processes or solvents.[19, 28] A key question is *what factors dictate the formation of cocrystals with different stoichiometry by solution-mediated processes?*

Efforts to enhance the success and efficiency of cocrystal screening methods have received considerable attention.[9, 10, 12, 29] However, relatively less is known about the factors affecting cocrystal formation and thermodynamic stability.[30, 31] Understanding the mechanisms and kinetics of cocrystallization, as well as the factors affecting cocrystal stability, is essential to control synthesis and phase transformations.[32-35] This contribution aims to identify the factors that affect the solution-mediated formation of cocrystals with different stoichiometry by examining the role of cocrystal and solution chemistry on crystallization and phase stability.

Carbamazepine−4-aminobenzoic acid (CBZ−4ABA) was studied as a model system. A 2:1 cocrystal has been reported.[27] Herein, we report the discovery of a 1:1 CBZ−4ABA cocrystal. Both cocrystals can be prepared by reaction crystallization method (RCM) by varying solution concentration of reactants. The relative thermodynamic stability and solubility of the two cocrystals and the crystalline drug are examined as a function of ligand (4ABA) solution concentration. Previous studies with carbamazepine-nicotinamide and carbamazepine-succinic acid cocrystals have shown that cocrystal solubility and stability are described by mathematical models based on solution complexation and solubility product behavior.[10, 30] In the current study this approach has been extended to: (i) develop models that describe the solubilities of cocrystals with different stoichiometry, (ii) generate phase diagrams that show crystallization and stability domains of various phases, and (iii) identify key parameters to determine the stability domains of cocrystals. Results from these studies are applicable for improving the success and efficiency of cocrystal screening and synthesis, as well as

to anticipate conditions under which process-induced transformation can lead to cocrystal formation or instability.

Experimental section

Materials

Anhydrous monoclinic form III carbamazepine (CBZ(III)) and α-form of 4-aminobenzoic acid (4ABA) were obtained from Sigma-Aldrich and were used as received. Both compounds were characterized by X-ray powder diffraction (XRPD) and Raman spectroscopy before carrying out experiments. Ethanol, obtained from Fisher Scientific, was dried using molecular sieves prior to use.

Methods

Cocrystal synthesis

1:1 and 2:1 carbamazepine−4-aminobenzoic acid cocrystals were synthesized using the reaction crystallization method[10, 31]. X-ray quality single crystals of 1:1 cocrystal were grown by slow evaporation of solvent.

Single crystal of 1:1 CBZ−4ABA cocrystal: A mixture of 100 mg (0.0042 mol) of CBZ (III) and 581.5 mg (0.042 mol) of 4ABA was dissolved in 5 ml ethanol. Slow evaporation of ethanol at room temperature yielded single crystals of the 1:1 cocrystal. The crystals were characterized by Raman microscopy prior to solving the crystal structure.

Reaction crystallization method for 2:1 and 1:1 cocrystal synthesis: The 2:1 cocrystal was prepared by suspending 200 mg of CBZ(III) in 3.25g of 0.6m 4ABA ethanolic solution. The 1:1 cocrystal was prepared by suspending 200 mg of CBZ(III) in

saturated 4ABA suspension. The suspensions were magnetically stirred at room temperature for 12 hours and the solid phases recovered after filtration was characterized by XRPD and Raman spectroscopy. XRPD patterns were compared with the simulated patterns of 2:1 and 1:1 cocrystal to confirm that the solid phases were pure cocrystals. Simulated XRPD pattern of 2:1 cocrystal was obtained from the crystal structure database (CSD Refcode: XAQRAJ) and that of the 1:1 cocrystal was obtained by solving the crystal structure.

CBZ(III)and cocrystal stability studies

CBZ(III) stability as a function of ligand concentration was studied by suspending 200mg CBZ(III) in 2ml of 0.1m, 0.6m and saturated 4ABA solution with excess solid 4ABA. All suspensions were magnetically stirred for 48-96 hours at 25 ºC and the solid phases were characterized by Raman spectroscopy and X-ray powder diffraction (XRPD).

The stability of 2:1 and/or 1:1 cocrystals in methanol, ethanol, isopropyl alcohol, acetonitrile, chloroform and water was studied by suspending 200mg of cocrystal in 2-3ml of organic solvent or water. The suspension was stirred magnetically at 25 °C for 2–7 days and the solid phases were characterized by XRPD. Transformation and stability of cocrystals in ethanol was also monitored in real-time by Raman spectroscopy.

Transition concentration measurement

Three transition concentrations or isothermal invariant points (c_1, c_2, and c_3) were identified for the CBZ−4ABA cocrystals in ethanol at 25˚C. The transition concentration

(c_1) for CBZ(III) and 2:1 cocrystal was determined by measuring reactant concentrations (CBZ and 4ABA) in ethanol saturated with CBZ(III) and 2:1 cocrystal. Saturation with respect to the two crystalline phases was achieved by suspending CBZ(III) in 0.12m and 0.5m 4ABA in ethanol. 2:1 cocrystal was added to the suspensions after 24 hours. The suspensions were allowed to reach equilibrium by magnetically stirring at 25°C. Solid phase and solution concentration were monitored. The equilibrium was considered to be achieved when solution concentrations reached a steady value while two solid phases coexist. The solid phases in suspension were characterized by Raman spectroscopy. Solutions were analyzed by HPLC for CBZ concentration and 4ABA concentration was determined by gravimetric method. The suspensions were filtered and the solid phases were characterized by XRPD.

The transition concentration c_2 was determined by saturating ethanol with 2:1 and 1:1 cocrystals. This was achieved by adding excess 2:1 and 1:1 cocrystals to 1.1m 4ABA. c_3 was determined by saturating ethanol with 1:1 cocrystal and 4ABA. The procedures for analysis of solid and liquid phases were similar to those described above.

Solubility studies

2:1 Carbamazepine−4-aminobenzoic acid cocrystal: Cocrystal solubility studies as a function of ligand (4ABA) concentration were performed by suspending excess 2:1 cocrystal in solutions of ethanol with varying ligand concentrations. The suspensions were allowed to reach equilibrium while magnetically stirring at 25 °C. Aliquots of solutions were withdrawn after 48, 70 and 90 hours using a syringe fitted with a 0.45µ PTFE filter. The solutions were diluted as needed and analyzed by HPLC to determine

the equilibrium concentration of CBZ. All the samples attained equilibrium by 70 hours. The equilibrium concentration of 4ABA in solution was then determined by mass balance. The solid phases at equilibrium were characterized by XRPD.

Carbamazepine (CBZ(III)): The solubility dependence of CBZ(III) on ligand (4ABA) concentration was determined by suspending excess drug in varying concentrations of the ligand in ethanol at 25˚C. The equilibrium concentration of the drug was determined using a procedure similar to that described for the 2:1 cocrystal. The solid phases at equilibrium were characterized by XRPD.

4-Aminobenzoic acid (4ABA): The solubility of 4ABA was determined by suspending excess 4ABA in ethanol. The suspension was allowed to reach equilibrium while magnetically stirring at 25°C. The equilibrium concentration of 4ABA in the solution was then determined using a gravimetric approach. The solid phase at equilibrium was characterized by XRPD.

Raman spectroscopy

Raman spectra was collected using a RXN1 Raman spectrometer equipped with an immersion probe or a Raman microprobe from Kaiser Optical Systems Inc., Ann Arbor, MI. Spectra were collected using 10 exposures and 1-3 accumulations using the vendor supplied Holograms software.

X-ray Diffraction

Powder: A bench top Rigaku Miniflex X-ray powder Diffractometer (Danvers, MA) using Cu Kα radiation (λ = 1.54Å), a tube voltage of 30kV, and a tube current of 15mA

was used to collect XRPD patterns of solid phases. Data was collected from 2˚ to 40˚ at a continuous scan rate of 2.5 deg/min.

Single crystal: Single crystal X-ray diffraction data for 1:1 cocrystal was collected on a Bruker SMART APEX CCD-based X-ray diffractometer (Mo Kα radiation, λ = 0.71073 Å) equipped with a low temperature device. Empirical absorption corrections using SADABS[36] were applied. Structure solution and refinement were performed with SHELXTL[37]. All non-hydrogen atoms were refined anisotropically with the hydrogen atoms placed in idealized positions except for those involved in hydrogen bonding which were allowed to refine isotropically.

High Performance Liquid Chromatography (HPLC)

A Waters system (Milford, MA) equipped with a 5µm C18 Atlantis column (4.6 x 250mm; Waters, Milford, MA) and UV/Vis detector was used to measure CBZ concentrations. The concentrations were measured using an isocratic method. Mobile phase consisting of 55% methanol and 0.1% trifluoroacetic acid in water was flowed through the column at 1ml/min. 20µL of samples was injected into the column and the absorbance of CBZ was monitored at 284nm. Data collection and processing was performed using the vendor provided Empower software.

Results

Crystal structure of 1:1 CBZ−4ABA

A 1:1 cocrystal of CBZ−4ABA was discovered by reaction crystallization method at high ligand concentrations in ethanol. Crystal structure analysis reveals an unexpected hydrogen bond pattern with carboxylic acid···acid and amide···amide homosynthons of 4ABA and CBZ (figure 2.1). The carboxamide dimer is not replaced by the frequently occurring amide-carboxylic acid dimer.[27, 38-40] As shown in figure 2.1, cyclic homodimers are linked by N–H···O hydrogen bonds between amine N–H donor and amide carbonyl acceptor to form a one dimensional tape. The anti N–H of amide group is not involved in any strong hydrogen bonding. Table 2.1 summarizes the crystallographic properties of 1:1 cocrystal. Figure 2.2 compares the simulated and experimental XRPD patterns of the 1:1 cocrystal.

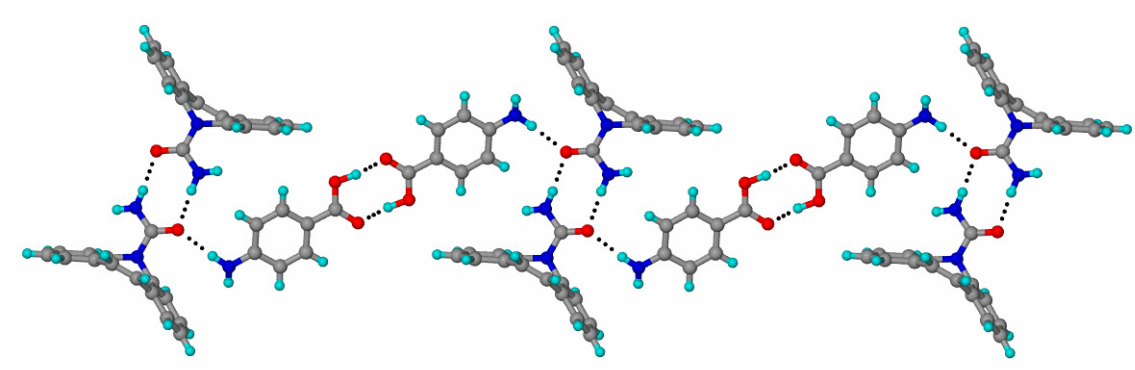

Figure 2.1: Amide···amide and acid···acid homosynthons in the crystal structure of 1:1 CBZ−4ABA cocrystal.

Table 2.1: Crystallographic data of 1:1 CBZ-4ABA cocrystal

Formula	$C_{22}H_{19}N_3O_3$
Formula weight	373.4
Crystal system	Monoclinic
Space group	$P2_1/n$
a (Å)	5.1909(4)
b (Å)	18.4126(13)
c (Å)	19.0481(14)
B (degrees)	97.7740(10)
V (Å^3)	1803.8(2)
Z	4
ρ_{cal} (g cm^{-3})	1.375
T (K)	85(2)
μ (mm^{-1})	0.093
$R1$	0.0460
$wR2$	0.1093
goodness-of-fit	1.058

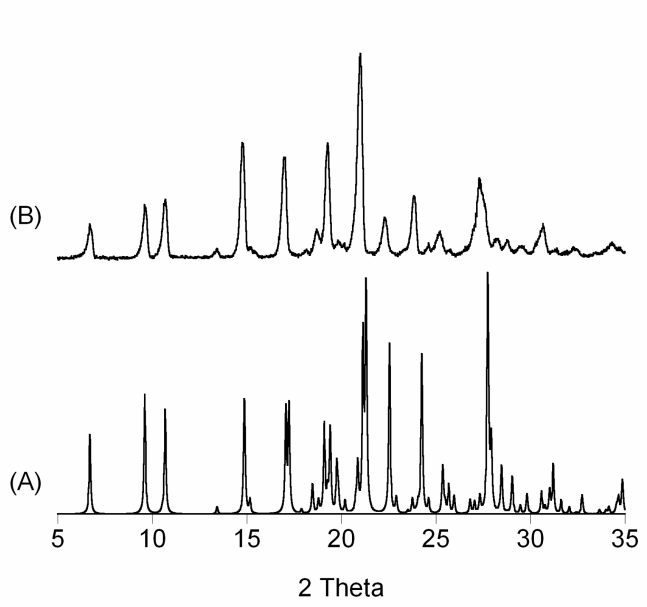

Figure 2.2: Comparison of (A) simulated, and (B) experimental XRPD patterns of 1:1 cocrystal.

Cocrystal formation and stability

Transformation of crystalline drug (CBZ(III)) to cocrystal (1:1 or 2:1) is dependent on the ligand (4ABA) concentration. The transformation was examined by slurrying CBZ(III) at three levels of ligand concentrations - 0.1m 4ABA, 0.6m 4ABA and in 4ABA suspension (saturated 4ABA solution with excess 4ABA solid). Figure 2.3 shows the XRPD patterns of solid phases recovered from these studies. The powder patterns indicate that CBZ(III) is stable in 0.1m 4ABA but transforms to 2:1 cocrystal in 0.6m 4ABA or to 1:1 cocrystal in solution saturated with 4ABA.

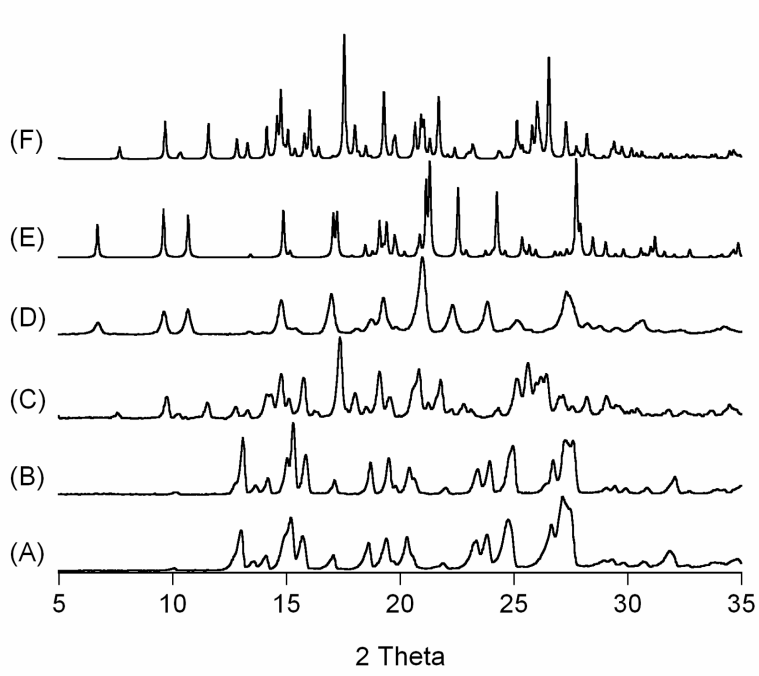

Figure 2.3: XRPD patterns showing ligand concentration dependent transformation of (A) CBZ(III) in (B) 0.1m 4ABA, (C) 0.6m 4ABA, and (D) 4ABA suspension; simulated XRPD patterns of (E) 1:1 cocrystal and (F) 2:1 cocrystal are shown as references.

Cocrystal stability studies in neat ethanol or water indicate that both cocrystals are unstable. In water, both cocrystals transform to 2:1 cocrystal hydrate indicating that cocrystal hydrate is less soluble than the anhydrous cocrystals (appendix A). In ethanol, the 2:1 cocrystal transforms to CBZ(III) while the 1:1 cocrystal transforms to 2:1 cocrystal (Figure 2.4). Figure 2.5 shows the Raman spectra acquired at different times during 1:1 cocrystal transformation in ethanol. The 1:1 cocrystal transforms to CBZ(III) and then to 2:1 cocrystal suggesting that the 1:1 cocrystal is more soluble than CBZ(III) and 2:1 cocrystal in ethanol. Peaks corresponding to these transformations are observed at 266 cm^{-1} for 1:1 cocrystal, 252 cm^{-1} for CBZ(III), and 259 cm^{-1} for 2:1 cocrystal.

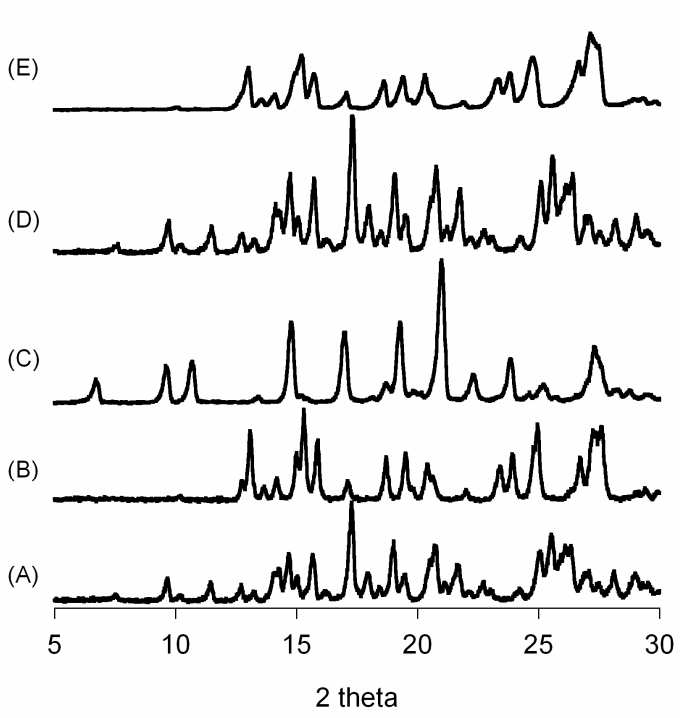

Figure 2.4: XRPD patterns indicating cocrystal instability in ethanol; 2:1 cocrystal (A) before slurrying, and (B) after slurrying in ethanol; 1:1 cocrystal (C) before slurrying, and (D) after slurrying in ethanol; (E) reference pattern of CBZ(III).

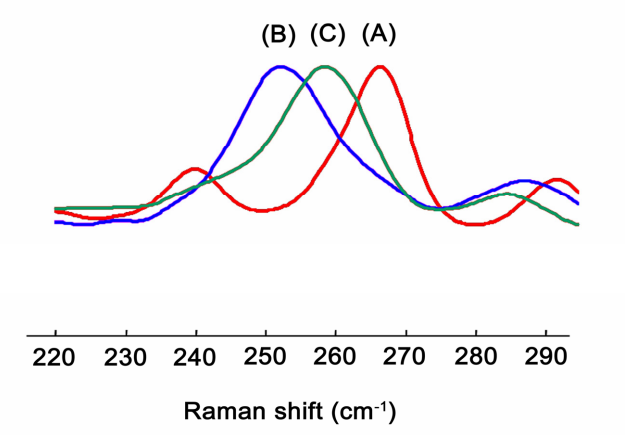

Figure 2.5: Raman spectra showing transformation of 1:1 cocrystal in ethanol (A) before slurrying, (B) after 1 minute showing transformation to CBZ(III), and (C) after 5 minutes indicating transformation to 2:1 cocrystal.

The stability of the cocrystals was also examined in other organic solvents. Table 2.2 summarizes the results from stability studies in various solvents. XRPD patterns of the solid phases from the stability studies are included in appendix A.

Table 2.2: Cocrystal stability in various solvents.

Solvent	2:1 cocrystal	1:1 cocrystal
Water	Unstable, transforms to cocrystal hydrate	Unstable, transforms to cocrystal hydrate
Ethanol	Unstable, transforms to CBZ(III)	Unstable, transforms to 2:1 cocrystal
Methanol	Unstable, transforms to CBZ(III)	Unstable, transforms to 2:1 cocrystal
IPA	Unstable, transforms to CBZ(III)	-
Acetonitrile	Stable	-
Chloroform	Unstable, transforms to 4ABA	Unstable, transforms to 4ABA

Results from stability studies in ethanol show that cocrystal formation and stability depend on the ligand concentration. Previous studies with CBZ-nicotinamide cocrystal in organic solvents and CBZ−Succinic acid cocrystal in water have shown similar dependence of drug and cocrystal stability on ligand concentration.[10, 30] The transformation of drug to cocrystal at high ligand concentrations is due to lower solubility of cocrystal relative to the crystalline drug, whereas the drug is least soluble and most stable phase at low ligand concentrations. This change in the relative order of solubility and stability of the crystalline phases with increasing ligand concentration gives rise to the transition concentration (C_{tr}), at which two solid phases are in equilibrium with the solution.[10, 30, 31] Since there are three components (API, ligand and solvent) and three phases (2 solid phases and liquid) at a fixed temperature and pressure, phase rule dictates that C_{tr} is an invariant point. Thus, based on the results from CBZ(III) and CBZ−4ABA cocrystal stability studies in ethanol (figures 2.3, 2.4 and 2.5), there must be invariant points at which CBZ(III)/2:1 cocrystal and 2:1 cocrystal/1:1 cocrystal are in equilibrium with the solution.

Phase diagrams representing the solution compositions in equilibrium with the drug or cocrystal phases indicate that the transition concentration is a useful parameter to identify cocrystal stability domains.[10, 30, 31] The stability domains of the two CBZ−4ABA cocrystals were identified by measuring the transition concentrations as described below.

Transition concentrations

Table 2.3 summarizes the transition concentrations or invariant points and the solid phases that coexist in equilibrium with the solution. From the invariant points, the stability domains of the different crystalline phases can be determined. The 2:1 cocrystal is stable at reactant concentrations between c_1 and c_2, while the 1:1 cocrystal is stable between c_2 and c_3. CBZ(III) is the stable phase at reactant concentrations below c_1, while 4ABA is stable above c_3.

Table 2.3: Solid phases and reactant concentrations at the invariant points for CBZ−4ABA−Ethanol system at 25 ˚C

Invariant point	Solid phases at equilibrium	[CBZ] (m)[a]	[4ABA] (m)[a]
c_1	CBZ(III), 2:1 cocrystal	0.150±0.005	0.168±0.004
c_2	2:1 cocrystal, 1:1 cocrystal	0.093±0.001	1.144±0.013
c_3	1:1 cocrystal, 4ABA	0.096±0.002	1.280±0.040

[a] Concentrations are the mean ± standard deviation

Reactant concentrations at the invariant points can also be used to identify trends in the solubility dependence of the crystalline phases on ligand concentration. Examination of the reactant concentration at the invariant points indicates that CBZ concentration at c_1 is higher than CBZ(III) solubility in ethanol (0.125m). This suggests an increase in CBZ(III) solubility with 4ABA concentration possibly due to solution complexation. Further, CBZ concentration at c_2 is less than that at c_1 suggesting a decrease in 2:1 cocrystal solubility with increase in 4ABA concentration. Similar results have been shown for other cocrystalline systems.[10, 30]

Phase solubility and triangular phase diagrams

The solubilities of the two CBZ−4ABA cocrystals and CBZ(III) crystal were measured as a function of 4ABA concentration. These results, along with the reactant concentrations at the invariant points, were used to generate phase solubility and triangular phase diagrams. The phase solubility diagram (PSD) shows the reactant concentrations in solution at equilibrium with the different solid phases-crystalline drug, cocrystal and ligand. The reactant concentrations are usually in molarity or molality. The PSD is useful for determining the solubility dependence of the phases on solution composition, and for studying solution complexation.[30, 41] Unlike the PSD, the triangular phase diagram (TPD) shows the total composition of the system, including that in the solid and liquid phases.[10, 42]

Figure 2.6 presents the PSD for the CBZ−4ABA−Ethanol system. The PSD shows the CBZ concentration dependence on 4ABA when CBZ(III), 2:1 cocrystal, 1:1 cocrystal, or 4ABA are in equilibrium with the solution. The concentrations of the drug and ligand in solution are expressed as analytical or total concentrations measured at equilibrium, $[CBZ]_T$ and $[4ABA]_T$. This concentration is the sum of the concentrations of unbound (free) and bound reactant in solution. Symbols in figure 2.6 represent experimental data from solubility studies of CBZ(III), 2:1 cocrystal and 1:1 cocrystal performed as a function of 4ABA concentration. The solid lines ac_1, c_1c_2, and c_2c_3 are the predicted solubilities of CBZ(III), 2:1 cocrystal and 1:1 cocrystal, respectively. The predictions are made using mathematical models described in a later section.

From the PSD, it is evident that the solubility of the different crystalline phases is dependent on ligand concentration. The solubility of CBZ(III) increases while that of the cocrystals decreases with increasing 4ABA concentration. The solubility curves intersect at the invariant points (c_1, c_2, or c_3) where two solid phases coexist in equilibrium with the solution. Thus the PSD shows the stability domains for the different phases and the solution concentrations. The solubility of the cocrystals in neat ethanol is given by the intersection of the cocrystal solubility curves with the stoichiometric lines, 1:1 or 2:1. It is evident that in neat ethanol, the 2:1 cocrystal will transform to CBZ(III) and the 1:1 cocrystal will transform to 2:1 cocrystal. This is in agreement with results of cocrystal stability studies in ethanol (figures 2.4 and 2.5).

The solubilities and stability domains of the different crystalline phases are also represented on a triangular phase diagram (TPD) as shown in figure 2.7. The solubility of CBZ(III), 2:1 cocrystal, 1:1 cocrystal and 4ABA, in mass fractions, are represented by the curves ac_1, c_1c_2, c_2c_3, and c_3b, respectively. The stability domain of CBZ(III), 2:1 cocrystal, 1:1 cocrystal and 4ABA are represented by regions 1, 2, 3 and 4, respectively. Regions 5, 6, and 7 represent regions where two solid phases are in equilibrium with the solution - CBZ(III)/2:1 cocrystal in region 5; 2:1 cocrystal/1:1 cocrystal in region 6; and 1:1 cocrystal/4ABA in region 7. The solution composition in regions 5, 6, and 7 correspond to the invariant points c_1, c_2, and c_3, respectively.

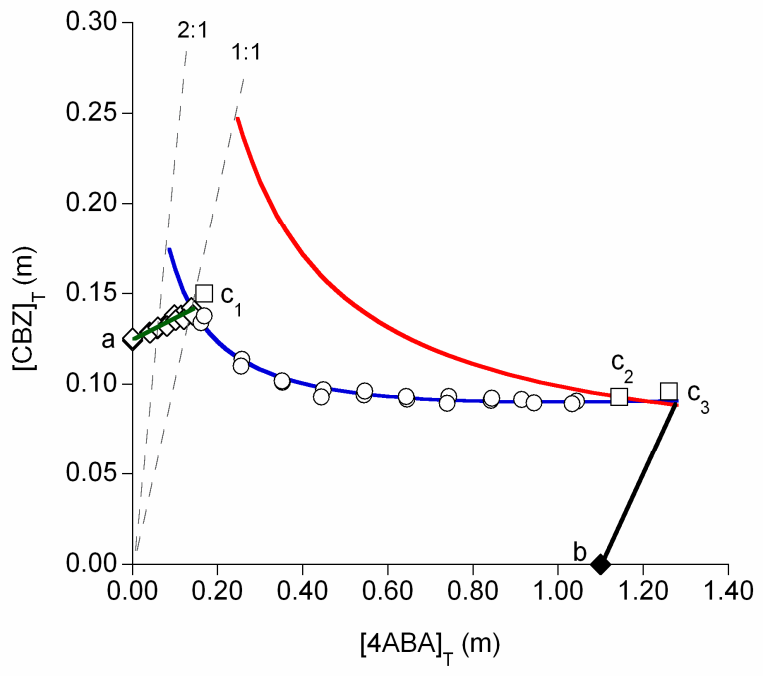

Figure 2.6: Phase solubility diagram for CBZ−4ABA−Ethanol system at 25˚C showing reactant solution concentrations ($[CBZ]_T$ and $[4ABA]_T$) at equilibrium with CBZ(III) (◇), 2:1 cocrystal (○), or 4ABA (◆). Measured solubility of CBZ(III) and 4ABA in neat ethanol are indicated by the points 'a' and 'b', respectively. Invariant points c_1, c_2, and c_3 are represented by □. Dashed lines correspond to solution reactant stoichiometries equal to that of cocrystals. Predicted solubility dependence on ligand concentration for CBZ(III), 2:1 cocrystal and 1:1 cocrystal according to equations (10), (5) and (12) are represented by green, blue and red solid lines, respectively.

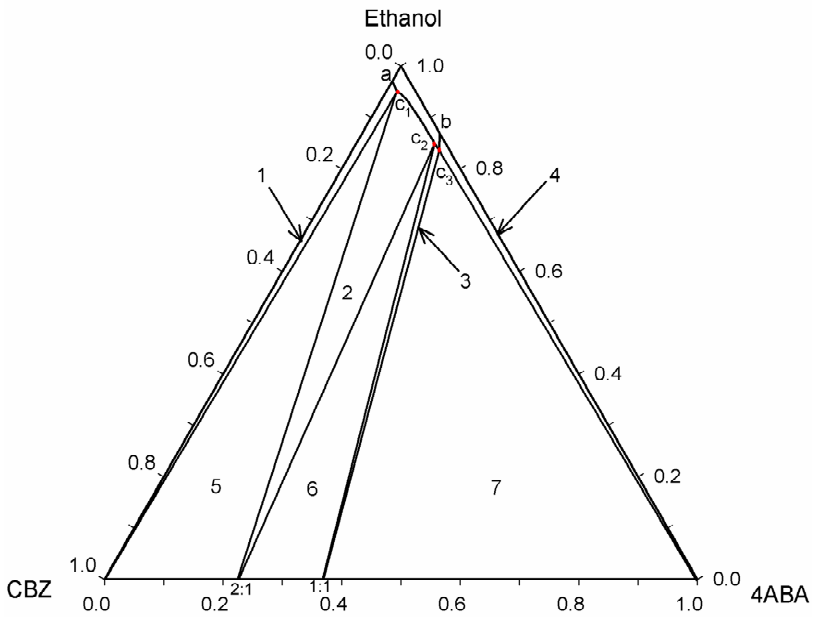

Figure 2.7: Triangular phase diagram for CBZ−4ABA-ethanol system at 25˚C generated from experimental and calculated solubilities. For clarity, each experimental value is not shown. c_1, c_2, and c_3 are the invariant points where the solubility curves intersect. Stability regions for different phases are as follows: 1 - CBZ(III), 2 – 2:1 cocrystal, 3 – 1:1 cocrystal, 4 – 4ABA, 5 – CBZ(III)/2:1 cocrystal, 6 – 2:1 cocrystal/1:1 cocrystal, and 7 – 1:1 cocrystal/4ABA. Compositions shown are on mass fraction basis.

Mathematical models predicting the solubility of cocrystals and drug

The phase diagrams presented in the previous section show that the solubilities of CBZ(III), 2:1 cocrystal and 1:1 cocrystal are dependent on ligand concentration. In this section, mathematical models predicting this dependence for the drug and the cocrystals will be presented. The models enable estimation of cocrystal solubility in pure solvents which are otherwise experimentally inaccessible due to cocrystal instability and transformation. Further, the models allow for prediction of solubility dependence on ligand concentration with a minimum number of experiments as will be illustrated for 1:1 CBA−4ABA cocrystal.

Models predicting 2:1 cocrystal solubility

For the 2:1 cocrystal, the solubility decreases with increase in ligand concentration between c_1 and c_2 (figure 2.6). Previous studies from our lab with other cocrystalline systems have shown that this dependence can be explained by the solubility product principle[10, 30]. Thus for a 2:1 cocrystal D_2L, where D is the drug and L is the ligand, the equilibrium reaction for cocrystal dissociation in solution is given as:

$$D_2L_{(solid)} \overset{K}{\rightleftharpoons} 2D_{(soln)} + L_{(soln)} \qquad (1)$$

where K is the equilibrium constant for the reaction and is given by

$$K = \frac{a_D^2 a_L}{a_{D_2L}}$$

a_D and a_L are the activities of D and L in solution, and a_{D2L} is the activity of the solid.

If the activity of the solid D_2L is equal to 1, the above relation yields the solubility product (K_{sp}) for the cocrystal:

$$K_{sp} = a_D^2 a_L$$

Under ideal conditions activities can be replaced with concentrations as follows:

$$K_{sp} = [D]^2[L] \quad (2)$$

For practical purposes henceforth, concentrations are used instead of activities.

If there is negligible solution complexation then the total or analytical reactant concentrations in solution are

$$[D]_T = [D] \text{ and } [L]_T = [L] \quad (3)$$

From equations (2) and (3):

$$[D]_T = \sqrt{\frac{K_{sp}}{[L]_T}} \quad (4)$$

Equation (4) predicts that the drug concentration ($[D]_T$) decreases with increase in ligand concentration ($[L]_T$) when the cocrystal is in equilibrium with the solution. Further, according to equation (4), a plot of $[D]_T$ against $\frac{1}{\sqrt{[L]_T}}$ must yield a straight line through the origin. The K_{sp} of the cocrystal can then be evaluated from the slope of the line. K_{sp} of the 2:1 cocrystal estimated in this manner is 8.4×10^{-4} m^3. This model however underpredicts the cocrystal solubility dependence on ligand concentration.

The cocrystal solubility model (equation 4) does not consider solution complexation which may explain why the model underpredicts cocrystal solubility. In fact, results from the current study show an increase in CBZ(III) solubility with 4ABA concentration suggesting solution complexation (figure 2.6). Solution complexation has

been shown to affect the solubility of crystal and cocrystal phases.[30, 41, 43] Models that describe 2:1 cocrystal solubility dependence on ligand concentrations were therefore developed by considering 1:1 and 2:1 solution complexation equilibria. These models along with the equilibrium reactions are shown in table 2.4.

Equations (5) – (9) in table 3 predict non-linear dependence of drug concentration on ligand concentration for the 2:1 cocrystal. Therefore the thermodynamic constants (K_{11}, K_{21}, and K_{sp}) can be evaluated by non-linear fit of the equations to the experimental data. Detailed derivations of equations (5) – (9) for the models presented, as well as the procedure for evaluating the constants, are included in appendix B.

Figure 2.8 shows the fit of models I, II and III to the experimental data. Models I and II give a better fit than model III. At low ligand concentrations model III overestimates the dependence, while at high ligand concentrations it underestimates the dependence. Table 2.5 summarizes the values of the thermodynamic constants, R^2 and F-values for models I − III. Based on the R^2 and F-value as well as the p-values for the constants, we note that the best fit is obtained with model II, equation (7). Further, we observe that the constants evaluated using equations (5) and (7) are similar and suggest negligible 2:1 solution complexation. Thus the 2:1 cocrystal solubility dependence on ligand concentration is explained by 1:1 solution complexation and equation (5) or (7) can be used to describe 2:1 cocrystal solubility. In addition to evaluating complexation constants from cocrystal solubility studies, complexation constants were also evaluated from CBZ(III) solubility studies as discussed below.

Table 2.4: Models based on cocrystal and solution chemistry to predict drug concentration dependence on ligand concentration for 2:1 cocrystal (D_2L).

Model	Complexation	Equilibrium reactions	[a]$[D]_T$ dependence on $[L]_T$	Equation
I	1:1 + 2:1	$D_2L_{(solid)} \overset{K_{sp}}{\rightleftharpoons} 2D_{(soln)} + L_{(soln)}$ $D_{(soln)} + L_{(soln)} \overset{K_{11}}{\rightleftharpoons} DL_{(soln)}$ $DL_{(soln)} + D_{(soln)} \overset{K_{21}}{\rightleftharpoons} D_2L_{(soln)}$	$[D]_T = \sqrt{\frac{K_{sp}}{A_1}} + K_{11}\sqrt{A_1 K_{sp}} + 2K_{21}K_{11}K_{sp}$ where, $A_1 = \left(2([L]_T - K_{11}K_{21}K_{sp}) + K_{11}^2 K_{sp} - 2K_{11}\sqrt{K_{sp}[L]_T}\right)/2$	5
			$[D]_T = \sqrt{\frac{K_{sp}}{A_2}} + K_{11}\sqrt{A_2 K_{sp}} + 2K_{21}K_{11}K_{sp}$ where, $A_2 = \left(2([L]_T - K_{11}K_{21}K_{sp}) + K_{11}^2 K_{sp} + 2K_{11}\sqrt{K_{sp}[L]_T}\right)/2$	6
II	1:1	$D_2L_{(solid)} \overset{K_{sp}}{\rightleftharpoons} 2D_{(soln)} + L_{(soln)}$ $D_{(soln)} + L_{(soln)} \overset{K_{11}}{\rightleftharpoons} DL_{(soln)}$	$[D]_T = \sqrt{\frac{K_{sp}}{A_1}} + K_{11}\sqrt{A_1 K_{sp}}$ where, $A_1 = \left(2[L]_T + K_{11}^2 K_{sp} - 2K_{11}\sqrt{K_{sp}[L]_T}\right)/2$	7
			$[D]_T = \sqrt{\frac{K_{sp}}{A_2}} + K_{11}\sqrt{A_2 K_{sp}}$ where, $A_2 = \left(2[L]_T + K_{11}^2 K_{sp} + 2K_{11}\sqrt{K_{sp}[L]_T}\right)/2$	8

Table 2.4 (continued)

Model	Complexation	Equilibrium reactions	[a][D]$_T$ dependence on [L]$_T$	Equation
III	2:1	$D_2L_{(solid)} \overset{K_{sp}}{\rightleftharpoons} 2D_{(soln)} + L_{(soln)}$ $2D_{(soln)} + L_{(soln)} \overset{K'_{21}}{\rightleftharpoons} D_2L_{(soln)}$	$[D]_T = \sqrt{\frac{K_{sp}}{[L]_T - K'_{21}K_{sp}}} + 2K'_{21}K_{sp}$	9

[a][D]$_T$ and [L]$_T$ are the analytical concentrations of the drug and ligand in equilibrium with the cocrystal.

Table 2.5: Complexation and solubility product constants evaluated from 2:1 cocrystal solubility studies.

Model	Complexation	Equation	K_{sp} (m^3)	K_{11} (m^{-1})	K_{21} (m^{-1})	K'_{21} (m^{-2})	R^2	F-value
I	1:1 + 2:1	5	$(1.95\pm0.60^{a,b})\times10^{-3}$	1.04±0.20	0.0 ± 5.0[c]	-	0.97	10773
		6	$(2.37\pm1.52)\times10^{-3}$**	0.84±0.20	0.0 ± 8.0[d]	-	0.96	7783
II	1:1	7	$(1.95\pm0.06)\times10^{-3}$	1.04±0.05	-	-	0.97	17109
		8	$(2.37\pm0.08)\times10^{-3}$	0.84±0.04	-	-	0.96	12362
III	2:1	9	$(6.3 \pm 0.9)\times10^{-4}$	-	-	49 ±10[e]	0.92	6560

[a]Standard error. [b] Statistically significant, $p < 0.05$. [c] Statistically insignificant, $p > 0.05$. [d] Statistically insignificant, $p > 0.05$.
[e]Statistically significant, $p < 0.05$. ** Statistically insignificant, $p > 0.05$

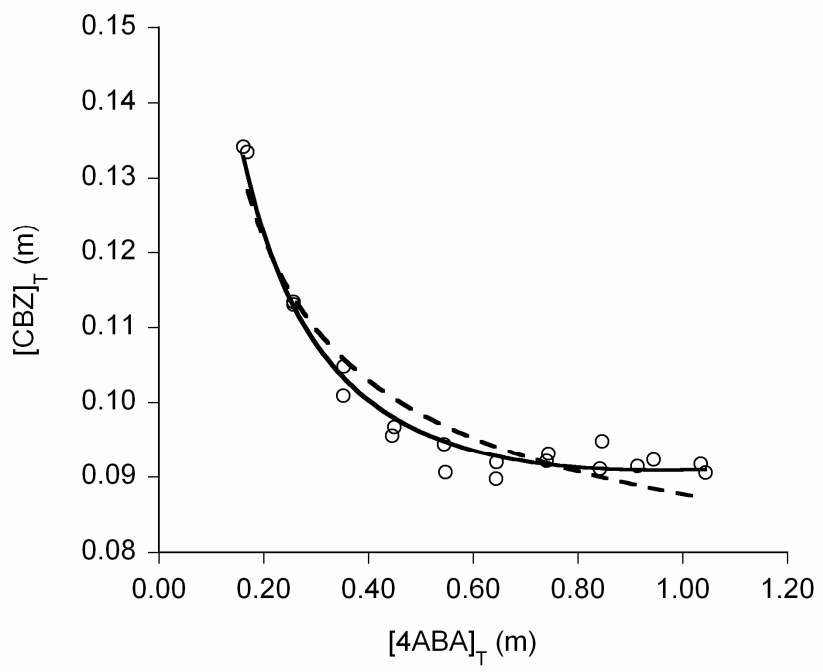

Figure 2.8: Phase solubility diagram showing the experimental and predicted dependence of $[CBZ]_T$ on $[4ABA]_T$ when the 2:1 cocrystal is in equilibrium with the solution. Symbols indicate experimental data. Solid line represents the predicted dependence according to models I and II. Dashed line is the predicted dependence of model III.

Models predicting carbamazepine (CBZ(III)) solubility

The solubility of CBZ(III) increases linearly with ligand concentration (figure 2.9) suggesting the formation of a first order complex with respect to the ligand i.e, D_mL. Complexation constants from these studies were evaluated using previously developed mathematical models based on 1:1 and 2:1 solution complexation.[41, 43, 44] These models are shown in table 2.6.

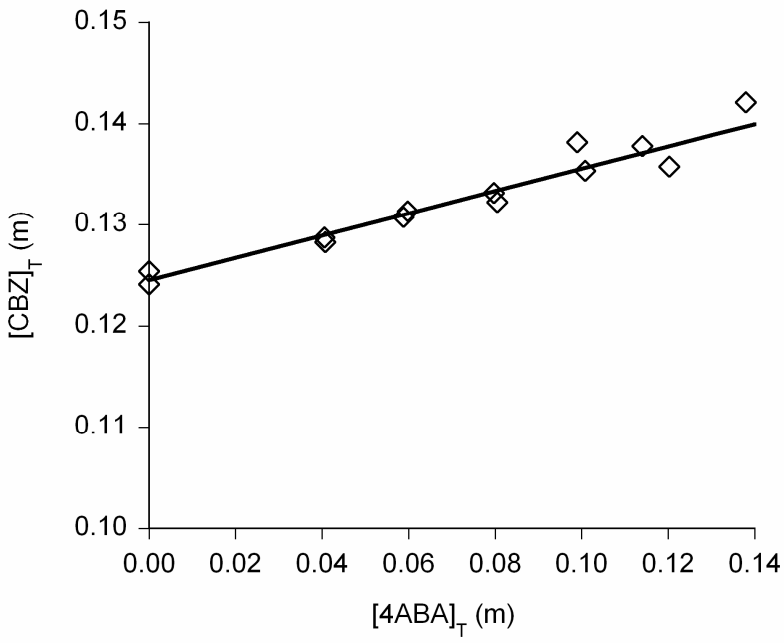

Figure 2.9: CBZ(III) solubility as a function of 4ABA concentration in ethanol at 25˚C. Symbols represent experimental data and the line represents the predicted dependence according to models IV−VI (table 2.6).

Table 2.6**:** Mathematical models to predict the dependence of drug solubility on ligand concentration for the drug crystal (D).

Model	Complexation	Equilibrium reactions	[a][D]$_T$ dependence on [L]$_T$	Equation
IV	1:1 + 2:1	$D_{(soln)} + L_{(soln)} \overset{K_{11}}{\rightleftharpoons} DL_{(soln)}$ $DL_{(soln)} + D_{(soln)} \overset{K_{21}}{\rightleftharpoons} D_2L_{(soln)}$	$[D]_T = D_o + \left(\frac{K_{11}D_o(1+2K_{21}D_o)}{1+K_{11}D_o(1+K_{21}D_o)}\right)[L]_T$	10
V	1:1	$D_{(soln)} + L_{(soln)} \overset{K_{11}}{\rightleftharpoons} DL_{(soln)}$	$[D]_T = D_o + \left(\frac{K_{11}D_o}{1+K_{11}D_o}\right)[L]_T$	11
VI	2:1	$2D_{(soln)} + L_{(soln)} \overset{K'_{21}}{\rightleftharpoons} D_2L_{(soln)}$	$[D]_T = D_o + \left(\frac{2K'_{21}D_o^2}{1+K'_{21}D_o^2}\right)[L]_T$	12

[a][D]$_T$ and [L]$_T$ are the total drug and ligand concentration when the drug crystal is in equilibrium with the solution. D_o is the drug solubility in the absence of the ligand.

Table 2.7: Complexation constants evaluated from CBZ(III) solubility study.

Model	Complexation	K_{11} (m^{-1})	K_{21} (m^{-1})	K'_{21} (m^{-2})	R^2	F-value
IV	1:1 + 2:1	0.99 ± 0.09[a]	0.00 ± 0.01[b]	-	0.93	59896
V	1:1	0.99 ± 0.09	-	-	0.93	59896
VI	2:1	-	-	3.80 ± 0.35	0.93	59896

[a] Standard error [b]Statistically insignificant, $p > 0.05$.

Models IV – VI in table 2.6 predict a linear dependence of drug solubility on ligand concentration. Thus a plot of $[D]_T$ against $[L]_T$ for these models will yield a straight line and the complexation constants can be evaluated from the slope of the line. Model IV has two unknowns (K_{11} and K_{21}) in the expression for the slope and therefore the constants can only be evaluated from cocrystal solubility studies.[44] Since results from 2:1 cocrystal solubility studies indicate negligible 2:1 solution complexation, we therefore assume K_{21}= 0 in model IV, and evaluate K_{11} from the slope. Models IV and V are identical when K_{21} = 0 in model IV.

The complexation constants (K_{11}, K_{21}, and K'_{21}), R^2, and F-values obtained using models IV−VI are summarized in table 2.7. The R^2 and F-values are equal for all the models. K_{11} from model IV, evaluated by assuming K_{21}=0, and model V are in agreement with that evaluated for the 2:1 cocrystal using models I and II (equations 5 and 7). However, K'_{21} obtained from model VI for drug solubility is significantly different from that evaluated for 2:1 cocrystal using model III (table 2.5). These results suggest 1:1 complexation with negligible 2:1 complex formation in solution. Similar analysis to evaluate thermodynamic constants and determine the nature of the complex in solution has been carried out for other complexes.[43, 45]

Model predicting 1:1 cocrystal solubility

The 1:1 cocrystal solubility is not experimentally accessible below the invariant point c_2 because of fast conversion to the 2:1 cocrystal. The 1:1 cocrystal is stable in the region between c_2 and c_3 and the solubility could be measured by equilibrium methods. However, the region of 1:1 cocrystal stability is very narrow as indicated by the small

range of 4ABA concentration in Table I. Therefore the solubility dependence on ligand concentration was calculated by the following equation.[30]

$$S_{cocrystal} = [D]_T = \frac{K_{sp}}{[L]_T} + K_{11}K_{sp} \quad (13)$$

The K_{sp} of 4.85×10^{-2} m^2 was evaluated using the total drug and ligand concentration at c_2 (table 2.3). K_{11} was evaluated from 2:1 cocrystal and drug solubility studies. The predicted solubility of the 1:1 cocrystal as a function of ligand concentration is shown in figure 2.6.

Equation (13) can be used to evaluate the K_{sp}, and hence predict the cocrystal solubility dependence on ligand concentration, if the complexation constant and the equilibrium reactant concentrations at equilibrium with the 1:1 cocrystal at any point are known.

Discussions

This study reports the discovery of a 1:1 cocrystal of CBZ and 4ABA by the reaction crystallization method. The crystal structure shows amide···amide and acid···acid homosynthons. This is unusual as acid···amide heterosynthon is expected to form in 1:1 stoichiometry based on hydrogen bond complementarity.[27, 38-40] In fact, the crystal structure of the previously reported 2:1 CBZ−4ABA anhydrous cocrystal exhibits an acid···amide heterosynthon along with an amide···amide homosynthon.[27] A CSD search for organic compounds with only primary amide and carboxylic acid groups without other hydrogen bond competing groups resulted in 33 hits. Crystal structure analysis of

these compounds showed 28 structures with acid···amide heterosynthon indicating 85% probability for heterosynthon formation. The remaining structures show acid···acid homosynthon (3%), amide-amide homosynthon (6%) and acid···amide catamer (6%). None of the crystal structures in the CSD show both acid···acid and amide···amide homosynthons. To our knowledge, the 1:1 CBZ−4ABA cocrystal is the first example where both homosynthons are present in the crystal structure.

The studies reported here show that the stability of cocrystals with different stoichiometry is dependent on ligand concentration. The cocrystal richer in ligand component is more stable at higher ligand solution concentrations. As shown for the CBZ−4ABA cocrystals, 1:1 cocrystal is more stable at higher 4ABA concentrations whereas the 2:1 cocrystal is more stable at lower 4ABA concentrations in ethanol. The ability to form and sustain both cocrystals in a given solvent will depend on the solubility of the reactants.

The stability domains for the different crystalline phases can be identified using phase solubility and triangular phase diagrams. These diagrams indicate that the crystallization outcomes and phase stability are governed by the solution composition of the drug and ligand. This is illustrated by the transformation pathways E for evaporation, and R_1 and R_2 for reaction crystallization in figure 2.10.

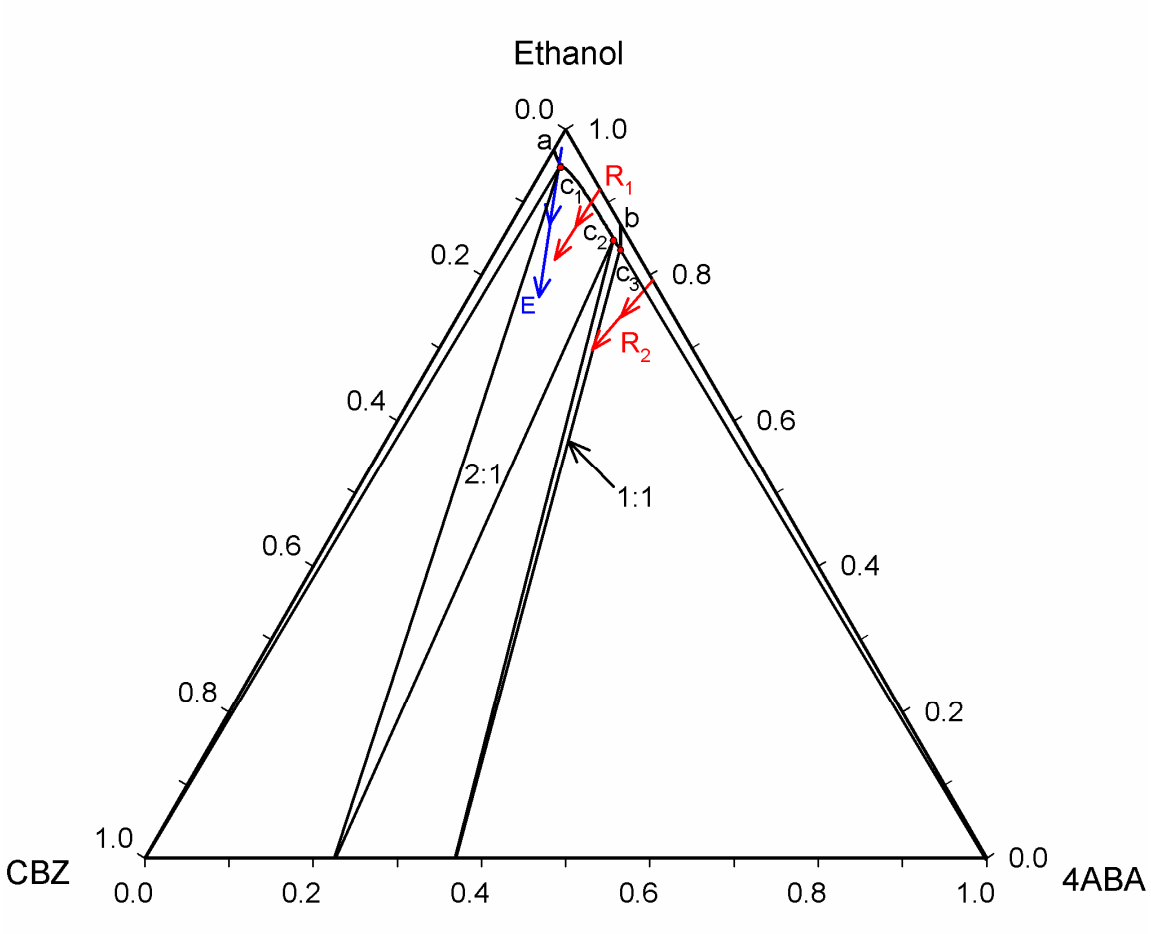

Figure 2.10: TPD showing how transformation pathways R_1 and R_2 in reaction crystallization and pathway E during evaporation lead to supersaturation with respect to cocrystal or to a region where cocrystal is the thermodynamically stable phase. 2:1 cocrystal is obtained along paths E and R_1. 1:1 cocrystal is obtained along R_2.

During solvent evaporation, the initial reactant concentrations in solution as well as the extent and rate of solvent evaporation determine the solution composition of reactants, and hence the phase with respect to which supersaturation is generated. For instance, the pathway E in figure 2.10 represents evaporation of solvent from a solution of reactants in 1:1 mol ratio. Solvent evaporation in this case leads into the region where supersaturation with respect to 2:1 cocrystal is generated. This may explain why a 2:1

CBZ−4BA cocrystal was obtained by solvent evaporation in an earlier study.[27] Further solvent evaporation along pathway E can result in a mixed phase of 1:1 and 2:1 cocrystal depending on the rates of solvent evaporation and crystallization. If the ratio of reactant concentrations in solution is changed such that it lies between the invariant points c_2 and c_3, solvent evaporation will lead into the region where supersaturation with respect to 1:1 cocrystal is achieved. It is important to note that the 1:1 cocrystal stability domain as shown in figure 2.10 is narrower than that of the 2:1 cocrystal and may require careful control of evaporation rates to form 1:1 cocrystal.

In contrast to solvent evaporation, supersaturation with respect to the cocrystals in reaction crystallization method is generated by reactant dissolution. The solution concentration of reactants depends on the relative amounts of reactants added as indicated by the pathways R_1 and R_2 in figure 2.10. R_1 represents the change in composition by the addition of drug to an undersaturated 4ABA solution. R_2 shows the change in solution composition when the drug is added to a suspension of 4ABA saturated with 4ABA. At a given total drug composition, the equilibrium solution composition is different for the two pathways. Consequently, the crystallization outcomes due to drug addition along the two pathways are also different. As shown in figure 2.10, the 1:1 cocrystal is obtained along R_2 but not along R_1.

From the phase diagrams, PSD (figure 2.6) and TPD (figures 2.7 and 2.10), the equilibrium composition of the reactants in solution varies along a-c_1-c_2-c_3-b. ‘a’ and ‘b’ correspond to drug and ligand solubility in the pure solvent. c_1, c_2, and c_3 are the invariant points. Therefore, the key parameters essential to identify the stability domains of the crystalline phases are the reactant solubility in pure solvent (points ‘a’ and ‘b’) and their

concentrations at the invariant points (c_1, c_2, and c_3). The number of invariant points in a system depends on the number of crystalline phases. The CBZ−4ABA-ethanol system presented in this study has 4 crystalline phases (CBZ(III), 2:1 cocrystal, 1:1 cocrystal and 4ABA) and three invariant points. Studies with other cocrystals and molecular complexes show three crystalline phases (A, B, AB) and two invariant points.[10, 42, 46]

The equilibrium solution composition of the reactants for the different crystalline phases, as shown in the phase diagrams, can be determined from solubility studies of the crystalline phases as a function of ligand concentration. The solution concentrations of reactants in equilibrium with solid phases can also be predicted using mathematical models based on heterogenous and homogenous equilibria as illustrated for the 1:1 CBZ−4ABA cocrystal. The models are also useful predicting cocrystal solubility which are otherwise experimentally inaccessible due to cocrystal instability.

The solubility models developed in this study for the CBZ−4ABA cocrystals show that the solubility of 2:1 cocrystal is explained by 1:1 solution complexation. Calculation of the species distribution based on the K_{11} value indicates that the concentration of the 1:1 solution complex varies from 10% to 50% of the total drug concentration under equilibrium conditions between the invariant points c_1 and c_2 (figure 2.11). Thus, a significant fraction of the drug remains uncomplexed in solution. According to the classical theory of crystallization, nucleation is preceded by the formation and growth of molecular clusters.[47] While there is 1:1 complexation at saturated conditions, the molecular assemblies at supersaturated conditions are not known for this system.

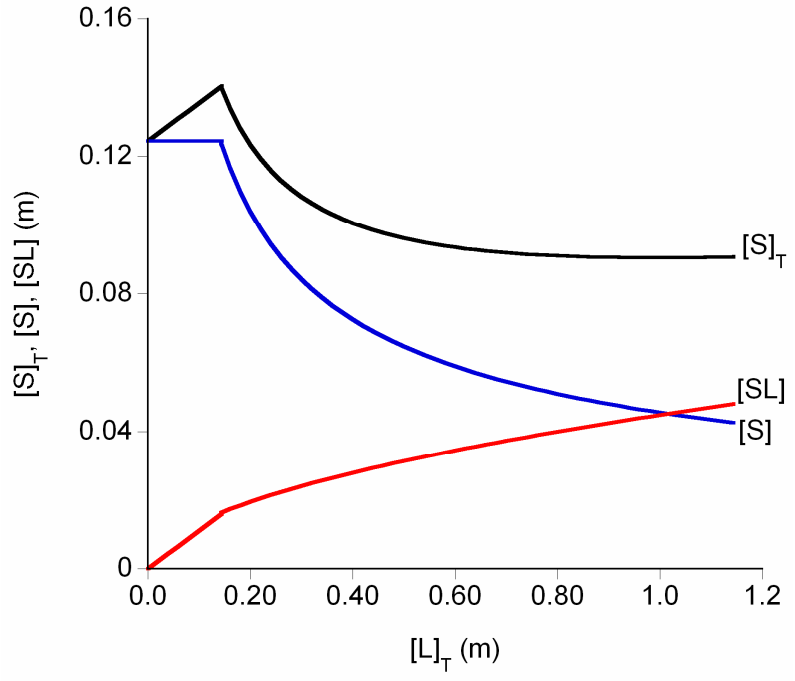

Figure 2.11: Species distribution plot showing concentration dependence of total drug ($[S]_T$), free drug ([S]) and complex ([SL]) on total ligand concentration ($[L]_T$).

Previous studies show that solution complexation at saturation is not an indicator of cocrystal formation or its stoichiometry. For instance, while the stoichiometry of the solution complex of sacrosine anhydride with aminobenzoic acids and hydroxybenzoic acids correspond to the stoichiometry of the solid complexes,[43] studies on molecular complexes of hydroxybenzoic acids with ethyl theobromine and N, N, N', N' - methylterephthalamide indicate that the stoichiometry of the solution complex is different from that of the solid complex.[45, 48] In fact, significantly large values of complexation constants have been reported in systems where no cocrystal formation has been observed.[41] Also, solubility studies with carbamazepine-nicotinamide cocrystal in

ethanol indicate negligible complex formation in solution, yet this cocrystal can be synthesized from ethanol.[30] This is because the driving force for crystallization is supersaturation and not solution complexation.

Conclusions

Two different stoichiometric cocrystals of CBZ−4ABA (2:1 and 1:1) are synthesized using reaction crystallization method (RCM) by varying ligand concentration. Stability of these cocrystals is dependent on reactant solution composition. Identification of isothermal invariant points is essential to establish the regions of cocrystal stability. The solubilities of cocrystals and equilibrium solution composition of reactants to generate phase diagrams can be predicted using mathematical models. The findings from this study have potential applications for cocrystal screening and synthesis and to control process-induced transformations.

References

1. Gould, P. L. Salt Selection for Basic Drugs. *Int. J. Pharm.* **1986,** *33*, 201-217.

2. Hancock, B. C.; Zografi, G. Characteristics and Significance of the Amorphous State in Pharmaceutical Systems. *J. Pharm. Sci.* **1997,** *86*, 1-12.

3. Huang, L.-F.; Tong, W.-Q. T. Impact of Solid State Properties on Developability Assessment of Drug Candidates. *Adv. Drug. Del. Rev.* **2004,** *56*, 321-334.

4. Miller, J. M.; Collman, B.M.; Greene, L.R.; Grant, D.J.W.; Blackburn, A.C.; Identifying the Stable Polymorph Early in the Drug Discovery-Development Process. *Pharm. Dev. Tech.* **2005,** *10*, 291-297.

5. Murphy, D.; Rodríguez-Cintrón, F.; Langevin, B.; Kelly, R. C.; Rodríguez-Hornedo, N. Solution-Mediated Phase Transformation of Anhydrous to Dihydrate Carbamazepine and the Effect of Lattice Disorder. *Int. J. Pharm.* **2002,** *246*, 121-134.

6. Pan, X.H.; Julian, T.; Augsburger, L. Increasing the Dissolution Rate of a Low-Solubility Drug through a Crystalline-Amorphous Transition: A Case Study with Indomethacin. *Drug Dev. Ind. Pharm.* **2008,** *34*, 221-231.

7. Rodríguez-Spong, B.; Price, C. P.; Jayasankar, A.; Matzger, A. J.; Rodríguez-Hornedo, N. General Principles of Pharmaceutical Solid Polymorphism: A Supramolecular Perspective. *Adv. Drug. Del. Rev.* **2004,** *56*, 241-274.

8. Serajuddin, A. T. M. Salt Formation to Improve Drug Solubility. *Adv. Drug. Del. Rev.* **2007,** *59*, 603-616.

9. Berry, D. J.; Seaton, C. C.; Clegg, W.; Harrington, R. W.; Coles, S. J.; Horton, P. N.; Hursthouse, M. B.; Storey, R.; Jones, W.; Friščić, T.; Blagden, N. Applying Hot-Stage Microscopy to Co-Crystal Screening: A Study of Nicotinamide with Seven Active Pharmaceutical Ingredients. *Cryst. Growth Des.* **2008,** *8*, 1697-1712.

10. Childs, S. L.; Rodríguez-Hornedo, N.; Reddy, L. S.; Jayasankar, A.; Maheshwari, C.; McCausland, L.; Shipplett, R.; Stahly, B. C. Screening Strategies Based on Solubility and Solution Composition Generate Pharmaceutically Acceptable Cocrystals of Carbamazepine. *CrystEngComm.* **2008**, 856-864.

11. Cui, Y.; Yao, E. Evaluation of Hydrate Screening Methods. *J. Pharm. Sci.* **2008,** *97*, 2730-2744.

12. Lu, E.; Rodríguez-Hornedo, N.; Suryanarayanan, R. A Rapid Thermal Method for Cocrystal Screening. *CrystEngComm.* **2008,** *10*, 665-668.

13. Morissette, S. L.; Almarsson, Ö.; Peterson, M. L.; Remenar, J. F.; Read, M. J.; Lemmo, A. V.; Ellis, S.; Cima, M. J.; Gardner, C. R. High-Throughput Crystallization: Polymorphs, Salts, Co-Crystals and Solvates of Pharmaceutical Solids. *Adv. Drug. Del. Rev.* **2004,** *56*, 275-300.

14. Sacchetti, M. General Equations for In Situ Salt Screening of Multibasic Drugs in Multiprotic Acids. *Pharm. Dev. Tech.* **2000,** *5*, 579-582.

15. Childs, S. L.; Chyall, L. J.; Dunlap, J. T.; Smolenskaya, V. N.; Stahly, B. C.; Stahly, P. G. Crystal Engineering Approach to Forming Cocrystals of Amine Hydrochlorides with Organic Acids. Molecular Complexes of Fluoxetine Hydrochloride with Benzoic, Succinic, and Fumaric Acids. *J. Am. Chem. Soc.* **2004,** *126*, 13335-13342.

16. McNamara, D. P.; Childs, S.L.; Giordano, J.; Iarriccio, A.; Cassidy, J.; Shet, M. S.; Mannion, R.; O'Donnell, E.; Park, A. Use of a Glutaric Acid Cocrystal to Improve Oral Bioavailability of a Low Solubility API. *Pharm. Res.* **2006,** *23*, 1888-1897.

17. Rodríguez-Hornedo, N.; Nehm, S. J.; Jayasankar, A. Cocrystals: Design, Properties and Formation Mechanisms. In *Encyclopedia of Pharmaceutical Technology,* 3rd ed.; Swarbrick, J., Eds.; Informa Health Care: New York, **2006**, pp.615-635.

18. Sun, C. C.; Hou, H. Improving Mechanical Properties of Caffeine and Methyl Gallate Crystals by Cocrystallization. *Cryst. Growth Des.* **2008,** *8*, 1575-1579.

19. Trask, A. V.; Motherwell, W. D. S.; Jones, W. Pharmaceutical Cocrystallization: Engineering a Remedy for Caffeine Hydration. *Cryst. Growth Des.* **2005,** *5*, 1013-1021.

20. Trask, A. V.; Motherwell, W. D. S.; Jones, W. Physical Stability Enhancement of Theophylline Via Cocrystallization. *Int. J. Pharm.* **2006,** *320*, 114-123.

21. Remenar, J. F.; Peterson, M. L.; Stephens, P. W.; Zhang, Z.; Zimenkov, Y.; Hickey, M. B. Celecoxib : Nicotinamide Dissociation: Using Excipients to Capture the Cocrystal's Potential. *Mol. Pharm.* **2007,** *4*, 386-400.

22. Babu, N. J.; Reddy, L. S.; Nangia, A. Amide- N -Oxide Heterosynthon and Amide Dimer Homosynthon in Cocrystals of Carboxamide Drugs and Pyridine N-Oxides. *Mol. Pharm.* **2007,** *4*, 417-434.

23. Bučar, D.-K.; Henry, R. F.; Lou, X.; Duerst, R. W.; Borchardt, T. B.; MacGillivray, L. R.; Zhang, G. G. Z. Co-Crystals of Caffeine and Hydroxy-2-Naphthois Acids: Unusual Formation of the Carboxylic Acid Dimer in the Presence of a Heterosynthon. *Mol. Pharm.* **2007,** *4*, 339-346.

24. Caira, M. R. Sulfa Drugs as Model Cocrystal Formers. *Mol. Pharm.* **2007,** *4*, 310-316.

25. Childs, S. L.; Hardcastle, K. I. Cocrystals of Piroxicam with Carboxylic Acids. *Cryst. Growth Des.* **2007,** *7*, 1291-1304.

26. Fleischman, S. G.; Kuduva, S. S.; McMahon, J. A.; Moulton, B.; Walsh, R. D. B.; Rodríguez-Hornedo, N.; Zaworotko, M. J. Crystal Engineering of the Composition of Pharmaceutical Phases: Multiple-Component Crystalline Solids Involving Carbamazepine. *Cryst. Growth Des.* **2003,** *3*, 909-919.

27. McMahon, J. A.; Bis, J. A.; Vishweshwar, P.; Shattock, T. R.; McLaughlin, O. L.; Zaworotko, M. J. Crystal Engineering of the Composition of Pharmaceutical Phases. 3. Primary Amide Supramolecular Heterosynthons and Their Role in the Design of Pharmaceutical Cocrystals. *Z. Kristallogr.* **2005,** *220*, 340-350.

28. Trask, A. V.; van de Streek, J.; Motherwell, W. D. S.; Jones, W. Achieving Polymorphic and Stoichiometric Diversity in Cocrystal Formation: Importance of Solid-State Grinding, Powder X-Ray Structure Determination, and Seeding. *Cryst. Growth Des.* **2005,** *5*, 2233-2241.

29. Karki, S.; Friščić, T.; Jones, W.; Motherwell, W. D. S. Screening for Pharmaceutical Cocrystal Hydrates Via Neat and Liquid-Assisted Grinding. *Mol. Pharm.* **2007,** *4*, 347-354.

30. Nehm, S. J.; Rodríguez-Spong, B.; Rodríguez-Hornedo, N. Phase Solubility Diagrams of Cocrystals Are Explained by Solubility Product and Solution Complexation. *Cryst. Growth Des.* **2006,** *6*, 592-600.

31. Rodríguez-Hornedo, N.; Nehm, S. J.; Seefeldt, K. F.; Pagán-Torres, Y.; Falkiewicz, C. J. Reaction Crystallization of Pharmaceutical Molecular Complexes *Mol. Pharm.* **2006,** *3*, 362-367.

32. Bak, A.; Gore, A.; Yanez, E.; Stanton, M.; Tufekcic, S.; Syed, R.; Akrami, A.; Rose, M.; Surapaneni, S.; Bostick, T.; King, A.; Neervannan, S.; Ostovic, D.; Koparkar, A. The Co-Crystal Approach to Improve the Exposure of a Water Insoluble Compounds: AMG 517 Sorbic Acid Co-Crystal Characterization and Pharmacokinetics. *J. Pharm. Sci.* **2008,** *97*, 3942-3956.

33. Jayasankar, A.; Good, D. J.; Rodríguez-Hornedo, N. Mechanisms by Which Moisture Generates Cocrystals. *Mol. Pharm.* **2007,** *4*, 360-372.

34. Jayasankar, A.; Somwangthanaroj, A.; Shao, J. Z.; Rodríguez-Hornedo, N. Cocrystal Formation During Cogrinding and Storage Is Mediated by Amorphous Phase. *Pharm. Res.* **2006,** *23*, 2381-2392.

35. Seefeldt, K. J.; Miller, J.; Alvarez-Núñez, F.; Rodríguez-Hornedo, N. Crystallization Pathways and Kinetics of Carbamazepine-Nicotinamide Cocrystals from the Amorphous State by in Situ Thermomicroscopy, Spectroscopy and Calorimetry

Studies. *J. Pharm. Sci.* **2007,** *96*, 1147-1158.

36. Sheldrick, G. M. *SADABS*, v. 2.10; Program for empirical absorption correction of area detector data, University of Gottingen: Gottingen, Germany, 2003.

37. Sheldrick, G. M. *SHELXTL*, v. 6.12; Bruker Analytical X-ray: Madison, Wisconsin, 2001.

38. Leiserowitz, L. Molecular Packing Modes. Carboxylic Acids. *Acta Crystallogr.* **1976,** *B32*, 775-801.

39. Leiserowitz, L.; Schmidt, G. M. J. Molecular Packing Modes .3. Primary Amides. *J. Chem. Soc. A*. **1969,** *16*, 2372.

40. Vishweshwar, P.; McMahon, J. A.; Bis, J. A.; Zaworotko, M. J. Pharmaceutical Co-Crystals. *J. Pharm. Sci.* **2006,** *95*, 499-516.

41. Higuchi, T.; Connors, K. A. Phase-Solubility Techniques. In *Advances in Analytical Chemistry and Instrumentation*; Reilley, C., Eds.; **1965**, pp.117-212.

42. Chiarella, R. A.; Davey, R. J.; Peterson, M. L. Making Co-Crystals - the Utility of Ternary Phase Diagrams. *Cryst. Growth Des.* **2007,** *7*, 1223-1226.

43. Poole, J. W.; Higuchi, T. Complexes Formed in Aqueous Solutions by Sarcosine Anhydride; Interactions with Organic Acids, Phenols, and Aromatic Alcohols. *J. Am. Pharm. Assoc.* **1959**, 592-601.

44. Zughul, M. B.; Badwan, A. A. Rigorous Analysis of S_2L-Type Phase Solubility Diagrams to Obtain Individual Formation and Solubility Product Constants of Both SL- and S_2L-Type Complexes. *Int. J. Pharm.* **1997,** *151*, 109-119.

45. Kostenbauder, H. B.; Higuchi, T. Formation of Molecual Complexes by Some Water-Soluble Amides I. *J. Am. Pharm. Assoc.* **1956,** *45*, 518-522.

46. Ito, K.; Sekiguchi, K. Studies on the Molecular Compounds of Organic Medicinals II. Application of the Solubility Product Principle and Consideration by the Phase Rule to the Solubility Phenomena of the Molecular Compound of Sulfanilamide and Sulfathiazole. *Chem. Pharm. Bull.* **1966,** *14*, 255-262.

47. Mullin, J. W., *Crystallization*, 4th ed.; Butterworth-Heinemann: Oxford; **2001**.

48. Bolton, S.; Guttman, D.; Higuchi, T. Complexes Formed in Solution by Homologs of Caffeine - Interactions between P-Hydroxybenzoic Acid and Ethyl, Propyl, and Butyl Derivatives of Theobromine, and Theophylline. *J. Am. Pharm. Assoc.* **1957,** *46*, 38-41.

CHAPTER III

MECHANISMS BY WHICH MOISTURE GENERATES COCRYSTALS

Introduction

The effects of moisture on drug stability are of central importance for the development of pharmaceutical products. Water can cause chemical instability and solid phase transformations that will compromise product safety and bioavailability. Relative humidity dependent phase transformations are well documented and include anhydrous to hydrate,[1-6] polymorphic,[7] and amorphous to crystalline transformations.[8, 9] Recent studies from our laboratory demonstrated that amorphous regions mediate transformations of solid reactants to cocrystal and that moisture enhances reactivity.[10, 11] These studies showed that the mechanism involves increased molecular mobility and is associated with the plasticizing effects of water.[10, 12]

Moisture sorption by hygroscopic materials can also lead to deliquescence.[13-15] This process refers to the formation of an aqueous solution by the absorption of water vapor at a characteristic relative humidity or deliquescent relative humidity (DRH).[16] DRH is a function of the chemistry of a solid, solid phase composition, and temperature.[14, 15, 17-21] It is well established that the presence of a second solid component decreases the DRH. Materials used in pharmaceutical formulations that

exhibit deliquescence include sugars, organic and inorganic salts.[19, 22-24] Deliquescence dependent phase transformations for hydrates[4] and deliquescence mediated chemical degradation have also been published.[24-26] Although cocrystals have been shown to prevent formation of hydrated API during storage at high RH,[27-30] various cocrystals have shown RH dependent transformation to hydrated API.[29, 30] Therefore, it appears that identifying the mechanisms for cocrystal formation and stability would be of practical importance if cocrystals are to be developed as pharmaceutical products.

The research reported here is based on the premise that deliquescence can lead to cocrystal nucleation and growth because cocrystal solubility and thermodynamic stability are dependent on solution chemistry. Earlier reports from our laboratory have shown that cocrystal solubility is a function of the cocrystal components in solution and is described by solubility product and solution speciation.[27, 31, 32] This means that cocrystal solubility decreases as the liquid becomes richer in one of the cocrystal components. The important implication of this mechanism is that supersaturation with respect to cocrystal can be generated by dissolving nonequivalent amounts of its components. Supersaturation is dependent on solution composition and for a binary cocrystal AB is expressed by:[32]

$$\sigma = \left(\frac{[A][B]}{K_{sp}} \right)^{1/2} \qquad (1)$$

Hence, if the required supersaturation for cocrystal nucleation is attained then cocrystals are formed. Evidence has been presented to show increase in cocrystal transformation rates with increasing solution concentration of the more soluble reactant.[32, 33]

The thermodynamic stability of a cocrystal relative to pure API crystal has been demonstrated to vary with the concentration of reactants in solution.[31, 32] Moreover, in solvents where cocrystal is more soluble than pure API there is a reactant transition concentration (C_{tr}) at which the cocrystal solubility is equal to the solubility of pure API or API solvate. At this concentration, both crystalline forms are at equilibrium. Above the C_{tr}, cocrystal solubility is below that of API, and therefore cocrystal is the thermodynamically stable form. Rapid transformation of API to API cocrystal has been shown in aqueous media for API that readily transforms to API hydrate in pure water e.g., carbamazepine (CBZ) to carbamazepine-nicotinamide (CBZ-NCT) cocrystal.[32]

The present study is based on the hypothesis that cocrystals are produced when solid reactants are exposed to deliquescent conditions, since dissolution of cocrystal reactants in the sorbed moisture can generate the supersaturation necessary for nucleation and growth of cocrystals. Cocrystal systems were selected from previously reported pharmaceutical cocrystals with APIs that form hydrates.[29, 30, 34] This initial report presents results of cocrystal formation at constant RH in (1) binary blends of cocrystal reactants (CBZ/NCT), and (2) ternary blends of cocrystal reactants with a deliquescent additive that is not consumed by the reaction (CBZ/NCT, CBZ/SAC, caffeine/dicarboxylic acids, theophylline/dicarboxylic acids with sucrose or fructose). The influence of deliquescent additive, solid blend composition, and RH on the transformation rate to cocrystal was studied by on-line Raman spectroscopy during deliquescence. To our knowledge this is the first report on cocrystal formation induced by deliquescence and on the indicators of cocrystal stability under deliquescence processes.

Experimental section

Materials

All chemicals were obtained from Sigma Chemical Company (St. Louis, MO), and were of USP grade. Chemicals were used as received without further purification. All chemicals were characterized prior to use by X-ray powder diffraction (XRPD) and infra-red spectroscopy. XRPD of carbamazepine and theophylline agreed with the Cambridge Structural Database (CSD) simulated XRPD pattern of form III monoclinic CBZ (CSD refcode: CBMZPN01) and anhydrous theophylline (CSD refcode: BAPLOT01). The pattern of caffeine agreed with form II anhydrous caffeine.[5]

All samples were sieved to collect particle size fractions of 45-63μm and 106-125μm. Large crystals were hand ground prior to sieving. Samples were annealed and characterized again by XRPD and FTIR prior to using them in our studies. These fractions were used in preparing samples to study deliquescence by gravimetric sorption analysis and cocrystal formation in bulk samples at constant RH. The composition of the deliquescent additives is expressed on a weight percent basis unless otherwise specified.

Within the scope of this paper we can define the materials used as APIs, cocrystal formers or ligands, and deliquescent additives as listed in table 3.1. The term reactant refers to cocrystal components, i.e. API and ligand. The deliquescence behavior of some of the cocrystal formers (shown in italics in table 3.1) and additives has been published.[17, 19, 35]

Table 3.1: List of the materials used to study moisture uptake and phase stability

APIs	Cocrystal formers (ligands)	Deliquescent additives
Carbamazepine	*Nicotinamide*	Fructose
Theophylline	Saccharin	Sucrose
Caffeine	*Oxalic acid*	
Sulfadimidine	*Glutaric acid*	
	Malonic acid	
	Maleic acid	
	Anthranilic acid	
	Salicylic acid	

Methods

Gravimetric Vapor Sorption

Vapor sorption studies were conducted to determine DRH or to monitor the progress of moisture sorption towards equilibrium under constant RH and temperature. Both types of gravimetric vapor sorption studies use samples of 5-10mg with particle size of all components between 45 and 63μm unless otherwise noted. All studies were done on an SGA-100 symmetrical gravimetric analyzer from VTI Corp. (Hialeah, FL). The instrument uses a microbalance (CI Electronics, Wiltshire, UK) to monitor sample weight and a chilled dew point analyzer (Edgetech, Milford, MA) to detect and control humidity in the sample chamber. Temperature is controlled to within 0.01^{o}C and the instrument RH resolution is ±1%. All experiments were conducted at 25^{o}C.

Deliquescent RH Determinations

The DRH for single components and binary blends was determined using a non-equilibrium sorption method. This is an isothermal method that ramps RH by 2% increments. The relative humidity is increased incrementally when the sample changes weight by less than 0.036% in fifteen minutes or 240 minutes whichever comes first at constant RH. While the samples only adsorb small levels of moisture below the DRH a large weight increase from moisture absorption is observed once the DRH is reached.

Moisture Sorption Kinetics

The time course of moisture sorption, and desorption in some instances, at fixed temperature and humidity was also studied for a variety of sample compositions. In these studies a constant RH and temperature was maintained over the course of several days until the sample reached an equilibrium moisture sorption level.

Bulk Sample Studies in RH Chambers

The effects of DRH, storage RH, particle size, and the amount of deliquescent materials on the rate of cocrystal formation was studied using ternary mixtures of CBZ (III), with NCT or saccharin (SAC), and a deliquescent additive (fructose, sucrose or citric acid). In these studies the cocrystal reactant ratio in the solid phases was held constant at equimolar concentrations and the composition of the deliquescent additive was varied. Raman spectroscopy has been shown to be valuable for real-time monitoring of cocrystal formation[32, 36] and was used to study cocrystal formation at constant RH and temperature.

Desired RH conditions during storage at 25°C were generated in glass desiccators with appropriate saturated salt solution: NaCl for 75%, KCl for 85%, and K_2SO_4 for 98%. An aluminum plate with holes was suspended above the solution to hold samples and a 1/8th inch thick quartz glass lid was used to seal the chamber. The relative humidity in the chambers was confirmed using a HydroClip SC05 RH probe from Rotronics (Huntington, NY). Probe accuracy is ±1.5%RH / ±0.2°C.

Solid blends were stored at 0%RH in a P_2O_5 desiccator and analyzed by XRPD and IR prior to introduction into RH chambers. Quartz cuvettes containing 30-60mg of 45-63μm (unless otherwise specified) crystalline blends were introduced into the RH chambers. Phase transformation in the blends was monitored by Raman spectroscopy. A non-contact fiber optic probe was used to collect Raman spectra through the quartz chamber lid. Spectra were collected frequently over random areas of the sample for several days. A time course of the change in spectral features was used to monitor cocrystal formation. HoloReact™ software, from Kaiser Optical Systems (Ann Arbor, MI), was used for multivariate curve resolution to plot the change in spectral features correlating to reactants and cocrystal. The analysis region for CBZ-NCT systems was 924-1182cm^{-1} and CBZ-SAC was 225-300cm^{-1}. Samples were promptly analyzed by XRPD and IR once removed from the chamber. The mass of the blends before and after storage were also noted to determine the amount of moisture sorbed.

Slurry Studies

Screening for cocrystals was carried out according to methods published earlier.[31, 32] Cocrystal reactants were added to aqueous solutions such that non-stoichiometric

reactant concentrations would favor cocrystal formation. The slurries were placed in a 25^{o}C recirculation water bath and stirred continuously. No nucleating seeds were added to these samples. Once removed from the water bath the slurries were dried by vacuum filtration and promptly analyzed by XRPD.

Moisture uptake and stability of cocrystals during storage

Approximately 50 mg cocrystal of CBZ, caffeine and theophylline cocrystals with various ligands were stored at different relative humidities (85%, 91% and 98% RH) to investigate moisture uptake and stability. Moisture uptake of cocrystals was determined by noting the mass change during storage. Solid phase stability during storage was monitored by Raman spectroscopy using a non-contact fiber optic probe. Solid phases were also characterized by XRPD.

Raman Spectroscopy

Raman spectra of solid phases were collected with a Kaiser Optical Systems, Inc. (Ann Arbor, MI), RXN1 Raman spectrometer equipped with a 785 nm laser. Crystallization in bulk samples was monitored in-situ with a fiber optic non-contact probe. Crystallization was also monitored in micro-scale using a Leica DMLP (Wetzlar, Germany) Raman microscope. Acquisition conditions were optimized so that the spectra collected for bulk studies had maximum intensity around 30-40k counts. The spectra collected had a spectral resolution of 4 cm^{-1} and were collected between 100 and 3200 cm^{-1}.

Attenuated Total Reflectance Fourier Transform Infrared (ATR-FTIR) Spectroscopy

IR spectra of solid phases were collected on a Bruker Vertex 70 FT-IR (Billerica, MA) unit equipped with a DTGS detector. Samples were placed on a zinc selenide (ZnSe) attenuated total reflectance (ATR) crystal accessory, and 64 scans were collected for each sample at a resolution of 4 cm^{-1} over a wavenumber region of 4000-600 cm^{-1}.

X-ray Powder Diffraction (XRPD)

XRPD was used to identify crystalline phases and phase transformations after exposure to various storage conditions. XRPD patterns of solid phases were recorded with a Rigaku MiniFlex X-ray diffractometer (Danvers, MA) using Cu Kα radiation (λ = 1.54 Å), a tube voltage of 30 kV, and a tube current of 15 mA. The intensities were measured at 2θ values from 2° to 40° at a continuous scan rate of 2.5°/min. Samples, prior to and after RH storage experiments, were analyzed by XRPD. Results were compared to diffraction patterns reported in literature or calculated from crystal structures reported in the Cambridge Structural Database (CSD).

Polarized Optical Light Microscopy Studies

Particles of cocrystal reactants and deliquescent additives were placed in contact with each other on a slide and introduced into a variable relative humidity microscope stage from Surface Measurement Systems (VGI 2000M. Middlesex, UK). This stage provides temperature and humidity control capability during optical microscopy studies. The stage is computer controlled and receives a flow of dry nitrogen that is saturated in-

situ with water to the appropriate extent as monitored by internal sensors. Water uptake, deliquescence, dissolution, and crystallization were visually monitored with a Leica DMPL polarizing optical microscope (Wetzlar, Germany). Images were collected with a Spot Insight FireWire 4 Megasample Color Mosaic camera controlled with Spot software (Diagnostics Inc, Sterling Heights, MI). Solid phases were identified by Raman microscopy.

Results

Microscopy study

Figure 3.1 shows optical microscopy images of deliquescence-induced cocrystal formation of an initially dry ternary system of cocrystal reactants and a sugar. CBZ, NCT, and sucrose crystals were arranged on the controlled RH microscope stage as shown in figure 3.1(A) and exposed to 95%RH. These images illustrate the sequence of events that lead to cocrystal formation: moisture uptake, dissolution, and crystallization.

The first stage in the formation of cocrystals is the formation of a liquid phase as moisture is sorbed and deliquescence proceeds as shown by the liquid domain in figure 3.1(B). This is followed by dissolution of sucrose and cocrystal reactants as indicated by the change in size and shape of particles. NCT dissolves faster than CBZ as expected based on their different aqueous solubilities. A new phase is observed to crystallize from solution (figure 3.1(D)) near the surface of CBZ crystals. This new phase was determined to be CBZ-NCT cocrystal by Raman microscopy.

Cocrystallization in bulk samples

The microscopy results presented above suggest that cocrystal formation can occur in solid blends of cocrystal reactants exposed to deliquescence conditions. In this section we present results on the moisture uptake behavior of bulk samples, and the factors that determine cocrystal formation by monitoring solid phase changes by spectroscopic and XRPD analysis.

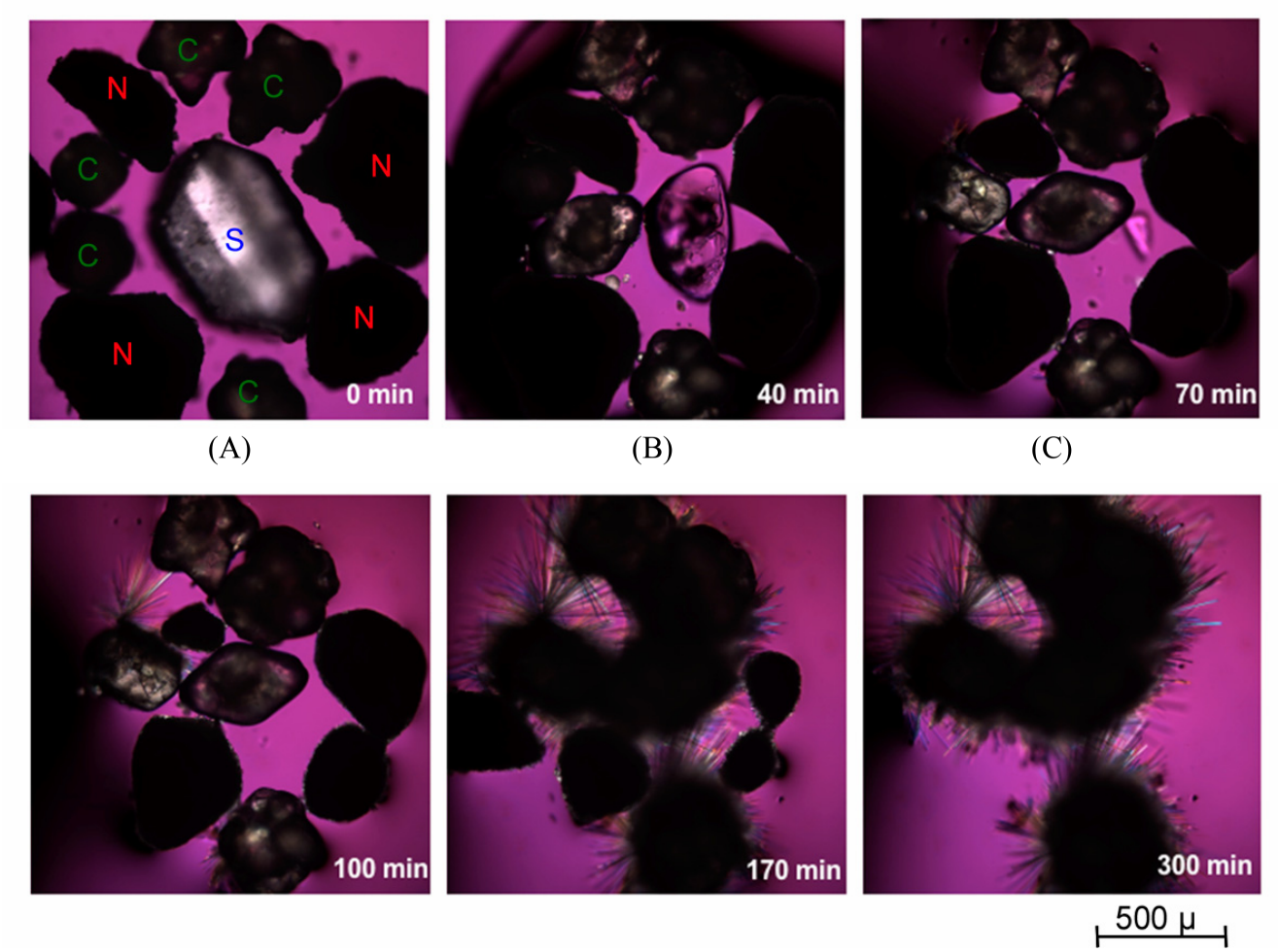

Figure 3.1: Optical microscopy images showing moisture sorption, deliquescence, dissolution and cocrystallization in CBZ/NCT/Sucrose system at 25°C and 95%RH. Symbols C, N and S represent CBZ, NCT and sucrose respectively.

DRH of single components and binary blends

To determine the DRH of blends composed of cocrystal reactants and deliquescent additives, moisture sorption isotherms were obtained under non-equilibrium conditions while the RH was ramped (figure 3.2). DRHs were determined for pure components and binary mixtures of a deliquescent additive (sucrose or fructose) with the most water soluble cocrystal reactant (nicotinamide or saccharin) and are shown in table 3.2. The weight percent of deliquescent additive in all the binary mixtures listed would be 50% if one molar equivalent of CBZ is added. The weight ratios of SAC blends are lower than NCT blends because SAC has a higher molecular weight.

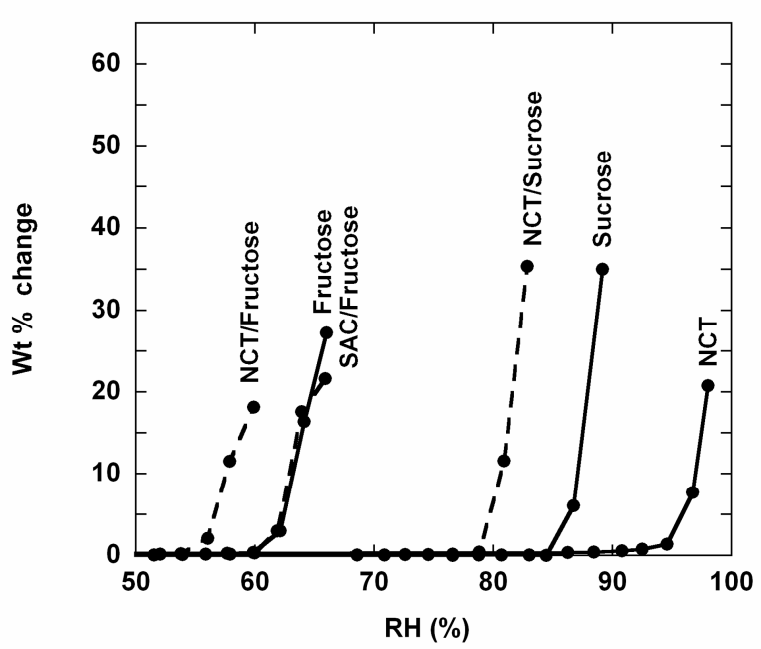

Figure 3.2: Moisture sorption isotherms of single components and binary blends.

Table 3.2: Deliquescent RH of single components and binary blends (S.D. = ±0.3).

Deliquescent components and blends	**Weight ratio**	**Mole ratio**	**DRH(%) at 25°C**
Sucrose	-	-	86.1
Fructose	-	-	62.0
Nicotinamide	-	-	94.5
NCT/Sucrose	1.0 : 2.9	1.0 : 1.1	80.0
NCT/Fructose	1.0 : 2.9	1.0 : 2.0	55.3
SAC/Fructose	1.0 : 2.3	1.0 : 2.3	61.5

The DRH values of the pure components are in good agreement with those available in the literature. The reported DRH for fructose and sucrose is 62% and 85% respectively.[19, 24] Slight differences between the reported DRH values and those observed in this study for sucrose may be due to instrument accuracy of 1%RH and the specific equilibrium conditions used for each RH step listed in the methods section. The DRH of a pure substance is decreased by the addition of a second deliquescent component. Similar deliquescence behavior has been observed in binary and ternary systems with inorganic and organic components,[15, 17, 19, 20] and is explained by the effect of solute composition on the water activity of solutions. While in this study we report the DRH of blends at only one composition for the purpose of investigating transformation to cocrystal, the dependence of DRH on composition is currently being investigated.

The DRH of binary mixtures was determined to avoid rapid cocrystal formation associated with ternary mixtures containing CBZ since transformation to cocrystal can affect the resolution of DRH measurements. Furthermore, the low solubility of CBZ in

water means it should have negligible impact on the DRH and water activity of solutions with sugar and NCT or SAC. The DRH of ternary blends is not expected to change in the presence of CBZ. Indeed CBZ exhibits no deliquescence as anticipated from its low solubility.[28, 37] Consequently, ternary blends of CBZ with cocrystal former in equimolar ratios and 50% deliquescent additive referenced in the next section can be assumed to have the same DRH as blends listed in table 3.2.

Cocrystallization in ternary blends

Figure 3.3(A) shows the changes in the Raman spectra as CBZ-NCT cocrystal formation proceeds in CBZ/NCT/50% sucrose. Peaks at 1026.5 and 1035.0 cm^{-1}, characteristic of CBZ-NCT cocrystal, are observed as cocrystal formation occurs. This is accompanied by a decrease in the intensity of the peak characteristic of CBZ at 1041.5 cm^{-1}. Figure 3.3(B) shows the changes in Raman spectra as CBZ-SAC cocrystal formation occurs in CBZ/SAC/50% fructose blends at 85%RH. A peak at 231.7cm^{-1}, characteristic of CBZ-SAC cocrystal, is observed as cocrystal formation occurs. A decrease in peak intensity for peaks characteristic of SAC and CBZ at 246.0 cm^{-1} and 272.5 cm^{-1} respectively is also observed with cocrystal formation. These changes in the spectra were used to measure cocrystal formation in ternary blends during storage as a function of ambient RH and deliquescent additive.

The progress of cocrystal formation in CBZ/NCT/sugar (fructose or sucrose) blends at 75% and 85%RH was monitored over a two day period by Raman spectroscopy. The initial composition of sugar in these blends was 10%, 20%, or 50%

while the cocrystal reactant molar ratio (CBZ/NCT) was constant at 1:1. A control sample without sugar is included at 85% RH for reference.

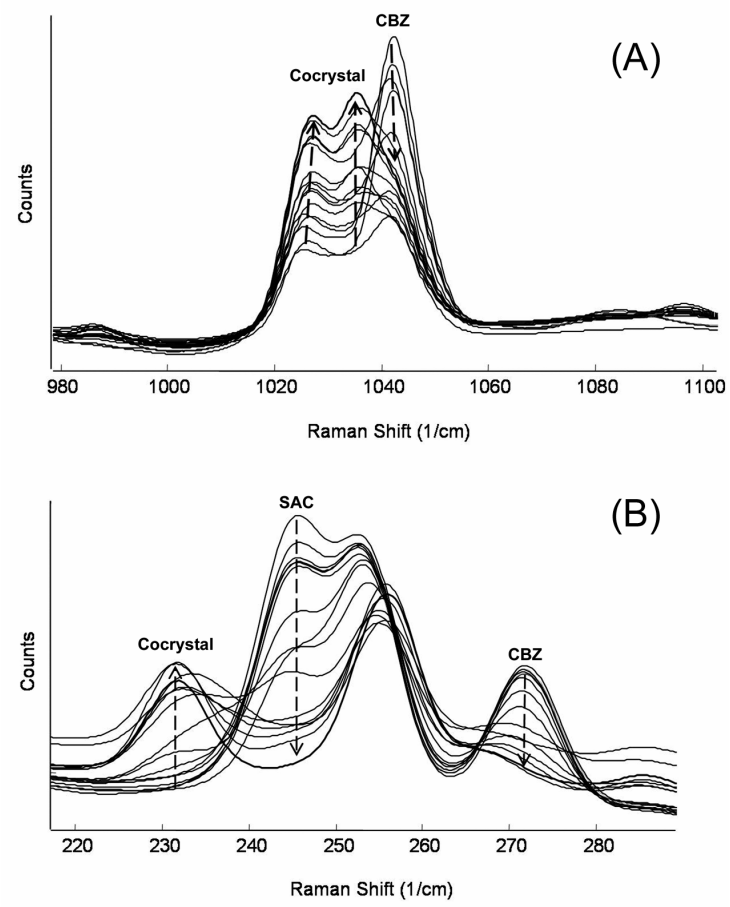

Figure 3.3: Raman spectra showing cocrystal formation and CBZ depletion in (A) CBZ/NCT/50% Sucrose and (B) CBZ/SAC/50% Fructose at 85%RH.

It is evident from figure 3.4 that deliquescence generates cocrystals. Significant cocrystal formation was observed in CBZ/NCT/sugar blends above their DRH, while no cocrystal formation was detected in mixtures below their DRH. For instance, cocrystal formation occurred in ternary blends with sucrose or fructose at 85%RH. In contrast, neither the control sample at 85% RH, nor the ternary mixtures with sucrose at 75% RH

transformed to cocrystal during the course of the study because RH was below DRH. The DRH for NCT is greater than 85% and for NCT/sucrose is greater than 75% as shown in table 3.2.

The rate and extent of cocrystal formation appears to be dependent on the sugar, the percentage of sugar, and the ambient RH as shown in figure 3.4. At 85%RH the fructose blends transformed faster than sucrose blends. Faster rate of cocrystal formation was also observed in fructose blends stored at 85%RH than those stored at 75%RH. It can be seen that the rate of transformation decreases with time. Time intervals at the beginning of the transformation have rapid cocrystal formation followed by a slow conversion period or plateau region. Samples with less deliquescent additive (sugar) exhibit a more gradual conversion to cocrystal as shown by the 10% fructose at 75%RH. After the initial interval of rapid conversion producing a small fraction of cocrystal the progress of transformation is slow as indicated by the slope of the plateau region. In contrast, higher sugar compositions experience faster and extensive transformation to cocrystal during the initial time interval. This behavior is also observed with increasing ambient RH farther above DRH as seen by comparing the 75% and 85%RH fructose samples.

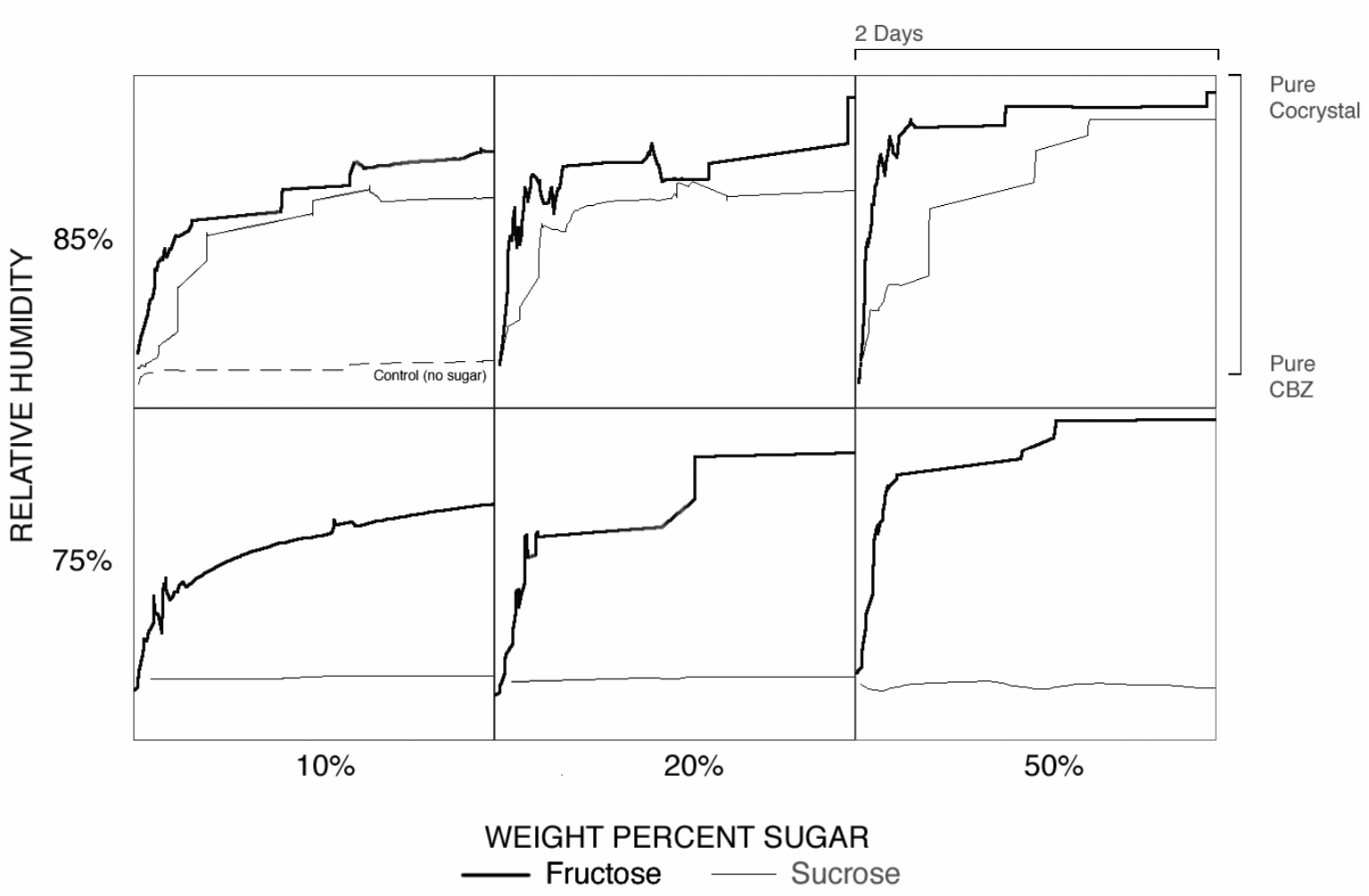

Figure 3.4: Effect of RH and sugar composition on CBZ-NCT cocrystal formation in CBZ/NCT/Sugar blends. Six separate panes corresponding to two relative humidity conditions and three different sugar compositions are shown. Each pane has the same time and composition axis scaling presented for the top right pane. The maximum of the y-axis corresponds to pure cocrystal, while the minimum corresponds to pure reactants.

Lower rates of cocrystal formation at low sugar composition may be associated with small volumes of water uptake and small domains of supersaturation leading to isolated regions of cocrystal formation in the bulk of the sample. In fact, the curves in figure 3.4 have jagged features corresponding to the non-uniform distribution of cocrystal nucleation and growth sites throughout the bulk of the sample. To resolve this spatial distribution of transformation sites, spectra were randomly collected from different regions of the samples. Together the spectra collected represent the average level of transformation in the bulk.

The data in figure 3.4 has been shown over a two day time frame to highlight the dependence of cocrystal formation rates as a function of blend composition and RH. Transformation was monitored over a longer period by Raman until full conversion to cocrystal was achieved at which point the samples were analyzed by XRPD. Figure 3.5 compares the XRPD patterns of CBZ and NCT blends containing 20% sugar (fructose or sucrose) before and after storage at 85%RH with the CBZ-NCT cocrystal XRPD pattern calculated from CSD. XRPD pattern homology between the stored blends and the cocrystal indicate cocrystal formation during storage. XRPD patterns of blends containing 10% and 50% sugars similarly showed evidence for cocrystal formation during storage.

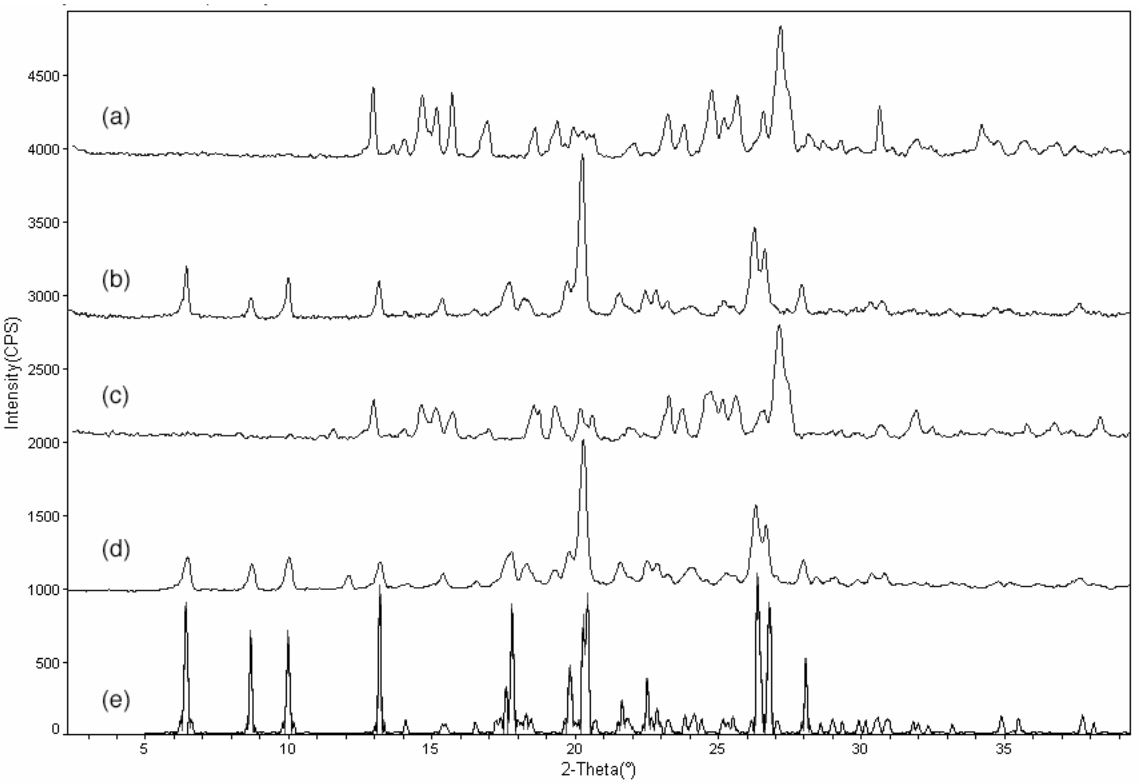

Figure 3.5: XRPD of CBZ/NCT/20% Sugar blends confirms cocrystal formation after storage at 85%RH: 20% fructose (a) before storage and (b) after storage; 20% sucrose (c) before storage and (d) after storage; (e) CBZ-NCT calculated from CSD.

The moisture sorption behavior of reactive blends was investigated since water uptake is an important factor affecting solution composition, supersaturation, and consequently cocrystal formation. Figure 3.6 shows the moisture sorption behavior of CBZ and NCT blends containing 50% sucrose or fructose at 85%RH. An increase in weight due to water uptake through deliquescence is observed for both blends. Moisture sorption is faster in the fructose blend than the sucrose blend. Both curves are characterized by a maximum in the moisture sorption behavior followed by desorption and leveling off. Desorption correlates with the depletion of NCT from solution as it is

consumed by cocrystal formation. Previous moisture uptake studies of pure CBZ-NCT cocrystal indicate very low moisture uptake (<1%) compared to NCT (>50%) at 98% RH.[28]

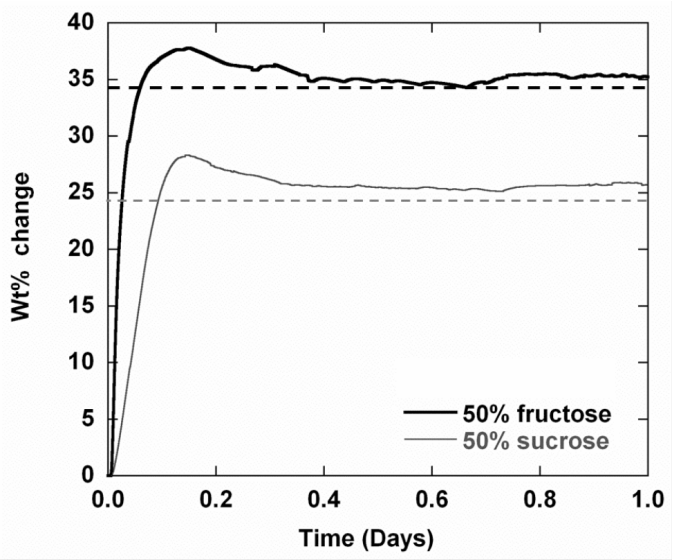

Figure 3.6: Moisture sorption in CBZ/NCT/50% Sugar (fructose or sucrose) at 85% RH. Dashed horizontal lines indicate equilibrium moisture sorption level of pure sugars scaled to the percent in the blends.

Comparison with the progress of cocrystal formation in these blends (figure 3.4) indicates that moisture sorption and cocrystal formation begin quickly and occur simultaneously. Both systems shown in figure 3.6 achieved an equilibrium level of water sorption in about half a day indicating that phase transformation to cocrystal has reached a steady state or is mostly complete. The timeframe within which this plateau is attained agrees with that shown in figure 3.4 for transformation in bulk samples with 50% sugar stored at 85%RH, and corresponds to a high level of conversion to cocrystal. Analysis of

the ternary blends by XRPD and FTIR after exposure to 85%RH in the vapor sorption analyzer confirmed cocrystal formation.

The final water content in the ternary blend containing fructose is ~35% while that containing sucrose is ~25% (figure 3.6). The equilibrium water content at 85% RH for pure sugar scaled to the amount in each blend is shown by a horizontal dashed line in figure 3.6. Thus the final water content in the ternary blends is proportional to the amount of sugars in these blends and the equilibrium moisture content of the sugars at 85%RH.

The rates of moisture sorption and reactant dissolution depend on surface area and hence particle size of the components in the blend. A decrease in cocrystal formation rate was observed in blends of larger particles (106-125μm).

Cocrystallization in binary blends

The preceding section showed that deliquescence generates cocrystals in ternary blends containing a deliquescent additive (sugar) and cocrystal reactants. However, cocrystal formation can also occur in binary blends if one or both cocrystal reactants are deliquescent. Figure 3.7(A) shows the moisture sorption behavior for an equimolar CBZ/NCT blend at 98%RH. An increase in weight is observed due to deliquescence of NCT (DRH = 94.5%) until a maximum is achieved after which desorption dominates as CBZ-NCT cocrystal (non-hygroscopic) forms. This behavior is similar to that of ternary blends with sugars shown in figure 3.6. Beyond the maximum, the weight of the binary blend decreases continuously due to depletion of NCT (hygroscopic) from solution. XRPD after storage of the binary blend for 4 days at 98%RH confirmed cocrystal formation (figure 3.7(B)).

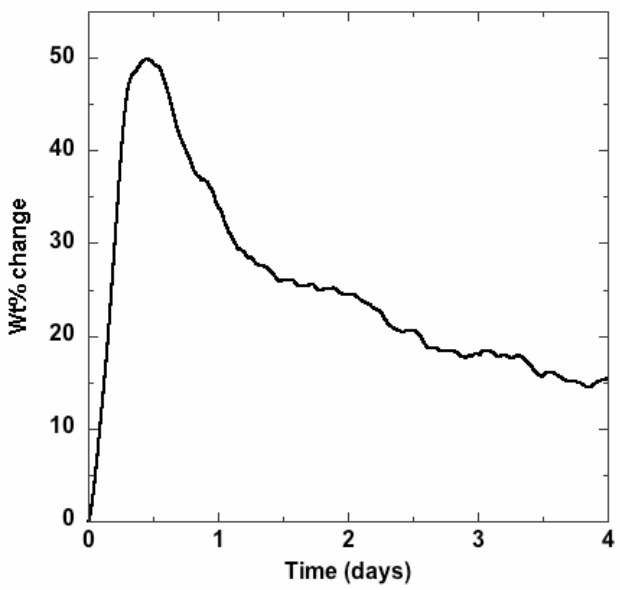

(A)

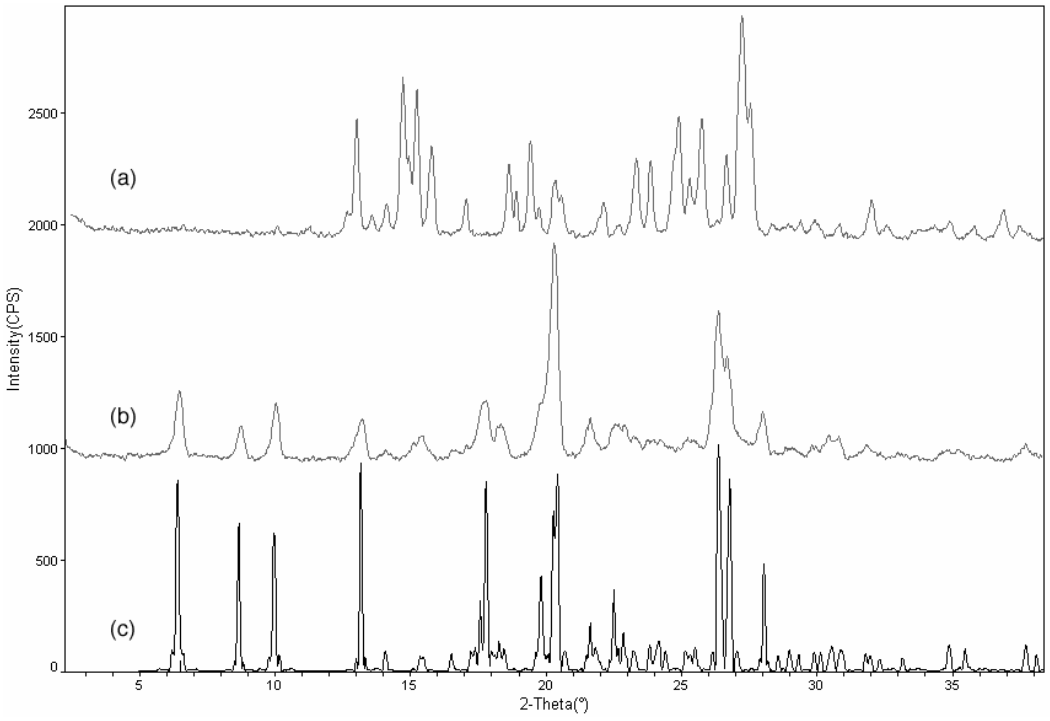

(B)

Figure 3.7: (A) Moisture sorption behavior of equimolar CBZ/NCT blend at 98% RH. (B) XRPD confirms CBZ-NCT cocrystal formation in CBZ/NCT blend after storage at 98%RH: CBZ/NCT blend (a) before storage (b) after storage and (c) CBZ-NCT cocrystal calculated from CSD.

Effect of reactant properties on cocrystal formation

The effect of cocrystal reactant properties on moisture sorption and cocrystal formation was studied by replacing NCT with SAC as the cocrystal reactant. NCT is highly hygroscopic and water soluble while SAC is non-hygroscopic, ionizable (pK_a =1.8),[38] and has lower aqueous solubility than NCT. The DRH of the SAC/fructose blend shown in table 3.2 is similar to that of pure fructose. This is due to non-hygroscopic nature and low aqueous solubility of SAC.

Figure 3.8 compares CBZ-NCT and CBZ-SAC cocrystal formation rates at 85%RH in ternary blends of CBZ/50% fructose and NCT or SAC. Clearly the rate of CBZ-SAC cocrystal formation is slower than that of CBZ-NCT. This may be a result of cocrystal solubilities, reactant dissolution rate, and ionization in the sorbed moisture.

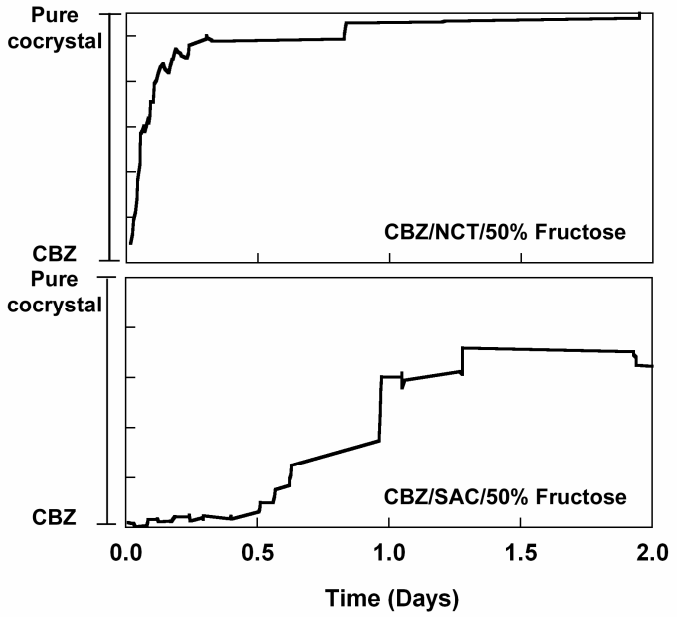

Figure 3.8: Comparison of CBZ-NCT and CBZ-SAC cocrystal formation rates at 85%RH.

Figure 3.9(A) shows CBZ-SAC cocrystal formation in ternary blends of CBZ/SAC with fructose at 85% RH. Cocrystal formation is more extensive and faster in blends with higher sugar level. Figure 3.9(B) compares cocrystal formation rates during storage of CBZ/SAC/50% fructose blends at 75% and 85%RH. These results are similar to those of CBZ/NCT/sugar blends where cocrystal formation rate increases with storage RH and sugar composition.

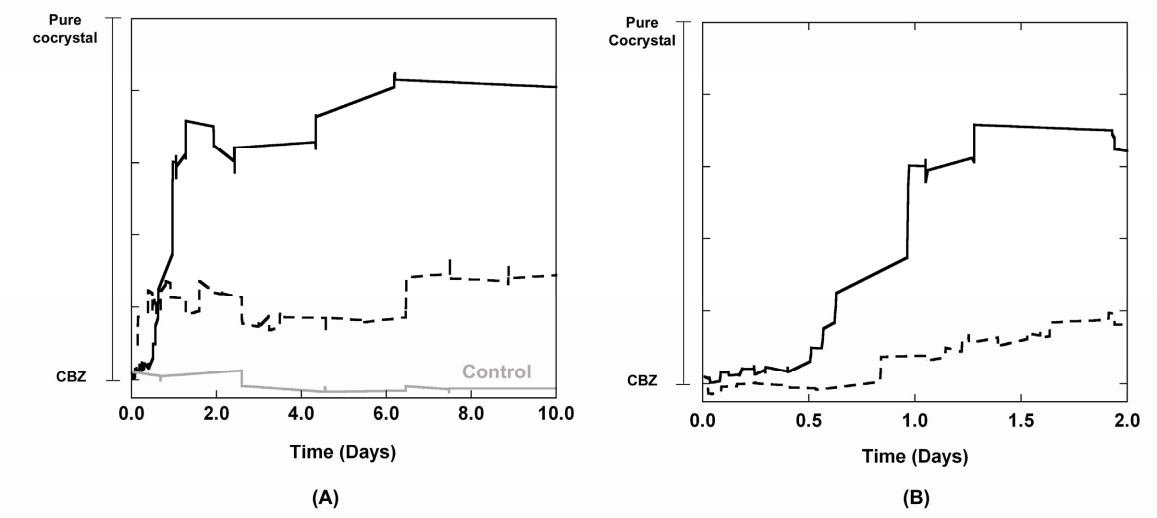

Figure 3.9: CBZ-SAC cocrystal formation rate dependence on (A) fructose composition in ternary blends exposed to 85%RH: control sample without sugar (—), 10% (- - -) and 50% (——) fructose, and (B) storage RH in CBZ/SAC/ 50% Fructose blends at 75% RH (- - -) and 85% RH (—).

Figure 3.10 shows the CBZ-SAC cocrystal formation in ternary blends of CBZ/SAC with fructose or citric acid at 85% RH. Cocrystal formation is faster in blends with citric acid and blends with higher level of additive. The transformation dependence on composition between 10% and 50% additive is similar to that of the CBZ/NCT/sugar blends.

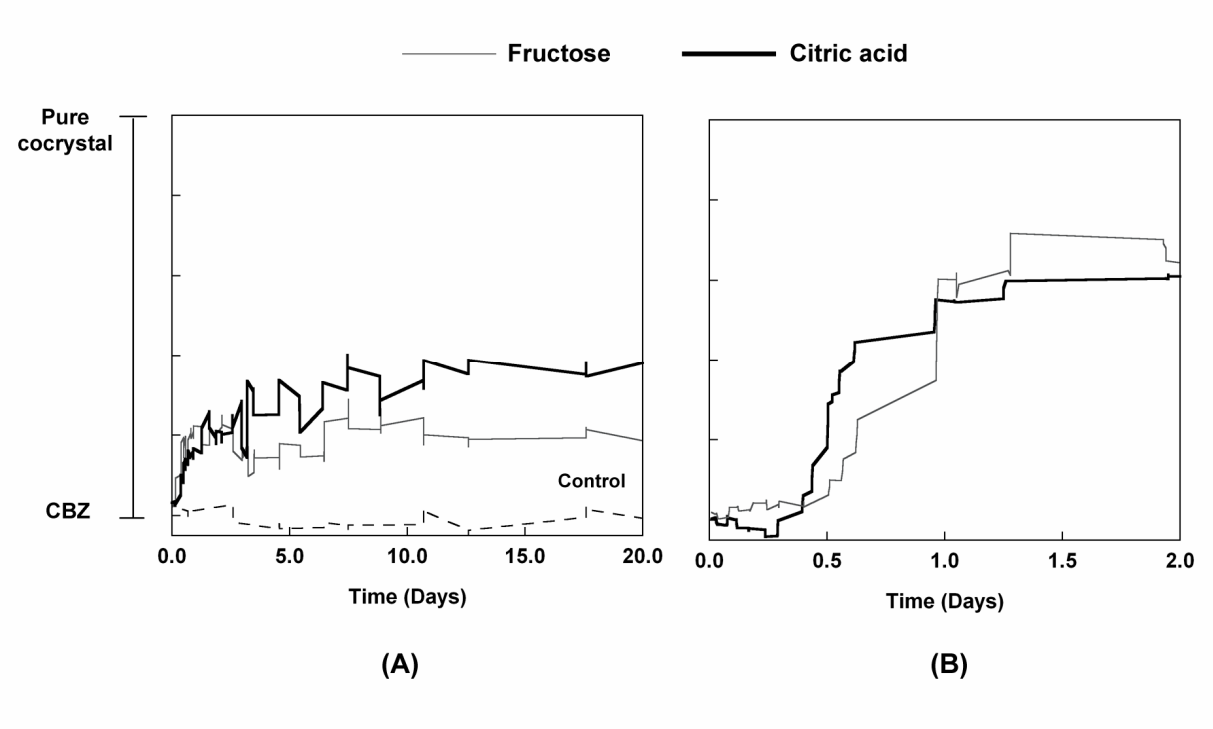

Figure 3.10: Effect of deliquescent additive (CA or fructose) composition on CBZ-SAC cocrystal formation in ternary blends exposed to 85%RH. (A) 10% additive and (B) 50% additive.

Cocrystal formation via deliquescence is broadly applicable to other compounds

Based on the above findings, transformation to cocrystal induced by deliquescence was studied with caffeine and theophylline systems. These APIs have been reported to form cocrystals from organic solvents and by co-grinding.[29, 30] Our studies show that the cocrystals in table 3.3 are generated both by slurrying the reactants in aqueous solutions and by storing ternary blends with 20% fructose above the DRH. All cocrystals have equimolar composition except theophylline-maleic acid, theophylline-oxalic acid, caffeine-malonic acid, and caffeine-oxalic acid, which have the cocrystal reactants in 2:1 (API:ligand) molar ratio. Cocrystal formation was confirmed by XRPD

analysis. These results illustrate broad applicability of the concepts presented to other APIs with a variety of cocrystal components. The kinetics of deliquescent mediated cocrystal formation in these systems is currently being investigated in our laboratory.

Table 3.3: API and corresponding ligands that formed cocrystals by both slurrying in water and deliquescence.

API	Ligand
Carbamazepine	Nicotinamide
	Saccharin
Caffeine	Oxalic acid
	Maleic acid
	Glutaric acid
	Malonic acid
Theophylline	Oxalic acid
	Maleic acid
	Glutaric acid
	Malonic acid
Sulfadimidine	Salicylic acid
	Anthranilic acid

Moisture uptake and stability of cocrystals

Results in the preceding sections show that moisture sorption can induce cocrystal formation in reactant mixtures. However, moisture uptake by cocrystals can also induce cocrystal instability. Figures 3.11 and 3.12 show the XRPD patterns of theophylline and caffeine cocrystals stored at 98%RH. Significant moisture uptake leading to deliquescence and transformation to API hydrate was observed for the cocrystals.

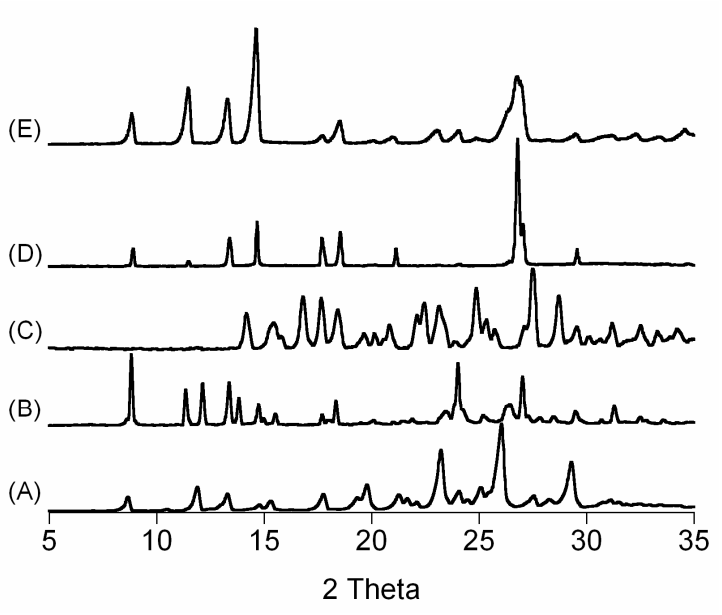

Figure 3.11: XRPD patterns showing theophylline cocrystal instability during storage at 98%RH. Theophylline-glutaric acid (A) before storage, and (B) after storage; theophylline-citric acid hydrate (C) before storage, and (D) after storage; (E) theophylline monohydrate reference pattern.

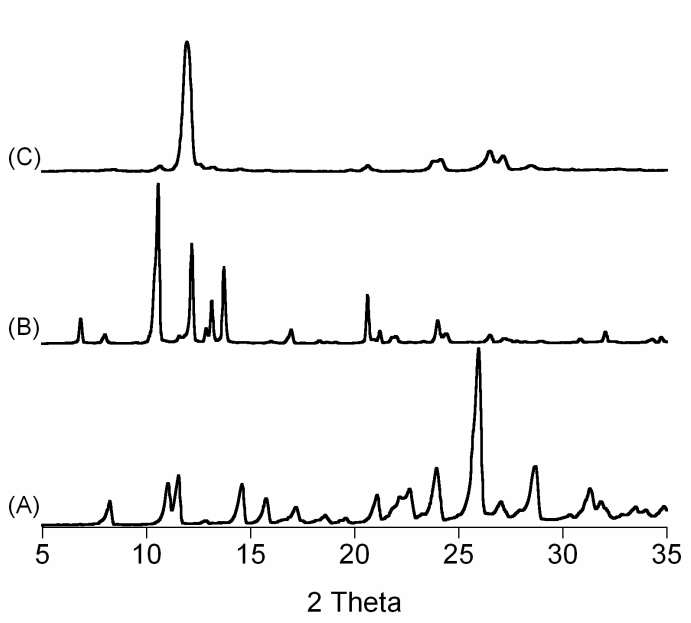

Figure 3.12: XRPD patterns indicating caffeine-glutaric acid cocrystal instability during storage at 98%RH. Caffeine-glutaric acid (A) before storage, and (B) after storage; (C) caffeine hydrate reference pattern.

Table 3.4 summarizes the moisture uptake and stability of some carbamazepine, theophylline and caffeine cocrystals at 85%, 91% and 98% RH. Moisture uptake of cocrystals increases with increase in RH. While caffeine and theophylline cocrystals deliquesce and transform to corresponding API hydrates at 98%RH, CBZ cocrystals are stable even after 6 months of storage. Raman spectra showing the stability of some of the cocrystals shown in table 3.4 are included in appendix C.

Table 3.4: Moisture uptake and stability of carbamazepine (CBZ), theophylline(THP) and caffeine(CAFF) cocrystals during storage.

Cocrystal	**Weight gain (%) and stability due to moisture uptake**		
	85% RH	**91% RH**	**98% RH**
CBZ-maleic	-	2.02 (stable)	5.44 (stable)
CBZ-Glutaric acid	-	6.3 (stable)	28.5 (stable)
THP-Glutaric acid	-	2.7 (stable)	88.4 (unstable)*
CAFF-Glutaric acid	-	2.4 (stable)	209.4 (unstable)**
THP-Citric acid (anhydrous)	6.4 (stable)	7.4 (stable)	89.4 (unstable)[1]
THP-Citric acid (hydrate)	3.8 (stable)	4.2 (stable)	202.8 (unstable)[1]

*solid phase is theophylline hydrate.
** solid phase is caffeine hydrate + unknown phase

Discussions

The results of this study indicate that cocrystals can form spontaneously when solid mixtures with cocrystal reactants deliquesce. The mechanism for deliquescence-induced cocrystal formation involves three important processes as revealed by microscopy studies (figure 3.1) and illustrated in scheme 3.1: water uptake, dissolution of cocrystal reactants, and crystallization of molecular complex. Several factors that determine transformation kinetics are nucleation rate, growth rate, and the density and distribution of nucleation sites. Cocrystal nucleation and growth rates will depend on supersaturation. Supersaturation is determined by how fast cocrystal reactants dissolve and this in turn depends on the amount and rate of water uptake.

How dissolution of cocrystal reactants leads to supersaturation with respect to cocrystal is illustrated in scheme 3.1(ii) and is explained by considering the solution and cocrystal chemistry.[31, 32] As the reactants dissolve in the sorbed moisture, their concentrations increase in solution. Unequal reactant dissolution rates, due to different solubilities and/or surface areas, result in non-stoichiometric concentrations of reactants in the sorbed moisture. As the deliquesced solution becomes rich in one of the cocrystal components, the cocrystal solubility decreases leading to ever increasing supersaturated conditions where cocrystal is the least soluble phase as shown in figure 3.13. Cocrystal formation will be initiated when the critical supersaturation for nucleation is achieved. The CBZ and NCT system is particularly interesting since their aqueous solubilities are very different. Due to the higher dissolution rate of the more soluble reactant (NCT), cocrystal nucleation occurs on the surface or in the vicinity of the less soluble reactant (CBZ) (figure 3.1).

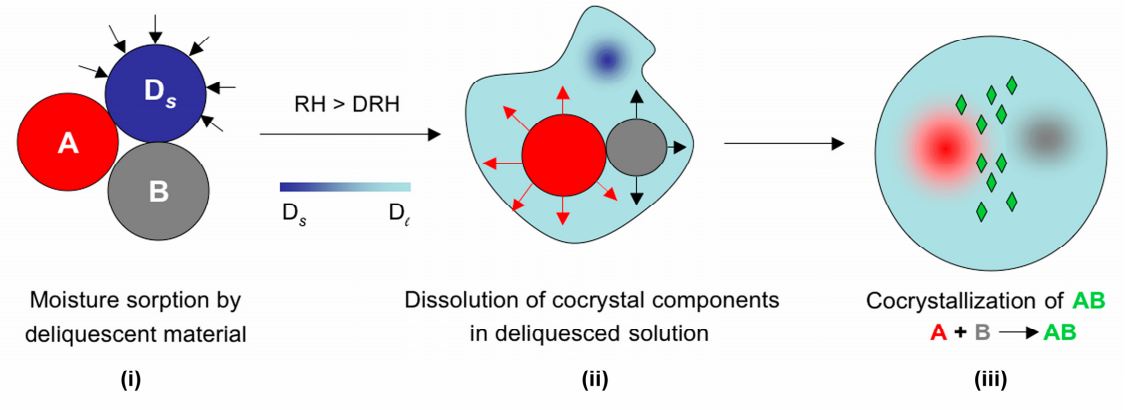

Scheme 3.1: Illustration of the moisture uptake process leading to deliquescence, reactant dissolution and cocrystal formation. A and B are cocrystal reactants, D_s is solid deliquescent additive and D_l is the solution phase created by deliquescence at RH greater than DRH.

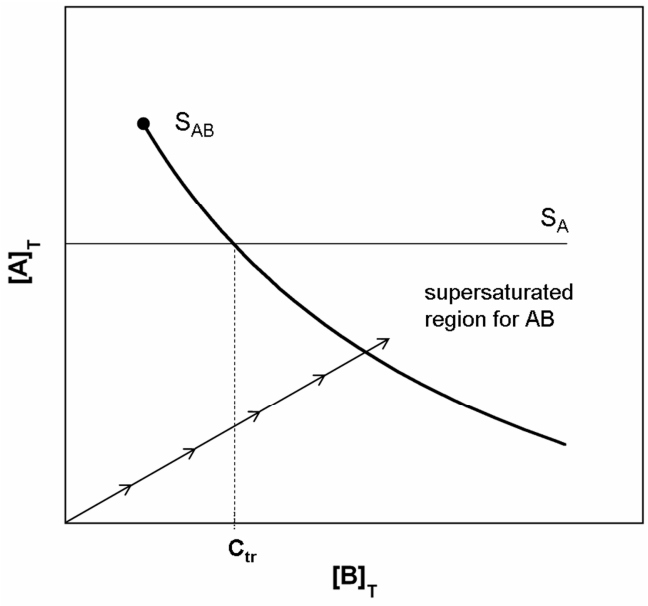

Figure 3.13: Schematic showing the solubility of cocrystal AB (S_{AB}) and pure component crystal A (S_A) as a function of ligand concentration B, the ligand transition concentration (C_{tr}) and a hypothetical cocrystallization pathway. Supersaturation is generated by the unequal dissolution rates of reactant components A and B.

Cocrystal stability

Our results show that deliquescence leads to cocrystal formation even with certain APIs that readily form hydrates during storage or by slurry conversion in water.[1-3, 5, 37, 39-42] Carbamazepine, caffeine, and theophylline spontaneously transformed to cocrystal when mixtures of cocrystal reactants with deliquescent additive were stored above the DRH of the dry mixtures. This indicates that cocrystal nucleation and growth rates were faster than the rate of hydrate formation under the conditions studied. The stability of cocrystal is also confirmed by the lack of transformation to single components or hydrates thereof.

Although deliquescence in mixtures reported here exhibited cocrystal formation and stability, a reversal can occur given the right conditions. This is shown for some theophylline and caffeine cocrystals at high relative humidity where moisture uptake leading to deliquescence and transformation of cocrystals to API hydrates occurred during storage. The transformation of cocrystals to API hydrates is indicative of higher cocrystal solubility relative to the hydrated reactant, and occurs since the reactant concentrations resulting from cocrystal dissolution in the sorbed moisture are below the transition concentration as indicated in the phase diagram (figure 3.13).[31, 32] Previous studies from our laboratory have shown that although in pure water CBZ-NCT cocrystals transform to CBZ dihydrate within minutes, the transformation is reversed (CBZ to cocrystal) at high NCT solution concentrations.[32, 33] CBZ cocrystals of NCT or SAC are not hygroscopic at 98%RH and have been shown to be stable.[27, 28] CBZ cocrystal formation during deliquescence is thus explained by the relationship between solution composition and thermodynamic stability of reactant and cocrystal phases.

Caffeine and theophylline cocrystals shown in table 3.3 formed during deliquescence of blends of API/ligand/fructose (as well as in highly concentrated aqueous solutions of ligand) even though some of these cocrystals transform to hydrated API when exposed to moisture. Caffeine-maleic acid cocrystals and theophylline cocrystals with maleic acid, malonic acid, and glutaric acid have been reported to transform to hydrated API when exposed to 98%RH.[29, 30] Caffeine-glutaric acid has been reported to transform to hydrated caffeine at 43%RH.[29] These results clearly indicate that for the direction of transformation to be reversed by aqueous solution composition there must be a transition concentration above which solubility of cocrystal is less than pure API and cocrystal formation is favorable. Therefore deliquescence will generate conditions of cocrystal stability or instability depending on solution chemistry including ionization and complexation processes.

Deliquescence and cocrystal formation

Previous studies on deliquescence and crystallization have shown hydrate formation in solid mixtures.[3, 4, 6] There are also reports of crystallization as a result of moisture loss and efflorescence due to changes in ambient RH or DRH as composition of solution changes.[35, 43, 44] It is important to note that in the studies reported here there was no RH cycling and crystallization was a result of solution composition. To our knowledge this is the first report of cocrystal formation induced by deliquescence. This finding also makes apparent the opportunity for producing cocrystals by green chemistry methods. Aqueous media can generate cocrystals as illustrated for carbamazepine, caffeine, theophylline and sulfadimidine systems.

The ability of a deliquescent material to generate cocrystals depends on its potency for moisture uptake and on its ability to modify the mode and rate of nucleation. Blends stored below their DRH did not result in cocrystal formation during the course of the study as shown by binary blends of CBZ/NCT at 85%RH and ternary blends of CBZ/NCT/sucrose at 75%RH. Transformation to cocrystal was however associated with moisture uptake and storage RH above DRH as indicated by binary blends of CBZ/NCT at 98%RH and ternary blends of CBZ/NCT/sucrose at 85%RH.

The interplay between moisture uptake and dissolution determines the liquid phase composition, supersaturation and subsequent nucleation. This is shown by the rapid initial cocrystal formation rates of CBZ-NCT at both low and high sugar composition when stored at RH above DRH. Moreover, low small levels of moisture (< 7%) are capable of producing the necessary cocrystal supersaturation to initiate nucleation as shown for the transformation to CBZ-NCT in blends with 10% sucrose or fructose at 85% RH. Deliquescent additives can also influence nucleation by their effects on solution viscosity, molecular associations that precede nucleation, and to the extent that material surfaces serve as catalysts for nucleation.

Generally one expects the amount of moisture uptake to control the transformation rate based on its temporal and spatial distribution. Low levels of deliquescent additive and low moisture uptake will have the effect of reducing the regions of deliquescence. Consequently, small domains of supersaturation can develop in a liquid phase that is not uniformly distributed throughout the sample leading to isolated regions of cocrystal formation. In this case high supersaturations are initially achieved and transformation rate to cocrystal is initially fast, but the rate will slow or even level off

before extensive conversion. This mechanism explains the transformation to CBZ-NCT cocrystal at the lower fructose composition (10%) and 75%RH.

High levels of moisture sorption allow for greater exposure of reactants to the crystallization medium and to larger extent of cocrystal formation during the initial time period, provided the kinetics and distribution of moisture sorption maintain adequate supersaturation for cocrystal formation. This behavior is observed with the CBZ/NCT/fructose at higher RH (85%) or higher fructose (20 and 50%) showing faster and more extensive conversion compared to the CBZ/NCT/fructose at 10% fructose and 75%RH. Similar behavior was observed with CBZ/SAC/fructose blends. These results clearly indicate that for low fructose composition at low RH, the transformation is occurring at relatively low moisture uptakes where solute transport tends to be limited to small domains of liquid phase. Faster transformation rates with more deliquescent additive at RH above DRH were also observed for CBZ/NCT/sucrose, CBZ/SAC/fructose, and CBZ/SAC/citric acid.

Quite a different situation arises when high amounts of moisture uptake lead to low supersaturation, saturation, or undersaturation with respect to cocrystal and consequently slow, prevent, or reverse the transformation to cocrystal. High moisture uptake levels are associated with the hygroscopic nature of the blend components, the amount of hygroscopic or deliquescent additive, and high RH values above DRH. A reversal in the transformation to cocrystal was observed at CBZ/NCT/50% fructose at 98%RH. CBZ dihydrate formed after initial formation of cocrystal (results not shown).

Moisture sorption and deliquescence of solid mixtures are a complex function of phase composition, relative humidity, and temperature.[17, 20, 21] The study presented here

has focused on identifying the mechanism by which deliquescence induces cocrystal formation. Deliquescence and phase diagrams of composition and water activity (i.e, relative humidity) for the systems reported here are currently being investigated in our laboratory.

In this first report we have compared the transformation to cocrystal with the moisture uptake behavior and deliquescence under non-equilibrium conditions. Our results show that moisture uptake behavior is an indicator of cocrystal formation as shown by binary blends with deliquescent reactant (NCT) in figure 3.7(A) and by ternary blends with deliquescent additive (sugars) in figure 3.6.

Cocrystal formation during deliquescence is also dependent on the properties of cocrystal reactants, cocrystals, and solution chemistry. Reactant properties that increase solution concentrations in the sorbed moisture such as dissolution rate and solubility are expected to increase the rate of transformation to cocrystal as shown by the CBZ-NCT cocrystal formation rate relative to CBZ-SAC. In addition, particle size and solid-state form of reactants (amorphous, polymorphs and solvated forms) will influence the transformation rate to cocrystal when dissolution is the rate-limiting step.

CBZ-NCT cocrystal formation was faster than CBZ-SAC in blends of cocrystal reactants and fructose. This behavior is explained by the dependence of supersaturation on cocrystal solubility (K_{sp} in equation 1), reactant solubility and ionization.[27] Previous studies in our laboratory have shown that the aqueous solubility of CBZ-SAC cocrystal is slightly higher than that of CBZ-NCT.[28] NCT has an aqueous solubility much higher than SAC, 8.19 M versus 0.011 M at 20^{o}C.[45] SAC is an acid (pK_a of 1.8)[38] and at solution pH higher than pK_a (> $2pK_a$) it will be largely in the ionized form. This

ionization can lower the transformation to cocrystal by decreasing the concentration of reactant available for cocrystal formation. This is applicable to cocrystals with neutral components.[46] Deliquescent additives with acidic or basic properties will therefore regulate the rate of cocrystal formation by altering the pH of the sorbed moisture. The pH of the deliquesced sugar blends will be closer to neutrality. Consequently SAC is largely in its ionized form. Citric acid solutions on the other hand can reach pH values as low as 0.5[47] and therefore a greater fraction of SAC is non-ionized. This may be the reason for the faster CBZ-SAC cocrystal formation in blends with citric acid compared to blends with fructose. The effect of deliquescent additive on moisture uptake however, needs to be determined to fully evaluate the effect of solution pH.

The mechanisms for cocrystal formation reported here are valuable to design stable formulations and predict conditions that will preserve cocrystal. The amount of deliquescent additive required to prevent or reverse the transformation to cocrystal can in principle be estimated if one knows the moisture sorption of the blend at a given composition, temperature and RH, and the C_{tr} in the sorbed moisture. For example, the C_{tr} in water at which the solubility of the CBZ-NCT cocrystal is equal to the solubility of CBZ dihydrate is around 1m.[33] As a first approximation it is assumed that additives do not change C_{tr}. Consequently, levels of moisture sorption that lead to NCT concentrations above 1m will favor cocrystal formation at adequate CBZ solution concentration as shown in figure 3.13. Based on the results for the CBZ/NCT/50% fructose at 85%RH the moisture sorbed is about 35% and corresponds to moisture retained by fructose (70% for pure fructose at 85%RH). If one considers that NCT will fully dissolve in the sorbed moisture of the ternary blend then the mass of water required to dilute NCT to the C_{tr} can

be calculated. The percentage of fructose in the dry blend that will lead to the transition concentration at 85% RH was calculated to be 80%. Therefore if CBZ-NCT cocrystal is to be preserved in such ternary blend, fructose compositions must be lower than 80% in the dry blend. Our results of cocrystal formation and stability in fructose blends are in agreement with this estimate.

Conclusions

This work demonstrates that moisture can generate cocrystals when particulate systems with cocrystal reactants are exposed to deliquescent conditions. Cocrystals of carbamazepine, caffeine, and theophylline were formed during deliquescence even when these APIs can form hydrates. The mechanisms responsible for cocrystal formation involve moisture uptake, dissolution of cocrystal reactants, cocrystal nucleation and growth. These mechanisms are important to design formulations and predict conditions that will preserve cocrystals. Cocrystal solubility dependence on aqueous solution composition and chemistry are good predictors of cocrystal formation and stability during deliquescence. Our findings have important implications for a green chemistry based approach in the use of aqueous media to produce cocrystals.

References

1. Airaksinen, S.; Karjalainen, M.; Kivikero, N.; Westermarck, S.; Shevchenko, A.; Rantanen, J.; Yliruusi, J. Excipient Selection can Significantly Affect Solid-State Phase Transformation in Formulation During Wet Granulation. *AAPS PharmSciTech.* **2005,** *6*, E311-E322.

2. Kaneniwa, N.; Yamaguchi, T.; Watari, N.; Otsuka, M. Hygroscopicity of Carbamazepine Crystalline Powders. *Yakugaku. Zasshi.* **1984,** *104*, 184-190.

3. Kesavan, J. G.; Peck, G. E. Solid-State Stability of Theophylline Anhydrous in Theophylline Anhydrous-Polyvinylpyrrolidone Physical Mixtures. *Drug Dev. Ind. Pharm.* **1996,** *22*, 189-199.

4. Otsuka, M.; Matsuda, Y. The Effect of Humidity on Hydration Kinetics of Mixtures of Nitrofurantoin Anhydride and Diluents. *Chem. Pharm. Bull.* **1994,** *42*, 156-159.

5. Pirttimaki, J.; Laine, E. The Transformation of Anhydrate and Hydrate Forms of Caffeine at 100-percent RH and 0-percent RH. *Eur. J. Pharm. Sci.* **1994,** *1*, 203-208.

6. Salameh, A. K.; Taylor, L. S. Physical Stability of Crystal Hydrates and their Anhydrates in the Presence of Excipients. *J. Pharm. Sci.* **2006,** *95*, 446-461.

7. Yoshinari, Y.; Forbes, R. T.; York, P.; Kawashima, Y. Moisture Induced Polymorphic Transition of Mannitol and Its Morphological Transformation. *Int. J. Pharm.* **2002,** *247*, 69-77.

8. Andronis, V.; Yoshioka, M.; Zografi, G. Effects of Sorbed Water on the Crystallization of Indomethacin from the Amorphous State. *J. Pharm. Sci.* **1997,** *86*, 346-351.

9. Tong, P.; Zografi, G. Effects of Water Vapor Absorption on the Physical and Chemical Stability of Amorphous Sodium Indomethacin. *AAPS PharmSciTech.* **2004,** *5*, Art. No. 26.

10. Jayasankar, A.; Somwangthanaroj, A.; Shao, Z. J.; Rodríguez-Hornedo, N. Cocrystal Formation During Cogrinding and Storage is Mediated by Amorphous Phase. *Pharm. Res.* **2006,** *23*, 2381-2392.

11. Seefeldt, K. J.; Miller, J.; Alvarez-Núñez, F.; Rodríguez-Hornedo, N. Crystallization Pathways and Kinetics of Carbamazepine-Nicotinamide Cocrystals from the Amorphous State by In-situ Thermomicroscopy, Spectroscopy and Calorimetry studies. *J. Pharm. Sci.* **2007,** *96*, 1147-1158.

12. Hancock, B. C.; Zografi, G. The Relationship Between the Glass-Transition Temperature and the Water Content of Amorphous Pharmaceutical Solids. *Pharm.*

Res. **1994,** *11*, 471-477.

13. Kontny, M. J.; Conners, J. J., Water Sorption of Drugs and Dosage Forms. In *Encyclopedia of Pharmaceutical Technology*, 2nd ed; Swarbrick, J.; Boylan, J. C.; Marcel Dekker, Inc.: New York, 2002; pp.2970-2986.

14. Kontny, M. J.; Zografi, G. Moisture Sorption Kinetics for Water-Soluble Substances IV: Studies with Mixtures of Solids. *J. Pharm. Sci.* **1985,** *74*, 124-127.

15. Salameh, A. K.; Taylor, L. S. Deliquescence in Binary Mixtures. *Pharm. Res.* **2005,** *22*, 318-324.

16. Campen, L. V.; Amidon, G. L.; Zografi, G. Moisture Sorption Kinetics for Water-Soluble Substances I: Theoretical Considerations of Heat Transport Control. *J. Pharm. Sci.* **1983,** *72*, 1381-1388.

17. Brooks, S. D.; Wise, M. E.; Cushing, M.; Tolbert, M. A. Deliquescence Behavior of Organic/Ammonium Sulfate Aerosol. *Geophys. Res. Lett.* **2002,** *29*, Art. No. 1917.

18. Carroll, S.; Craig, L.; Wolery, T. J. Deliquescence of NaCl-$NaNO_3$, KNO_3-$NaNO_3$, and NaCl-KNO_3 Salt Mixtures from 90 to 120 Degrees C. *Geochem. Trans.* **2002,** *6*, 19-30.

19. Salameh, A. K.; Mauer, L. J.; Taylor, L. S. Deliquescence Lowering in Food Ingredient Mixtures. *J. Food. Sci.* **2006,** *71*, E10-E16.

20. Salcedo, D. Equilibrium Phase Diagrams of Aqueous Mixtures of Malonic Acid and Sulfate/Ammonium Salts. *J. Phys. Chem. A.* **2006,** *110*, 12158-12165.

21. Wexler, A. S. Second-Generation Inorganic Aerosol Model. *Atmos. Environ.* **1991,** *25A*, 2731-2748.

22. Parsons, M. T.; Mak, J.; Lipetz, S. R.; Bertram, A. K. Deliquescence of Malonic, Succinic, Glutaric and Adipic Acid Particles. *J. Geophys. Res.* **2004,** *109*, Art. No. D06212.

23. Salameh, A. K.; Taylor, L. S. Deliquescence-Induced Caking in Binary Powder Blends. *Pharm.. Dev. Technol.* **2006,** *11*, 453-464.

24. Salameh, A. K.; Taylor, L. S. Role of Deliquescence Lowering in Enhancing Chemical Reactivity in Physical Mixtures. *J. Phys. Chem. B.* **2006,** *110*, 10190-10196.

25. Carstensen, J. T.; Attarchi, F.; Hou, X.-P. Decomposition of Aspirin in the Solid-State in the Presence of Limited Amounts of Moisture. *J. Pharm. Sci.* **1985,** *74*, 741-745.

26. Teraoka, R.; Otsuka, M.; Matsuda, Y. Effects of Temperature and Relative-Humidity on the Solid-State Chemical-Stability of Ranitidine Hydrochloride. *J. Pharm. Sci.* **1993,** *82*, 601-604.

27. Rodríguez-Hornedo, N.; Nehm, S. J.; Jayasankar, A. Cocrystals: Design, Properties and Formation Mechanisms. In *Encyclopedia of Pharmaceutical Technology,* 3rd ed.; Swarbrick, J., Eds.; Informa Health Care: New York, **2006**, pp.615-635.

28. Rodríguez-Spong, B. Enhancing the Pharmaceutical Behavior of Poorly Soluble Drugs Through the Formation of Cocrystals and Mesophases. Ph.D. Thesis, University of Michigan, Ann Arbor, **2005**.

29. Trask, A. V.; Motherwell, W. D. S.; Jones, W. Pharmaceutical Cocrystallization: Engineering a Remedy for Caffeine Hydration. *Cryst. Growth Des.* **2005,** *5*, 1013-1021.

30. Trask, A. V.; Motherwell, W. D. S.; Jones, W. Physical Stability Enhancement of Theophylline via Cocrystallization. *Int. J. Pharm.* **2006,** *320*, 114-123.

31. Nehm, S. J.; Rodríguez-Spong, B.; Rodríguez-Hornedo, N. Phase Solubility Diagrams of Cocrystals are Explained by Solubility Product and Solution Complexation. *Cryst. Growth Des.* **2006,** *6*, 592-600.

32. Rodríguez-Hornedo, N.; Nehm, S. J.; Seefeldt, K. F.; Pagán-Torres, Y.; Falkiewicz, C. J. Reaction Crystallization of Pharmaceutical Molecular Complexes. *Mol. Pharm.* **2006,** *3*, 362-367.

33. Jayasankar, A.; Nehm, S. J.; Rodríguez-Hornedo, N. The Use of Raman Spectroscopy for Real-Time Monitoring of Cocrystal Formation During Wet Granulation. *AAPS J.* **2006,** *8*, R6165.

34. Fleischman, S. G.; Kuduva, S. S.; McMahon, J. A.; Moulton, B.; Walsh, R. D. B.; Rodríguez-Hornedo, N.; Zaworotko, M. J. Crystal Engineering of the Composition of Pharmaceutical Phases: Multiple-component Crystalline Solids Involving Carbamazepine. *Cryst. Growth Des.* **2003,** *3*, 909-919.

35. Parsons, M. T.; Riffell, J. L.; Bertram, A. K. Crystallization of Aqueous Inorganic-Malonic Acid Particles: Nucleation Rates, Dependence on Size and Dependence on the Ammonium-to-Sulfate Ratio. *J. Phys. Chem. A.* **2006,** *110*, 8108-8115.

36. Rodríguez-Hornedo, N.; Nehm, S. J.; Jayasankar, A. Process Analytical Technologies to Analyze and Control Cocrystallization. *Am. Pharm. Rev.* **2007** *10*, 46-55.

37. Murphy, D.; Rodríguez-Cintrón, F.; Langevin, B.; Kelly, R. C.; Rodríguez-Hornedo, N. Solution-mediated Phase Transformation of Anhydrous to Dihydrate

Carbamazepine and the Effect of Lattice Disorder. *Int. J. Pharm.* **2002,** *246*, 121-134.

38. Zubair, M. U.; Hassan, M. M. A., Saccharin. In *Analytical Profiles of Drug Substances*; Florey, K., Eds.; Academic Press: Orlando, **1984,** pp. 487-519.

39. Rodríguez-Hornedo, N.; Lechuga-Ballesteros, D.; Wu, H. J. Phase-Transition and Heterogenous Epitaxial Nucleation of Hydrated and Anhydrous Theophylline Crystals. *Int. J. Pharm.* **1992,** *85*, 149-162.

40. Rodríguez-Hornedo, N.; Murphy, D. Surfactant-Facilitated Crystallization of Dihydrate Carbamazepine During Dissolution of Anhydrous Polymorph. *J. Pharm. Sci.* **2004,** *93*, 449-460.

41. Ticehurst, M. D.; Storey, R. A.; Watt, C. Application of Slurry Bridging Experiments at Controlled Water Activities to Predict the Solid-State Conversion between Anhydrous and Hydrated Forms Using Theophylline as a Model Drug. *Int. J. Pharm.* **2002,** *247*, 1-10.

42. Zhu, H.; Yuen, C.; Grant, D. J. W. Influence of Water Activity in Organic Solvent + Water Mixtures on the Nature of the Crystallizing Drug Phase . 1. Theophylline. *Int. J. Pharm.* **1996,** *135*, 151-160.

43. Braban, C. F.; Abbatt, J. P. D. A Study of the Phase Transition Behavior of Internally Mixed Ammonium Sulfate-Malonic Acid Aerosols. *Atmos. Chem. Phys.* **2004,** *4*, 1451-1459.

44. Zhang, Y. H.; Hu, Y. A.; Ding, F.; Zhao, L. J. FTIR-ATR Chamber for Observation of Efflorescence and Deliquescence Processes of $NaClO_4$ Aerosol Particles on ZnSe Substrate. *Chinese Sci. Bull.* **2005,** *50*, 2149-2152.

45. O'Neil, M. J., *The Merck index*. 13th Merck & Co., Inc: New Jersey, 2001.

46. Bethune, S. J. Thermodynamic and Kinetic Parameters that Explain Solubility and Crystallization of Pharmaceutical Cocrystals. Ph.D. thesis, University of Michigan, Ann Arbor, **2008**.

47. Maffia, M. C.; Meirelles, A. J. A. Water Activity and pH in Aqueous Polycarboxylic Acid Systems. *J. Chem. Eng. Data.* **2001,** *46*, 582-587.

CHAPTER IV

FACTORS THAT AFFECT THE FORMATION AND THERMODYNAMIC STABILITY OF COCRYSTAL HYDRATES

Introduction

Water-solid interactions are frequently encountered during processing and storage of pharmaceutical solids. Such interactions often lead to phase transformations such as amorphous to crystalline conversions and polymorphic transformations.[1-3] Water, when incorporated in the crystal lattice along with a drug molecule, results in the formation of hydrates.[4] Hydrate formation during processing or storage can adversely affect pharmaceutical performance and processability.[5-10]

Recent studies have shown that pharmaceutical cocrystals or crystalline complexes, consisting of an API and coformer, provide greater stability against hydration. Cocrystals of carbamazepine, caffeine and theophylline are shown to prevent API hydrate formation at relative humidities where the anhydrous APIs generally transform to hydrates.[11-13] Cocrystals are also shown to prevent deliquescence as with carbamazepine-nicotinamide cocrystal.[13] Cocrystal design based on crystal engineering strategies and principles further allows modulation of other API properties such as solubility, dissolution rates and bioavailability as well as mechanical properties.[13-20] Cocrystals are therefore pursued as potential solid forms in drug development, and screening strategies for API cocrystals have received considerable attention.[21-27]

While the majority of API cocrystals are anhydrous,[11, 12, 28-30] few are also reported to exist as hydrates.[24, 26, 31] In most cases, cocrystal hydrates were serendipitously identified using organic solvents,[24, 31] and the conditions governing the formation of cocrystal hydrates are not known. This study therefore aims to identify the factors and conditions that govern their formation and stability.

Water activity is well known to affect the stability of pharmaceutical hydrates.[32-34] Since the water activity is dependent on solution compositions,[35, 36] it can be altered by varying the solution composition. This is achieved by addition of solution additives or excipients to aqueous solution. Studies from our lab have shown that coformer aqueous concentration affects cocrystal stability. Thus, the addition of coformer to aqueous solutions can also alter the water activity. Further, water activity when expressed in percentage is equal to relative humidity (RH): RH = a_w x 100%.[37] Thus the stability of hydrates will also depend on RH. The current study examines (1) the effect of coformer, excipient and cosolvent aqueous concentrations on cocrystal hydrate formation and stability, (2) the effect of relative humidity (RH) on cocrystal hydrate and anhydrous cocrystal formation during storage of reactant mixtures, and (3) the relative thermodynamic stabilities of anhydrous and hydrated cocrystals. Results presented here have significant implications for anticipating phase transformations and controlling phase stability during processing and storage.

The model cocrystals selected in the current study include theophylline-citric acid (THP-CTA) and carbamazepine-4-aminobenzoic acid (CBZ-4ABA) cocrystals since anhydrous and hydrated cocrystalline phases have been identified for both systems.[24, 31] The hydrated cocrystalline phases in both systems were serendipitously identified by

slow evaporation using organic solvents or by cogrinding reactants.[24, 31] THP-CTA and CBZ-4ABA were further selected as models systems due to differences in properties of the coformers. Citric acid is highly water soluble, deliquescent coformer, and is known to decrease the water activity at high concentrations.[38] 4ABA, on the contrary, has low aqueous solubility.[39] These differences in coformer properties enable the evaluation of coformer effects on cocrystal hydrate formation and stability. The effect of excipients and cosolvents on water activity and cocrystal hydrate stability was examined using fructose and acetonitrile, respectively. Addition of fructose or acetonitrile to aqueous solutions is known to decrease the water activity.[40-42]

Experimental section

Materials

Anhydrous theophylline (THP), anhydrous form (III) monoclinic carbamazepine (CBZ), and α-form 4-aminobenzoic acid (4ABA) used in the studies were purchased from Sigma Aldrich. Anhydrous citric acid (CTA) was purchased from Fisher Scientific. All chemicals were characterized by X-ray powder diffraction (XRPD) and Raman spectroscopy prior to use. Ethanol and 2-propanol, purchased from Sigma Aldrich, were dried using molecular sieves prior to use.

Methods

Cocrystal preparation

Anhydrous and hydrated cocrystals of theophylline-citric acid (THP-CTA) and carbamazepine-4-aminobenzoic acid (CBZ-4ABA) were prepared by the reaction crystallization method.[21, 43]

Carbamazepine-4aminobenzoic acid cocrystal (CBZ-4ABA): 2:1 anhydrous CBZ-4ABA was prepared by suspending 200 mg of CBZ(III) in 3g of 0.6m 4ABA ethanolic solution. 2:1:1 CBZ-4ABA cocrystal hydrate was prepared by suspending 1.72g CBZ(III) in 0.5g 4ABA aqueous solution. The suspensions were magnetically stirred at room temperature for 12 hours. The solid phases after filtration were characterized by XRPD and Raman spectroscopy. XRPD patterns of the solid phases from ethanol and aqueous suspensions were compared with the simulated pattern of the anhydrous and hydrated cocrystals from the crystal structure database (CSD) to confirm they were cocrystals.

Theophylline-citric acid cocrystal (THP-CTA): Anhydrous THP-CTA cocrystal was prepared by suspending 200 mg anhydrous theophylline in 11.4g of 1.89m citric acid solution in ethanol. Cocrystal hydrate was prepared by suspending 1.5g anhydrous theophylline in 9.0g of 5m aqueous citric acid solution. The suspensions were stirred overnight and the solid phases were characterized by XRPD and Raman spectroscopy. XRPD patterns of the solid phases from ethanol and aqueous suspensions were compared with the simulated patterns of the anhydrous and hydrated cocrystals from CSD to confirm they were cocrystals.

Coformer, excipient and cosolvent effects on cocrystal hydrate stability

Theophylline-citric acid cocrystal: Cocrystal hydrate stability dependence on coformer (citric acid) solution concentration was examined by suspending excess cocrystal hydrate in aqueous solutions with varying coformer concentrations. The suspensions were magnetically stirred in a water bath at 25°C for 24 - 48 hours prior to adding anhydrous cocrystal. The suspensions were then stirred for 2-3 weeks to reach equilibrium. Solution concentrations of theophylline and citric acid at equilibrium were measured using HPLC. Equilibrium was considered to be achieved when the solution concentrations reached steady values. Solid phases were characterized by Raman spectroscopy and XRPD. The water activities of the equilibrated suspensions were determined by measuring the RH above the suspensions using a Hydroclip RH probe from Rotronics (Huntington, NY).

Excipient effect on water activity and cocrystal hydrate stability can be examined by selecting excipients that modulate the water activity of aqueous solutions. Sugars such as sucrose and fructose have been shown to decrease the water activity of water as well as citric acid aqueous solutions.[44] The chemical stability of sugars in the presence of acid is also reported in the literature. In this study fructose was selected as the excipient since it is reported to be stable in the presence of citric acid while sucrose undergoes acid catalyzed inversion.[44, 45]

Excess THP-CTA hydrate was suspended in aqueous fructose-citric acid solutions with varying fructose concentration but constant citric acid concentration (6.05moles/kg water) at 25°C. The suspensions were allowed to reach equilibrium as described above. Solid phase stability in suspensions was periodically monitored using Raman

spectroscopy and XRPD. The water activity of the suspensions was determined by measuring the RH as described above.

Carabamazepine-4-aminobenzoic acid cocrystal: Anhydrous and hydrated cocrystal stability in pure water, and cocrystal hydrate stability in saturated aqueous 4ABA solution was examined by suspending excess anhydrous or hydrated cocrystal in water or 4ABA solution. The suspensions were magnetically stirred for 7 days at 25°C, and the solid phases were characterized by Raman spectroscopy and XRPD.

Cocrystal hydrate stability was also studied in aqueous solutions with varying amounts of cosolvent by suspending excess cocrystal hydrate in cosolvent-water mixtures with varying water activity. The suspensions were magnetically stirred for 48 hours at 25°C prior to adding anhydrous cocrystal. The suspensions were then stirred for an additional two weeks. Solid phases were characterized by Raman spectroscopy and XRPD to monitor phase transformations.

The addition of a cosolvent such as methanol, ethanol, isopropyl alcohol (IPA) or acetonitrile (ACN) is known to decrease the water activity of aqueous solutions.[33, 42, 46] In the current study, acetonitrile was selected as the model cosolvent to examine the effect of cosolvent concentrations on cocrystal hydrate stability as well as to measure the critical water activity of cocrystal hydrate. Cosolvent selection was based on preliminary stability studies that showed transformation of anhydrous cocrystal to crystalline drug in neat alcohols and alcohol-water mixtures with low water activities, whereas the cocrystal was stable in neat ACN. A key requirement for critical water activity measurement is the coexistence of anhydrous and hydrated crystalline phases in equilibrium with the solution

at the critical water activity. Since the anhydrous cocrystal was stable in ACN, ACN-water mixtures were used to measure the critical water activity.

The water activity of ACN-water mixtures as a function of water composition has been reported in a previous study,[42] and is estimated using the following equations:

$$a_w = x_w.\gamma_w \quad (1)$$

a_w is the water activity, x_w is mole fraction water and γ_w is the activity coefficient of water in ACN-water mixtures. γ_w can be estimated using the Wilson equation:

$$\ln(\gamma_w) = -\ln(x_w + \Lambda_{w,acn} x_{acn}) + x_{acn}\left[\frac{\Lambda_{w,acn}}{x_w + \Lambda_{w,acn}} - \frac{\Lambda_{acn,w}}{\Lambda_{acn,w} x_w + x_{acn}}\right] \quad (2)$$

$\Lambda_{acn,w}$ and $\Lambda_{acn,w}$ in equation (2) are evaluated from the following equations:

$$\Lambda_{w,acn} = \frac{v_w}{v_{acn}} e^{\left[\frac{-(\lambda_{w,acn} - \lambda_{ww})}{RT}\right]} \quad (3)$$

$$\Lambda_{acn,w} = \frac{v_{acn}}{v_w} e^{\left[\frac{-(\lambda_{w,acn} - \lambda_{acn,acn})}{RT}\right]} \quad (4)$$

The values $(\lambda_{w,acn}-\lambda_{ww})$ and $(\lambda_{w,acn}-\lambda_{acn,acn})$ were obtained from literature, and are 6745 and 1379 J/mol, respectively.[42] The values of υ_{acn} and υ_w are 52.86 and 13 ml/mol, respectively.[42] The water activity dependence on solution composition for ACN-water mixtures, estimated from the above equations, is shown in figure 4.1.

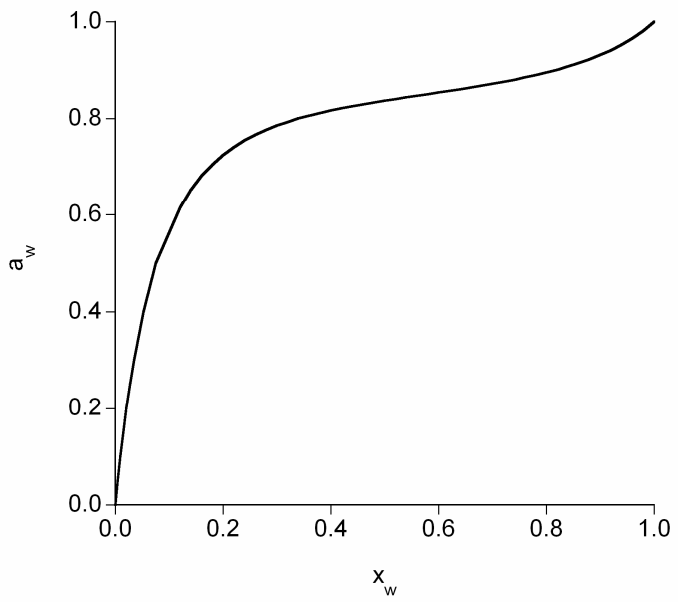

Figure 4.1: Water activity (a_w) as a function of mole fraction water (x_w) for ACN-water mixtures.

Transition concentration measurements for THP-CTA cocrystals

Three transition concentrations or eutectic points (c_1, c_2, and c_3) were identified for the THP-CTA cocrystals in water at 25˚C. The transition concentration (c_1) between theophylline hydrate and cocrystal hydrate was determined by measuring the reactant concentrations (theophylline and citric acid) in water saturated with theophylline hydrate and cocrystal hydrate. Saturation with respect to the two crystalline phases was achieved by suspending excess anhydrous theophylline in 1.8m citric acid aqueous solution. The suspensions were allowed to reach equilibrium by magnetically stirring at 25°C. Solid phase and solution concentration were monitored. Equilibrium was considered to be achieved when solution concentrations reached a steady value while two solid phases coexist. The solid phases in suspension were characterized by Raman spectroscopy.

Solutions were analyzed for theophylline and citric acid concentrations by HPLC. The suspensions were filtered and the solid phases were characterized by XRPD.

The transition concentration c_2 was determined by saturating water with anhydrous and hydrated cocrystals. This was achieved by adding anhydrous and hydrated cocrystals to 7.2m citric acid. c_3 was determined by saturating water with anhydrous cocrystal and citric acid hydrate. The procedures for analysis of solid and liquid phases were similar to those described above. The water activities corresponding to the transition concentrations were determined by measuring the RH above the equilibrated suspensions using the hydroclip RH probe.

Stability and transformations during storage

The role of deliquescence on cocrystal formation in solid mixtures of theophylline and anhydrous citric acid at 75%, 85% and 98%RH at 25°C was studied using the procedures described in an earlier study.[47] Approximately 50mg mixtures were stored in glass desiccators equilibrated to the desired RH using appropriate saturated salt solutions: NaCl for 75%, KCl for 85% and K_2SO_4 for 98%RH.[48] The particle size of the reactants used in the study was 45-63 microns. Transformation during storage was monitored using a non-contact fiber optic Raman probe. Solid phases were also characterized by XRPD.

Moisture uptake and stability of THP-CTA cocrystal hydrate was also investigated at 75%, 85% and 98%RH at 25°C. Solid phase stability and transformation was monitored Raman spectroscopy and XRPD.

Raman spectroscopy

Raman spectra of solid phases were collected with a Kaiser Optical Systems, Inc. (Ann Arbor, MI), RXN1 Raman spectrometer equipped with a 785 nm laser. Solid phase transformations were monitored using an immersion or non-contact fiber optic probe. The immersion probe was used to collect the spectra of solid phases in aqueous suspensions and the non-contact probe was used to monitor transformations in solid mixtures during storage. The spectra were collected between 100 and 1800 cm^{-1} with a resolution of 4 cm^{-1} using the vendor supplied Holograms software.

X-ray Powder Diffraction

A bench top Rigaku Miniflex X-ray powder Diffractometer (Danvers, MA) using Cu Kα radiation (λ = 1.54Å), a tube voltage of 30kV, and a tube current of 15mA was used to collect XRPD patterns of solid phases. Data was collected from 2˚ to 40˚ at a continuous scan rate of 2.5 deg/min.

High Performance Liquid Chromatography (HPLC)

A Waters system (Milford, MA) equipped with a 5µm C18 Atlantis column (4.6 x 250mm; Waters, Milford, MA) and UV/Vis detector was used to measure theophylline and citric acid concentrations with a gradient method. The mobile phase was flowed through the column at 1ml/min and the composition was varied from 40% methanol to 5% methanol in water with 0.1% trifluoroacetic acid. 20µL of samples were injected into the column, and data collection and processing was performed using the vendor provided Empower software.

Theophylline and citric acid concentrations were also measured using an isocratic method and a HPLC system from Agilant Technologies. Mobile phase composition was 0.2% trifluoroacetic acid and 30% methanol in water. Mobile phase flow rate was 1ml/min and sample injection volumes were 25μL.

Thermal analysis

Thermal analysis of samples was carried out using a TA 2590 DSC (TA instruments, New Castle, DE) which was calibrated for temperature and cell constants using indium and n-dodecane. Samples (3-5 mg), crimped in hermetic sealed pans with pinholes, were analyzed in the DSC from 15 to 200°C at a heating rate of 10 °C/min. Samples were continuously purged with nitrogen at 50 ml/min. Samples were also analyzed on a TA 2950 TGA (TA instruments, New Castle, DE) to determine the mass change in samples due to dehydration. Samples were heated from 25°C to 170°C at a heating rate of 10°C/min.

Results

Effect of coformer concentration on cocrystal hydrate stability

Cocrystal hydrate stability in aqueous solutions is dependent on coformer concentration. XRPD patterns in figure 4.2 show that theophylline-citric acid (THP-CTA) cocrystal hydrate is stable at coformer concentrations between 2.39m and 6.80m. Above 7.31m citric acid, cocrystal hydrate transforms to anhydrous cocrystal, while transformation to theophylline hydrate occurs below 1.62m citric acid. Previous studies have shown coformer concentration dependent stability and transformation of anhydrous

cocrystal to crystalline drug.[21, 26, 43, 49] To our knowledge, this is the first study showing coformer concentration dependent stability and transformation of a hydrated cocrystal to anhydrous cocrystal or crystalline drug hydrate.

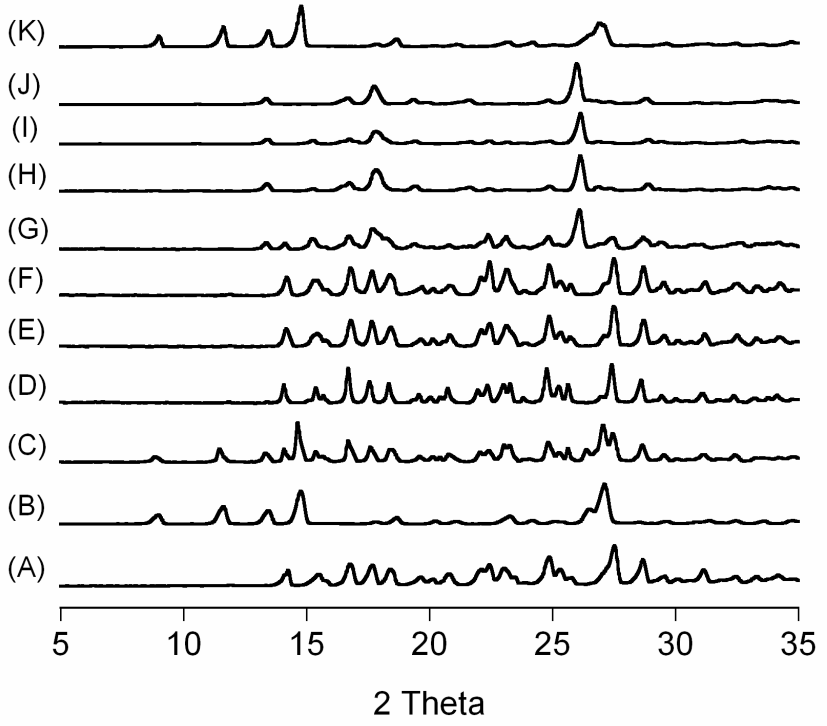

Figure 4.2: XRPD patterns showing transformation of (A) THP-CTA cocrystal hydrate in solutions of varying coformer concentrations (B) 0.19m, (C) 1.62m, (D) 2.39m, (E) 6.68m, (F) 6.80m, (G) 7.31m, (H) 7.76m, and (I) 9.12m; reference XRPD of (J) anhydrous cocrystal, and (K) theophylline hydrate.

Cocrystal stability domains

Studies with other cocrystalline systems have shown that the key parameter to identify cocrystal stability domains in coformer solutions is the transition concentration (C_{tr}), an isothermal invariant point at which two solid phases are in equilibrium with the solution.[21, 26, 43, 49] Results from stability studies of THP-CTA cocrystals suggest that

there are three transition concentrations (c_1, c_2 and c_3). The solid phases in equilibrium with the solution at c_1, c_2 and c_3 are API hydrate/cocrystal hydrate, cocrystal hydrate/anhydrous cocrystal, and anhydrous cocrystal/coformer hydrate, respectively. The reactant concentrations and solid phases at equilibrium at the transition concentrations are summarized in table 4.1.

Table 4.1: Reactant concentrations and solid phases at equilibrium at the transition concentrations (C_{tr}) for THP-CTA cocrystals at 25°C.

C_{tr}	[THP][a] (m)	[CTA][a] (m)	Solid phases at equilibrium
c_1	0.1225 ± 0.0003	1.62 ± 0.05	Theophylline hydrate, cocrystal hydrate
c_2	0.0313 ± 0.0030	7.31 ± 0.01	Cocrystal hydrate, anhydrous cocrystal
c_3	0.0278 ± 0.0004	9.44 ± 0.20	Anhydrous cocrystal, citric acid hydrate

[a]concentrations are mean ± standard deviation.

From the C_{tr} values, the stability domains of the different crystalline phases can be identified on a phase solubility diagram (PSD) as shown in figure 4.3. Lines and curves between experimentally measured values were drawn based on the behavior of the cocrystal solubility dependence on coformer for other systems.[26, 43, 49] Cocrystal hydrate is the solid phase in equilibrium with solutions having reactant concentrations between c_1 and c_2, while the anhydrous cocrystal is the equilibrium solid phase in solutions with reactant concentrations between c_2 and c_3. Theophylline hydrate is the equilibrium solid phase in solutions with reactant concentrations below c_1, and citric acid hydrate is the equilibrium solid phase at reactant concentrations between 'b' and c_3.

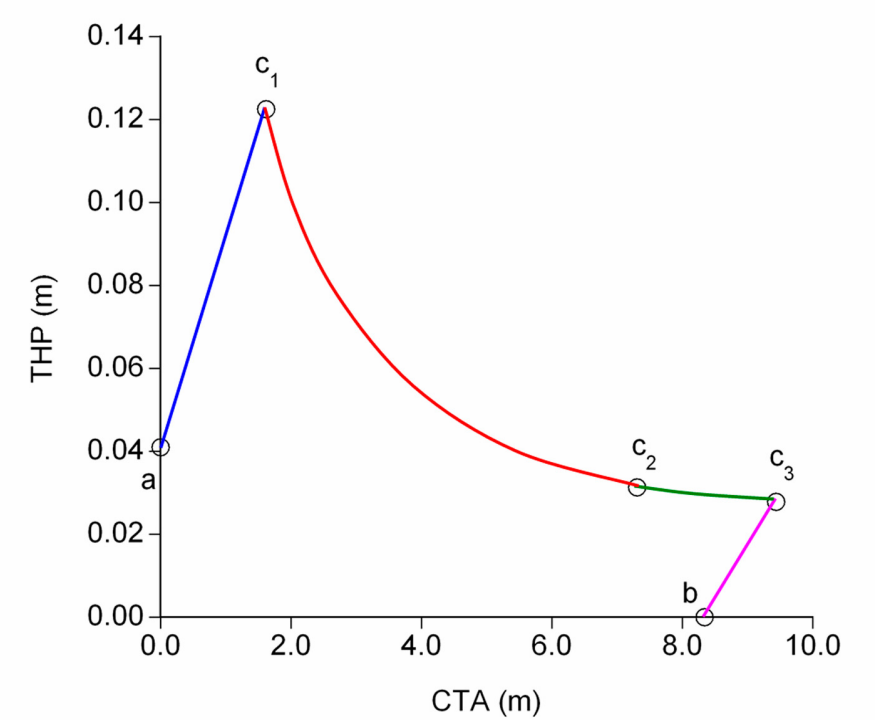

Figure 4.3: Phase solubility diagram of theophylline-citric acid cocrystals showing the stability domains and solubility dependence on coformer concentrations for the different crystalline phases. c_1, c_2, and c_3 represent transition concentrations. 'a' and 'b' represent the aqueous solubilities of theophylline hydrate and citric acid hydrate as obtained from literature.[9, 50] Lines through a, c_1, c_2, c_3, and b are drawn based on the behavior of the cocrystal solubility dependence on coformer for other cocrystal systems. The stability domains of crystalline phases are: ac_1 - theophylline hydrate, c_1c_2 - cocrystal hydrate, c_2c_3 - anhydrous cocrystal, bc_3 - citric acid hydrate.

Drug and cocrystal solubility dependence on coformer concentration can also be predicted from the C_{tr} values as shown in figure 4.3. Theophylline concentration at c_1 is higher than theophylline hydrate solubility in pure water[33] (point 'a' in PSD). This indicates that the drug solubility increases with coformer concentration from 'a' to c_1, possibly due to solution interactions such as complexation,[49, 51] hydrotropy,[52] etc. Theophylline concentration at c_2 is less than that at c_1 suggesting a decrease in cocrystal hydrate solubility with increase in coformer concentrations. Studies with other

cocrystalline systems showing similar cocrystal solubility dependence on coformer concentration have indicated that cocrystal solubility is described by the solubility product principle.[43, 49]

Conversion of cocrystal hydrate to anhydrous cocrystal at coformer concentrations beyond c_2 is explained by the effect of coformer concentration on water activity, a factor well known to affect the stability of pharmaceutical hydrates.[32, 33, 53] The water activities of aqueous citric acid solutions are reported in literature,[38, 54] and are slightly higher (~ 5%) than those measured in the current study (table 4.2). This may be due to differences in solution interactions in the presence of theophylline as well as differences in methods used to measure the water activity. The transformation of cocrystal hydrate to anhydrous cocrystal with increasing coformer concentration must be due to lowering of water activity by the coformer. The critical water activity above which cocrystal hydrate is stable is 0.80.

Table 4.2: Water activity and cocrystal hydrate stability dependence on citric acid concentration at 25.0 ± 0.5 °C.

Citric acid (m)	Water activity (a_w)	Solid phase at equilibrium
1.62[a]	0.95	Theophylline hydrate, cocrystal hydrate
2.39	0.89	Cocrystal hydrate
6.68	0.83	Cocrystal hydrate
6.80	0.81	Cocrystal hydrate
7.31[b]	0.80	Cocrystal hydrate, anhydrous cocrystal
7.76	0.80	Anhydrous cocrystal
9.12	0.78	Anhydrous cocrystal

[a]transition concentration $c_{1;}$ [b]transition concentration c_2

Effect of excipients on cocrystal hydrate stability

In addition to the coformer, excipients such as sugars used in pharmaceutical formulations can also lower the water activity of aqueous solutions. Fructose is reported to lower the water activity of aqueous solutions.[40, 41] The water activity of saturated solution of fructose is 0.64.[40, 41] Therefore, the addition of fructose to aqueous solutions is expected to alter cocrystal hydrate stability. Since cocrystal hydrate is unstable and transforms to crystalline drug hydrate in aqueous solution without citric acid, fructose effect on cocrystal hydrate stability was investigated by adding varying amounts of fructose to aqueous solutions with fixed coformer concentration (6.05 mol/kg water) in which cocrystal hydrate is the stable phase.

Table 4.3 shows the effect of fructose addition on water activity and cocrystal hydrate stability in aqueous citric acid solutions. Addition of fructose decreases the water activity of aqueous citric acid solutions. XRPD patterns in figure 4.4 show that cocrystal hydrate is the stable phase in aqueous citric acid solution without fructose (a_w = 0.84). As the water activity is lowered by fructose addition, cocrystal hydrate transforms to anhydrous cocrystal at a_w = 0.79. Based on these results, the critical water activity above which the cocrystal hydrate is stable is above 0.79. This is in agreement with the critical water activity reported in the preceding section.

Table 4.3: Water activity of fructose-citric acid aqueous solutions at 25.0 ± 0.5 °C

CTA (m)	Fructose (m)	a_w	Solid phases at equilibrium
6.05	0.00	0.84	Cocrystal hydrate
6.05	0.94	0.82	Cocrystal hydrate
6.05	3.72	0.79	Anhydrous cocrystal

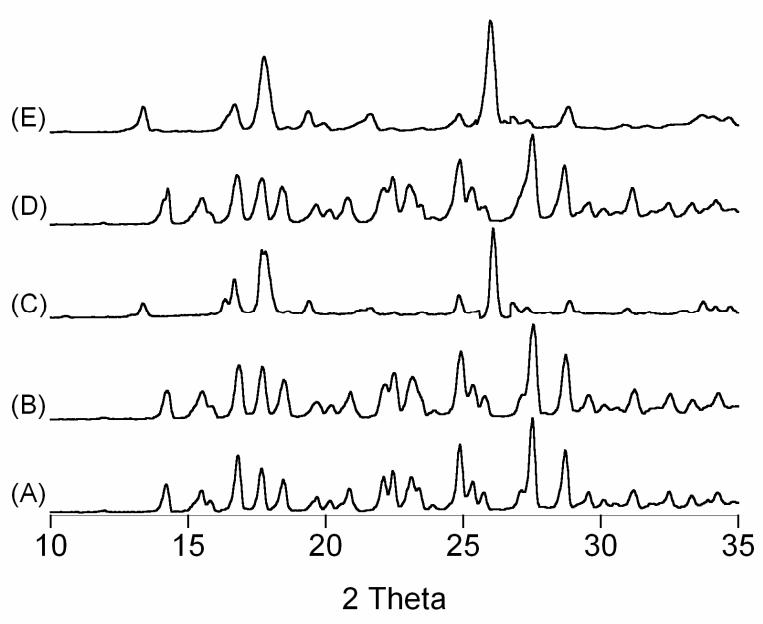

Figure 4.4: XRPD showing transformation of THP-CTA cocrystal hydrate as a function of water activity. Water activity was varied by addition of fructose to 6.05m aqueous CTA solutions. (A) $a_w = 0.84$, (B) $a_w = 0.82$, and (C) $a_w = 0.79$. Reference patterns of (D) cocrystal hydrate, and (E) anhydrous cocrystal. Solid phases were analyzed after 2 weeks.

Effect of relative humidity on cocrystal formation and stability

Results from the above studies show that the transformation of cocrystal hydrate to anhydrous cocrystal is governed by water activity. Water activity when expressed in percentage is equal to relative humidity (RH).[37] RH dependent transformation of reactant mixtures to cocrystal during storage has been shown in a previous study.[47] Transformation in these mixtures occurred due to deliquescence of reactants during storage. Citric acid is a deliquescent material and its deliquescence RH (DRH) is 75%RH at 25°C[44]. Therefore, the effect of RH on cocrystal formation and stability was studied in mixtures of THP/CTA at 75%, 85% and 98% RH at 25°C.

Figure 4.5 shows the XRPD patterns of theophylline/citric acid mixtures after storage at various RH. The powder pattern indicates anhydrous cocrystal formation after storage at 75%RH for 6 weeks. A mixed phase of anhydrous and hydrate cocrystal is observed at 85%RH after 4 weeks. Peaks characteristic of anhydrous cocrystal at 13.4° and 26.1° and that of cocrystal hydrate at 14.3° are observed. At 98%RH a mixed phase of theophylline hydrate (2Θ values at 11.6° and 14.8°) and cocrystal hydrate (2Θ = 14.3°, 18.5°, 27.5° and 28.7°) is observed after storage for 7 weeks.

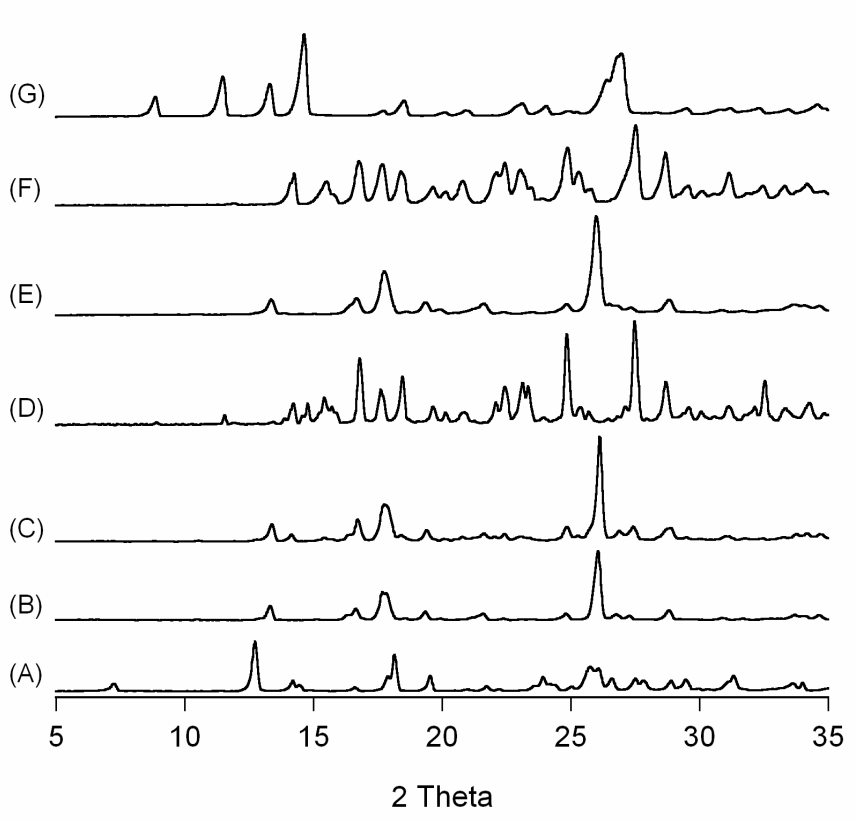

Figure 4.5: XRPD patterns of THP/CTA mixtures showing transformation after storage at 85% and 98%RH. (A) mixture before storage, mixture after storage at (B) 75%RH, (C) 85%RH, and (D) 98%RH. Reference patterns of (E) Anhydrous cocrystal, (F) Cocrystal hydrate and (G) Theophylline hydrate

The transformation pathways in mixtures stored at 85% and 98% RH were identified using Raman spectroscopy. At 85% and 98% RH, the mixture transforms to anhydrous cocrystal and then to cocrystal hydrate. Further transformation of cocrystal hydrate to theophylline hydrate was observed only at 98%RH (figure 4.6). Cocrystal formed at 85%RH was stable even after 6 weeks of storage.

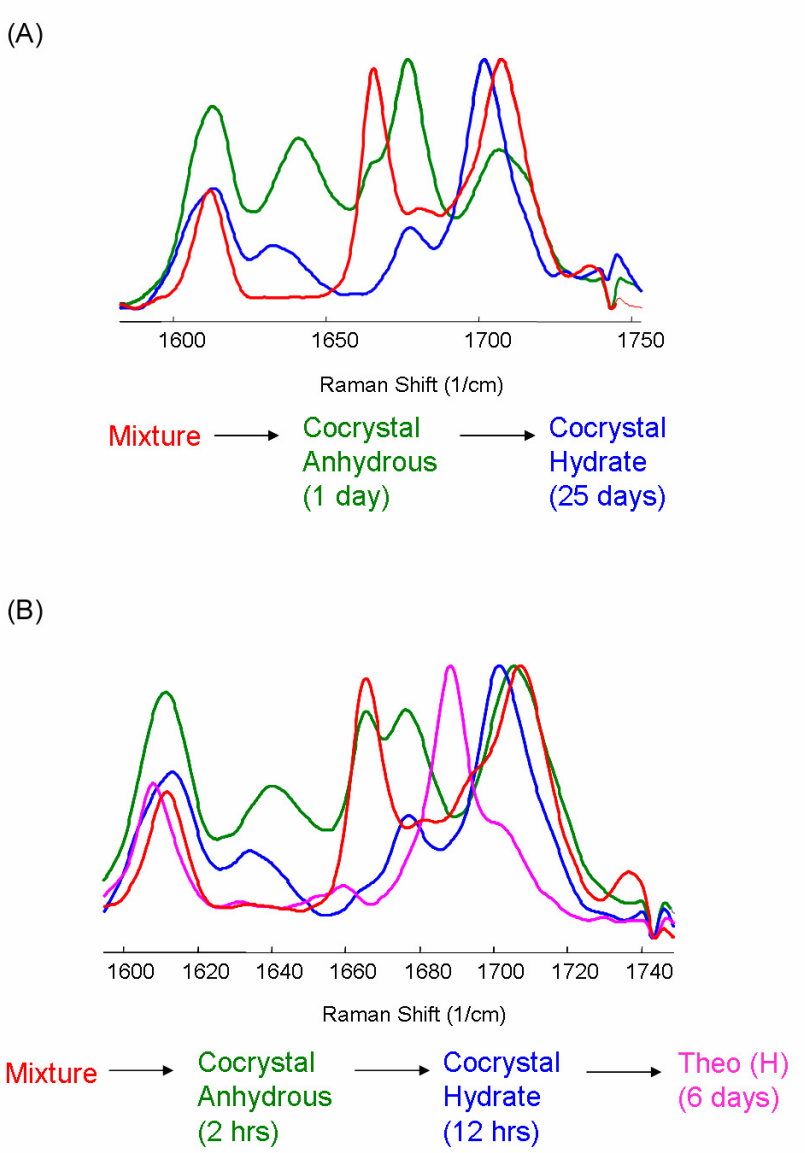

Figure 4.6: Raman spectra showing the transformation pathway in THP/CTA mixtures during storage at (A) 85% and (B) 98%RH.

Moisture uptake and stability of THP-CTA hydrate cocrystal at 85% and 98%RH was also investigated by storing the hydrated cocrystal under these conditions. Figure 4.7 shows the XRPD patterns after storage for 4.5 months. Cocrystal hydrate sorbs less than 2% moisture and remains stable at 85%RH after 16 weeks of storage. At 98%RH,

cocrystal hydrate deliquesces by sorbing 74 % water and transforms to theophylline hydrate. A previous study has reported the cocrystal hydrate to be stable at 98%RH.[24] However, cocrystal stability in this study was examined only for a week. The current study shows evidence for transformation over longer storage times.

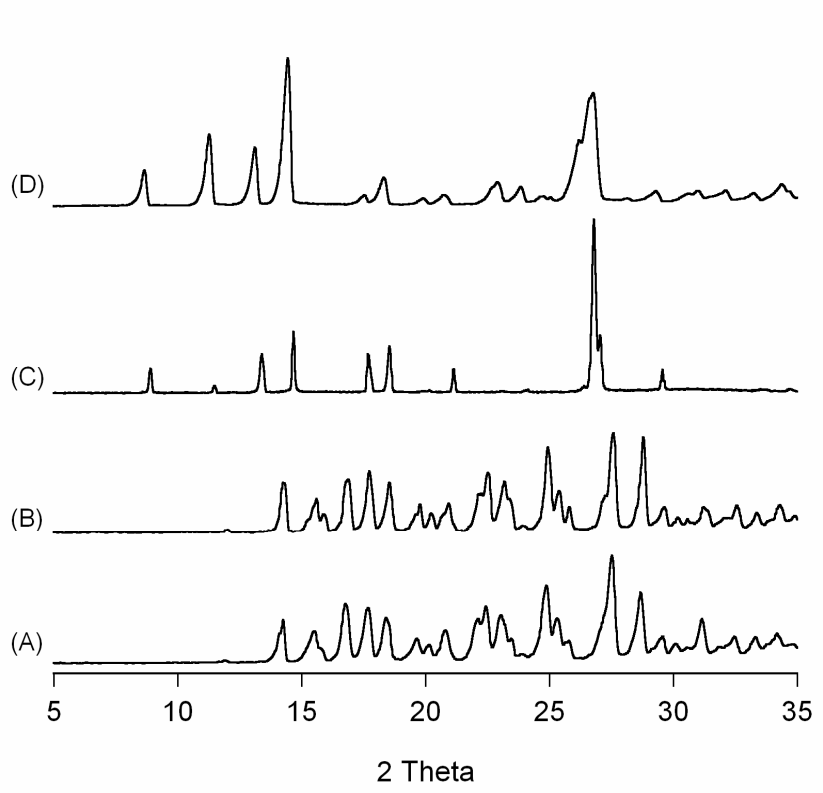

Figure 4.7: XRPD patterns of THP-CTA cocrystal hydrate: (A) before storage; after storage for 16 weeks at (B) 85%RH, and (C) 98%RH; (D) reference pattern of theophylline hydrate

Stability of carbamazepine-4-aminobenzoic acid (CBZ-4ABA) cocrystals in aqueous solutions

The stability of 2:1 CBZ-4ABA anhydrous and hydrated cocrystals in aqueous solutions was also studied. XPRD patterns in figure 4.8 indicate that both anhydrous and hydrated cocrystals are unstable in pure water. Cocrystal hydrate transforms to CBZ(D), while the anhydrous cocrystal transforms to cocrystal hydrate. In a saturated aqueous solution of the coformer (4ABA), cocrystal hydrate is the stable phase. These results indicate that CBZ-4ABA hydrate stability in aqueous solutions is dependent on coformer concentration. Cocrystal hydrate stability in saturated aqueous coformer solutions further suggests that the coformer concentration does not govern transformation between the hydrate and anhydrous cocrystals as shown for THP-CTA cocrystals. The critical water activity was therefore measured by examining cocrystal stability in acetonitrile-water mixtures of varying solvent composition and water activities.

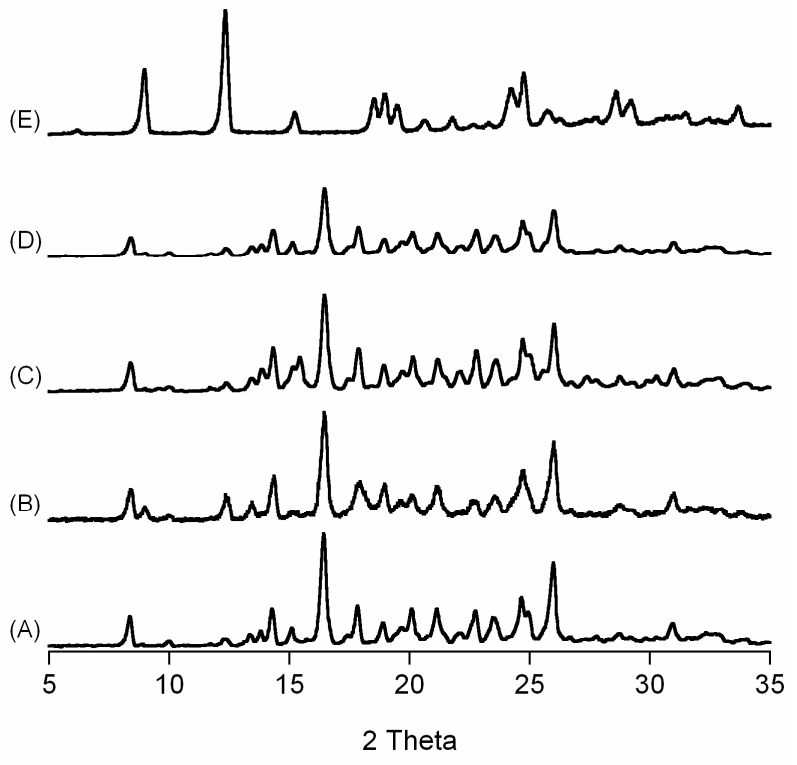

Figure 4.8: XRPD patterns showing the stability of CBZ-4ABA anhydrous and hydrated cocrystals after suspending for a week in aqueous solutions. CBZ-4ABA hydrate (A) reference pattern, and after suspending in (B) pure water, and (C) saturated 4ABA solution; Anhydrous cocrystal (D) reference pattern, and after suspending in (E) pure water; (F) reference pattern of CBZ(D).

XRPD patterns in figure 4.9 shows the dependence of anhydrous and hydrated cocrystal stability on water activity. The anhydrous cocrystal is stable at $a_w \leq 0.26$. Characteristic peaks corresponding to the anhydrous cocrystal are observed at 9.8° and 17.5°. Cocrystal hydrate is stable at $a_w \geq 0.30$. Thus the critical water activity above which the cocrystal hydrate is thermodynamically stable is 0.26 - 0.30.

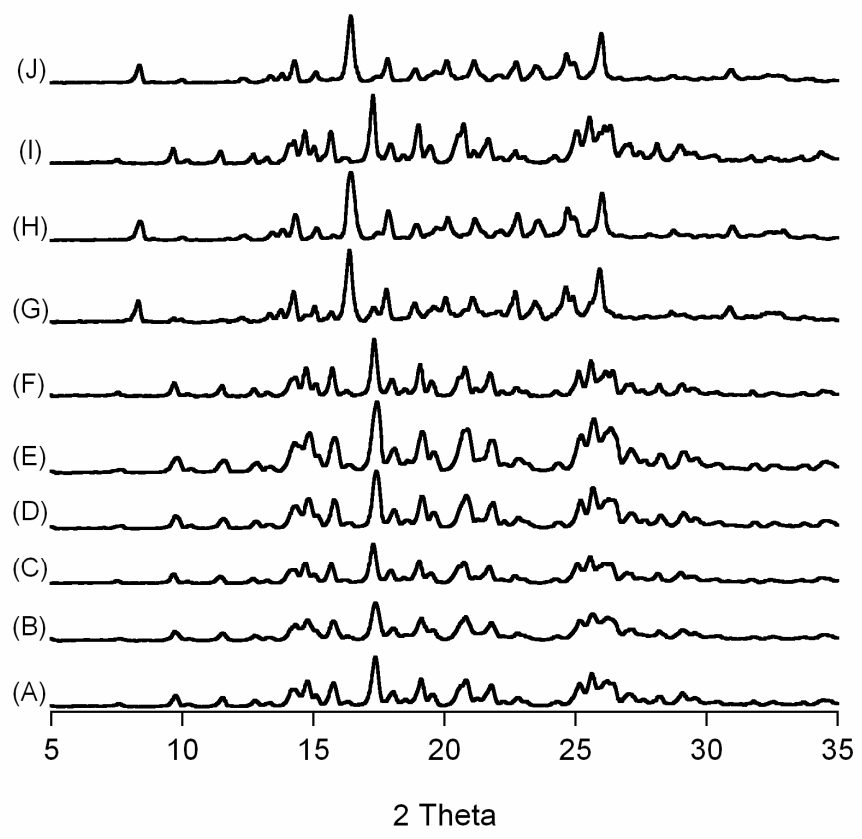

Figure 4.9: XRPD patterns showing transformation of CBZ-4ABA cocrystal hydrate as a function of water activity (a_w). Water activity was varied by addition of acetonitrile to water. (A) $a_w = 0.0$, (B) $a_w = 0.06$, (C) $a_w = 0.11$, (D) $a_w = 0.16$, (E) $a_w = 0.21$; (F) $a_w = 0.26$, (G) $a_w = 0.30$, (H) $a_w = 0.41$; reference patterns for (I) cocrystal hydrate, and (J) anhydrous cocrystal.

Thermal Analysis of cocrystal hydrates

Figure 4.10 shows the thermal data for CBZ-4ABA and THP-CTA cocrystal hydrates. An endotherm corresponding to dehydration is observed at 91.1±1.1°C for CBZ-4ABA hydrate in the DSC. The dehydration is followed by an exotherm indicating crystallization. This suggests dehydration of cocrystal hydrate results in amorphous phase

formation. The exothermic event is followed by endothermic events at 130°C, 139°C, and 153°C.

The DSC data of THP-CTA cocrystal hydrate shows an endotherm at 53.1±0.3°C followed by another endotherm at 88.6±1.1°C. Thermogravimetric analysis of the cocrystal hydrate shows a weight change between 50°C and 110°C corresponding to the two endothermic events observed in the DSC. This suggests that the dehydration of cocrystal hydrate proceeds in two steps. Cocrystal hydrate dehydration is followed by two endotherms at 145°C and 176°C.

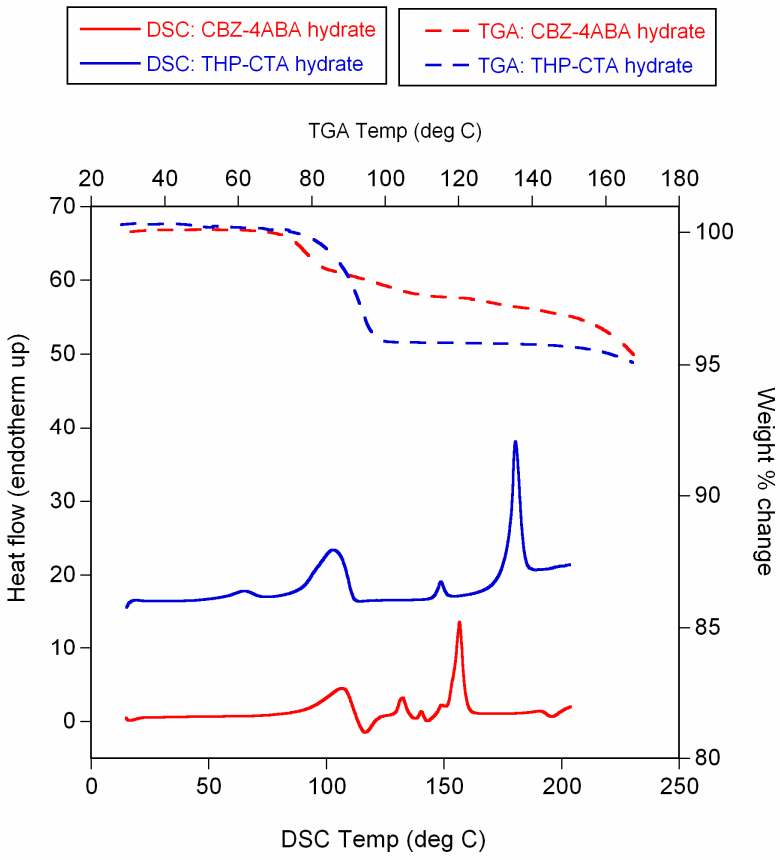

Figure 4.10: DSC and TGA traces of CBZ-4ABA and THP-CTA cocrystal hydrates.

The dehydration of cocrystal hydrates occur at higher temperatures when compared to the corresponding API hydrates. Carbamazepine dihydrate (CBZ(D)) and theophylline monohydrate (THP(H)) are reported to dehydrate at 25-80°C and 79°C, respectively.[55, 56]

Discussion

Results from our current study show that the coformer aqueous concentration affects the thermodynamic stability of cocrystal hydrates in aqueous solutions. Depending on the coformer concentration, cocrystal hydrate can transform to crystalline drug or anhydrous cocrystal. Transformation of cocrystal hydrate to anhydrous cocrystal in aqueous coformer solutions occurs when the coformer modulates the water activity significantly. This is demonstrated for THP-CTA cocrystal hydrate. Conversion of cocrystal hydrate to anhydrous cocrystal with increasing coformer concentrations did not occur for CBZ-4ABA. This is because 4ABA has low aqueous solubility and negligibly affects the water activity of aqueous solution. The a_w of saturated aqueous 4ABA (a_w =0.98) is significantly higher than the critical a_w of CBZ-4ABA hydrate (a_w = 0.26-0.30).

A key parameter to identify anhydrous and hydrated cocrystal stability domains is the transition concentration between the different crystalline phases. Using the transition concentrations, phase solubility diagrams (PSD) showing the reactant solution concentrations in molality or molarity at equilibrium with the different solid phases as well as the cocrystal stability domains can be plotted as shown in figure 4.3.[26, 49] Alternatively, the stability domains can also be represented on a triangular phase diagram (TPD) that shows the total composition of the system, including that in the solid and

liquid phase, in mole or mass fractions.[26, 49] Figure 4.11 shows the TPD for a hypothetical ternary system where the coformer modulates the water activity similar to THP/CTA/water system. A hypothetical ternary system is considered since the drug and cocrystal solubility in THP/CTA/water system cannot be represented on the TPD due to extremely low mole fractions of THP ($<10^{-2}$).

In figure 4.11, the solubility of the crystalline drug hydrate, cocrystal hydrate, anhydrous cocrystal, and ligand hydrate are represented by the solubility curves ac_1, c_1c_2, c_2c_3, and c_3b, respectively. The stability domains of cocrystal hydrate and anhydrous cocrystal are represented by regions 2 and 3. The hydrated drug and ligand are stable in regions 1 and 4, respectively. Mixed phases of crystalline drug hydrate/cocrystal hydrate, cocrystal hydrate/anhydrous cocrystal, and anhydrous cocrystal/ hydrated ligand will be present in regions 5, 6, and 7, respectively. Similar phase diagrams have been reported for cocrystals with different stoichiometry.[49] In these studies, the stability domains of the cocrystal with different stoichiometry are governed by cocrystal and solution chemistry. The current study with the theophylline-citric acid cocrystals suggests that the stability domains of the anhydrous and hydrated cocrystals are governed by water activity and solution chemistry.

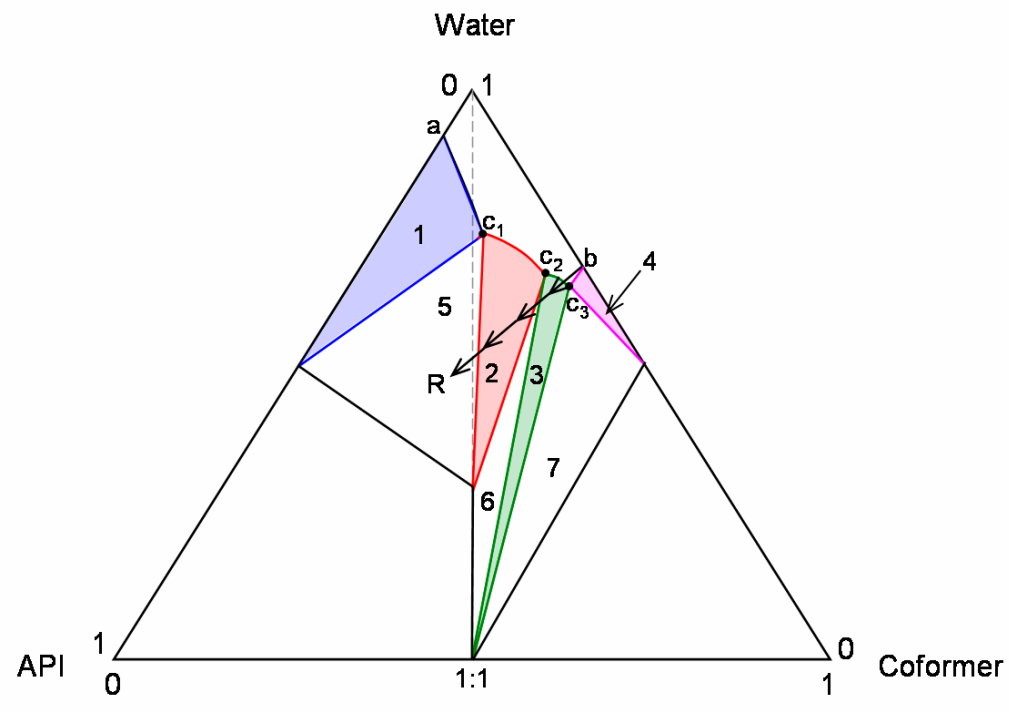

Figure 4.11: TPD showing the stability domains for anhydrous and hydrated cocrystals with coformers that modulate the water activity. Points 'a' and 'b' correspond to API hydrate and coformer hydrate aqueous solubility. c_1, c_2, and c_3 represent the transition concentrations or eutectic points. Curves ac_1, c_1c_2, c_2c_3, and c_3b represent the solubilities of crystalline drug hydrate, cocrystal hydrate, anhydrous cocrystal, and hydrated coformer respectively. Stability regions for the crystalline phases are: 1- crystalline drug hydrate; 2- cocrystal hydrate; 3-anhydrous cocrystal; 4- cocrystal hydrate; 5- crystalline drug hydrate/cocrystal hydrate; 6- anhydrous/hydrated cocrystals; 7- anhydrous cocrystal/hydrated coformer. Pathway R represents the transformation occurring during reaction crystallization or deliquescence in solid mixtures in storage.

From the phase diagrams, the transformation pathway and crystallization outcomes can be predicted as represented by the pathway 'R' for reaction crystallization or deliquescence in solid mixtures. The addition of drug to a saturated solution of the coformer during reaction crystallization generates supersaturation with respect to the anhydrous cocrystal as shown by the pathway. Further addition of drug generates supersaturation with respect to cocrystal hydrate.

During deliquescence in solid mixtures, supersaturation with respect to cocrystals is generated by non-equivalent reactant concentrations in the deliquesced solution. As deliquescence begins, the sorbed water is saturated with coformer.[37] Under these conditions, the anhydrous cocrystal is the least soluble and most stable phase. The dissolution of drug in this solution therefore generates supersaturation with respect to anhydrous cocrystal. Further transformation of anhydrous cocrystal to cocrystal hydrate will occur when supersaturation with respect to cocrystal hydrate is generated. This is achieved when the coformer concentration falls below that corresponding to transition concentration c_2.

The concentration of the coformer in a deliquesced solution depends on the RH. At the deliquescence RH, the deliquesced solution remains saturated with the coformer. However, at higher RH (RH > DRH), increased levels of water uptake lead to coformer dilution in the deliquesced solution thereby affecting cocrystal stability. Coformer dilution at high RH explains the observed transformation pathway in THP/CTA mixtures at 85% and 98%RH.

Cocrystal hydrate instability and transformation to theophylline hydrate due to cocrystal deliquescence at 98%RH is similarly explained by the effect of reactant solution concentrations on cocrystal stability. Cocrystal stability studies in aqueous coformer solution indicate that the cocrystal hydrate is more soluble and transforms to theophylline hydrate at coformer concentrations below 1.62m (c_1). Thus during cocrystal deliquescence, stoichiometric dissolution of the cocrystal in the sorbed water generates supersaturation with respect to the drug resulting in its crystallization.

In addition to the coformer, excipients and cosolvent that alter the water activity of aqueous solutions also affect cocrystal hydrate stability and transformation to anhydrous cocrystal as shown for THP-CTA and CBZ-4ABA cocrystal hydrates. Thus when the coformer does not alter water activity, the critical water activity for cocrystal hydrate formation and stability can be measured using excipients or cosolvents. When using these approaches to determine the critical water activity for cocrystal hydrate, it is important to ensure that transformation of cocrystal to crystalline drug does not occur in aqueous solutions with cosolvent or excipient. This is because the equilibrium solid phases at the critical water activity are the anhydrous and hydrated cocrystals.

The critical water activity of CBZ-4ABA and THP-CTA hydrates is different from those of the corresponding API hydrates. The critical a_w for carbamazepine and theophylline hydrates is 0.62-0.64.[33, 34, 46] The critical water activity is an indicator of the tendency to form hydrates, with lower water activities implying greater tendency for hydration. CBZ-4ABA cocrystal, therefore, has a higher tendency to transform to a hydrate than anhydrous CBZ, while THP-CTA cocrystal has a lower tendency to hydrate when compared to anhydrous theophylline. Differences in the critical water activities of API and cocrystal hydrates may be due to differences in the crystal structure, hydrogen bond interactions between water, API and/or coformer, as well as differences in solubility and free energy of these materials.

Conclusions

Coformers, excipients and cosolvents that modulate the water activity of aqueous solutions can affect cocrystal hydrate stability and induce transformation to anhydrous cocrystal. This is shown for theophylline-citric acid and carbamazepine-4-aminobenzoic acid cocrystal hydrates. Cocrystal stability can be evaluated by (i) examining cocrystal stability in aqueous suspensions with varying coformer, excipient or cosolvent concentrations, and (ii) storing the cocrystals at various RH. Key parameters to identify anhydrous and hydrated cocrystal stability domains are transition concentrations and critical water activity. THP-CTA and CBZ-4ABA cocrystal hydrates are stable at water activities above 0.79-0.83 and 0.26-0.30, respectively.

References

1. Otsuka, M.; Ofusa, T.; Matsuda, Y. Effect of Environmental Humidity on the Transformation Pathway of Carbamazepine Polymorphic Modifications During Grinding. *Colloids Surf. B Biointerfaces.* **1999,** 13, 263-273.

2. Matsuo, K.; Matsuoka, M. Solid-State Polymorphic Transition of Theophylline Anhydrate and Humidity Effect. *Cryst. Growth Des.* **2007,** 7, 411-415.

3. Andronis, V.; Yoshioka, M.; Zografi, G. Effects of Sorbed Water on the Crystallization of Indomethacin from the Amorphous State. *J. Pharm. Sci.* **1997,** 86, 346-351.

4. Morris, K. R. Structural Aspects of Hydrates and Solvates. In *Polymorphism in Pharmaceutical Solids*, ed.; Britain, H. G., Eds.; Marcel Dekker, Inc.: New York, **1999**; pp 126-180.

5. Zhang, G. G. Z.; Law, D.; Schmitt, E. A.; Qiu, Y. Phase Transformation Considerations During Process Development and Manufacture of Solid Oral Dosage Forms. *Adv. Drug Del. Rev.* **2004,** 56, 371-390.

6. Shefter, E.; Higuchi, T. Dissolution Behavior of Cryatlline Solvated and Nonsolvated Forms of Some Pharmaceuticals. *J. Pharm. Sci.* **1963,** 52, 781-791.

7. Murphy, D.; Rodríguez-Cintrón, F.; Langevin, B.; Kelly, R. C.; Rodríguez-Hornedo, N. Solution-Mediated Phase Transformation of Anhydrous to Dihydrate Carbamazepine and the Effect of Lattice Disorder. *Int. J. Pharm.* **2002,** 246, 121-134.

8. Khankari, R.; Chen, L.; Grant, D. J. W. Physical Characterization of Nedocromil Sodium Hydrates. *J. Pharm. Sci.* **1998,** 87, 1052-1061.

9. Debnath, S.; Suryanarayanan, R. Influence of Processing-Induced Phase Transformations on the Dissolution of Theophylline Tablets. *AAPS PharmSciTech.* **2004,** 5, 1-11.

10. Carino, S. R.; Sperry, D. C.; Hawley, M. Relative Bioavailability Estimation of Carbamazepine Crystal Forms Using an Artificial Stomach-Duodenum Model. *J. Pharm. Sci.* **2006,** 95, 116-125.

11. Trask, A. V.; Motherwell, W. D. S.; Jones, W. Physical Stability Enhancement of Theophylline Via Cocrystallization. *Int. J. Pharm.* **2006,** 320, 114-123.

12. Trask, A. V.; Motherwell, W. D. S.; Jones, W. Pharmaceutical Cocrystallization: Engineering a Remedy for Caffeine Hydration. *Cryst. Growth Des.* **2005,** 5, 1013-1021.

13. Rodríguez-Spong, B. Enhancing the Pharmaceutical Behavior of Poorly Soluble Drugs through the Formation of Cocrystals and Mesophases. Ph.D. Thesis, University of Michigan, Ann Arbor, **2005**.

14. Rodríguez-Hornedo, N.; Nehm, S. J.; Jayasankar, A. Cocrystals: Design, Properties and Formation Mechanisms. In *Encyclopedia of Pharmaceutical Technology*, 3rd ed.; Swarbrick, J., Eds.; Informa Health Care: New York, **2006**; pp 615-635.

15. Remenar, J. F.; Peterson, M. L.; Stephens, P. W.; Zhang, Z.; Zimenkov, Y.; Hickey, M. B. Celecoxib : Nicotinamide Dissociation: Using Excipients to Capture the Cocrystal's Potential. *Mol. Pharm.* **2007,** 4, 386-400.

16. Remenar, J. F.; Morissette, S. L.; Peterson, M. L.; Moulton, B.; MacPhee, J. M.; Guzman, H. R.; Almarsson, O. Crystal Engineering of Novel Cocrystals of a Triazole Drug with 1,4-Dicarboxylic Acids. *J. Am. Chem. Soc.* **2003,** 125, 8456-8457.

17. McNamara, D. P.; Childs, S. L.; Giordano, J.; Iarriccio, A.; Cassidy, J.; Shet, M. S.; Mannion, R.; O'Donnell, E.; Park, A. Use of a Glutaric Acid Cocrystal to Improve Oral Bioavailability of a Low Solubility Api. *Pharm. Res.* **2006,** 23, 1888-1897.

18. Childs, S. L.; Chyall, L. J.; Dunlap, J. T.; Smolenskaya, V. N.; Stahly, B. C.; Stahly, P. G. Crystal Engineering Approach to Forming Cocrystals of Amine Hydrochlorides with Organic Acids. Molecular Complexes of Fluoxetine Hydrochloride with Benzoic, Succinic, and Fumaric Acids. *J. Am. Chem. Soc.* **2004,** 126, 13335-13342.

19. Sun, C. C.; Hou, H. Improving Mechanical Properties of Caffeine and Methyl Gallate Crystals by Cocrystallization. *Cryst. Growth Des.* **2008,** 8, 1575-1579.

20. Reddy, L. S.; Bethune, S. J.; Kampf, J. W.; Rodríguez-Hornedo, N. Cocrystals and Salts of Gabapentin: Ph Dependent Cocrystal Stability and Solubility. *Cryst. Growth Des.* **2008,** accepted.

21. Rodríguez-Hornedo, N.; Nehm, S. J.; Seefeldt, K. F.; Pagán-Torres, Y.; Falkiewicz, C. J. Reaction Crystallization of Pharmaceutical Molecular Complexes. *Mol. Pharm.* **2006,** 3, 362-367.

22. Morissette, S. L.; Almarsson, Ö.; Peterson, M. L.; Remenar, J. F.; Read, M. J.; Lemmo, A. V.; Ellis, S.; Cima, M. J.; Gardner, C. R. High-Throughput Crystallization: Polymorphs, Salts, Co-Crystals and Solvates of Pharmaceutical Solids. *Adv. Drug Del. Rev.* **2004,** 56, 275-300.

23. Lu, E.; Rodríguez-Hornedo, N.; Suryanarayanan, R. A Rapid Thermal Method for Cocrystal Screening. *CrystEngComm.* **2008,** 10, 665-668.

24. Karki, S.; Friščić, T.; Jones, W.; Motherwell, W. D. S. Screening for Pharmaceutical Cocrystal Hydrates Via Neat and Liquid-Assisted Grinding. *Mol. Pharm.* **2007,** 4,

347-354.

25. Friščić, T.; Trask, A. V.; Jones, W.; Motherwell, W. D. S. Screening for Inclusion Compounds and Systematic Construction of Three Component Solids by Liquid Assisted Grinding. *Angew. Chem. Int. Ed.* **2006,** 45, 7546-7550.

26. Childs, S. L.; Rodríguez-Hornedo, N.; Reddy, L. S.; Jayasankar, A.; Maheshwari, C.; McCausland, L.; Shipplett, R.; Stahly, B. C. Screening Strategies Based on Solubility and Solution Composition Generate Pharmaceutically Acceptable Cocrystals of Carbamazepine. *CrystEngComm.* **2008**, 856-864.

27. Berry, D. J.; Seaton, C. C.; Clegg, W.; Harrington, R. W.; Coles, S. J.; Horton, P. N.; Hursthouse, M. B.; Storey, R.; Jones, W.; Friscic, T.; Blagden, N. Applying Hot-Stage Microscopy to Co-Crystal Screening: A Study of Nicotinamide with Seven Active Pharmaceutical Ingredients. *Cryst. Growth Des.* **2008,** 8, 1697-1712.

28. Childs, S. L.; Hardcastle, K. I. Cocrystals of Piroxicam with Carboxylic Acids. *Cryst. Growth Des.* **2007,** 7, 1291-1304.

29. Fleischman, S. G.; Kuduva, S. S.; McMahon, J. A.; Moulton, B.; Walsh, R. D. B.; Rodríguez-Hornedo, N.; Zaworotko, M. J. Crystal Engineering of the Composition of Pharmaceutical Phases: Multiple-Component Crystalline Solids Involving Carbamazepine. *Cryst. Growth Des.* **2003,** 3, 909-919.

30. Caira, M. R.; Nassimbeni, L. R.; Wildervanck, A. F. Selective Formation of Hydrogen Bonded Cocrystals between Sulfonamide and Aromatic Carboxylic Acids in the Solid State. *J. Chem. Soc. Perkin Trans.* **1995,** 2, 2213-2216.

31. McMahon, J. A.; Bis, J. A.; Vishweshwar, P.; Shattock, T. R.; McLaughlin, O. L.; Zaworotko, M. J. Crystal Engineering of the Composition of Pharmaceutical Phases. 3. Primary Amide Supramolecular Heterosynthons and Their Role in the Design of Pharmaceutical Cocrystals. *Z. Kristallogr.* **2005,** 220, 340-350.

32. Ticehurst, M. D.; Storey, R. A.; Watt, C. Application of Slurry Bridging Experiments at Controlled Water Activities to Predict the Solid-State Conversion between Anhydrous and Hydrated Forms Using Theophylline as a Model Drug. *Int. J. Pharm.* **2002,** 247, 1-10.

33. Zhu, H.; Yuen, C.; Grant, D. J. W. Influence of Water Activity in Organic Solvent + Water Mixtures on the Nature of the Crystallizing Drug Phase . 1. Theophylline. *Int. J. Pharm.* **1996,** 135, 151-160.

34. Qu, H.; Louhi-Kultanen, M.; Kallas, J. Solubility and Stability of Anhydrate/Hydrate in Solvent Mixtures. *Int. J. Pharm.* **2006,** 321, 101-107.
35. Ross, K. D. Estimation of Water Activity in Intermediate Moisture Foods. *Food Tech.* **1975,** 29, 26-34.

36. Salcedo, D. Equilibrium Phase Diagrams of Aqueous Mixtures of Malonic Acid and Sulfate/Ammonium Salts. *J. Phys. Chem. A.* **2006,** 110, 12158-12165.

37. Kontny, M. J.; Conners, J. J. Water Sorption of Drugs and Dosage Forms. In *Encyclopedia of Pharmaceutical Technology*, 2nd ed.; Swarbrick, J.; Boylan, J. C., Eds.; Marcel Dekker, Inc.: New York, **2002**; pp 2970-2986.

38. Maffia, M. C.; Meirelles, A. J. A. Water Activity and Ph in Aqueous Polycarboxylic Acid Systems. *J. Chem. Eng. Data.* **2001,** 46, 582-587.

39. Gracin, S.; Rasmuson, Å. C. Polymorphism and Crystallization of P-Aminobenzoic Acid *Cryst. Growth Des.* **2004,** 4, 1013-1023.

40. Salameh, A. K.; Mauer, L. J.; Taylor, L. S. Deliquescence Lowering in Food Ingredient Mixtures. *J. Food. Sci.* **2006,** 71, E10-E16.

41. Salameh, A. K.; Taylor, L. S. Deliquescence-Induced Caking in Binary Powder Blends. *Pharm. Dev. Technol.* **2006,** 11, 453-464.

42. Bell, G.; Janssen, A. E. M.; Halling, P. J. Water Activity Fails to Predict Critical Hydration Level for Enzyme Activity in Polar Organic Solvents: Interconversion of Water Concentrations and Activities. *Enzyme Microb. Tech.* **1997,** 20, 471-477.

43. Nehm, S. J.; Rodríguez-Spong, B.; Rodríguez-Hornedo, N. Phase Solubility Diagrams of Cocrystals Are Explained by Solubility Product and Solution Complexation. *Cryst. Growth Des.* **2006,** 6, 592-600.

44. Salameh, A. K.; Taylor, L. S. Role of Deliquescence Lowering in Enhancing Chemical Reactivity in Physical Mixtures. *J. Phys. Chem. B.* **2006,** 110, 10190-10196.

45. Karel, M.; Labuza, T. P. Nonenzymatic Browning in Model Systems Containing Sucrose. *J. Agric. Food. Chem.* **1968,** 16, 968.

46. Li, Y.; Chow, P. S.; Tan, R. B. H.; Black, S. N. Effect of Water Activity on the Transformation between Hydrate and Anhydrate of Carbamazepine. *Org. Process Res. Dev.* **2008,** 12, 264-270.

47. Jayasankar, A.; Good, D. J.; Rodríguez-Hornedo, N. Mechanisms by Which Moisture Generates Cocrystals. *Mol. Pharm.* **2007,** 4, 360-372.

48. O'Brien, F. E. M. The Control of Humidity by Saturated Salt Solutions. *J. Sci. Instrum.* **1948,** 25, 73-76.

49. Jayasankar, A.; Reddy, L. S.; Bethune, S. J.; Rodríguez-Hornedo, N. The Role of Cocrystal and Solution Chemistry on the Formation and Stability of Cocrystals with

Different Stoichiometry. *Cryst. Growth Des.* **2008,** submitted.

50. Peng, C.; Chan, M. N.; Chan, C. K. The Hygroscopic Properties of Dicarboxylic and Multifunctional Acids: Measurements and Unifac Predictions. *Environ. Sci. Technol.* **2001,** 35, 4495-4501.

51. Higuchi, T.; Connors, K. A. Phase-Solubility Techniques. In *Advances in Analytical Chemistry and Instrumentation*, ed.; Reilley, C., Eds.; **1965**; pp 117-212.

52. Suzuki, H.; Sunada, H. Mechanistic Studies of Hydrotropic Solubilization of Nifedepin in Nicotinamide Solution. *Chem. Pharm. Bull.* **1998,** 46, 125-130.

53. Sacchetti, M. Determining the Relative Physical Stability of Anhydrous and Hydrous Crystal Forms of GW2016. *Int. J. Pharm.* **2004,** 273, 195-202.

54. Peng, C.; Chow, A. H. L.; Chan, C. K. Hygroscopic Study of Glucose, Citric Acid, and Sorbitol Using an Electrodynamic Balance: Comparison with Unifac Predictions. *Aerosol Sci. Tech.* **2001,** 35, 753-758.

55. Li, Y.; Han, J.; Zhang, G. G.; Grant, D. J. W.; Suryanarayanan, R. In-Situ Dehydration of Carbamazepine Dihydrate: A Novel Technique to Prepare Amorphous Anhydrous Carbamazepine. *Pharm. Dev. Technol.* **2000,** 5, 257-266.

56. Phadnis, N. V.; Suryanarayanan, R. Polymorphism in Anhydrous Theophylline - Implications on the Dissolution Rate of Theophylline Tablets. *J. Pharm. Sci.* **1997,** 86, 1256-1263.

CHAPTER V

COCRYSTAL FORMATION DURING COGRINDING AND STORAGE IS MEDIATED BY AMORPHOUS PHASE

Introduction

Hydrogen bonds are the basis of molecular recognition phenomena in biological and pharmaceutical systems. They are also key elements in the design of molecular assemblies and supermolecules in the liquid and solid states. In the crystalline state, hydrogen bonds are responsible for the generation of families of molecular networks with the same molecular components (single component crystals and their polymorphs) or with different molecular components (multiple component crystals or cocrystals).[1-12]

Cocrystals, also referred to as molecular complexes, include two or more different components and often rely on hydrogen bonded assemblies between neutral molecules. Cocrystals with the same active pharmaceutical ingredient (API) can have strikingly different pharmaceutical properties (melting point, solubility, dissolution, bioavailability, moisture uptake, chemical stability, etc.), depending on the nature of the second component.[13-16] It is important to note that cocrystals are a homogeneous phase of stoichiometric composition and not a mixture of pure component crystalline phases.

Cocrystallization is a result of competing molecular associations between similar molecules, or homomers, and different molecules or heteromers.[6, 10] Most studies on

cocrystal formation focus on design and isolation for the purpose of crystal structure determination, and the factors that control cocrystallization have not been explicitly considered.[2, 3, 6, 9, 16-19] Cocrystals have therefore been prepared largely on a trial and error basis by solution, solid-state, or melt processes.[20] Key questions in the discovery of families of cocrystals are: (i) what are the criteria for cocrystal former selection, (ii) can cocrystal screening and cocrystallization methods be theoretically based, and (iii) can cocrystals form as a result of stresses encountered during pharmaceutical processes and storage? The objective of the current study is to address the latter question.

Solution-based methods in search of cocrystals have suffered from the risk of crystallizing the single component phases and often a very large number of solvents and experimental conditions need to be tested. Furthermore, transferability to large-scale crystallization processes has been limited. The success of crystallizing the molecular complex is significantly improved using the reaction crystallization method where nucleation and growth of cocrystals are directed by the effect of cocrystal components on decreasing the solubility of the molecular complex to be crystallized.[21, 22]

One way to cope with the complexities of solution-based methods has been to screen for cocrystals by cogrinding solid reactants.[4, 6, 8, 10, 18] Although examples of cocrystals formed by this process are abundant, the underlying mechanisms and the factors that determine cocrystallization by cogrinding are not known. Disorder induced by grinding or milling is well documented in the pharmaceutical literature and its effects on solid-state changes and reactivity have been thoroughly studied.[23-28] These include amorphous phase formation, polymorphic transformations, complexation, and chemical

reactivity. Therefore, the concepts of solid-state reactivity in pharmaceutical materials can be applied to understand the formation of cocrystals by solid-state methods.

Since the basis for reactivity in the solid-state lies on molecular mobility and complementarity, process-induced cocrystal formation must be related to the propensity of API and other components to form disordered or amorphous phases. That is, as long as the transformation does not occur through the melt caused by high local temperatures during a process. Cogrinding under cryogenic conditions is necessary to ascertain that the reaction does not proceed through the melt. Thus, if amorphous phases generate cocrystals, then cocrystals can form not only during the process that induced the disorder, but also during storage. Furthermore, the presence of plasticizers, such as water or other solvents that lower the T_g and enhance molecular mobility[23, 29, 30] will increase reactivity and cocrystallization rate in the solid state. To challenge these hypotheses is the focus of our work.

The objectives of the present study are to (i) investigate the underlying mechanisms of cocrystal formation during cogrinding and storage, and (ii) establish the effects of water by cogrinding hydrated crystal forms of reactants and by varying RH conditions during storage. The hydrogen bonded 1:1 carbamazepine-saccharin (CBZ-SAC) and carbamazepine-nicotinamide (CBZ-NCT) cocrystals are chosen as model systems since the crystal structures are reported.[31] Both cocrystals have functional groups that are commonly encountered in other pharmaceutical components and their crystal structures are known. Cocrystals of carbamazepine with saccharin or nicotinamide have been shown to improve dissolution, mechanical properties, moisture uptake behavior, and chemical stability relative to the pure carbamazepine crystal, anhydrous

monoclinic form III, (CBZ(III)).[13] Crystal structures have been reported and cocrystals are prepared by solution and solid-state methods.[13, 21] We have shown that carbamazepine-saccharin and carbamazepine-nicotinamide cocrystals can be formed from amorphous phases generated either by quenching the melt of components, or by grinding a blend of components.[32-34]

Findings from the current study have significant implications for anticipating the propensity of solid components to form cocrystals during storage as a result of disorder created during a pharmaceutical process such as grinding. Process induced transformations to cocrystal may thus be added to the list of transformations that can considerably affect product safety and performance in addition to transformations involving polymorphs and solvates.

Experimental section

Materials

Anhydrous monoclinic form III carbamazepine (CBZ(III)), saccharin (SAC), and form I nicotinamide (NCT)[35] were obtained from Sigma Aldrich and were used as received. The compounds were analyzed by infra-red spectroscopy (ATR-FTIR), X-ray powder diffraction (XRPD), and differential scanning calorimetry (DSC) before carrying out the experiments.

CBZ-SAC and CBZ-NCT cocrystals and carbamazepine dihydrate (CBZ(D)) were prepared according to the methods described earlier.[13, 24] Solid phases were analyzed by XRPD, ATR-FTIR, DSC and thermogravimetric analysis (TGA). Experimental XRPD of the cocrystal was in agreement with that calculated using the

Lorentz-polarisation correction by Mercury (ver.1.3) for the structure reported in the Cambridge Structural Database (reference code: UNEZAO).

Methods

Cogrinding

Cogrinding was carried out at room temperature in a ball mill and under liquid nitrogen using a cryogenic impact mill.

Room temperature cogrinding methodology

Anhydrous CBZ(III) was coground with SAC or NCT in stoichiometric ratio (1:1) in a 5100 SPEX CertiPrep Mixer/Mill (Metuchen, NJ) using a 3114 stainless steel vial having a grinding load volume of 0.6ml (0.5 inch diameter x 1 inch length). Two stainless steel beads about 0.25 inches in diameter were used for cogrinding. CBZ(III) and SAC were also coground in non-stoichiometric ratios (1:2 and 2:1). Total mass of each blend consisting of CBZ(III) and SAC or NCT was 0.5 grams. Cogrinding of the blends was carried out at room temperature for different time periods up to 30 minutes. The temperature of the grinding vial, determined by placing a thermometer to the outside of the vial, was 45°C after 30 minutes of cogrinding.

Cogrinding the dihydrate form of carbamazepine, CBZ(D), with SAC or NCT in stoichiometric ratio (1:1) of reactants was carried out in the room temperature mill. Due to the low bulk density of this blend, the total mass of the blend ground was 0.25 grams since the vial could not hold 0.5 grams of the blend. For comparison of the rate of cocrystal formation between the dihydrate and anhydrous system, a blend of CBZ(III) and SAC or NCT weighing 0.25 grams was also ground. Samples were analyzed by

ATR-FTIR, XRPD, and DSC to examine changes in crystallinity and in polymorph, solvate, and cocrystal forms during cogrinding and during storage.

Cryogenic cogrinding methodology

Cogrinding of CBZ(III) and SAC or NCT in stoichiometric ratio (1:1) was carried out in a 6750 SPEX CertiPrep cryogenic mill (Metuchen, NJ) using a polycarbonate vial with 4 ml capacity. A stainless steel rod was used as an impactor for grinding. The total mass of the blend was 1 gram. The mill was programmed to an impact frequency of 10Hz and 15 cycles, each cycle consisting of 2 minutes grinding followed by 2 minutes cooling period. Thus, the total grinding time was 30 minutes. The vial containing the coground sample was later transferred to a dessicator containing phosphorous pentoxide as the desiccant to allow the sample to reach room temperature and to prevent condensation of moisture on the sample due to low temperature of the sample. Ground samples were analyzed by the methods indicated above.

Cryogenic milling of CBZ-NCT cocrystal was also performed to investigate cocrystal stability during grinding. Approximately 1gram cocrystal was milled for different times, and the ground sample was characterized for changes in crystallinity and molecular interactions by XRPD and FTIR.

Storage of Samples

Ground CBZ(III)/SAC mixtures were stored in desiccators equilibrated at 0% and 75% relative humidities using phosphorous pentoxide and saturated sodium chloride solution respectively at room temperature (22-25°C).[36] XRPD and FTIR spectra of the

milled blends during storage were obtained to evaluate changes in crystallinity and to monitor cocrystal formation.

Attenuated Total Reflection Fourier Transform Infra-red (ATR-FTIR) Spectroscopy

ATR-FTIR was used to identify intermolecular interactions that reflect hydrogen bond directed molecular associations and to determine solid-state forms (polymorph, solvate, or cocrystal). The samples were analyzed using a Vertex 77 spectrometer from Bruker Optics (Billerica, MA) and a Nicolet 6700 spectrometer from Thermo Electron (Madison, WI). Both spectrometers were equipped with a DTGS detector and a single bounce ATR accessory with ZnSe crystal. Spectra (64 scans at $4cm^{-1}$ resolution) were collected in the 4000-600 cm^{-1} range.

Quantification of CBZ-SAC cocrystal formation during cogrinding and during storage was done according to IR quantitative methods reported for blends of polymorphs.[37, 38] Calibration curves were obtained as described below.

Calibration standards were prepared by blending CBZ(III) and SAC in 1:1 molar ratio with the required amount of CBZ-SAC cocrystal. Cocrystal used in the calibration was prepared by the solution method described previously.[13, 21] The total mass of each standard was 0.5 grams. The standards prepared had 0, 20, 40, 60, 80 and 100 per cent (by weight) CBZ-SAC cocrystal. Samples containing 10, 50 and 90 per cent CBZ-SAC cocrystal were used as validation standards for the calibration curve.

The standards were prepared by grinding 0.5 grams of each component separately for 2 to 3 minutes in the room temperature mill. This was done to reduce particle size

differences between these components and to obtain a homogeneous blend for the standards. The three components were then weighed and blended in a stainless steel vial without the grinding beads in the SPEX 5100 mill. The samples after blending were analyzed in the Nicolet 6700 spectrometer equipped with the ATR accessory. Three samples were taken from each standard and analyzed. The spectra of the replicates collected for each standard were compared to ensure homogeneity in the standards. If the spectra of the replicates of a particular standard differed from one another, the standard was prepared again by blending for a longer time. This procedure was repeated until a homogeneous blend was obtained. The spectra collected in this manner for all the standards were then used for obtaining a calibration curve using the Partial Least Square method in the Quant software for OPUS. The calibration curve obtained was then validated using the validation standards. The R^2 values for the calibration and validation were 0.99.

X-ray powder diffraction (XRPD)

XRPD was used to identify crystalline phases and to qualitatively examine changes in crystallinity. Measurements were done with a Scintag X1 diffractometer (Cupertino, CA) having a copper-target X-ray tube (CuKα radiation 1.54 Å). Data were collected at a scan rate of 2.5°/min over a 2θ range of 5° to 40°. The accelerating voltage was 35kV and the current was 20 Amperes.

XRPD was also done using a Rigaku miniflex diffractometer (The Woodlands, TX) having a copper target X-ray tube. Data were collected at a scan rate of 2.5°/min

over a 2θ range of 2.5° to 40°. The accelerating voltage was 30kV and the current was 15 mA.

Differential Scanning Calorimetry (DSC)

Thermal analysis of samples was carried out using a TA 2590 DSC (TA instruments, New Castle, DE) which was calibrated for temperature and cell constants using indium and n-dodecane. Samples (6-8 mg) crimped in aluminum pans were analyzed in the DSC from -20 to 200°C at a heating rate of 10 °C/min. Samples were continuously purged with nitrogen at 50 ml/min. Samples were also analyzed using modulated differential scanning calorimetry (MDSC) to determine the T_g of coground samples. The temperature modulation was ± 1°C with a 60 seconds period.

Results

FTIR spectra of crystalline and cocrystalline phases

Since cocrystal formation is a result of interactions between different molecular components that also exist in the single-component crystalline states, vibrational spectroscopy is an excellent technique to characterize and study cocrystallization. Differences in hydrogen bond interactions of CBZ-SAC and CBZ-NCT cocrystals as well as crystalline reactants (CBZ(III), CBZ(D), SAC and NCT) shown in figure 5.1, lead to significant changes in FTIR spectra as shown in figures 5.2 and 5.3.

The crystal structures of CBZ(III), CBZ(D) and both cocrystals, CBZ-SAC and CBZ-NCT (figure 5.1), show the formation of the carboxamide homodimer of CBZ with

the CBZ carboxamide unit acting as both a hydrogen bond donor (syn-NH) and acceptor (C=O). Compared to other primary amide crystals, CBZ(III) and all anhydrous CBZ polymorphs do not posses the conventional ribbons of carboxamide dimers because the azepine ring sterically blocks the exterior amide hydrogen bond donor (anti-NH) and acceptor. This anti-NH is however involved in linking CBZ and water molecules by N-H---O hydrogen bonds as shown for CBZ(D), while maintaining the carboxamide homodimer. Similar molecular interactions are observed in the acetone and DMSO solvates of CBZ.[31]

One of the strategies in designing CBZ cocrystals is to fulfill the donors and acceptors in the carboxamide dimers by linking the anti-NH hydrogen bond donor and acceptor (C=O) sites of CBZ that are not involved in the homodimer as shown in the cocrystals of CBZ with SAC or NCT (figure 5.1).[31] In the CBZ-SAC cocrystal, saccharin forms an N-H---O=C with the carbamazepine carbonyl, and an S=O---N-H with the additional donor of the carbamazepine amide. Compared to the crystal structure of pure saccharin, homomeric N-H---O=C dimers are replaced with heteromeric N-H---O=C dimers in the cocrystal, leaving the carbonyl group in SAC free. In addition, the free SO_2 in pure SAC is engaged in weak S=O---N-H bonds with CBZ in the cocrystal and forms S=O---H-C bonds between SAC molecules.[31] In the CBZ-NCT cocrystal, the anti-NH of CBZ hydrogen bonds with the carbonyl of NCT resulting in the heteromeric N-H---O=C dimer in the cocrystal.[31] These differences in hydrogen bond interactions are reflected in the FTIR spectra of these materials as discussed below, and were used to study cocrystallization by cogrinding solid reactants and during storage.

The IR spectrum of CBZ(III) (figure 5.2) shows peaks at 3465 and 3157 cm^{-1} that correspond to the free anti-NH and hydrogen bonded syn-NH respectively in CBZ(III).[39] A peak corresponding to the carbonyl stretch is observed in the spectrum at 1676 cm^{-1}. [40, 41] Peaks corresponding to NH and carbonyl stretch of the amide are also observed in the spectrum of CBZ(D). A peak at 3432 cm^{-1} for NH stretch, lower than that observed at 3465 cm^{-1} in CBZ(III), is observed in the spectrum of CBZ(D). The shift of the peak towards lower wavenumber is due to hydrogen bonding between the free NH of CBZ and the oxygen of water.[40, 41] The peak corresponding to the carbonyl stretch in CBZ(D) is observed at 1677 cm^{-1} and is similar to that observed in CBZ(III). These spectral differences reflect the hydrogen bond pattern differences between the anhydrous (III) and hydrated forms of CBZ as presented in figure 5.1.

The spectrum of pure SAC also shows peaks corresponding to NH and CO stretch of the secondary amide at 3094 and 1719 cm^{-1}. [42-44] In addition, peaks corresponding to asymmetric and symmetric stretching of $-SO_2$ group in SAC are also observed at 1332 and 1175 cm^{-1} respectively.[40, 41, 43, 45]

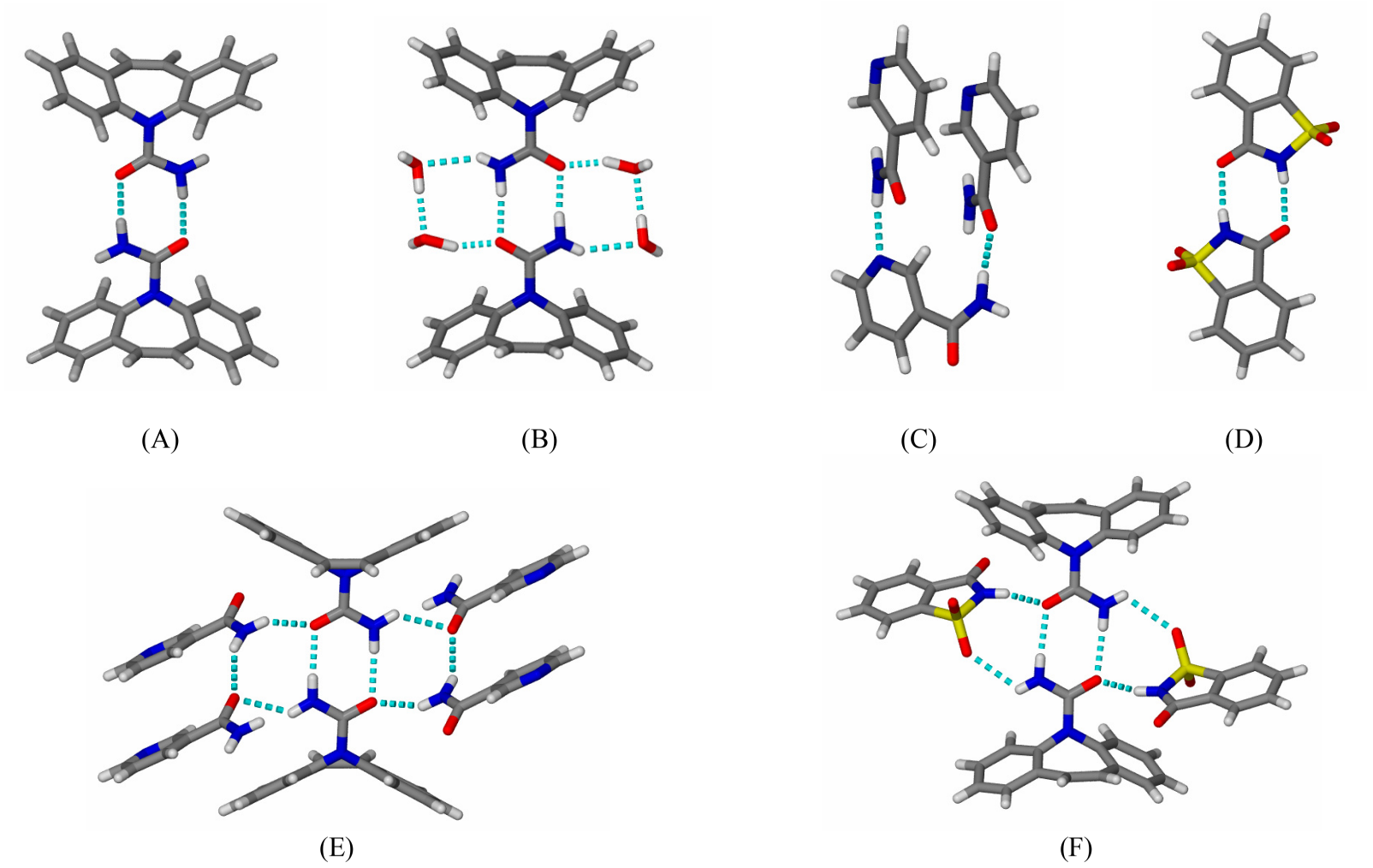

Figure 5.1: Hydrogen bonding in (A) CBZ(III), (B) CB(D), (C) NCT, (D) SAC, (E) CBZ-NCT, and (F) CBZ-SAC

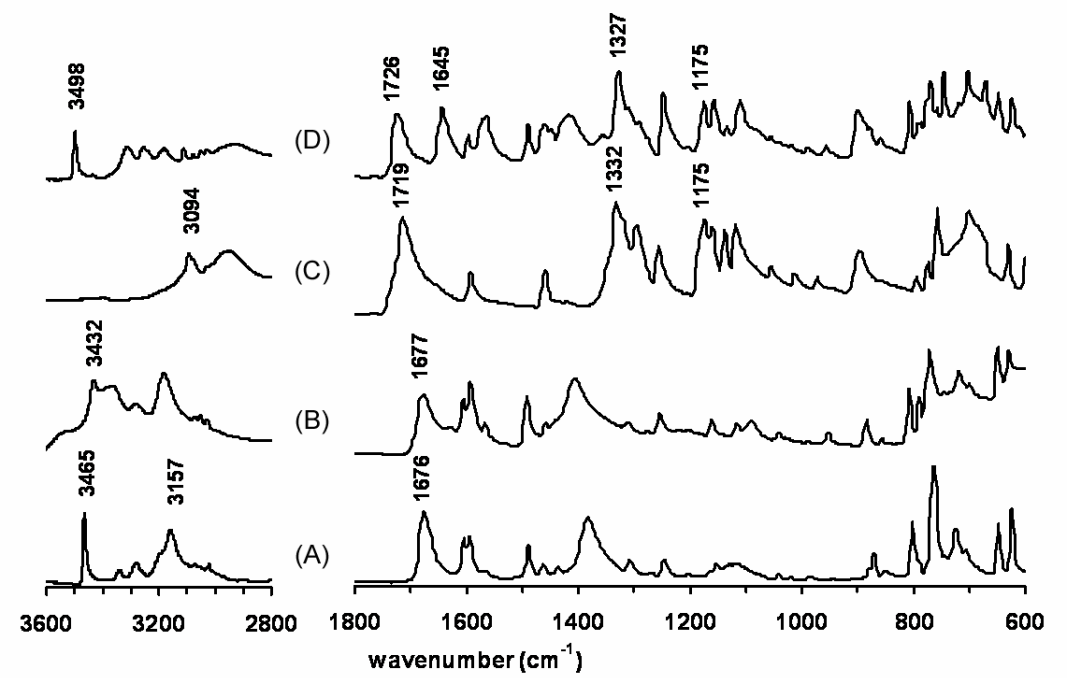

Figure 5.2: Infra-red spectra of (A) CBZ(III) (B) CBZ(D) (C) SAC and (D) CBZ-SAC cocrystal prepared from solution.

Comparison of the spectrum of CBZ-SAC cocrystal with that of CBZ(III) and SAC (figure 5.2) shows peak shifts in the carbonyl, amide, and SO_2 regions in the cocrystal spectrum that relate to hydrogen bond interactions in their crystal structures. Peaks corresponding to free carbonyl of SAC and hydrogen bonded carbonyl of CBZ are observed at 1726 and 1645 cm^{-1}, respectively in the spectrum of the cocrystal.[13, 40, 41] A peak shift is observed corresponding to NH stretch of the amide from 3465 cm^{-1} for CBZ(III) to 3498 cm^{-1} for the cocrystal. Comparison of the spectrum of SAC and CBZ-SAC cocrystal shows a peak shift corresponding to the asymmetric stretch of $–SO_2$ from 1332 cm^{-1} in the spectrum of SAC to 1327 cm^{-1} in the spectrum of the cocrystal. Similar

peak shifts due to hydrogen bond differences are also observed in CBZ-NCT cocrystal spectrum (figure 5.3). CBZ-NCT cocrystal spectrum shows peaks at 3447 and 3389 cm^{-1} corresponding to the amide NH. Peaks corresponding to the carbonyl stretch are observed at 1682 and 1657cm^{-1}.

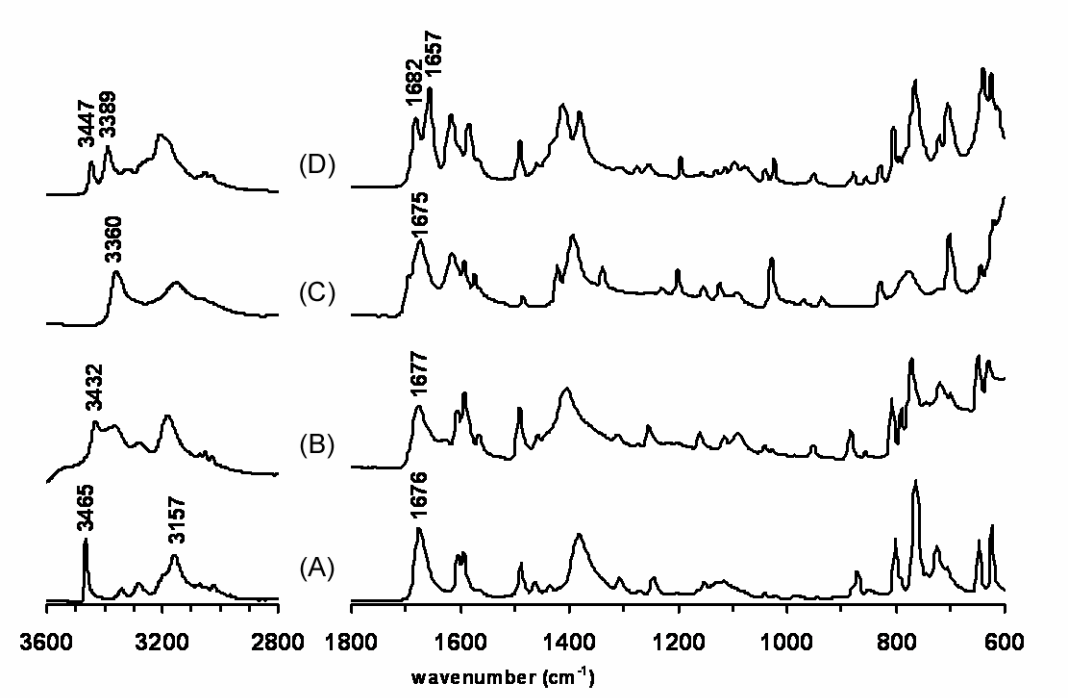

Figure 5.3: Infra-red spectra of (A) CBZ(III) (B) CBZ(D) (C) NCT and (D) CBZ-NCT cocrystal prepared from solution.

Cocrystal formation by cogrinding anhydrous CBZ(III) and SAC

XRPD patterns and FTIR spectra before and after cogrinding CBZ(III) and SAC equimolar blends for 30 minutes under ambient and cryogenic conditions are shown in figures 5.4 and 5.5. A decrease in XRPD peak intensities was observed, with the decrease being greater for the blend milled under cryogenic conditions (figure 5.4). This indicates

a larger reduction in the crystallinity of reactant materials under cryogenic conditions, with a few low intensity peaks that are common to cocrystal or reactants. Ambient temperature cogrinding resulted in transformation to the cocrystalline phase as indicated by the diffraction peaks at 7.08° and 28.3° unique to the CBZ-SAC cocrystal. A low intensity broad peak around 27.0° corresponding to CBZ and or SAC suggests the presence of unreacted crystalline material.

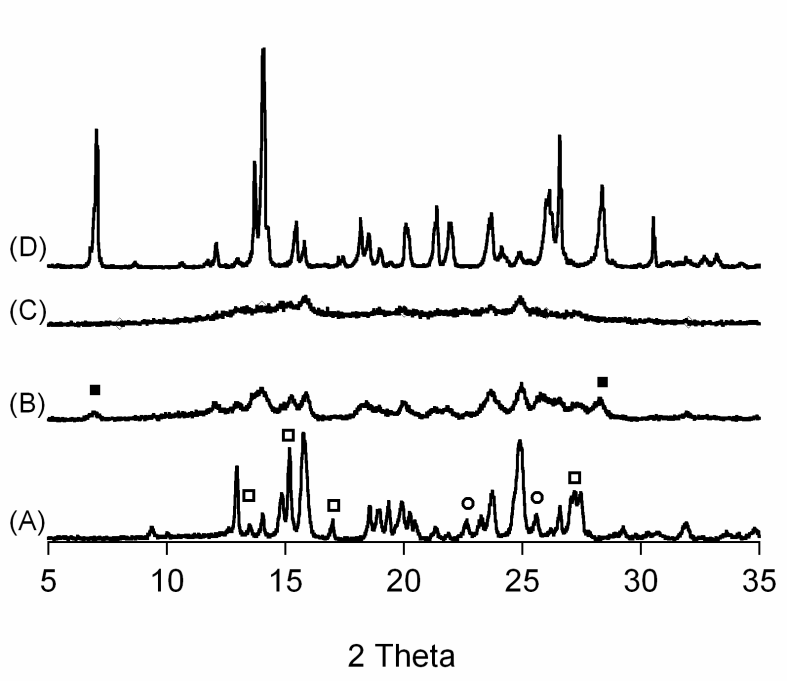

Figure 5.4: XRPD patterns showing cocrystal and amorphous phase formation after room temperature and cryogenic cogrinding of CBZ(III) and SAC. (A) before cogrinding, (B) after 30 minutes room temperature cogrinding, (C) after 30 minutes cryogenic cogrinding and (D) CBZ-SAC cocrystal prepared from solution (symbols □, ○, and ■ indicate CBZ(III), SAC and CBZ-SAC cocrystal prepared from solution)

FTIR analysis provided information regarding the intermolecular interactions and phase transformations occurring in these processes (figure 5.5). Infrared spectra show stronger peaks corresponding to CBZ-SAC cocrystal at 3498, 1726 and 1645 cm^{-1} after ambient temperature cogrinding. These observations are consistent with the XRPD analysis and suggest that hydrogen bond heteromeric associations between CBZ and SAC, similar to those in the cocrystal, occur at a faster rate during cogrinding at ambient temperature than under cryogenic conditions. Peaks characteristic of CBZ(III) and SAC are also observed, indicating some unreacted components.

Spectral shifts after cryogenic cogrinding also reflect changes in intermolecular interactions between CBZ and SAC in the XRPD disordered phase. A broad shoulder between 3475 and 3520 cm^{-1}, corresponding to $-NH_2$ stretch in the amide group, and spectral changes in the carbonyl stretching region that reflect changes in hydrogen bond interactions preceding complex formation are observed. Further studies of spectral shifts and chemical interpretations are currently under investigation in our laboratory.

To confirm the presence of a disordered or an amorphous phase, DSC analysis was carried out. Figure 5.6 shows the presence of an amorphous phase in the cryogenically coground sample with a T_g around 41°C, followed by a crystallization event (exotherm) around 69°C before an endotherm at 174°C that agrees with the melt of the CBZ-SAC cocrystalline phase at 176°C. XRPD analysis of the sample after the exothermic crystallization event and before the melt, shows peaks corresponding to cocrystal and a few peaks with weak intensities due to unreacted components (appendix D). The presence of unreacted components would cause a decrease in the melting point and may be the reason for the slightly lower melting points measured. Cogrinding under

ambient conditions showed a single endothermic event at 174°C. Pure CBZ(III) has been reported to exhibit an endothermic transition to CBZ(I) at 174°C followed by the melt of form I at 189°C.[46] The melting point of pure SAC was determined to be 228°C. Due to chemical degradation of CBZ, thermal analysis studies were done below 200°C.

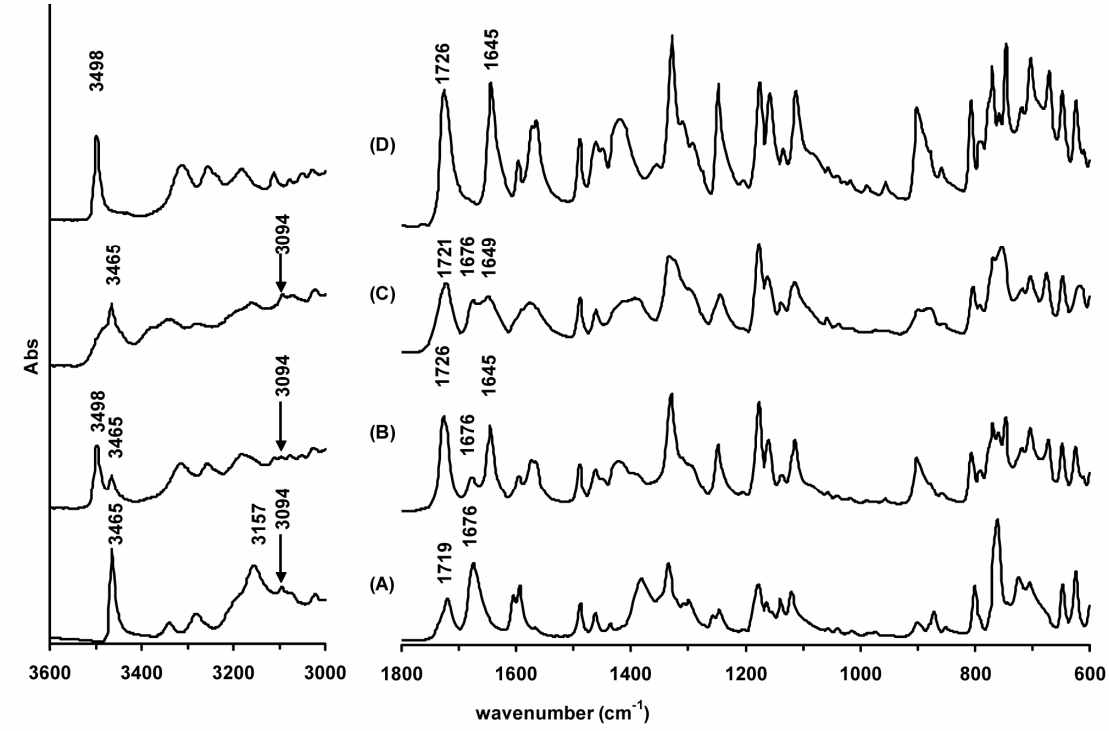

Figure 5.5: Infra-red spectra showing interactions between CBZ and SAC after 30 minutes room temperature and cryogenic cogrinding of CBZ(III) and SAC. (A) before cogrinding, (B) after room temperature cogrinding, (C) after cryogenic cogrinding and (D)CBZ-SAC cocrystal prepared from solution.

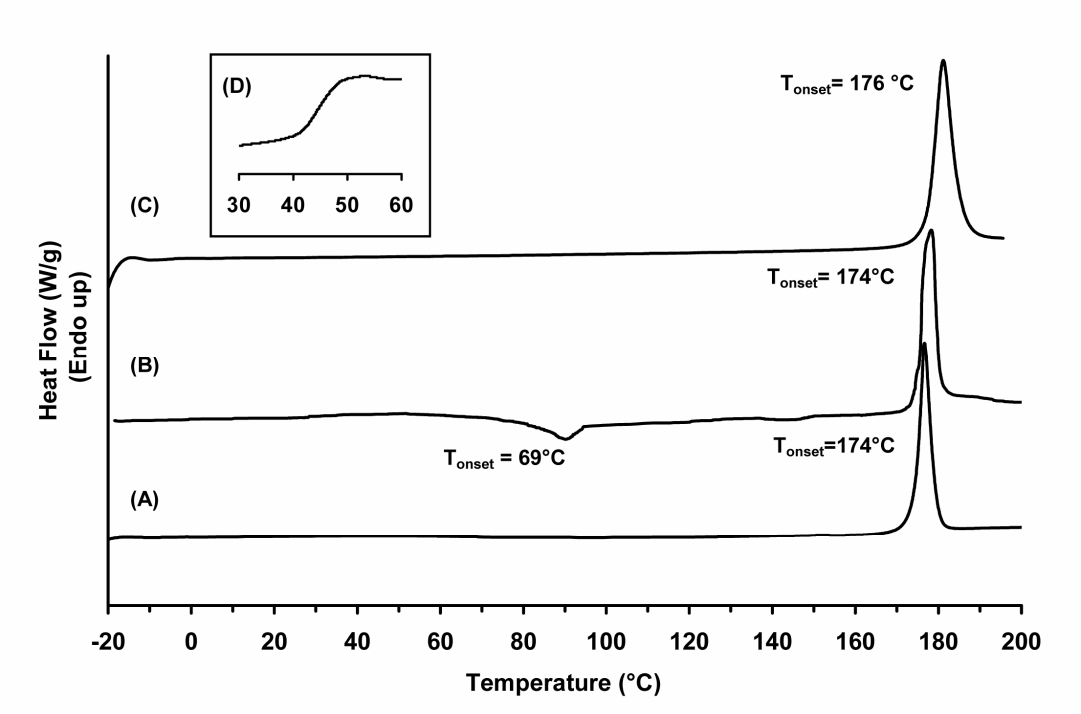

Figure 5.6: DSC analysis of CBZ(III) and SAC blends after cogrinding for 30 minutes under the following conditions: (A) room temperature, (B) cryogenic condition, (C) CBZ-SAC cocrystal prepared from solution, and (D) inset showing the T_g determined using MDSC after cryogenic cogrinding.

The glass transition temperature of amorphous materials is an important property that determines molecular mobility and reactivity,[47] and is thus considered in examining the results from cogrinding under ambient and cryogenic conditions. The T_g values, measured by melt-quenching the reactants in the DSC, are 52°C for anhydrous CBZ[24] and 85°C for SAC. Since the temperature in the cryogenic mill is below the glass transition temperature of the blend and individual components by at least 200°C, molecular mobility decreases under these conditions and the amorphous state generated by cogrinding is maintained.[23, 48] This explains the high degree of disorder observed in the XRPD pattern of the equimolar blend of CBZ(III) and SAC after 30 min cogrinding

under cryogenic conditions. In contrast, the temperature in the room temperature mill after 30 minutes cogrinding was observed to rise to 45°C which is close to the glass transition temperatures of CBZ and the equimolar blend. Under these conditions, molecular mobility increases in the amorphous phases leading to faster crystallization, and in this case cocrystallization of CBZ-SAC.

The extent of cocrystallization during cogrinding at room temperature is shown in figure 5.7. Quantification was done by FTIR analysis as described in the methods section. These results indicate the quick formation of the CBZ-SAC cocrystal with a faster rate of cocrystallization in the early stages of the process and approximately 85% cocrystal formed after cogrinding for 30 minutes.

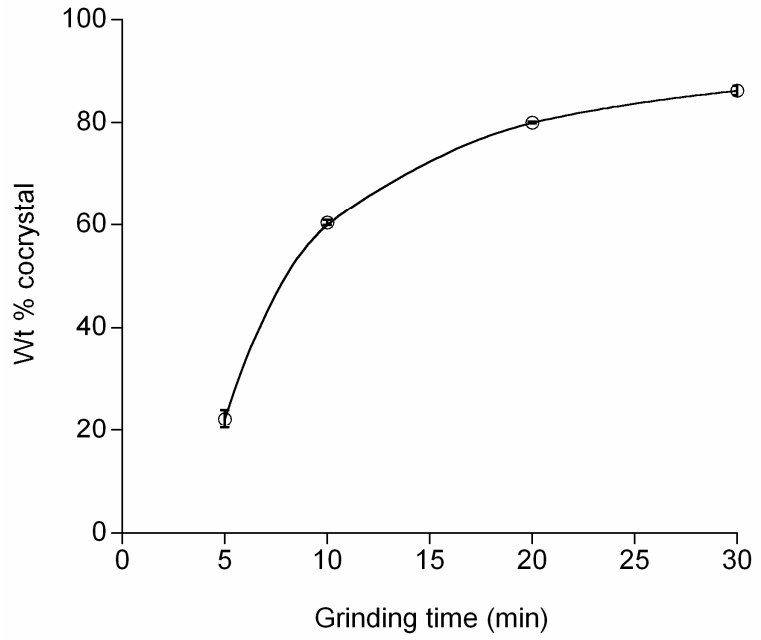

Figure 5.7: Cocrystal formation during cogrinding at room temperature.

Cocrystal formation during storage

Cocrystallization during solid state cogrinding under ambient temperatures has been reported for a number of systems.[4, 6, 9, 10, 49] However the formation of cocrystals during storage, to our knowledge, has not been reported. Based on the current understanding of amorphization induced by grinding, and considering the factors that affect the stability of amorphous phases and crystallization of single component crystals from the amorphous state, we studied cocrystal formation during storage after cogrinding solid reactants. Coground equimolar blends of CBZ(III) and SAC were stored at room temperature (22 to 25°C) under 0% and 75% RH. Cocrystallization was monitored by XRPD and FTIR.

Figure 5.8 shows that cocrystallization occurs at 0% and 75% RH after cryogenic cogrinding. Based on these findings we studied the extent of cocrystallization after 5 minute ambient temperature cogrinding. Results show that cocrystal formation initiated during cogrinding proceeds during storage (figure 5.9) and that the rate of cocrystallization increases with RH.

Cocrystal formation during storage after mechanical activation of the solid and the rate dependence on RH suggests an amorphous phase mediated transformation. Water, a potent plasticizer, has a T_g of -138°C and has been shown to decrease the glass transition temperature of amorphous solids.[29, 30] Therefore, moisture sorption will increase the molecular mobility and the rate of crystallization of amorphous phases. Higher rate of cocrystal formation during storage at high RH may therefore be due to a decrease in T_g and a consequent increase in molecular mobility in the disordered regions of the ground blend.

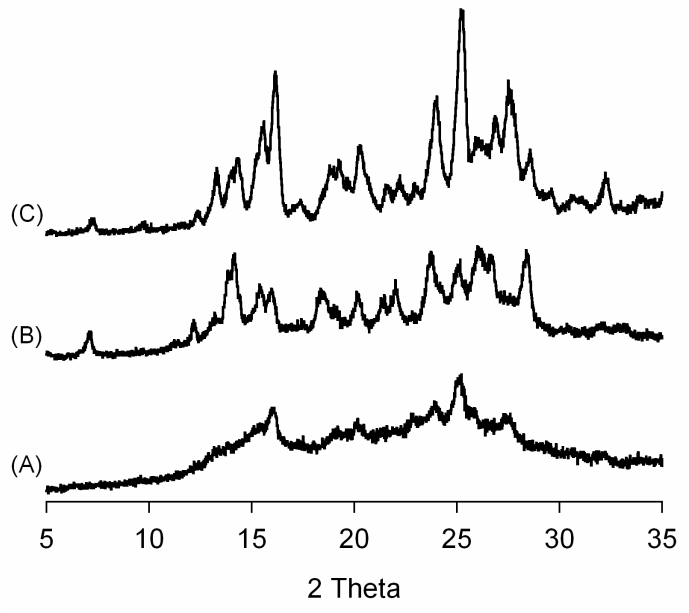

Figure 5.8: XRPD patterns showing cocrystal formation during storage after cryogenic cogrinding of CBZ(III) and SAC for 30 minutes. (A) freshly ground blend (day 0) after storage for 1 day at (B) room temperature and 0%RH , and (C) room temperature and 75%RH.

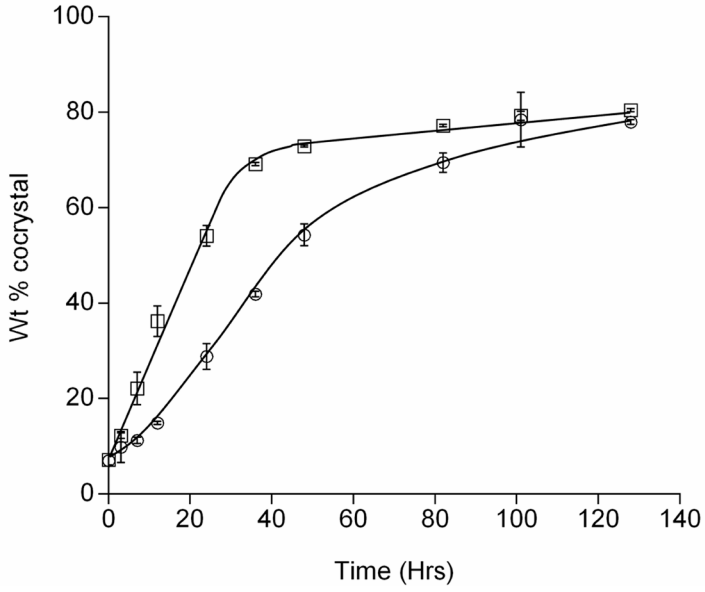

Figure 5.9: Cocrystal formation during storage under 0%RH and 75%RH at room temperature after cogrinding CBZ(III) and SAC for 5 minutes at room temperature. (○) storage at 0%RH; (□) storage at 75%RH.

Cocrystal formation by cogrinding carbamazepine dihydrate and saccharin

Since our results indicate that cocrystal formation proceeds through amorphous phases induced by grinding and that the rate of cocrystallization during storage increases on exposure to high relative humidities, one would anticipate that the use of crystalline solvates in cogrinding would increase the rate of cocrystallization. In this case, the solvent in the crystal structure serves as a potent plasticizer. Cogrinding with the dihydrate form of CBZ was therefore carried out to test this hypothesis.

XRPD and FTIR analysis confirm our hypothesis. XRPD patterns (figure 5.10) shows transformation to cocrystal during cogrinding under ambient conditions for 10 minutes, since the pattern of the coground reactants is in agreement with the pattern of the cocrystal prepared from solution. Peaks characteristic of CBZ(D), CBZ anhydrous polymorphs or SAC were absent after cogrinding.

To compare the rate of cocrystallization between CBZ(D) and CBZ(III) systems, the same cogrinding protocol was used with CBZ(III) and SAC. The XRPD pattern after cogrinding for 10 minutes (figure 5.11) shows evidence for cocrystal formation and unreacted components.

The FTIR spectra (figure 5.12) provided further evidence for cocrystallization. The spectrum of cocrystal prepared by cogrinding the dihydrate is very similar to that of the cocrystal prepared from solution. Peaks corresponding to unreacted components were not detected. The spectrum of the coground anhydrous CBZ (III) shows peaks characteristic of cocrystal as well as those corresponding to unreacted CBZ and SAC. These results suggest that the rate of cocrystallization is increased by cogrinding with the hydrated form of CBZ.

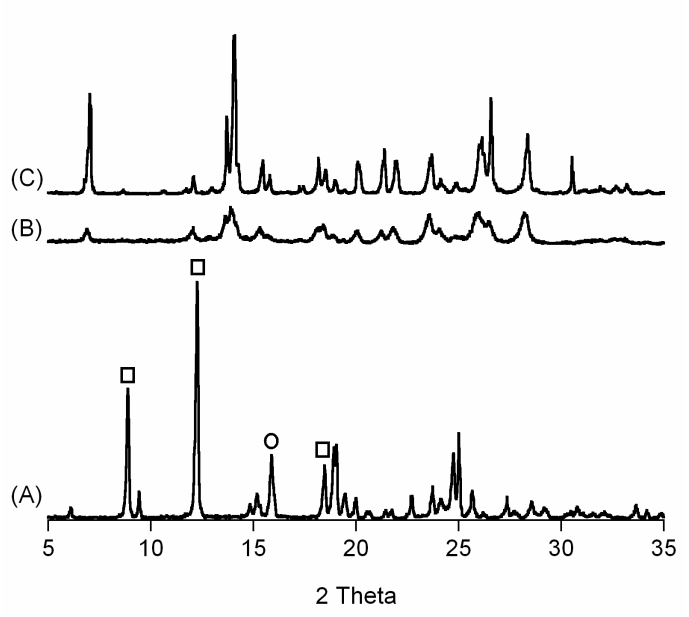

Figure 5.10: XRPD pattern showing cocrystal formation after cogrinding CBZ(D) and SAC at room temperature for 10 minutes. (A) before cogrinding, (B) after cogrinding and (C) CBZ-SAC cocrystal prepared from solution. (Symbols □ and ○ indicate CBZ(D) and SAC respectively)

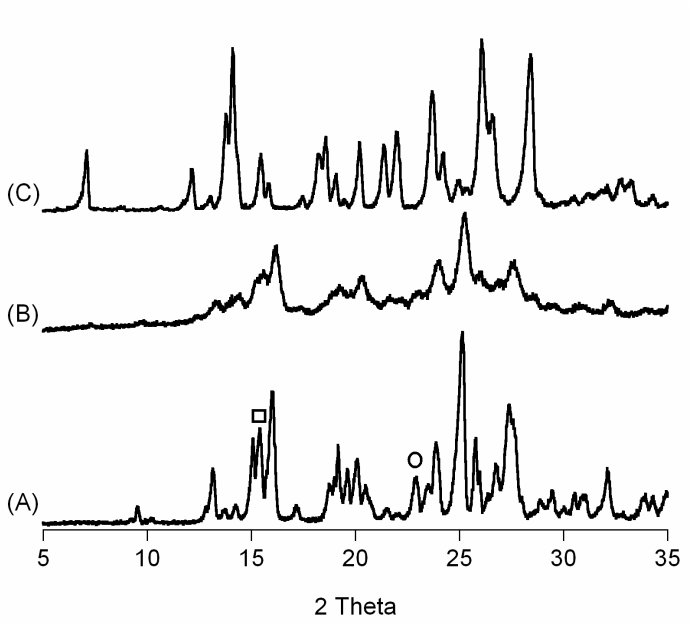

Figure 5.11: XRPD pattern of CBZ(III) and SAC showing cocrystal formation after 10 minutes cogrinding at room temperature. (A) before cogrinding, (B) after cogrinding and (C) CBZ-SAC cocrystal prepared from solution. (Symbols □ and ○ indicate CBZ(III) and SAC respectively)

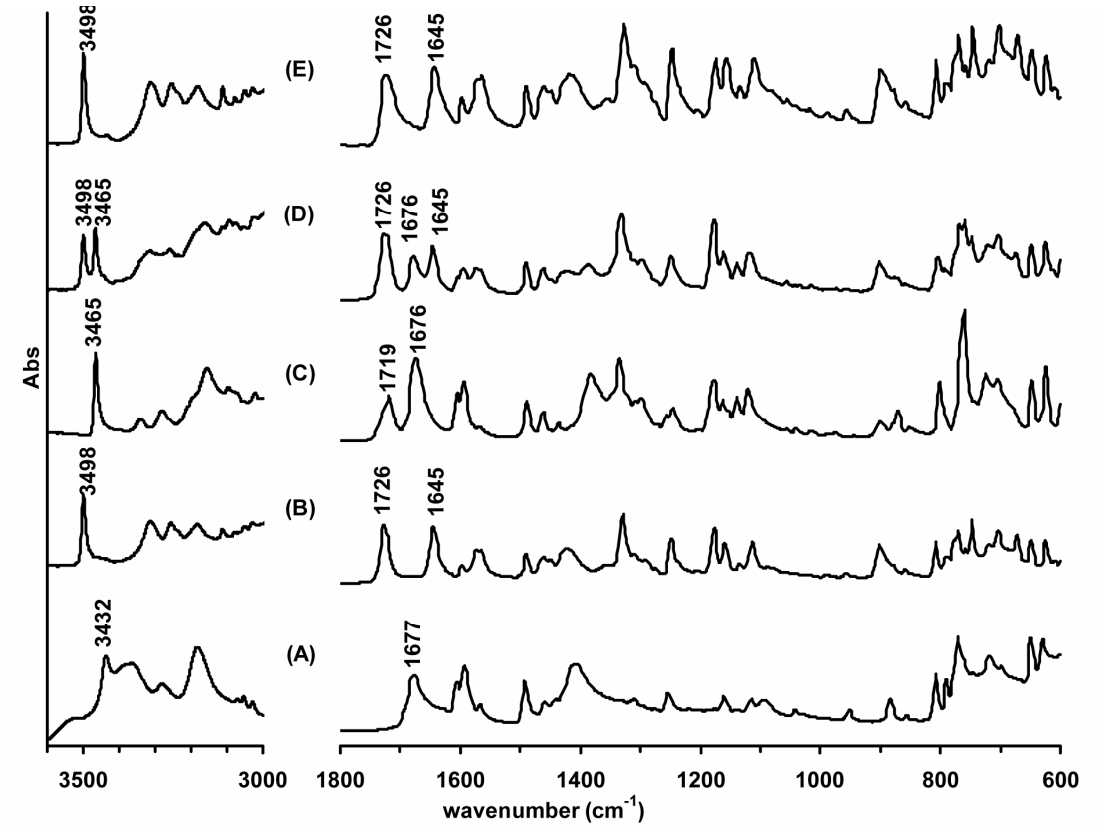

Figure 5.12: FTIR spectra showing interactions between CBZ and SAC after 10 minutes room temperature cogrinding of SAC with either CBZ(D) or CBZ(III). CBZ(D)/SAC mixture (A) before cogrinding, and (B) after cogrinding; CBZ(III)/SAC mixture (C) before cogrinding, and (D) after cogrinding; (E) CBZ-SAC cocrystal from solvent

Faster rate of cocrystallization by cogrinding with CBZ(D) may be due to the potent plasticizing action of water from the hydrate in reducing the T_g of the amorphous phase. CBZ(D) has 13.5% water and upon dehydration there is 7.9% water in the blend. This leads to significant plasticizing effects since solvents at low concentrations have the greatest plasticizing effects.[30]

Cocrystal formation in non-stoichiometric anhydrous CBZ(III) blends

Cocrystal formation was observed by cogrinding CBZ(III) and SAC in 1:2 and 2:1 ratios at ambient temperature for 30 minutes. The results also suggested the presence of unreacted CBZ and unreacted SAC in the 2:1 and 1:2 blends respectively after cogrinding.

Cocrystal formation by cogrinding CBZ(III) and NCT

Cocrystal formation during cogrinding was also studied in CBZ(III)/NCT mixtures. Figure 5.13 shows the XRPD patterns of CBZ(III)/NCT mixture after cogrinding at ambient and cryogenic conditions. Cogrinding CBZ(III) and NCT at ambient condition results in cocrystal formation. Peaks characteristic of the cocrystal are observed in the XRPD pattern at 2 theta values of 6.4°, 8.7° and 9.9° after cogrinding the mixture. The pattern also shows evidence for unreacted CBZ and NCT (2 theta = 14.7 and 15.8). However, cogrinding CBZ(III) and NCT at cryogenic conditions does not result in cocrystal formation. The XRPD pattern after cryogenic grinding resembles the mixture but shows a reduction in peak intensities suggesting disorder induced due to grinding.

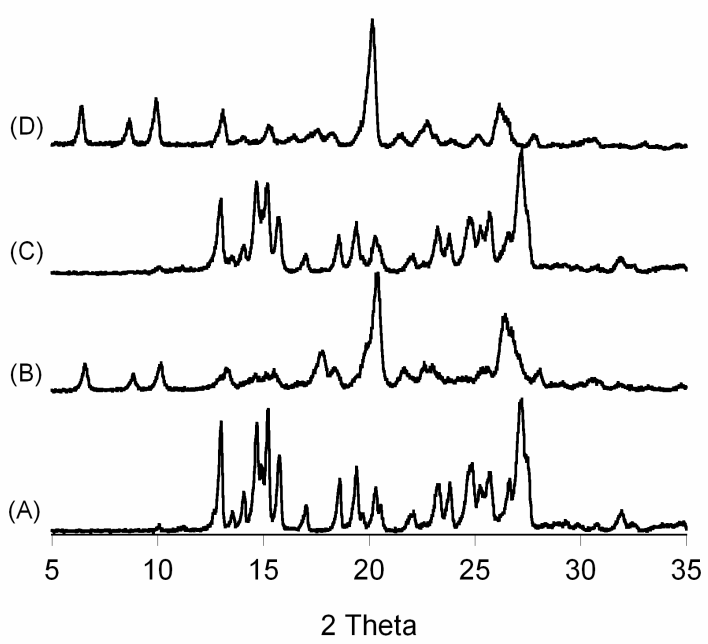

Figure 5.13: XRPD of CBZ(III)/NCT mixture after 30 minutes grinding at ambient and cryogenic conditions showing cocrystal formation and disorder. CBZ(III)/NCT mixture (A) before grinding; after grinding at (B) ambient, and (C) cryogenic conditions; (D) reference pattern of CBZ-NCT cocrystal

FTIR spectrum of CBZ(III)/NCT mixture after grinding is shown in figure 5.14. The spectrum of the mixture after grinding at ambient conditions shows peaks at 3446, 3389, 1683 and 1658cm^{-1} indicating cocrystal formation. Shifts in the IR spectrum are also observed after cryogenic grinding. Peaks at 3448 and 1658cm^{-1} suggest interactions between the reactants similar to those observed in the cocrystal. In addition, the spectrum also shows evidence for unreacted components as indicated by the peaks at 3464 and 1677cm^{-1}, consistent with results from XRPD patterns. Since the XRPD pattern does not show evidence for cocrystal after cryogenic grinding, it is possible that interactions between CBZ and NCT in the cryogenic ground mixture occur in the disordered regions induced by milling.

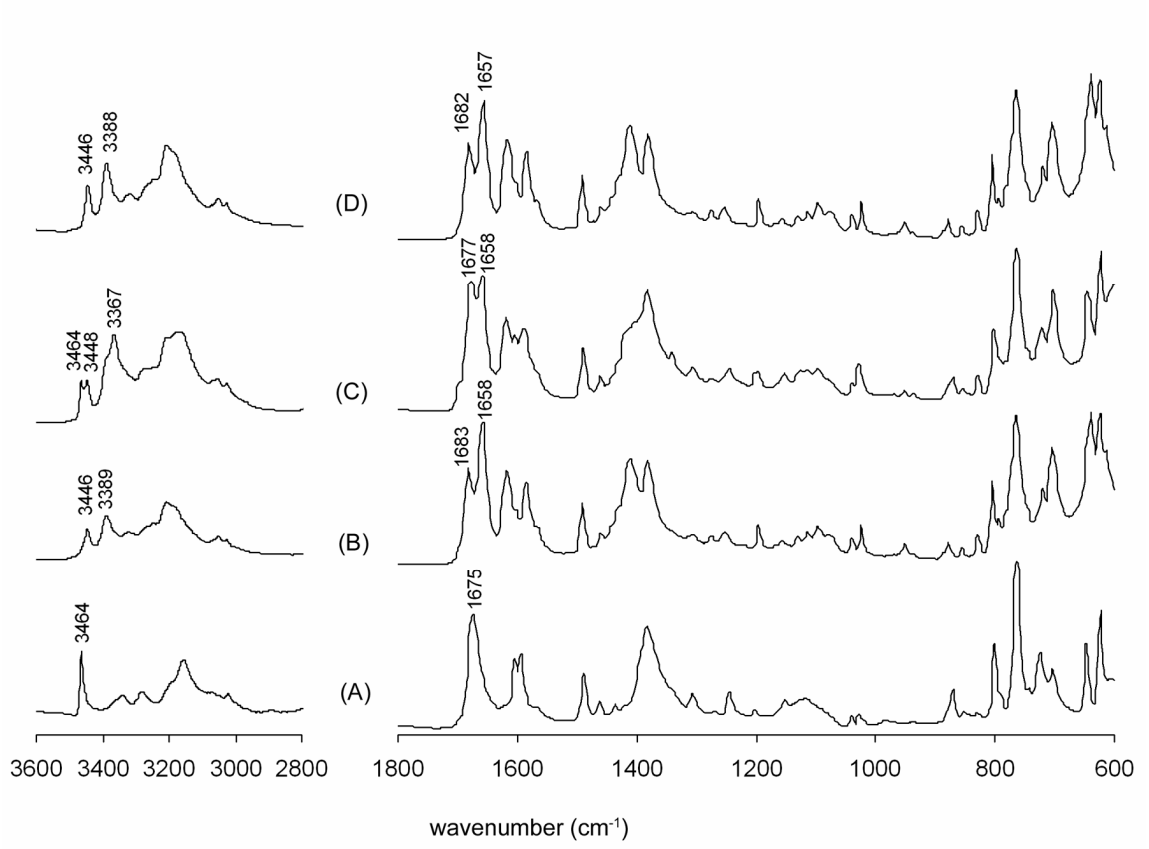

Figure 5.14: Infra-red spectra showing interactions between CBZ and NCT after room temperature and cryogenic grinding of CBZ(III)/NCT mixture. CBZ(III)/NCT mixture (A) before grinding; after grinding at (B) ambient conditions, and (C) cryogenic conditions; (D) reference pattern of CBZ-NCT cocrystal.

Thermal analysis of cryogenic ground mixture shows an exotherm with onset at 99.1°C and an endotherm with onset at 119.1°C, followed by another endotherm at 157.7°C that corresponds to cocrystal melting point of 158.7°C (figure 5.15). These events are different from those observed in CBZ or NCT. NCT exhibits an endotherm corresponding to melting with an onset at 126-128°C.[35] Analysis of the mixture ground under ambient conditions shows an endotherm corresponding to cocrystal melting at

157.5°C. Lower melting points of the cocrystal in the ground mixtures may be due to the presence of some unreacted components.

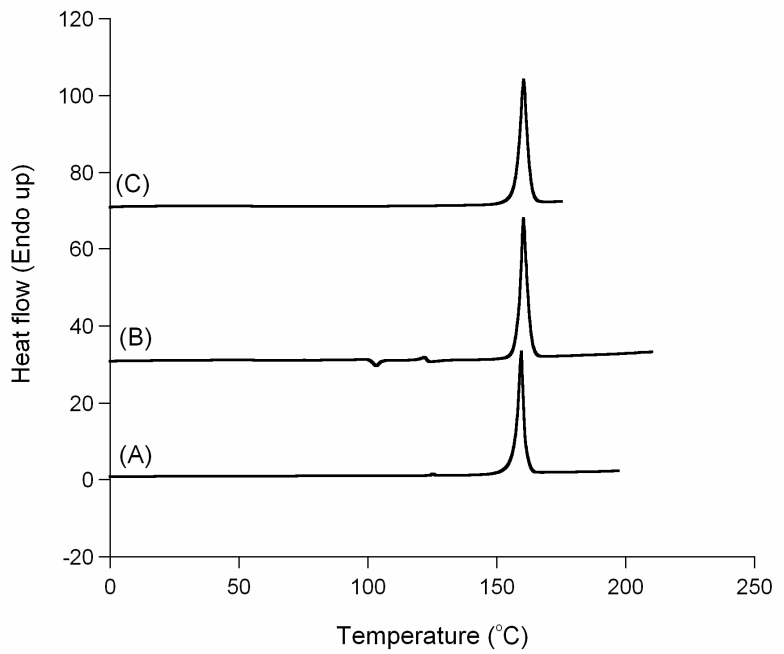

Figure 5.15: Thermal analysis of CBZ(III)/NCT mixture after 30 minutes grinding at (A) ambient condition, and (B) cryogenic condition; (C) CBZ-NCT cocrystal.

Results from the above study show that cocrystal formation by cogrinding reactants is dependent on temperature. Since cryogenic cogrinding of reactants did not result in cocrystal formation, cryogenic grinding of CBZ-NCT cocrystal was performed to investigate cocrystal stability.

CBZ-NCT stability during cryogenic grinding

Figure 5.16 shows the XRPD pattern of CBZ-NCT cocrystal after 5, 10, 30, and 60 minutes cryogenic grinding. Conversion of cocrystal to CBZ(III) and NCT after 5 minutes grinding indicates cocrystal instability. Reduction in peak intensities with longer grinding times indicates amorphous phase formation due to grinding. Cocrystal stability under cryogenic conditions was also investigated without any mechanical activation. In this case, cocrystal was stable even after 60 minutes of storage under cryogenic conditions. This suggests that mechanical activation is necessary to induce cocrystal instability under cryogenic conditions.

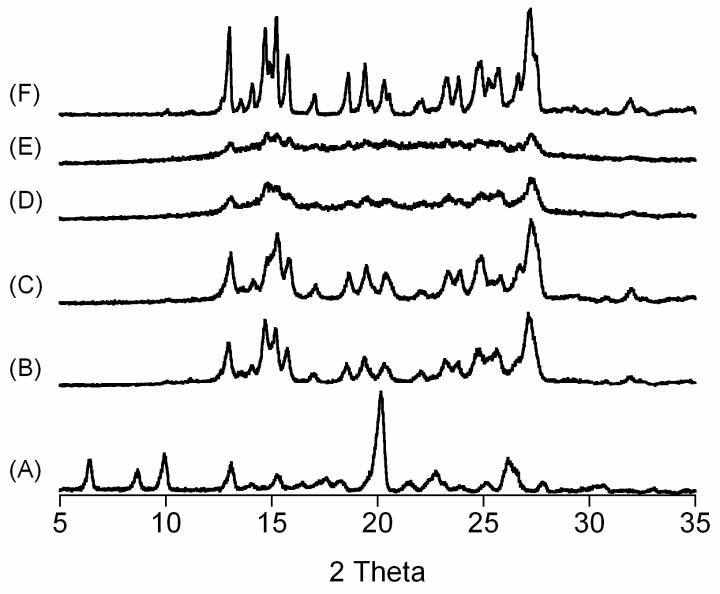

Figure 5.16: XRPD showing CBZ-NCT cocrystal instability after cryogenic grinding for different times. CBZ-NCT cocrystal (A) before grinding, and after grinding for (B) 5 min, (C) 10 min, (D) 30 min, and (E) 60 min; (F) reference pattern of CBZ(III)/NCT mixture.

Cocrystal formation by cogrinding CBZ(D) and NCT

Water present in hydrated reactants has been shown to affect cocrystal formation during cogrinding in a preceding section. Cogrinding of CBZ(D) and NCT was therefore performed at cryogenic and ambient conditions to study the effect of hydrated reactants on crystallization outcomes during cogrinding. Unlike CBZ(III)/NCT mixture, cryogenic grinding of CBZ(D)/NCT mixture results in cocrystal formation (figure 5.17). Cogrinding CBZ(D) and NCT at ambient conditions similarly facilitates cocrystal formation and enhances the rate of cocrystallization. Figure 5.18 shows the XRPD patterns of CBZ(III)/NCT and CBZ(D)/NCT mixtures after 5 minute grinding under ambient conditions. The patterns indicate complete conversion of CBZ(D)/NCT mixture to cocrystal. In contrast, the pattern of CBZ(III)/NCT mixture after 5 minutes cogrinding shows evidence for unreacted components in addition to cocrystal formation. Results from FTIR spectral analysis of the ground mixtures are in agreement with the above findings. Faster rates of cocrystal formation with hydrated reactants may be due to enhanced molecular mobility in the amorphous phase as a result of plasticizing action of water.[30]

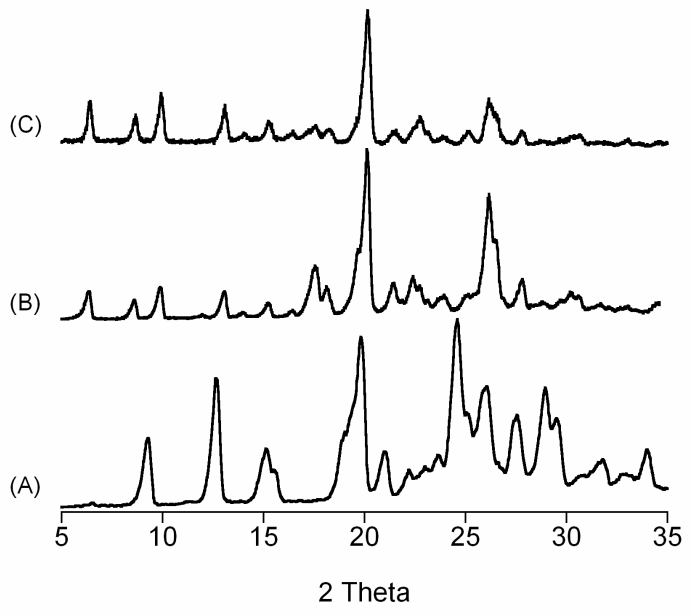

Figure 5.17: XRPD pattern showing cocrystal formation after 12 minutes cryogenic grinding of CBZ(D)/NCT mixture. CBZ(D)/NCT mixture (A) before grinding, and (B) after cryogenic grinding; (C) CBZ-NCT reference pattern.

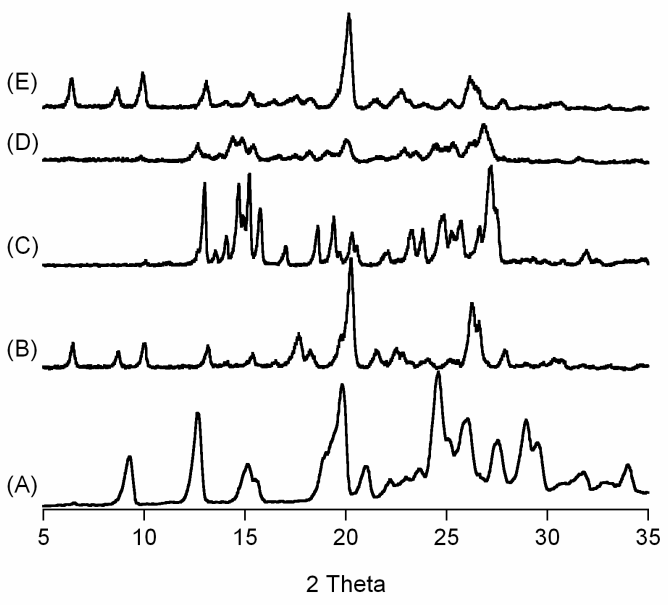

Figure 5.18: XRPD pattern showing the effect of anhydrous and hydrated reactant (CBZ) on CBZ-NCT cocrystal formation during cogrinding at ambient conditions for 5 min. CBZ(D)/NCT mixture (A) before grinding, and (B) after grinding; CBZ(III)/NCT mixture (C) before grinding, and (D) after grinding; (E) CBZ-NCT cocrystal.

Discussion

Our results demonstrate that cocrystal formation during storage is mediated by the formation of disordered regions or amorphous phases induced by cogrinding reactants. The rate of cocrystal formation during cogrinding of solid reactants depends on the grinding temperature and on the solid-state form of the reactants. Cogrinding CBZ(III) and SAC under cryogenic conditions results in amorphous phase formation. This is possibly due to reduced molecular mobility under cryogenic conditions, and hence reduced rate of cocrystal formation. Amorphization by low temperature grinding (4°C and cryogenic conditions) has been demonstrated for indomethacin (T_g of 43°C),[23] while grinding in the proximity of the T_g yielded partially amorphous materials.[23, 27] In the case of CBZ(III) and NCT, cryogenic cogrinding shows evidence for disorder and crystalline reactants.

Studies on the solid-state complexation of coground mixtures of cholic acid with either methyl p-hydroxybenzoate or ibuprofen demonstrated the formation of crystalline inclusion complexes during room temperature grinding and the formation of an amorphous phase under cryogenic conditions.[26] The amorphous phase transformed to the crystalline complex after 1 hour of heat treatment at 60°C. Crystalline complex formation was suggested to be a result of two factors: (i) amorphous phase formation by mechanical force and (ii) crystallization of complex by thermal activation. This behavior is similar to that observed in our studies with CBZ and SAC, however, we observed crystallization of the complex at room temperature.

Studies on cogrinding of ursodeoxycholic acid (UDCA) with anthrone and/or phenanhrene exhibited different behavior. Crystalline complex formation between UDCA

and phenanthrene or anthrone occurred during cogrinding at ambient temperature, while cogrinding the reactant mixture at low temperatures (0°C, -55°C and -70°C) resulted in amorphous UDCA and crystalline phenanthrene or anthrone.[25] Cogrinding the crystalline complex of UDCA and phenanthrene or anthrone at low temperature also resulted in amorphous UDCA and crystalline second component. Heating the mixture of amorphous UDCA and crystalline anthrone and/or crystalline phenanthrene at 75°C for 40 minutes formed a mixture of the single component crystalline phases.[25] This behavior is similar to that observed with CBZ and NCT. However, in our studies crystalline components were observed after cryogenic cogrinding for short times. Longer grinding times resulted in amorphization.

In-situ studies with binary amorphous phases of CBZ and NCT have shown that crystallization outcome form amorphous phase is dependent on heating rates. Low heating rates resulted in cocrystal formation from amorphous phase, while high heating rates resulted in cocrystallization.[33, 34] Cocrystallization may thus be a result of molecular mobility in the amorphous state coupled with favorable interactions between heteromeric molecular complexes, so that crystallization of the pure phases is prevented. The conversion of CBZ-NCT cocrystal to crystalline CBZ and NCT during cryogenic cogrinding may be preceded by the generation of amorphous phase. A rapid change in temperature from cryogenic to ambient conditions after cryogenic grinding of cocrystal or reactant mixture may have induced the transformation of amorphous phase to crystalline reactants.

The rate of cocrystal formation during cogrinding, besides depending on the grinding temperature, also depends on the solvated crystal form of reactants. Faster rate

of cocrystal formation by cogrinding CBZ(D) and SAC or NCT suggests that water in the crystal lattice of CBZ(D) acts as a plasticizer. Matsuda et al. have shown that CBZ(D) forms an amorphous phase upon dehydration before conversion to the anhydrous CBZ(III) during grinding at room temperature.[28] Water from CBZ(D) may thus be present in the amorphous phase formed during cogrinding and serves as a plasticizer to reduce the T_g. The predicted T_g of the amorphous phases of CBZ/SAC and CBZ/NCT in the presence of this water is at least 20°C below room temperature. The T_g was calculated from the modified Gordon Taylor equation and the Simha-Boyer rule[50] using the following values: T_g of amorphous CBZ/SAC of 29°C, T_g of amorphous CBZ/NCT 21°C, T_g of water -138°C and K value of 0.25 generally found for small molecules.[30] Similar behavior has been reported for crystallization of indomethacin polymorphs during grinding of its solvates.[23]

Cocrystal formation during storage and its dependence on relative humidity demonstrates that moisture facilitates cocrystallization in blends ground under ambient and cryogenic conditions. This behavior is explained by the effect of water on molecular mobility and is consistent with the increased transformation to cocrystal during cogrinding the hydrated form of CBZ as discussed above.

The formation of cocrystal during cogrinding or during storage of mechanically activated blends in preference to the formation of crystalline CBZ and SAC or NCT raises an interesting question regarding competition between the kinetics of cocrystal formation and crystallization of the individual components from the disordered state. At the molecular level this may be regarded as a competition between heteromeric and homomeric interactions. The formation of CBZ-SAC cocrystal from the amorphous

phase suggests that under the conditions in which the experiments were performed heteromeric interactions are favored over homomeric interactions. Similar mechanisms are used in the stabilization of amorphous phases of drugs. Hydrogen bond directed stabilization of amorphous phases with drugs has been demonstrated for amorphous molecular dispersions with polymers[51-53] and from amorphous dispersions with granules of adsorbent.[54] In these cases, crystallization of the homomeric drug crystals is prevented by heteromeric interactions with the polymers or the adsorbents.

Comparison of the FTIR spectra after cogrinding under ambient and cryogenic conditions shows that heteromeric aggregation occurs in the disordered state and at low temperatures, although at a slower rate than that at ambient temperature conditions. Similarly, the formation of cocrystal by cogrinding CBZ(D) and SAC or NCT suggests that molecular associations between CBZ and coformer resulting in cocrystal are more favored than those observed between CBZ and water in carbamazepine dihydrate.

The thermodynamic stability of the cocrystal with respect to the individual component crystal phases needs to be considered. The free energies of cocrystal formation for CBZ-SAC and CBZ-NCT, estimated from cocrystal and reactant solubilities at 25°C, are -5.9 and -4.8 KJ/mol respectively.[55] The negative free energies for the cocrystal indicate that cocrystal is the stable phase at room temperature.

Conclusions

The results of this study show that amorphous phases generated during cogrinding can lead to cocrystal formation during storage. Water has a significant effect and increases the rate of cocrystallization during (i) cogrinding hydrated form of reactants, and (ii) storage of co-ground reactants at high RH. This study demonstrates that amorphous phases can lead to cocrystal formation under conditions where there is increased molecular mobility, and when hydrogen bond associations between different components are more favorable than those between similar components. Perhaps the most relevant implication of these findings is that cocrystals can be formed during pharmaceutical unit operations and during storage. Therefore, transformations to cocrystal may be added to the list of process-induced transformations to consider besides the well-documented transformations involving polymorphs and solvates.

References

1. Aakeroy, C. B.; Salmon, D. J. Building Co-Crystals with Molecular Sense and Supramolecular Sensibility. *CrystEngComm.* **2005**, *7*, 439-448.

2. Bettinetti, G.; Caira, M.; Callegari, A.; Merli, M.; Sorrenti, M.; Tadini, C. Structure and Solid-State Chemistry of Anhydrous and Hydrated Crystal Forms of the Trimethoprim-Sulfamethoxypyridazine 1:1 Molecular Complex. *J. Pharm. Sci.* **2000**, *89*, 478-488.

3. Caira, M. R. Molecular Complexes of Sulfonamides. 2. 1/1 Complexes between Drug Molecules - Sulfadimidine Acetylsalicylic Acid and Sulfadimidine-4-Aminosalicylic Acid. *J. Cryst. Spectrosc.* **1992**, *22*, 193-200.

4. Caira, M. R.; Nassimbeni, L. R.; Wildervanck, A. F. Selective Formation of Hydrogen Bonded Cocrystals between Sulfonamide and Aromatic Carboxylic Acids in the Solid State. *J. Chem. Soc. Perkin Trans.* **1995**, *2*, 2213-2216.

5. Desiraju, G. R. Hydrogen Bridges in Crystal Engineering: Interactions without Borders. *Acc. Chem. Res.* **2002**, *35*, 565-573.

6. Etter, M. C. Hydrogen Bonds as Design Elements in Organic Chemistry. *J. Phys. Chem.* **1991**, *95*, 4601 - 4610.

7. Etter, M. C.; Frankenbach, G. M. Hydrogen-Bond Directed Cocrystallization as a Tool for Designing Acentric Organic Solids. *Chem. Mater.* **1989**, *1*, 10-12.

8. Etter, M. C.; Frankenbach, G. M.; Adsmond, D. A. Using Hydrogen Bonds to Design Acentric Organic Materials for Nonlinear Optical Users. *Mol. Cryst. Liq. Cryst.* **1990**, *187*, 25-39.

9. Etter, M. C.; Reutzel, S. M. Hydrogen-Bond Directed Cocrystallization and Molecular Recognition Properties of Acyclic Imides. *J. Am. Chem. Soc.* **1991**, *113*, 2586-2598.

10. Etter, M. C.; Reutzel, S. M.; Choo, C. G. Self-Organization of Adenine and Thymine in the Solid State. *J. Am. Chem. Soc.* **1993**, *115*, 4411-4412.

11. Nangia, A.; Desiraju, G. R. Supramolecular Structures - Reason and Imagination. *Acta Crystallogr.* **1998**, *A54*, 934-944.

12. Rodríguez-Spong, B.; Price, C. P.; Jayasankar, A.; Matzger, A. J.; Rodríguez-Hornedo, N. General Principles of Pharmaceutical Solid Polymorphism: A Supramolecular Perspective. *Adv. Drug. Del. Rev.* **2004**, *56*, 241-274.

13. Rodríguez-Spong, B. Enhancing the Pharmaceutical Behavior of Poorly Soluble Drugs through the Formation of Cocrystals and Mesophases, Ph.D. Thesis. University of Michigan, **2005**.

14. Rodríguez-Spong, B.; Zocharski, P.; Billups, J.; McMahon, J.; Zaworotko, M. J.; Rodríguez-Hornedo, N. Enhancing the Pharmaceutical Behavior of Carbamazepine through the Formation of Cocrystals. *AAPS J.* **2003**, *5*, Abstract M1298.

15. Rodríguez-Hornedo, N.; Nehm, S. J.; Jayasankar, A. Cocrystals: Design, Properties and Formation Mechanisms. In *Encyclopedia of Pharmaceutical Technology,* 3rd ed.; Swarbrick, J.; Informa Health Care: **2006**, pp.615-635.

16. Trask, A. V.; Motherwell, W. D. S.; Jones, W. Pharmaceutical Cocrystallization: Engineering a Remedy for Caffeine Hydration. *Cryst. Growth Des.* **2005**, *5*, 1013-1021.

17. Etter, M. C.; Urbanczyk-Lipkowska, Z.; Zia-Ebrahimi, M.; Panunto, T. W. Hydrogen Bond Directed Cocrystallization and Molecular Recognition Properties of Diarylureas. *J. Am. Chem. Soc.* **1990**, *112*, 8415-8426.

18. Pedireddi, V. R.; Jones, W.; Chorlton, A. P.; Docherty, R. Creation of Crystalline Supramolecular Arrays: A Comparison of Co-Crystal Formation from Solution and by Solid State Grinding. *Chem. Comm.* **1996**, *8*, 987-988.

19. Trask, A. V.; Motherwell, W. D. S.; Jones, W. Solvent-Drop Grinding: Green Polymorph Control of Cocrystallisation. *Chem. Comm.* **2004**, *7*, 890-891.

20. Morissette, S. L.; Örn Almarsson; Peterson, M. L.; Remenar, J. F.; Read, M. J.; Lemmo, A. V.; Ellis, S.; Cima, M. J.; Gardner, C. R. High-Throughput Crystallization: Polymorphs, Salts, Co-Crystals and Solvates of Pharmaceutical Solids. *Adv. Drug. Del. Rev.* **2004**, *56*, 275-300.

21. Nehm, S. J.; Rodríguez-Hornedo, N.; Rodríguez-Spong, B. Phase Solubility Diagrams of Cocrystals Are Explained by Solubility Product and Solution Complexation. *Cryst. Growth Des.* **2005**, *6*, 592-600.

22. Rodríguez-Hornedo, N.; Nehm, S. J.; Seefeldt, K. F.; Pagán-Torres, Y.; Falkiewicz, C. J. Reaction Crystallization of Pharmaceutical Molecular Complexes. *Mol. Pharm.* **2006**, *3*, 362-367.

23. Crowley, K. J.; Zografi, G. Cryogenic Grinding of Indomethacin Polymorphs and Solvates: Assessment of Amorphous Phase Formation and Amorphous Phase Physical Stability. *J. Pharm. Sci.* **2002**, *91*, 492-507.

24. Murphy, D.; Rodríguez-Cintrón, F.; Langevin, B.; Kelly, R. C.; Rodríguez-Hornedo, N. Solution-Mediated Phase Transformation of Anhydrous to Dihydrate Carbamazepine and the Effect of Lattice Disorder. *Int. J. Pharm.* **2002**, *246*, 121-134.

25. Oguchi, T.; Kazama, K.; Fukami, T.; Yonemochi, E.; Yamamoto, K. Specific Complexation of Ursodeoxycholic Acid with Guest Compounds Induced by Co-Grinding. II. Effect of Grinding Temperature on the Mechanochemical Complexation. *Bull. Chem. Soc. Jpn.* **2003**, *76*, 515-521.

26. Oguchi, T.; Tozuka, Y.; Hanawa, T.; Mizutani, M.; Sasaki, N.; Limmatvapirat, S.; Yamamoto, K. Elucidation of Solid-State Complexation in Ground Mixtures of Cholic Acid and Guest Compounds. *Chem. Pharm. Bull.* **2002**, *50*, 887-891.

27. Otsuka, M.; Matsumoto, T.; Kaneniwa, N. Effect of Environmental Temperature on Polymorphic Solid-State Transformation of Indomethacin During Grinding. *Chem. Pharm. Bull.* **1986**, *34*, 1784-1793.

28. Otsuka, M.; Ofusa, T.; Matsuda, Y. Effect of Environmental Humidity on the Transformation Pathway of Carbamazepine Polymorphic Modifications During Grinding. *Colloids Surf. B Biointerfaces.* **1999**, *13*, 263-273.

29. Andronis, V.; Yoshioka, M.; Zografi, G. Effects of Sorbed Water on the Crystallization of Indomethacin from the Amorphous State. *J. Pharm. Sci.* **1997**, *86*, 346-351.

30. Hancock, B. C.; Zografi, G. The Relationship between the Glass Transition Temperature and the Water Content of Amorphous Pharmaceutical Solids. *Pharm. Res.* **1994**, *11*, 471-477.

31. Fleischman, S. G.; Kuduva, S. S.; McMahon, J. A.; Moulton, B.; Walsh, R. D. B.; Rodríguez-Hornedo, N.; Zaworotko, M. J. Crystal Engineering of the Composition of Pharmaceutical Phases: Multiple-Component Crystalline Solids Involving Carbamazepine. *Cryst. Growth Des.* **2003**, *3*, 909-919.

32. Jayasankar, J.; Somwangthanaroj, A.; Sirinutsomboon, B.; Shao, Z. J.; Rodríguez-Hornedo, N. Cocrystal Formation by Solid-State Grinding and During Storage. *AAPS J.* **2004**, *6*, R6159.

33. Seefeldt, K.; Miller, J.; Ding, S.; Rodríguez-Hornedo, N. Crystallization of Carbamazepine-Nicotinamide Cocrystal from the Amorphous Phase. *AAPS J.* **2004**, *6*, R6172.

34. Seefeldt, K. J.; Miller, J.; Alvarez-Núñez, F.; Rodríguez-Hornedo, N. Crystallization Pathways and Kinetics of Carbamazepine-Nicotinamide Cocrystals from the Amorphous State by in-Situ Thermomicroscopy, Spectroscopy and Calorimetry Studies *J. Pharm. Sci.* **2007**, *96*, 1147-1158.

35. Hino, T.; Ford, J. L.; Powell, M. W. Assessment of Nicotinamide Polymorphs by Differential Scanning Calorimetry. *Thermochim. Acta.* **2001**, *374*, 85-92.

36. O'Brien, F. E. M. The Control of Humidity Using Saturated Salt Solutions. *J. Sci. Instrum.* **1948**, *25*, 73-76.

37. Patel, A. D.; Luner, P. E.; Kemper, M. S. Quantitative Analysis of Polymorphs in Binary and Multi-Component Powder Mixtures by near-Infrared Reflectance Spectroscopy. *Int. J. Pharm.* **2000**, *206*, 63-74.

38. Salari, A.; Young, R. E. Application of Attenuated Total Reflectance FTIR Spectroscopy to the Analysis of Mixtures of Pharmaceutical Polymorphs *Int. J. Pharm.* **1998**, *163*, 157-166.

39. Nair, R.; Nyamweya, N.; Gonen, S.; Martinez-Miranda, L. J.; Hoag, S. W. Influence of Various Drugs on the Glass Transition Temperature of Poly(Vinylpyrrolidone): A Thermodynamic and Spectroscopic Investigation. *Int. J. Pharm.* **2001**, *225*, 83-96.

40. Colthup, N. B.; Daly, L. H.; Wiberley, S. E. *Introduction to Infrared and Raman Spectroscopy*. 3rd ed.; Harcourt Brace & Company, Publishers: Boston, **1990**.

41. Mayo, D. W.; Miller, F. A.; Hannah, R. W. *Course Notes on the Interpretation of Infrared and Raman Spectra*. John Wiley & Sons Publication: Hoboken, NJ, **2004**.

42. Hase, Y. The Infrared and Raman Spectra of Phthalimide, N-D-Phthalimide and Potassium Phthalimide. *J. Mol. Struct.* **1978**, *48*, 33-42.

43. Jovanovski, G. Metal Saccharinates and Their Complexes with N-Donor Ligands. *CCACAA.* **2000**, *73*, 843-868.

44. Teleb, S. M. Spectral and Thermal Studies of Saccharinato Complexes. *J. Argent. Chem. Soc.* **2004**, *92*, 31-40.

45. Jovanovski, G.; Tanceva, S.; Soptrajanov, B. The SO_2 Stretching Vibrations in Some Metal Saccharinates: Spectra-Structure Correlations. *Spectrosc. Lett.* **1995**, *28*, 1095-1109.

46. Behme, R. J.; Brooke, D. Heat of Fusion Measurement of a Low Melting Polymorph of Carbamazepine That Undergoes Multiple-Phase Changes During Differential Scanning Calorimetry Analysis. *J. Pharm. Sci.* **1991**, *80*, 986-990.

47. Hancock, B. C.; Zografi, G. Characteristics and Significance of the Amorphous State in Pharmaceutical Systems. *J. Pharm. Sci.* **1997**, *86*, 1-12.

48. Hancock, B.; Shamblin, S.; Zografi, G. Molecular Mobility of Amorphous Pharmaceutical Solids Below Their Glass Transition Temperatures. *Pharm. Res.* **1995**, *12*, 799-806.

49. Trask, A.; Jones, W. Crystal Engineering of Organic Cocrystals by the Solid-State Grinding Approach. *Top. Curr. Chem.* **2005**, *254*, 41-70.

50. Schneider, H. A. The Gordon-Taylor Equation. Additivity and Interaction in Compatible Polymer Blends. *Makromol. Chem.* **1988**, *189*, 1941-1955.

51. Gupta, P.; Bansal, A. Molecular Interactions in Celebcoxib-PVP-Meglumine Amorphous System. *J. Pharm. Pharmacol.* **2005**, *57*, 303-310.

52. Taylor, L. S.; Zografi, G. Spectroscopic Characterization of Interactions between PVP and Indomethacin in Amorphous Molecular Dispersions. *Pharm. Res.* **1997**, *14*, 1691-1698.

53. Tong, P.; Zografi, G. A Study of Amorphous Molecular Dispersions of Indomethacin and Its Sodium Salt. *J. Pharm. Sci.* **2001**, *90*, 1991-2004.

54. Gupta, M. K.; Vanwert, A.; Bogner, R. H. Formation of Physically Stable Amorphous Drugs by Milling with Neusilin. *J. Pharm. Sci.* **2003**, *92*, 536-551.

55. Maheshwari, C.; Jayasankar, A.; Khan, N. K.; Amidon, G. E.; Rodríguez-Hornedo, N. Factors That Influence the Spontaneous Formation of Cocrystals in Solid Mixtures. *CrystEngComm.* **2008** (submitted).

CHAPTER VI

CONCLUSIONS AND FUTURE WORK

This dissertation has focused on investigating the mechanisms, thermodynamics, and kinetics of cocrystallization. The specific goals of the study were to (i) identify the factors and conditions governing the formation and stability of cocrystals with different stoichiometry, (ii) examine the propensity and underlying mechanisms of cocrystal formation in solid mixtures due to moisture sorption, (iii) examine the effect of coformer, excipients and cosolvent concentration in aqueous solutions on the formation and thermodynamic stability of cocrystal hydrates, and (iv) identify the mechanisms by which mechanical activation of reactant mixtures induces cocrystal formation.

The formation, stability, and solubility of cocrystals with different stoichiometry are dependent on coformer solution concentration. 1:1 and 2:1 carbamazepine-4-aminobenzoic acid (CBZ-4ABA) cocrystals were synthesized by varying the coformer concentration using the reaction crystallization method. Cocrystal stability studies indicate that the cocrystal richer in ligand (1:1 cocrystal) is more stable at higher ligand concentrations. The stability domains of the cocrystals can be identified by measuring the transition concentration between the different crystalline phases (drug/2:1 cocrystal, 2:1 cocrystal/1:1 cocrystal, 1:1 cocrystal/ligand). Cocrystal and drug solubilities as well as

the equilibrium solution composition of reactants to generate phase diagrams can be predicted using mathematical models based on cocrystal and solution chemistry.

The solubility models developed in this study for CBZ-4ABA cocrystals indicate 1:1 complex formation in solutions equilibrated with the 2:1 cocrystal. Thus, the stoichiometry of the complex in solution at equilibrium does not correspond to cocrystal stoichiometry. Crystallization occurs under supersaturated conditions, and is governed by molecular recognition, thermodynamics and kinetics. The current study identifies the nature of complex in solution at equilibrium with cocrystal, while the molecular interactions and nature of complex leading to cocrystal formation under supersaturated conditions are not known. Studies evaluating the nature of these interactions and complexes, as well as the effect of complexation on cocrystal nucleation rates, will provide valuable insights regarding the mechanistic aspects of cocrystallization from solutions. Further, solvent effects on complex formation, cocrystal solubility, and stability also needs to be explored.

Water is commonly encountered during processing and storage of pharmaceutical materials. Water-solid interactions can induce phase transformations such as hydrate formation, polymorphic conversions, or amorphous to crystalline conversions. In this study, moisture sorption and deliquescence of solid mixtures of cocrystal reactants is shown to induce cocrystal formation. Cocrystals of carbamazepine-nicotinamide (CBZ-NCT) and carbamazepine-saccharin (CBZ-SAC), caffeine and theophylline with carboxylic acid ligands such as oxalic acid, maleic acid, malonic acid, glutaric acid and citric acid were formed during deliquescence even at conditions when the APIs are reported to form hydrates. The mechanisms responsible for cocrystal formation involve

moisture uptake, dissolution of cocrystal reactants, cocrystal nucleation and growth. Cocrystal formation rates in reactant mixtures depends on RH, amount of moisture sorbed, surface area of reactant particles, reactant hygroscopicity, solubilities and dissolution rates. This is demonstrated for cocrystals of carbamazepine with nicotinamide and saccharin. Mixtures of CBZ/NCT transformed to cocrystal faster than CBZ/SAC mixtures. Higher reactivity in CBZ/NCT mixtures is due to the deliquescent nature and high aqueous solubility of NCT relative to SAC.

The propensity for cocrystal formation in reactant mixtures is altered by the presence of hygroscopic additives in reactant mixtures. Small amounts of deliquescent additives such as fructose, sucrose and citric acid in the reactant mixtures are shown to induce cocrystal formation even at conditions when the cocrystal reactants do not deliquesce. The transformation rate in this case depends on the nature of deliquescent additive and solid composition. Hygroscopic polymers such as PVP that are non-deliquescent and exhibit different moisture uptake behavior are well known to affect solid phase stability and induce phase transformations. Future studies need to examine the effect of moisture uptake by hygroscopic polymers on cocrystal formation in reactant mixtures.

While moisture uptake and deliquescence in reactant mixtures induces transformation of drug to cocrystal, a reversal in transformation can occur due to cocrystal deliquescence. This is shown for cocrystals of theophylline with glutaric acid and citric acid, and caffeine-glutaric acid cocrystal. Cocrystals of carbamazepine with maleic and glutaric acid however did not deliquesce under similar storage conditions. Further studies examining the underlying cause for differences in the moisture uptake

behavior and stability of these cocrystals during storage can provide valuable insights for designing cocrystals with the desired hygroscopicity and stability.

Cocrystal solubility dependence on aqueous solution composition and chemistry are good predictors of cocrystal formation and stability during deliquescence. The transformation of a drug to cocrystal in a saturated aqueous solution of coformer is an indicator for cocrystal formation due to deliquescence in solid reactant mixtures. This is shown for cocrystals of carbamazepine, caffeine and theophylline with various coformers. Similarly, cocrystal transformation to crystalline drug in pure water is indicative of the propensity for cocrystal instability due to moisture uptake and deliquescence.

Most cocrystals identified to date are anhydrous, and a few have been serendipitously identified to exist as hydrates. The formation and stability of pharmaceutical hydrates is well known to depend on water activity (a_w). In this dissertation, coformers that modulate the water activity of aqueous solutions are shown to affect cocrystal hydrate formation and stability. Increasing the coformer concentration is shown to decrease the water activity resulting in transformation of theophylline-citric acid (THP-CTA) cocrystal hydrate to anhydrous cocrystal. Increasing the coformer concentration however did not result in the conversion of CBZ-4ABA cocrystal hydrate to anhydrous cocrystal. This is because 4ABA has low aqueous solubility and negligible decreases the water activity to 0.98, while the critical water activity of cocrystal hydrate is 0.26-0.30.

In addition to the coformer, excipients and cosolvent addition to aqueous solutions can also affect a_w and cocrystal hydrate stability. Fructose addition to aqueous

citric acid solutions is shown to decrease the a_w resulting in transformation of THP-CTA cocrystal hydrate to anhydrous cocrystal. The addition of acetonitrile to water similarly decreased the a_w resulting in conversion of CBZ-4ABA cocrystal hydrate to anhydrous cocrystal.

Anhydrous and hydrate cocrystals can also form in reactant solid mixtures due to deliquescence. The formation of these cocrystalline phases and their stability in this case is dependent on the coformer concentration in the deliquesced solution which in turn is dependent on the level of water uptake. THP/CTA mixture transforms to anhydrous cocrystal at 75%RH. At 85% and 98%RH, the mixture transforms to anhydrous cocrystal and then to cocrystal hydrate. Transformation of anhydrous to hydrated cocrystal is explained by the effect of water uptake on coformer concentration that affects the stability of cocrysalline phases.

In the solid-state, cocrystal formation due to mechanical activation of reactants is shown to be amorphous phase mediated. Enhanced molecular mobility in the amorphous phase generates cocrystals as long as heteromeric associations are favored over homomeric associations. This is shown for cocrystals of carbamazepine (CBZ) with saccharin (SAC) and nicotinamide (NCT). Cogrinding carbamazepine and saccharin at ambient conditions forms CBZ-SAC cocrystals, while cogrinding under cryogenic conditions results in amorphous phase formation due to low molecular mobility at low temperature. Cocrystals of CBZ and NCT also form by cogrinding at ambient conditions. However, mechanical activation of CBZ-NCT cocrystal under cryogenic conditions results in mixture of crystalline reactants.

Cocrystal formation from amorphous phases depends on the glass transition temperature (T_g) of cocrystal reactants and the presence of additives. Water present in the crystal lattice or in the vapor phase facilitates cocrystallization from amorphous phases by serving as a plasticizer. Amorphous phases of CBZ and SAC, generated by cogrinding, transform to cocrystal during storage at high RH. Cogrinding CBZ(D) with SAC or NCT enhances cocrystal formation rates during cogrinding.

The current study demonstrates the influence of molecular recognition and kinetics on cocrystallization. However, the thermodynamics of cocrystal formation also needs to be considered. Cocrystal formation during storage, and free energies of cocrystal formation evaluated from cocrystal and reactant solubilities suggest that CBZ-SAC and CBZ-NCT cocrystals are the thermodynamically stable phase at room temperature. Future studies should therefore explore the propensity for spontaneous cocrystal formation without mechanical activation of cocrystal reactants.

Stresses encountered during processing and storage can induce phase transformations such as amorphous to crystalline conversion, hydrate formation, and polymorphic conversions. The conversion of crystalline drug to cocrystals can be added to the existing list of possible phase transformations. This dissertation has identified the mechanisms and kinetics of cocrystallization, and factors affecting cocrystal stability. Results presented herein have potential implications for anticipating cocrystal formation, and controlling reactant and cocrystal stability during processing and storage of pharmaceutical materials.

APPENDICES

APPENDIX A

2:1 and 1:1 CBZ-4ABA cocrystal stability in various organic solvents

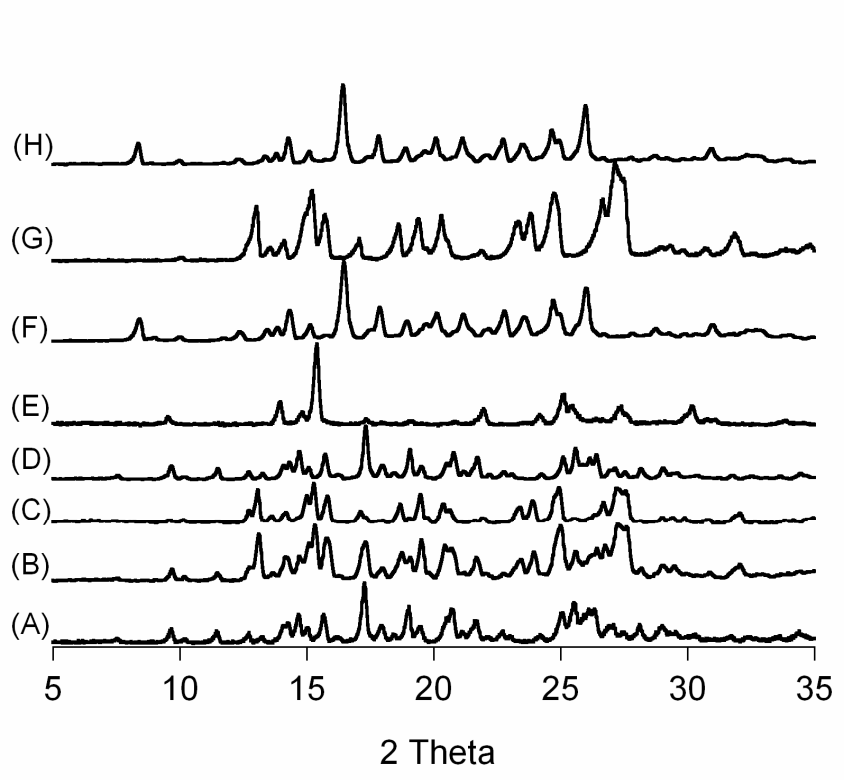

Figure A-1: XRPD showing 2:1 CBZ-4ABA cocrystal stability in various solvents. (A) 2:1 CBZ-4ABA anhydrous cocrystal reference; Cocrystal stability in (B) methanol, (C) isopropyl alcohol, (D) acetonitrile, (E) water, (F) chloroform, (G) CBZ(III), and (H) CBZ-4ABA cocrystal hydrate reference.

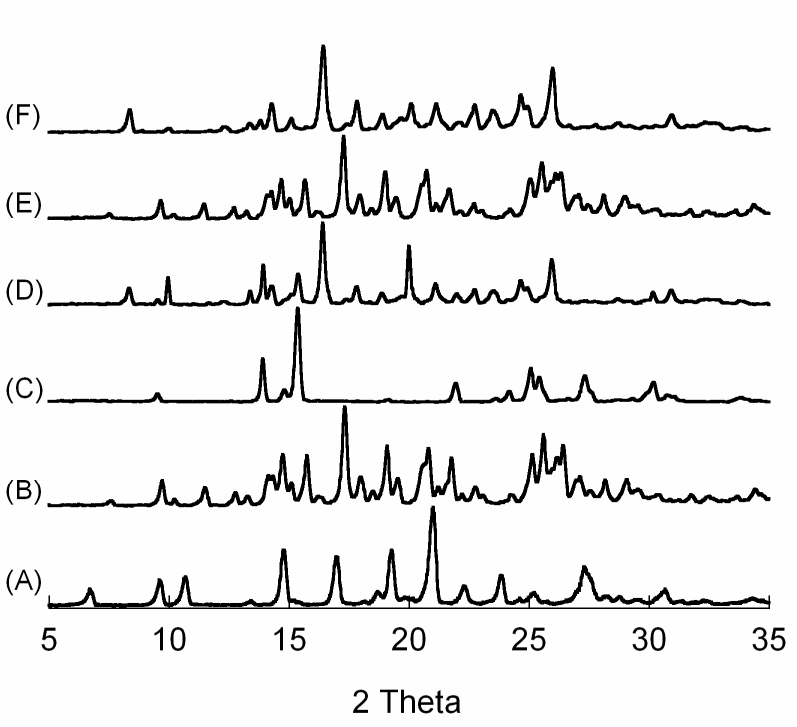

Figure A-2: XRPD showing 1:1 CBZ-4ABA cocrystal stability in various solvents. (A) 1:1 CBZ-4ABA anhydrous cocrystal reference; Cocrystal stability in (B) methanol, (C) Chloroform, (D) Water; reference patterns of (E) 2:1 anhydrous CBZ-4ABA, and (F) 2:1 CBZ-4ABA hydrate.

APPENDIX B

Mathematical models based on cocrystal and solution chemistry to predict cocrystal 2:1 cocrystal solubility

In this section, detailed derivations of mathematical models predicting the solubility of a 2:1 cocrystal (D_2L) as a function of ligand concentration are presented. The models presented consider the effect of 1:1 and 2:1 solution complexation on cocrystal solubility.

Model I – 1:1+ 2:1 solution complexation

The equilibrium reactions for cocrystal dissociation in solution and solution complexation can be written as shown below.

$$D_2L_{(solid)} \overset{K_{sp}}{\rightleftharpoons} 2D_{(soln)} + L_{(soln)} \quad (1)$$

$$D_{(soln)} + L_{(soln)} \overset{K_{11}}{\rightleftharpoons} DL_{(soln)} \quad (2)$$

$$DL_{(soln)} + D_{(soln)} \overset{K_{21}}{\rightleftharpoons} D_2L_{(soln)} \quad (3)$$

K_{sp} is the solubility product constant and is given as $K_{sp} = [D]^2[L]$ (4)

K_{11} and K_{21} are the complexation constants for the reactions and are given as:

$$K_{11} = \frac{[DL]}{[D][L]} \quad (5)$$

$$K_{21} = \frac{[D_2L]}{[DL][D]} \quad (6)$$

Rearranging equation (5) and substituting for [D] from equation (4) gives the following expression for the concentration of complex DL:

$$[DL] = K_{11}\sqrt{K_{sp}[L]} \quad (7)$$

Rearranging equation (6) and substituting for [D] and [DL] from equations (4) and (7) yields:

$$[D_2L] = K_{11}K_{21}K_{sp} \quad (8)$$

Mass balance for the concentration of the drug and ligand in solution can be written as shown below:

$$[D]_T = [D] + [DL] + 2[D_2L] \quad (9)$$

$$[L]_T = [L] + [DL] + [D_2L] \quad (10)$$

Substituting for [D], [DL] and $[D_2L]$ from equations (4), (7) and (8) gives

$$[D]_T = \sqrt{\frac{K_{sp}}{[L]}} + K_{11}\sqrt{K_{sp}[L]} + 2K_{11}K_{21}K_{sp} \quad (11)$$

$$[L]_T = [L] + K_{11}\sqrt{K_{sp}[L]} + K_{11}K_{21}K_{sp} \quad (12)$$

Re-arranging equation (12):

$$[L]_T - K_{11}K_{21}K_{sp} - [L] = K_{11}\sqrt{K_{sp}[L]} \quad (13)$$

Squaring both sides of equation (13) and re-arranging gives the following quadratic equation in [L]:

$$[L]^2 - [L]\left(2\left([L]_T - K_{11}K_{21}K_{sp}\right) + K_{11}^2K_{sp}\right) + \left([L]_T - K_{11}K_{21}K_{sp}\right)^2 = 0 \quad (14)$$

Let $c = [L]_T - K_{11}K_{21}K_{sp}$ (15)

Therefore, $[L]^2 - [L]\left(2c + K_{11}^2K_{sp}\right) + c^2 = 0$ (16)

Equation (16) is a quadratic equation and can be solved to obtain an expression for [L] as a function of $[L]_T$.

$$[L] = \frac{2c + K_{11}^2 K_{sp} \pm \sqrt{K_{11}^4 K_{sp}^2 + 4cK_{11}^2 K_{sp}}}{2} \tag{17}$$

Substituting for 'c' from equation (15):

$$[L] = \frac{2\left([L]_T - K_{11}K_{21}K_{sp}\right) + K_{11}^2 K_{sp} \pm \sqrt{K_{11}^4 K_{sp}^2 + 4K_{11}^2 K_{sp}[L]_T - 4K_{11}^3 K_{sp}^2 K_{21}}}{2} \tag{18}$$

If $K_{11}^4 K_{sp}^2$ and $4K_{11}^3 K_{sp}^2 K_{21} << 4K_{11}^2 K_{sp}[L]_T$ then equation (18) simplifies to:

$$[L] = \frac{2\left([L]_T - K_{11}K_{21}K_{sp}\right) + K_{11}^2 K_{sp} \pm 2K_{11}\sqrt{K_{sp}[L]_T}}{2} \tag{19}$$

Equation (19) gives an expression for the free ligand concentration ([L]) as a function of the thermodynamic constants (K_{sp}, K_{11}, K_{21}) and $[L]_T$. There are two solutions for [L] and these two solutions differ in the sign of the term $2K_{11}\sqrt{K_{sp}[L]_T}$. Substituting the above expressions for [L] in equation (9) yields the following two expressions relating $[D]_T$ to $[L]_T$, K_{11}, K_{21} and K_{sp}.

$$[D]_T = \sqrt{\frac{K_{sp}}{A_1}} + K_{11}\sqrt{K_{sp}A_1} + 2K_{11}K_{21}K_{sp} \tag{20}$$

where $A_1 = \frac{2\left([L]_T - K_{11}K_{21}K_{sp}\right) + K_{11}^2 K_{sp} - 2K_{11}\sqrt{K_{sp}[L]_T}}{2}$

$$[D]_T = \sqrt{\frac{K_{sp}}{A_2}} + K_{11}\sqrt{K_{sp}A_2} + 2K_{11}K_{21}K_{sp} \tag{21}$$

where $A_2 = \frac{2\left([L]_T - K_{11}K_{21}K_{sp}\right) + K_{11}^2 K_{sp} + 2K_{11}\sqrt{K_{sp}[L]_T}}{2}$

Equations (20) and (21) predict a non-linear dependence of $[D]_T$ on $[L]_T$ when the 2:1 cocrystal is in equilibrium with the solution. The thermodynamic constants K_{11}, K_{21} and K_{sp} can be evaluated by non-linear regression. The initial estimates for the constants were obtained assuming no solution complexation. Hence, the initial values for K_{11} and K_{21} were 0. The slope of the line obtained by plotting $[D]_T$ against $[L]_T^{-1/2}$ yielded the initial value of K_{sp}. All the constants were allowed to vary during the regression procedure. The values of the constants for subsequent iterations were determined using the Levenberg-Marquadt algorithm subject to the constraint that the constants are all greater than 0. The best fit was obtained by minimizing $\sum_{i=1}^{N}\left([D]_{T,i}^{exp} - [D]_{T,i}^{pred}\right)^2$, where $[D]_T^{pred}$ and $[D]_T^{exp}$ are the predicted and experimental total drug concentrations, respectively.

Model II – 1:1 solution complexation

The equilibrium reactions for cocrystal dissociation in solution and solution complexation can be written as shown below.

$$D_2L_{(solid)} \overset{K_{sp}}{\rightleftharpoons} 2D_{(soln)} + L_{(soln)} \quad (22)$$

$$D_{(soln)} + L_{(soln)} \overset{K_{11}}{\rightleftharpoons} DL_{(soln)} \quad (23)$$

K_{sp} and K_{11} are cocrystal solubility product and complexation constants and are given by equations (4) and (5).

Mass balance for the concentration of the drug and ligand in solution gives:

$$[D]_T = [D] + [DL] \quad (24)$$

$$[L]_T = [L] + [DL] \tag{25}$$

Substituting for [D] and [DL] from equations (4) and (7) gives

$$[D]_T = \sqrt{\frac{K_{sp}}{[L]}} + K_{11}\sqrt{K_{sp}[L]} \tag{26}$$

$$[L]_T = [L] + K_{11}\sqrt{K_{sp}[L]} \tag{27}$$

Re-arranging equation (27):

$$[L]_T - [L] = K_{11}\sqrt{K_{sp}[L]} \tag{28}$$

Squaring both sides of equation (28) and re-arranging yields the following quadratic equation in [L].

$$[L]^2 - [L]\left(K_{11}^2 K_{sp} + 2[L]_T\right) + [L]_T^2 = 0$$

Solving the above equation for [L]:

$$[L] = \frac{2[L]_T + K_{11}^2 K_{sp} \pm \sqrt{4[L]_T K_{11}^2 K_{sp} + K_{11}^4 K_{sp}^2}}{2} \tag{29}$$

If $K_{11}^4 K_{sp}^2 << 4[L]_T K_{11}^2 K_{sp}$ then equation (29) reduces to

$$[L] = \frac{2[L]_T + K_{11}^2 K_{sp} \pm 2K_{11}\sqrt{K_{sp}[L]_T}}{2} \tag{30}$$

Equation (30) expresses the free ligand concentration ([L]) as a function of the thermodynamic constants and $[L]_T$. There are two solutions for [L] and these two solutions differ in the sign of the term $2K_{11}\sqrt{K_{sp}[L]_T}$. Substituting the above expressions for [L] in equation (26) gives the following two expressions relating $[D]_T$ to terms of $[L]_T$, K_{11}, and K_{sp}.

$$[D]_T = \sqrt{\frac{K_{sp}}{A_1}} + K_{11}\sqrt{K_{sp}A_1} \tag{31}$$

where $A_1 = \frac{2[L]_T + K_{11}^2 K_{sp} - 2K_{11}\sqrt{K_{sp}[L]_T}}{2}$

$$[D]_T = \sqrt{\frac{K_{sp}}{A_2}} + K_{11}\sqrt{K_{sp}A_2} \quad (32)$$

where $A_2 = \frac{2[L]_T + K_{11}^2 K_{sp} + 2K_{11}\sqrt{K_{sp}[L]_T}}{2}$

Equations (31) and (32) predict a non-linear dependence of $[D]_T$ on $[L]_T$ when the 2:1 cocrystal is in equilibrium with the solution. The thermodynamic constants K_{11} and K_{sp} can be evaluated by non-linear regression as described earlier.

Model III – 2:1 solution complexation

The equilibrium reactions for cocrystal dissociation and 2:1 complex formation in solution are as follows:

$$D_2L_{(solid)} \overset{K_{sp}}{\rightleftharpoons} 2D_{(soln)} + L_{(soln)} \quad (33)$$

$$2D_{(soln)} + L_{(soln)} \overset{K'_{21}}{\rightleftharpoons} D_2L_{(soln)} \quad (34)$$

K_{sp} is the cocrystal solubility product and is given by $K_{sp} = [D]^2[L]$ (35)

K'_{21} is the complexation constant and is given as $K'_{21} = \frac{[D_2L]}{[D]^2[L]}$ (36)

From equations (35) and (36), $[D_2L] = K'_{21}K_{sp}$ (37)

Mass balance on drug and ligand concentration is written as:

$[D]_T = [D] + 2[D_2L]$ (38)

$[L]_T = [L] + [D_2L]$ (39)

Substituting for [D] from equation (35) and $[D_2L]$ from equation (37):

$$[D]_T = \sqrt{\frac{K_{sp}}{[L]}} + 2K'_{21}K_{sp} \quad (40)$$

$$[L] = [L]_T - K'_{21}K_{sp} \quad (41)$$

From equations (40) and (41) the following relation is obtained between $[D]_T$ and $[L]_T$:

$$[D]_T = \sqrt{\frac{K_{sp}}{[L]_T - K'_{21}K_{sp}}} + 2K'_{21}K_{sp} \quad (42)$$

Equation (42) predicts non-linear dependence of $[D]_T$ on $[L]_T$ for the 2:1 cocrystal. Therefore, the constants can be evaluated by non-linear regression. Initial estimates for the constants were obtained assuming no complexation. Thus, $K'_{21} = 0$ and K_{sp} was estimated from the slope of the line obtained by plotting $[D]_T$ against $[L]_T^{-1/2}$. The values of the constants in subsequent iterations were evaluated using the Levenberg-Marquadt algorithm. Best fit was obtained by minimizing $\sum_{i=1}^{N}\left([D]_{T,i}^{exp} - [D]_{T,i}^{pred}\right)^2$, where $[D]_T^{pred}$ and $[D]_T^{exp}$ are the predicted and experimental total drug concentrations, respectively.

Alternatively, the constants can be evaluated by linear regression as described below. As a first approximation, we assume $K'_{21}K_{sp} << [L]_T$. Equation (42) then becomes:

$$[D]_T = \sqrt{\frac{K_{sp}}{[L]_T}} + 2K'_{21}K_{sp} \quad (43)$$

The values of the constants K_{sp} and K'_{21} in equation (43) are evaluated from the slope and intercept of the line obtained by plotting $[D]_T$ against $[L]_T^{-1/2}$. These values of the constants are then used to evaluate $\left([L]_T - K'_{21}K_{sp}\right)^{-1/2}$ in equation (42). New values of

K_{sp} and K'_{21} are then obtained by plotting $[D]_T$ against $\left([L]_T - K'_{21}K_{sp}\right)^{-1/2}$. The procedure is repeated till convergence is achieved.

APPENDIX C

Effect of RH on the stability of carbamazepine, theophylline and caffeine cocrystals during storage

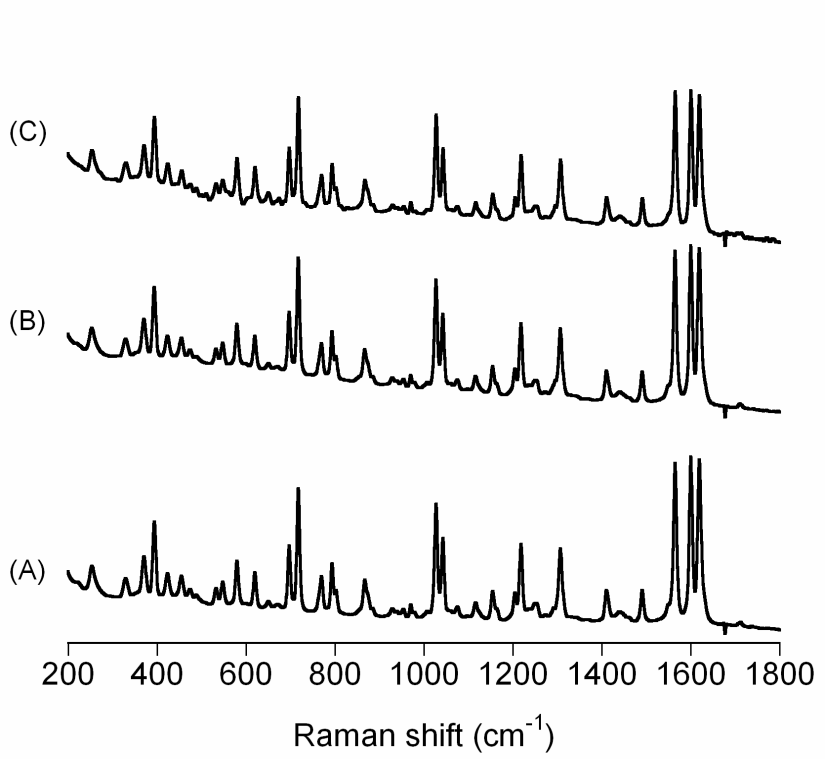

Figure C-1: Raman spectra showing the stability of (A) carbamazepine-glutaric acid cocrystal after storage at (B) 91%RH, and (C) 98%RH for 4.5 months.

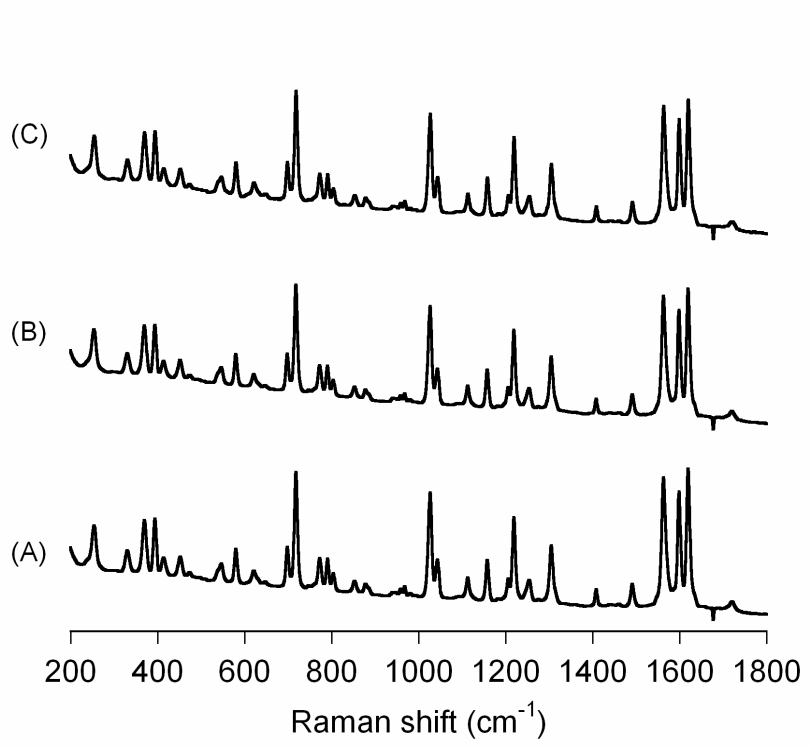

Figure C-2: Raman spectra showing the stability of (A) carbamazepine-maleic acid cocrystal after storage at (B) 91%RH, and (C) 98%RH for 4.5 months.

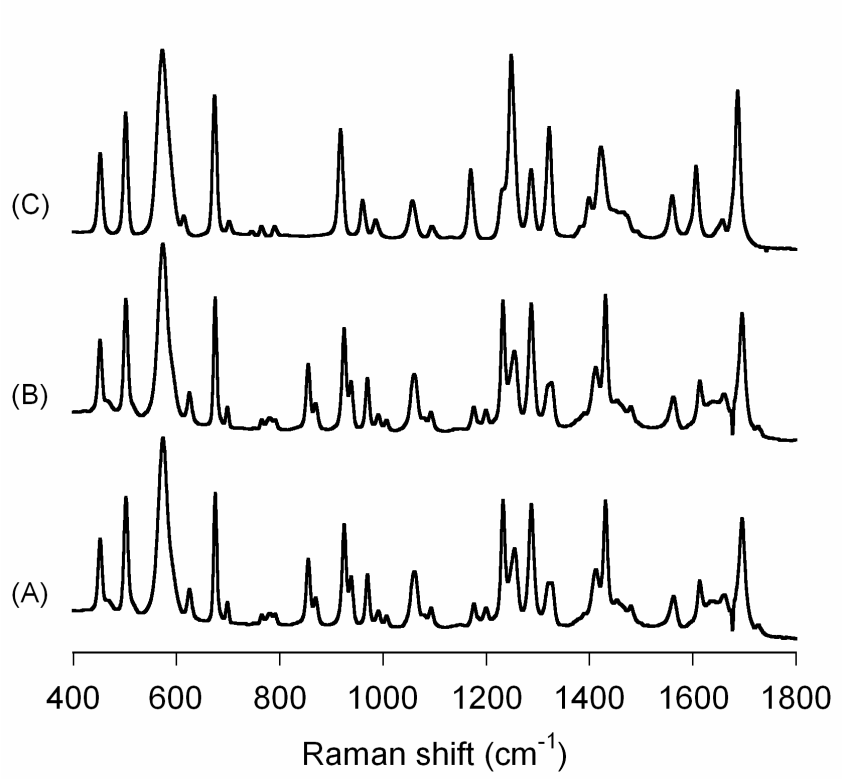

Figure C-3: Raman spectra showing the stability of (A) theophylline-glutaric acid cocrystal after storage at (B) 91%RH for 4.5 months; (C) Theophylline hydrate (reference spectrum).

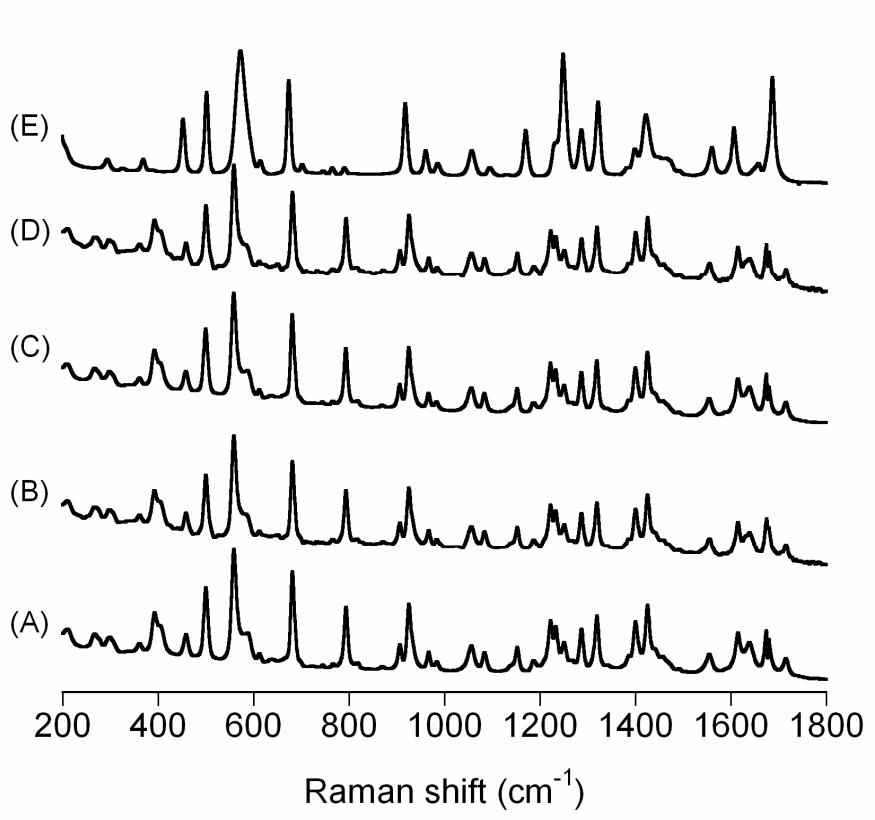

Figure C-4: Raman spectra showing the stability of (A) anhydrous theophylline-citric acid cocrystal after storage at (B) 85%RH, (C) 91%RH, and (D) 98%RH for 4.5 months; (E) Theophylline hydrate (reference spectrum).

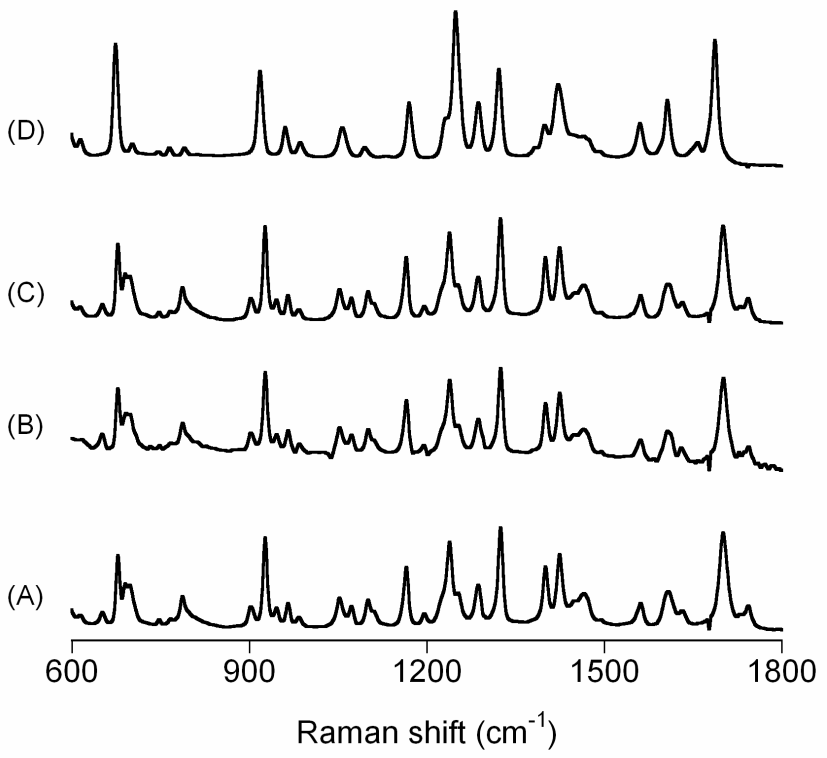

Figure C-5: Raman spectra showing the stability of (A) theophylline-citric acid hydrate cocrystal after storage at (B) 85%RH, and (C) 91%RH for 4.5 months; (D) Theophylline hydrate (reference spectrum).

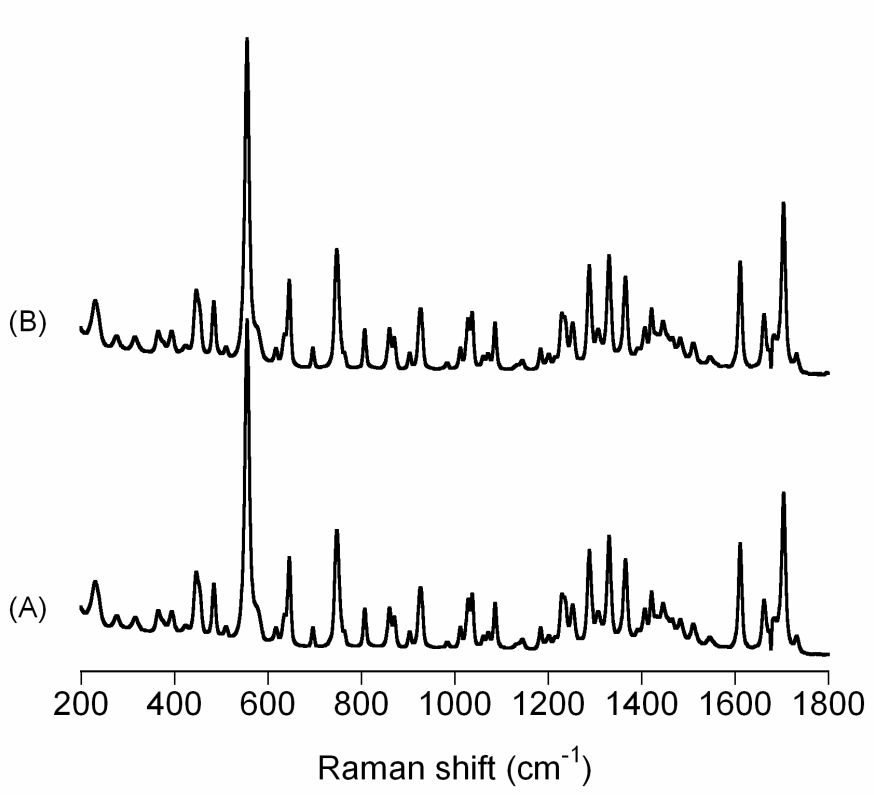

Figure C-6: Raman spectra showing the stability of (A) caffeine-glutaric acid cocrystal after storage at (B) 91%RH for 4.5 months.

APPENDIX D

XRPD pattern showing disorder in CBZ-SAC cocrystal after cryogenic grinding

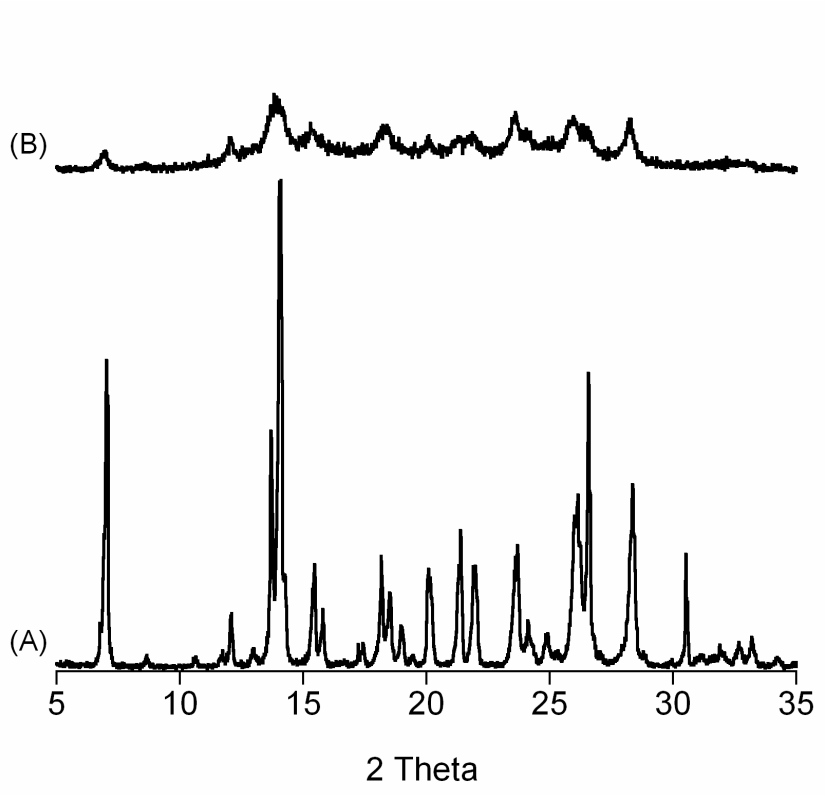

Figure D-1: XRPD showing disorder induced in CBZ-SAC cocrystal after 30 minutes cryogenic grinding. CBZ-SAC cocrystal (A) before grinding, and (B) after grinding.

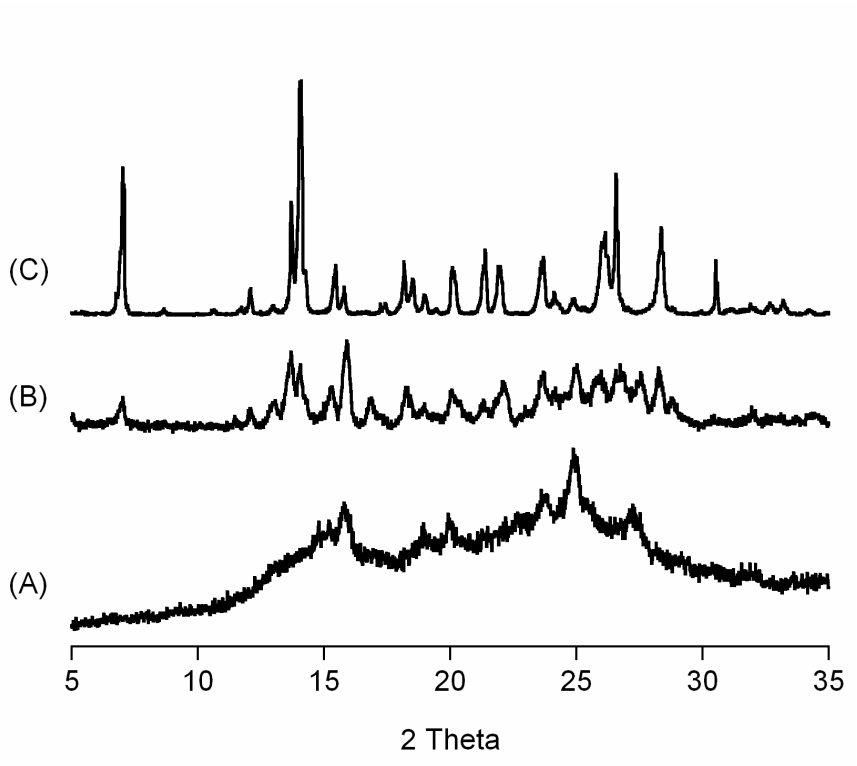

Figure D-2: XRPD pattern showing CBZ-SAC formation after heating the amorphous phase generated by 30 minute cryogenic cogrinding of CBZ(III) and SAC. (A) CBZ(III)/SAC mixture after 30 min cryogenic cogrinding, and (B) coground mixture after heating in DSC to 115°C; (C) CBZ-SAC cocrystal (reference)